

UCLA

UCLA Electronic Theses and Dissertations

Title

Total Synthesis of Picrinine

Permalink

<https://escholarship.org/uc/item/6d93p334>

Author

Smith, Joel Michael

Publication Date

2015

Peer reviewed|Thesis/dissertation

UNIVERSITY OF CALIFORNIA

Los Angeles

Total Synthesis of Picrinine

A dissertation submitted in partial satisfaction of the
requirements for the degree Doctor of Philosophy
in Chemistry

by

Joel Michael Smith

2015

© Copyright by
Joel Michael Smith
2015

ABSTRACT OF THE DISSERTATION

Total Synthesis of Picrinine

by

Joel Michael Smith

Doctor of Philosophy in Chemistry

University of California, Los Angeles, 2015

Professor Neil K. Garg, Chair

Throughout history, organisms have ensured their survival by producing a wide variety of small molecule natural products. These entities commonly serve roles in cell function and signaling, and have also provided a defense system to combat infectious parasites. In the realm of synthetic chemistry, natural products serve as an architectural inspiration for the development of novel chemical transformations and molecular cascade processes. Ultimately, the synthesis of natural products that have biological importance holds promise toward the understanding of a plethora of biochemical pathways and the treatment of disease.

This dissertation describes synthetic efforts toward the alkaloid picrinine. This molecule is a member of the akuammiline alkaloid class, and it bears a complex molecular scaffold unaddressed by synthetic chemistry. Central to the synthetic approach is the use of the Fischer indolization reaction as a platform for rapidly building molecular complexity and constructing the salient furanoindoline core of picrinine. The earlier part of this dissertation describes a first-generation approach to the synthesis of picrinine, while the ensuing chapter concerns a second-generation route, which resulted in its total synthesis. This dissertation's final section concerns the development of a unified and enantioselective approach to the akuammiline alkaloid family, in addition to a formal enantioselective synthesis of both aspidophylline A and picrinine. In summary, the synthetic endeavors described emphasize the importance natural products hold for the development of novel synthetic strategies and transformations.

The dissertation of Joel Michael Smith is approved.

Patrick G. Harran

Tatiana Segura

Neil K. Garg, Committee Chair

University of California, Los Angeles

2015

For my parents, Dr. Michael K. Smith and Mrs. Joleen M. Smith

TABLE OF CONTENTS

Abstract.....	ii
Committee Page.....	iv
Dedication Page.....	v
Table of Contents.....	vi
List of Figures.....	x
List of Schemes.....	xviii
List of Abbreviations	xx
Acknowledgments.....	xxiv
Biographical Sketch	xxvii
CHAPTER ONE: Cascade Reactions: A Driving Force in Akuammiline Alkaloid Total Synthesis	1
1.1 Abstract.....	1
1.2 Introduction.....	1
1.3 Total Syntheses of Vincorine	7
1.3.1 Qin’s Cyclopropanation Approach	8
1.3.2 Ma’s Oxidative Coupling Approach	11
1.3.3 MacMillan’s Organocatalytic Approach.....	15
1.4 Total Syntheses of Aspidophylline A and Picrinine	18
1.4.1 Garg’s Interrupted Fischer Approach	18
1.4.2 Garg’s Synthesis of Picrinine.....	21
1.4.3 Zhu’s Oxidative Azidoalkoxylation Approach	21

1.4.4 Ma's Oxidative Coupling Approach	23
1.5 Total Syntheses of Scholarisine A	26
1.5.1 Smith's Reductive Cyclization Approach	26
1.5.2 Snyder's Radical Functionalization Approach	29
1.6 Conclusions	31
1.7 References	32
CHAPTER TWO: First-Generation Approach to the Total Synthesis of Picrinine	40
2.1 Abstract	40
2.2 Introduction	40
2.3 Initial Forays and First Generation Retrosynthetic Analysis	44
2.4 Synthesis of [3.3.1]-Azabicyclic and Elaboration to Substrate 2.30	46
2.5 Fischer Indolization and Unsuccessful Late-Stage Studies	49
2.6 Conclusions	52
2.7 Experimental Section	53
2.7.1 Materials and Methods	53
2.7.2 Experimental Procedures	54
2.8 References	69
APPENDIX ONE: Spectra Relevant to Chapter Two	73
CHAPTER THREE: Second-Generation Approach and Total Synthesis of Picrinine	100
3.1 Abstract	100

3.2 Introduction.....	100
3.3 Second-Generation Retrosynthetic Analysis	101
3.4 Development of a Synthetic Route to Access Fischer Indolization Substrate 3.5	102
3.5 Failed Oxidation and Modification of Synthetic Route	107
3.6 Earlier Oxidation, Successful Fischer Indolization, and Late-Stage Challenges.....	109
3.7 Completion of the Total Synthesis of Picrinine (3.1)	111
3.8 Conclusion	112
3.9 Experimental Section	112
3.9.1 Materials and Methods.....	112
3.9.2 Experimental Procedures	114
3.10 References.....	138
APPENDIX TWO: Spectra Relevant to Chapter Three	142
CHAPTER FOUR: Unified and Enantioselective Approach to the Akuammiline Alkaloids.....	191
4.1 Abstract.....	191
4.2 Introduction.....	191
4.3 Unified Route to the Akuammiline Alkaloids	192
4.4 Enantioselective Approach to the Akuammiline Alkaloids.....	195
4.5 Conclusion	197
4.6 Experimental Section	198
4.6.1 Materials and Methods.....	198
4.6.2 Experimental Procedures	199

4.6.2.1 Synthesis of Lactone 4.4	199
4.6.2.2 Enantioselective Synthesis of Azabicyclic 4.10	205
4.7 References	209
APPENDIX THREE: Spectra Relevant to Chapter Four	211

LIST OF FIGURES

CHAPTER ONE

- Figure 1.1 Representative biologically active akuammiline alkaloids2
- Figure 1.2 Proposed biosynthesis of several monoterpenoid indole alkaloid classes ...4

CHAPTER TWO

- Figure 2.1 Picrinine (**2.1**) and 3D representation from X-ray structure.....41
- Figure 2.2 Summary of total synthesis of aspidophylline A (**2.7**) and initial synthetic plan for picrinine (**2.1**) utilizing the key Fischer indolization reaction43
- Figure 2.3 Unsuccessful Fischer indolization of **2.9** and design of new substrate.....45

APPENDIX ONE

- Figure A1.1 ¹H NMR (500 MHz, CDCl₃) of compound **2.22**.....74
- Figure A1.2 Infrared spectrum of compound **2.22**.....75
- Figure A1.3 ¹³C NMR (125 MHz, CDCl₃) of compound **2.22**.....75
- Figure A1.4 ¹H NMR (500 MHz, CDCl₃) of compound **2.23**.....76
- Figure A1.5 Infrared spectrum of compound **2.23**.....77
- Figure A1.6 ¹³C NMR (125 MHz, CDCl₃) of compound **2.23**.....77
- Figure A1.7 ¹H NMR (500 MHz, CDCl₃) of compound **2.24**.....78
- Figure A1.8 Infrared spectrum of compound **2.24**.....79
- Figure A1.9 ¹³C NMR (125 MHz, CDCl₃) of compound **2.24**.....79
- Figure A1.10 ¹H NMR (300 MHz, CDCl₃) of compound **2.26**.....80

Figure A1.11	Infrared spectrum of compound 2.26	81
Figure A1.12	¹³ C NMR (125 MHz, CDCl ₃) of compound 2.26	81
Figure A1.13	¹ H NMR (500 MHz, CDCl ₃) of compound 2.20	82
Figure A1.14	Infrared spectrum of compound 2.20	83
Figure A1.15	¹³ C NMR (125 MHz, CDCl ₃) of compound 2.20	83
Figure A1.16	¹ H NMR (500 MHz, CDCl ₃) of compound 2.19	84
Figure A1.17	Infrared spectrum of compound 2.19	85
Figure A1.18	¹³ C NMR (125 MHz, CDCl ₃) of compound 2.19	85
Figure A1.19	¹ H NMR (500 MHz, CDCl ₃) of compound 2.18	86
Figure A1.20	Infrared spectrum of compound 2.18	87
Figure A1.21	¹³ C NMR (125 MHz, CDCl ₃) of compound 2.18	87
Figure A1.22	¹ H NMR (500 MHz, CDCl ₃) of compound 2.28	88
Figure A1.23	Infrared spectrum of compound 2.28	89
Figure A1.24	¹³ C NMR (125 MHz, CDCl ₃) of compound 2.28	89
Figure A1.25	¹ H NMR (500 MHz, CDCl ₃) of compound 2.29	90
Figure A1.26	Infrared spectrum of compound 2.29	91
Figure A1.27	¹³ C NMR (125 MHz, CDCl ₃) of compound 2.29	91
Figure A1.28	¹ H NMR (500 MHz, CDCl ₃) of compound 2.30	92
Figure A1.29	Infrared spectrum of compound 2.30	93
Figure A1.30	¹³ C NMR (125 MHz, CDCl ₃) of compound 2.30	93
Figure A1.31	¹ H NMR (500 MHz, CDCl ₃) of compound 2.34	94
Figure A1.32	Infrared spectrum of compound 2.34	95
Figure A1.33	¹³ C NMR (125 MHz, CDCl ₃) of compound 2.34	95

Figure A1.34	^1H NMR (500 MHz, CDCl_3) of compound 2.35	96
Figure A1.35	Infrared spectrum of compound 2.35	97
Figure A1.36	^{13}C NMR (125 MHz, CDCl_3) of compound 2.35	97
Figure A1.37	^1H NMR (500 MHz, CDCl_3) of compound 2.38	98
Figure A1.38	Infrared spectrum of compound 2.38	99
Figure A1.39	^{13}C NMR (125 MHz, CDCl_3) of compound 2.38	99

CHAPTER THREE

Figure 3.1	Attempted olefin oxidation of indolenine substrate 3.3	108
Figure 3.2	Hypothesis for oxidation difficulties and revision of strategy.....	109

APPENDIX TWO

Figure A2.1	^1H NMR (500 MHz, CDCl_3) of compound 3.9	143
Figure A2.2	Infrared spectrum of compound 3.9	144
Figure A2.3	^{13}C NMR (125 MHz, CDCl_3) of compound 3.9	144
Figure A2.4	^1H NMR (500 MHz, CDCl_3) of compound 3.8	145
Figure A2.5	Infrared spectrum of compound 3.8	146
Figure A2.6	^{13}C NMR (125 MHz, CDCl_3) of compound 3.8	146
Figure A2.7	^1H NMR (500 MHz, CDCl_3) of compound 3.7	147
Figure A2.8	Infrared spectrum of compound 3.7	148
Figure A2.9	^{13}C NMR (125 MHz, CDCl_3) of compound 3.7	148
Figure A2.10	^1H NMR (500 MHz, CDCl_3) of compound 3.11	149
Figure A2.11	Infrared spectrum of compound 3.11	150

Figure A2.12	^{13}C NMR (125 MHz, CDCl_3) of compound 3.11	150
Figure A2.13	^1H NMR (500 MHz, CDCl_3) of compound 3.12	151
Figure A2.14	Infrared spectrum of compound 3.12	152
Figure A2.15	^{13}C NMR (125 MHz, CDCl_3) of compound 3.12	152
Figure A2.16	^1H NMR (500 MHz, CDCl_3) of compound 3.14	153
Figure A2.17	Infrared spectrum of compound 3.14	154
Figure A2.18	^{13}C NMR (125 MHz, CDCl_3) of compound 3.14	154
Figure A2.19	^1H NMR (500 MHz, CDCl_3) of compound 3.15	155
Figure A2.20	Infrared spectrum of compound 3.15	156
Figure A2.21	^{13}C NMR (125 MHz, CDCl_3) of compound 3.15	156
Figure A2.22	^1H NMR (500 MHz, CDCl_3) of compound 3.16	157
Figure A2.23	Infrared spectrum of compound 3.16	158
Figure A2.24	^{13}C NMR (125 MHz, CDCl_3) of compound 3.16	158
Figure A2.25	^1H NMR (500 MHz, CDCl_3) of compound 3.18	159
Figure A2.26	Infrared spectrum of compound 3.18	160
Figure A2.27	^{13}C NMR (125 MHz, CDCl_3) of compound 3.18	160
Figure A2.28	^1H NMR (500 MHz, CDCl_3) of compound 3.21	161
Figure A2.29	Infrared spectrum of compound 3.21	162
Figure A2.30	^{13}C NMR (125 MHz, CDCl_3) of compound 3.21	162
Figure A2.31	^1H NMR (500 MHz, CDCl_3) of compound 3.23	163
Figure A2.32	Infrared spectrum of compound 3.23	164
Figure A2.33	^{13}C NMR (125 MHz, CDCl_3) of compound 3.23	164
Figure A2.34	^1H NMR (500 MHz, CDCl_3) of compound 3.35	165

Figure A2.35	Infrared spectrum of compound 3.35	166
Figure A2.36	¹³ C NMR (125 MHz, CDCl ₃) of compound 3.35	166
Figure A2.37	¹ H NMR (500 MHz, CDCl ₃) of compound 3.20	167
Figure A2.38	Infrared spectrum of compound 3.20	168
Figure A2.39	¹³ C NMR (125 MHz, CDCl ₃) of compound 3.20	168
Figure A2.40	¹ H NMR (500 MHz, CD ₂ Cl ₂) of compound 3.34	169
Figure A2.41	Infrared spectrum of compound 3.34	170
Figure A2.42	¹³ C NMR (125 MHz, CD ₂ Cl ₂) of compound 3.34	170
Figure A2.43	¹ H NMR (500 MHz, CDCl ₃) of compound 3.24	171
Figure A2.44	Infrared spectrum of compound 3.24	172
Figure A2.45	¹³ C NMR (125 MHz, CDCl ₃) of compound 3.24	172
Figure A2.46	¹ H NMR (500 MHz, CDCl ₃) of compound 3.25	173
Figure A2.47	Infrared spectrum of compound 3.25	174
Figure A2.48	¹³ C NMR (125 MHz, CDCl ₃) of compound 3.25	174
Figure A2.49	¹ H NMR (500 MHz, CDCl ₃) of compound 3.5	175
Figure A2.50	Infrared spectrum of compound 3.5	176
Figure A2.51	¹³ C NMR (125 MHz, CDCl ₃) of compound 3.5	176
Figure A2.52	¹ H NMR (500 MHz, CDCl ₃) of compound 3.3	177
Figure A2.53	Infrared spectrum of compound 3.3	178
Figure A2.54	¹³ C NMR (125 MHz, CDCl ₃) of compound 3.3	178
Figure A2.55	¹ H NMR (500 MHz, CDCl ₃) of compound 3.28	179
Figure A2.56	Infrared spectrum of compound 3.28	180
Figure A2.57	¹³ C NMR (125 MHz, CDCl ₃) of compound 3.28	180

Figure A2.58	^1H NMR (500 MHz, CDCl_3) of compound 3.29	181
Figure A2.59	Infrared spectrum of compound 3.29	182
Figure A2.60	^{13}C NMR (125 MHz, CDCl_3) of compound 3.29	182
Figure A2.61	^1H NMR (500 MHz, CDCl_3) of compound 3.30	183
Figure A2.62	Infrared spectrum of compound 3.30	184
Figure A2.63	^{13}C NMR (125 MHz, CDCl_3) of compound 3.30	184
Figure A2.64	^1H NMR (500 MHz, CDCl_3) of compound 3.27	185
Figure A2.65	Infrared spectrum of compound 3.27	186
Figure A2.66	^{13}C NMR (125 MHz, CDCl_3) of compound 3.27	186
Figure A2.67	^1H NMR (500 MHz, CDCl_3) of compound 3.32	187
Figure A2.68	Infrared spectrum of compound 3.32	188
Figure A2.69	^{13}C NMR (125 MHz, CDCl_3) of compound 3.32	188
Figure A2.70	^1H NMR (500 MHz, CDCl_3) of compound 3.1	189
Figure A2.71	^{13}C NMR (125 MHz, CDCl_3) of compound 3.1	190

CHAPTER FOUR

Figure 4.1	Unified retrosynthetic strategy of akuammilines 4.1–4.3	193
------------	--	-----

APPENDIX THREE

Figure A3.1	^1H NMR (500 MHz, CDCl_3) of compound 4.6	212
Figure A3.2	Infrared spectrum of compound 4.6	213
Figure A3.3	^{13}C NMR (125 MHz, CDCl_3) of compound 4.6	213
Figure A3.4	^1H NMR (500 MHz, CDCl_3) of compound 4.7	214

Figure A3.5	Infrared spectrum of compound 4.7	215
Figure A3.6	¹³ C NMR (125 MHz, CDCl ₃) of compound 4.7	215
Figure A3.7	¹ H NMR (500 MHz, CDCl ₃) of compound 4.8a	216
Figure A3.8	Infrared spectrum of compound 4.8a	217
Figure A3.9	¹³ C NMR (125 MHz, CDCl ₃) of compound 4.8a	217
Figure A3.10	¹ H NMR (500 MHz, CDCl ₃) of compound 4.8b	218
Figure A3.11	Infrared spectrum of compound 4.8b	219
Figure A3.12	¹³ C NMR (125 MHz, CDCl ₃) of compound 4.8b	219
Figure A3.13	¹ H NMR (500 MHz, CDCl ₃) of compound 4.9	220
Figure A3.14	Infrared spectrum of compound 4.9	221
Figure A3.15	¹³ C NMR (125 MHz, CDCl ₃) of compound 4.9	221
Figure A3.16	¹ H NMR (500 MHz, CDCl ₃) of compound 4.4	222
Figure A3.17	Infrared spectrum of compound 4.4	223
Figure A3.18	¹³ C NMR (125 MHz, CDCl ₃) of compound 4.4	223
Figure A3.19	¹ H NMR (500 MHz, CDCl ₃) of compound 4.18	224
Figure A3.20	Infrared spectrum of compound 4.18	225
Figure A3.21	¹³ C NMR (125 MHz, CDCl ₃) of compound 4.18	225
Figure A3.22	¹ H NMR (500 MHz, CDCl ₃) of compound 4.13	226
Figure A3.23	Infrared spectrum of compound 4.13	227
Figure A3.24	¹³ C NMR (125 MHz, CDCl ₃) of compound 4.13	227
Figure A3.25	¹ H NMR (500 MHz, CDCl ₃) of compound 4.19	228
Figure A3.26	Infrared spectrum of compound 4.19	229
Figure A3.27	¹³ C NMR (125 MHz, CDCl ₃) of compound 4.19	229

Figure A3.28 Chiral SFC trace of racemic of compound 3.11	230
Figure A3.29 Chiral SFC trace of racemic of compound 4.10	230

LIST OF SCHEMES

CHAPTER ONE

Scheme 1.1	Divergent biosynthetic relationship of the akuammiline alkaloids.....	6
Scheme 1.2	Qin's key cyclopropanation step to construct 1.21	9
Scheme 1.3	Qin's synthetic endgame and completion of (\pm)-vincorine (1.15).....	10
Scheme 1.4	Ma's enantioselective synthesis of intermediate 1.31	12
Scheme 1.5	Ma's oxidative cyclization and completion of (-)-vincorine (1.15).....	14
Scheme 1.6	MacMillan's key cascade transformation	16
Scheme 1.7	MacMillan's radical cyclization and completion of (-)-vincorine (1.15)..	17
Scheme 1.8	Garg's synthesis of lactone 1.52	19
Scheme 1.9	Interrupted Fischer indolization and completion of aspidophylline A (1.4).....	20
Scheme 1.10	Zhu's oxidative key azidoalkoxylation transformation.....	22
Scheme 1.11	Zhu's completion of (\pm)-aspidophylline A (1.4).....	23
Scheme 1.12	Ma's key oxidative coupling to forge furoindoline 1.71	24
Scheme 1.13	Ma's completion of (\pm)-aspidophylline A (1.4).....	25
Scheme 1.14	Smith's key reductive cyclization cascade reaction.....	27
Scheme 1.15	Smith's completion of (+)-scholarisine A (1.14).....	28
Scheme 1.16	Snyder's radical cyclization/Keck allylation cascade.....	30
Scheme 1.17	Snyder's radical C-H activation and completion of (+)-scholarisine A (1.14).....	31

CHAPTER TWO

Scheme 2.1	Initial retrosynthetic plan for the total synthesis of picrinine (2.1).....	46
Scheme 2.2	Synthesis of [3.3.1]-azabicyclic 2.19	48
Scheme 2.3	Synthesis of Fischer indolization substrate 2.30	49
Scheme 2.4	Successful Fischer indolization of ketone 2.30	50
Scheme 2.5	Unsuccessful attempts to elaborate Fischer indolization product 2.34	52

CHAPTER THREE

Scheme 3.1	Revised retrosynthetic analysis of picrinine (3.1).....	102
Scheme 3.2	Assembly of the [3.3.1]-azabicyclic and attempted elaboration to enone 3.13	103
Scheme 3.3	Approaches to homologate and oxidize enone 3.11	104
Scheme 3.4	Diastereoselective reduction of enal 3.18	105
Scheme 3.5	Synthesis of cyclopentene 3.5 and Fischer indolization.....	107
Scheme 3.6	Synthesis of lactol 3.27 and failed late-stage <i>N,O</i> -acetal formation.....	110
Scheme 3.7	Completion of the total synthesis of picrinine (3.1).....	111

CHAPTER FOUR

Scheme 4.1	Synthesis of lactone 4.4 from enal 4.5 and elaboration to aspidophylline A (4.2).....	194
Scheme 4.2	Three approaches to the enantioselective synthesis of enone 4.10	196
Scheme 4.3	Asymmetric synthesis of enone 4.10	197

LIST OF ABBREVIATIONS

Å	angstrom
$[\alpha]_D$	specific rotation at wavelength of sodium D line
Ac	acetyl, acetate
AcOH	acetic acid
AIBN	Azobisisobutyronitrile
α	alpha
app.	apparent
aq.	aqueous
atm	atmosphere
Bz	benzoyl
Bn	benzyl
β	beta
br	broad
Boc	<i>tert</i> -butoxycarbonyl
BTPP	(<i>tert</i> -butylimino)tris(pyrrolidino)phosphorane
Bu	butyl
<i>i</i> -Bu	isobutyl
<i>n</i> -Bu	butyl (linear)
<i>t</i> -Bu	<i>tert</i> -butyl
<i>t</i> -BuOH	<i>tert</i> -butyl alcohol
BHT	butylated hydroxytoluene
<i>c</i>	concentration for specific rotation measurements
°C	degrees Celsius
CAN	Cerium (IV) ammonium nitrate
calcd	calculated
cat.	catalytic
CCDC	Cambridge Crystallographic Data Centre
COD	1,5-cyclooctadiene
d	doublet
DCB	1,2-dichlorobenzene
DCE	1,2-dichloroethane
(DHQ) ₂ PHAL	Hydroquinine 1,4-phthalazinediyl diether

DIC	<i>N,N'</i> -Diisopropylcarbodiimide
dig	digonal
DMAP	4-dimethylaminopyridine
DMF	<i>N,N</i> -dimethylformamide
DMP	Dess–Martin periodinane
DMPU	1,3-Dimethyl-3,4,5,6-tetrahydro-2(1H)-pyrimidinone
DMSO	dimethyl sulfoxide
dppf	1,1'-Bis(diphenylphosphino)ferrocene
ee	enantiomeric excess
equiv	equivalent
ESI	electrospray ionization
Et	ethyl
g	gram(s)
Glc	glucosyl
h	hour(s)
HMPA	Hexamethylphosphoramide
HRMS	high resolution mass spectroscopy
Hz	hertz
IBX	2-iodoxybenzoic acid
IR	infrared (spectroscopy)
<i>J</i>	coupling constant
L	liter
LiHMDS	lithium hexamethyldisilazide
M	molecular mass
m	multiplet or milli
<i>m</i>	meta
<i>m/z</i>	mass to charge ratio
μ	micro
<i>m</i> CPBA	3-chloroperbenzoic acid
Me	methyl
MHz	megahertz
min	minute(s)
mol	mole(s)
MOM	methoxymethyl ether

mp	melting point
MS	molecular sieves
NF- κ B	Nuclear Factor kappa B
NIS	<i>N</i> -iodosuccinimide
NMO	4-Methylmorpholine <i>N</i> -oxide
NMR	nuclear magnetic resonance
[O]	oxidation
<i>p</i>	para
π	pi
PCC	pyridinium chlorochromate
Ph	phenyl
pH	hydrogen ion concentration in aqueous solution
PhH	benzene
Piv	pivaloyl
PMP	1,2,2,6,6-Pentamethylpiperidine
PPh ₃	triphenylphosphine
ppm	parts per million
PPTS	Pyridinium <i>p</i> -toluenesulfonate
Pr	propyl
<i>i</i> -Pr	isopropyl
PSI	Pounds per square inch
pyr	pyridine
q	quartet
rt	room temperature
R _f	retention factor
s	singlet
sat.	saturated
SGLT2	sodium-glucose linked transporter 2
t	triplet
TBD	1,5,7-Triazabicyclo[4.4.0]dec-5-ene
TBDPS	<i>tert</i> -butyldiphenylsilyl
TBS	<i>tert</i> -butyldimethylsilyl
TBSCl	<i>tert</i> -butyldimethylsilyl chloride
TEBA	Benzyltriethylammonium
TES	triethylsilyl

Tf	trifluoromethanesulfonyl (trifyl)
TFA	trifluoroacetic acid
THF	tetrahydrofuran
TLC	thin layer chromatography
TMS	trimethylsilyl
TMSCl	trimethylsilyl chloride
TMSOTf	trimethylsilyl triflate
trig	trigonal
Ts	<i>p</i> -toluenesulfonyl (tosyl)
UV	ultraviolet

ACKNOWLEDGMENTS

Initially, I would like to acknowledge my doctoral advisor Neil K. Garg for his great mentorship throughout my time in graduate school. While I came to graduate school to primarily to be educated in organic chemistry, I did not expect such immense personal enrichment. Neil was instrumental in both of these respects – providing an arena for scholarly curiosity, as well as an opportunity to positively mature and grow as an individual. It need not be understated how appreciative I am for this guidance and bedrock on which I can continue to improve as a scientist and as a person.

Additionally, I want to express gratitude to my other committee members for their participation in my graduate school experience. Professors Patrick G. Harran, Catherine F. Clarke, and Tatiana Segura were all instrumental in my intellectual growth as a student by challenging me during my candidacy exam and reading my dissertation.

Other professors that I would like to thank include my undergraduate research advisors Professor Brian C. Goess and Professor Fernando Coelho. Both of them were influential in fostering my fervor for chemistry and helping me to hone my skills as a scientist. I still remember staying late into the evening with Professor Goess to rigorously analyze 2D NMR spectra, in addition to always putting my bowling scores to shame.

My labmates who graduated prior to me also deserve high acknowledgment. First, I am grateful to Dr. Alex Schammel for being such a wonderful laboratory mentor and fantastic friend. He has always been supportive of me and provided me with a great training background in order to build upon as a chemist. Dr. Ben Boal deserves my praise for being a wonderful coworker and an excellent friend. I learned so much from Ben while working in the akuammiline trenches alongside him, and his enthusiasm and intuition for chemistry has been inspiring. Dr.

Kyle Quasdorf was also a great labmate and close friend. He was an inspiration due to his exceedingly high intellect and modesty as a scientist. All I have to add about Kyle is the word “Georgia.” Dr. Tehetena Mesganaw was also a great friend and supportive coworker. She was very supportive of me and always provided me consistently stimulating conversation. Amongst my other older coworkers, I am thankful to Professor Liansuo Zu, Dr. Alex Hutters, Dr. Stephen Ramgren, Dr. Amanda Silberstein, and Dr. Grace Chiou. All of these coworkers were resourceful in intellectual conversation and fostering great laboratory comraderie. I am so happy that I was able to benefit from their friendship and professional association.

I also owe appreciation to all of my labmates that were concurrent with me as well as younger than me. Particular individuals deserve special attention. Noah Fine Nathel has always been a great friend and supportive individual. His immense kindness and stimulating intellect has helped me grow very much as a chemist over the past 5 years. Additionally, I would like to acknowledge Jesus Moreno, as he has been a great coworker in developing akuammiline synthesis in addition to being a wonderful friend. Elias Picazo and Lucas Morrill have also been a wonderful pair to work with on our akuammiline research, and I look forward to seeing them grow as scientists as they continue to learn. Another younger student who I owe much to is Michael Corsello. He is a talented and enthusiastic graduate student who has challenged me intellectually and helped me grow as a scientist. I am grateful to him for his strong friendship and his enthusiasm for science. Amongst other younger students, I thank José Medina, Junyong Kim, and Bryan Simmons for their friendship and support during the years in which we overlapped in the laboratory.

I also want to express my high gratitude to my family for their constant love and support. My brothers Ben Smith and Paul Smith, along with my sisters-in-law Alicia Smith and Heather

Smith, have always been supportive of me as a scientist. While chemistry may not be their trade, I am grateful for their constant encouragement and enthusiasm for my research and growth as an individual. I am also indebted to my father, Dr. Michael Smith, for his support of me. Much of my interest in chemistry came from his influence when I was a teenager, and his consistent interest in my work as a scientist has been unwavering. I still remember learning from him about the various oxidation states of polyatomic ions when I was taking chemistry in high school. Last, but certainly not least of my family, I must thank my mother Joleen Smith. She has been amazingly supportive during my time in graduate school, and I may not be where I am today without her love and encouragement. It is difficult to express in words how appreciative I am of her unwavering love for me as her son.

Finally, I want to thank my loving girlfriend Alexis Demeo for her support of me. It need not be understated the immense happiness I have with her in my life. I firmly believe that I would be a very different person today without her consistent love, support, and encouragement. I am deeply grateful for her being such a wonderful companion over the past 20 months.

Chapter 1 is a version of Smith, J. M.; Moreno, J.; Boal, B. W.; Garg, N. K. *Angew. Chem., Int. Ed.* **2015**, *54*, 400–412. Smith, Moreno, Boal, and Garg were responsible for writing the manuscript.

Chapter 2 is currently unpublished work performed by Smith, J. and Boal, B. W.

Chapter 3 is a blend of Smith et al. *J. Am. Chem. Soc.* 2014, *136*, 4504–4507 and unpublished work performed by Smith, J., Moreno, J., and Boal, B. W.

Chapter 4 is currently unpublished work performed by Smith, J. M., Moreno, J., and Picazo, E.

BIOGRAPHICAL SKETCH

Education

University of California, Los Angeles, CA

- Ph.D., Organic Chemistry, anticipated Spring 2015
- Graduate Research Assistant, July 2010 to present
- Current GPA: 3.99/4.00

Furman University, Greenville, CA

- Bachelor of Science, Chemistry and Music, with Honors, May 2010
- Cumulative GPA: 3.45/4.00

Professional and Academic Experience

Graduate Research Assistant: University of California, Los Angeles, CA

- July 2014 to July 2015; Advisor: Professor Neil K. Garg
- Developed and implemented synthetic strategies to construct complex akuammiline alkaloids.
- Completed asymmetric synthesis of akuammiline bicyclic scaffold.

NSF Graduate Research Fellow: University of California, Los Angeles, CA

- July 2011 to July 2014; Advisor: Professor Neil K. Garg
- Developed and implemented synthetic strategies to construct complex akuammiline alkaloids.
- Completed total syntheses of the long-standing akuammiline targets picrinine.

Teaching Assistant: University of California, Los Angeles, CA

- Led discussions for undergraduate organic chemistry (January 2011 to June 2011).
- Supervised and taught undergraduate experimental organic chemistry and laboratory technique (September 2010 to December 2010).

NSF REU Research Fellow: University of Campinas, Campinas, Brazil

- May 2009 to August 2009; Advisor: Professor Fernando Coelho
- Developed a new route to construct 1,3-oxazinanones from Morita-Baylis-Hillman adducts.

Teaching Assistant: Furman University, Greenville, SC

- September 2008 to May 2010
- Led discussions and conducted lectures for undergraduate chemistry and music theory courses.

Undergraduate Research Assistant: Furman University, Greenville, SC

- May 2008 to June 2010; Advisor: Brian C. Goess
- Investigated routes toward and completed the total synthesis of the furanosteroid hibiscone C.

Fellowships, Honors, and Awards

- UCLA Division of Organic Chemistry ACS Travel Grant, 2010 (ACS/San Francisco 2011)
- UCLA Dissertation Year Fellowship (7/2014–3/2015)
- NSF Predoctoral Graduate Research Fellowship (6/2011–6/2014)
- Keeler Music Scholarship (9/2009–5/2010)

- NSF-REU South America Fellowship (5/2009–7/2009)
- Furman Advantage Fellowship (5/2008–8/2008)
- Dreyfus Chemistry Scholar (9/2006–5/2010)
- Honor Scholar (9/2006–5/2010)
- Achiever Scholarship (9/2006–5/2010)

Publications

4. Smith, J. M.; Moreno, J.; Boal, B. W.; Garg, N. K. “Cascade Reactions as a Driving Force in Akuammiline Alkaloid Total Synthesis” *Angew. Chem. Int. Ed.* **2015**, *54*, 400–412.
3. Smith, J. M.; Moreno, J.; Boal, B. W.; Garg, N. K. “Total Synthesis of the Akuammiline Alkaloid Picrinine” *J. Am. Chem. Soc.* **2014**, *136*, 4504–4507.
2. Ungureanu, S.; Meadows, M.; Smith, J.; Duff, D. B.; Burgess, J. M.; Goess, B. C. “Total Synthesis of (±)-Hibiscone C” *Tetrahedron Lett.* **2011**, *52*, 1509–1511.
1. Rodrigues Jr., M. T.; Gomes, J. C.; Smith, J.; Coelho, F. “Simple and Highly Diastereoselective Access to 3,4-substituted tetrahydro-1,8-naphthyridines from Morita–Baylis–Hillman Adducts” *Tetrahedron Lett.* **2010**, *51*, 4988–4990.

Presentations

8. **Total Synthesis of the Akuammiline Alkaloid Picrinine (Talk).** Joel M. Smith*, Jesus Moreno, Ben W. Boal, and Neil K. Garg, *ACS National Meeting*, San Francisco, CA, August 2014.
7. **Total Synthesis of the Akuammiline Alkaloid Picrinine (Talk).** Joel M. Smith*, Jesus Moreno, Ben W. Boal, and Neil K. Garg, *DOC Graduate Research Symposium*, Irvine, CA, July 2014.
6. **Progress Towards the Total Synthesis of Picrinine (Poster).** Joel M. Smith*, Jesus Moreno, Ben W. Boal, and Neil K. Garg, *UCLA Seaborg Symposium*, Los Angeles, CA, October 2013.
5. **Progress Towards the Total Synthesis of Picrinine (Poster).** Joel M. Smith*, Jesus Moreno, Ben W. Boal, and Neil K. Garg, *UCLA Winstein Symposium*, Los Angeles, CA, October 2012.
4. **Progress Towards the Total Synthesis of Picrinine (Poster).** Joel M. Smith*, Ben W. Boal, and Neil K. Garg, *ACS National Meeting*, San Diego, CA, March 2012.
3. **Progress Towards the Total Synthesis of Picrinine (Poster).** Joel M. Smith*, Ben W. Boal, and Neil K. Garg, *SCALACS Western Regional Meeting*, Pasadena, CA, November 2011.
2. **Synthesis of 1,3-Oxazinanones from Morita–Baylis–Hillman Adducts (Talk).** Joel M. Smith* and Fernando Coelho, *SERMACS 2009*, San Juan, Puerto Rico, October 2009.
1. **Progress Towards the Synthesis of Hibiscone C (Poster).** Joel M. Smith*, Justin Goodwin, Ashley Windrum, and Brian C. Goess, *SERMACS 2008*, Nashville, TN, October 2008.

CHAPTER ONE

Cascade Reactions: A Driving Force in Akuammiline Alkaloid Total Synthesis

Adapted from: Joel M. Smith, Jesus Moreno, Ben W. Boal, and Neil K. Garg.

Angew. Chem. Int. Ed. **2015**, *54*, 400–412.

1.1 Abstract

The akuammiline alkaloids are a family of intricate natural products that have received considerable attention from scientists worldwide. Despite that many members of this alkaloid class were discovered over 50 years ago, synthetic chemistry has been unable to address their architectures until recently. This chapter provides a brief overview of the rich history of the akuammiline alkaloids, including their isolation, structural features, biological activity, and proposed biosyntheses. Furthermore, several recently completed total syntheses are discussed in detail. These examples not only serve to highlight modern achievements in alkaloid total synthesis, but also demonstrate how the molecular scaffolds of the akuammilines have provided inspiration for the discovery and implementation of innovative cascade reactions for the rapid assembly of complex structures.

1.2 Introduction

Natural products belonging to the akuammiline family of alkaloids have provided a fruitful area of scientific discovery for over one century.¹ Initial interest in the akuammilines stemmed from their role in traditional medicine, where inhabitants of southern and southeastern Asia utilized the leaves of native plants such as *Alstonia scholaris* to treat various ailments in

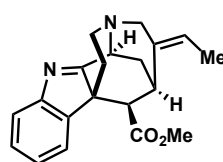
humans and livestock.² As a result, scientists have investigated the pharmacological effects of akuammiline alkaloids and discovered their wide range of biological properties, which range from anti-cancer to analgesic effects. For example, echitamine (**1.1**), which was first isolated in 1875,³ displays both in vitro and in vivo cytotoxicity,⁴ whereas strictamine (**1.2**)⁵ inhibits the transcription factor NF- κ B (Figure 1.1).⁶ Additionally, derivatives of picraline (**1.3**)⁷ inhibit the renal cortex protein SGLT2,⁸ while aspidophylline A (**1.4**) reverses drug-resistance in cancerous cell lines.⁹

Figure 1.1 Representative biologically active akuammiline alkaloids.



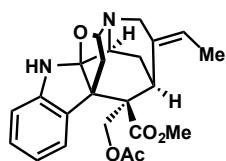
(-)-Echitamine (1.1)
(1875)

displays in vivo and
in vitro cytotoxicity



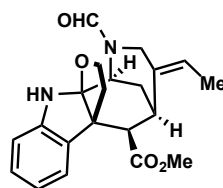
(+)-Strictamine (1.2)
(1966)

inhibits transcription
factor NF- κ B



(+)-Picraline (1.3)
(1954)

derivatives inhibit
SGLT2 protein



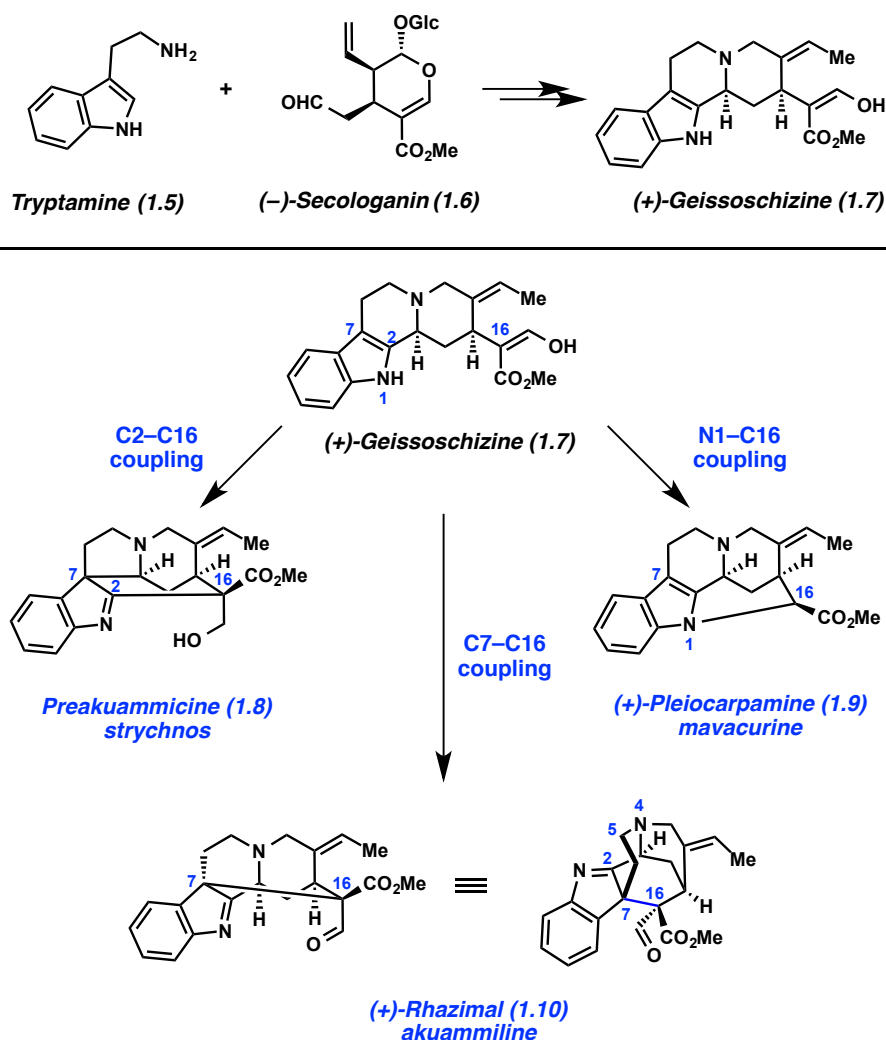
(-)-Aspidophylline A (1.4)
(2007)

reverses drug resistance
in cancer cells

As is apparent from the representative family members shown in Figure 1.1, there is a great deal of complexity and structural diversity amongst the >30 akuammiline alkaloids that have been isolated to date.¹ Although detailed biosynthetic studies have not been performed, the

proposed biogenesis of various akuammilines sheds light on how nature likely assembles these intricate scaffolds. As shown in Figure 1.2, the union of tryptamine (**1.5**) and the monoterpeneoid secologanin (**1.6**) first results in the formation of the natural product geissoschizine (**1.7**). In turn, **1.7** serves as the progenitor to many different alkaloid frameworks including the strychnos, mavacurine, and akuammiline varieties.¹⁰ For example, the strychnos alkaloid preakuammicine (**1.8**) would arise from a cyclization between C2 and C16, whereas the mavacurine alkaloid pleiocarpamine (**1.9**) stems from a cyclization between N1 and C16. The akuammiline framework, on the other hand, derives from an intramolecular oxidative coupling between C7 and C16 of geissoschizine (**1.7**). This constructs the caged indolenine framework of rhazimal (**1.10**).¹¹

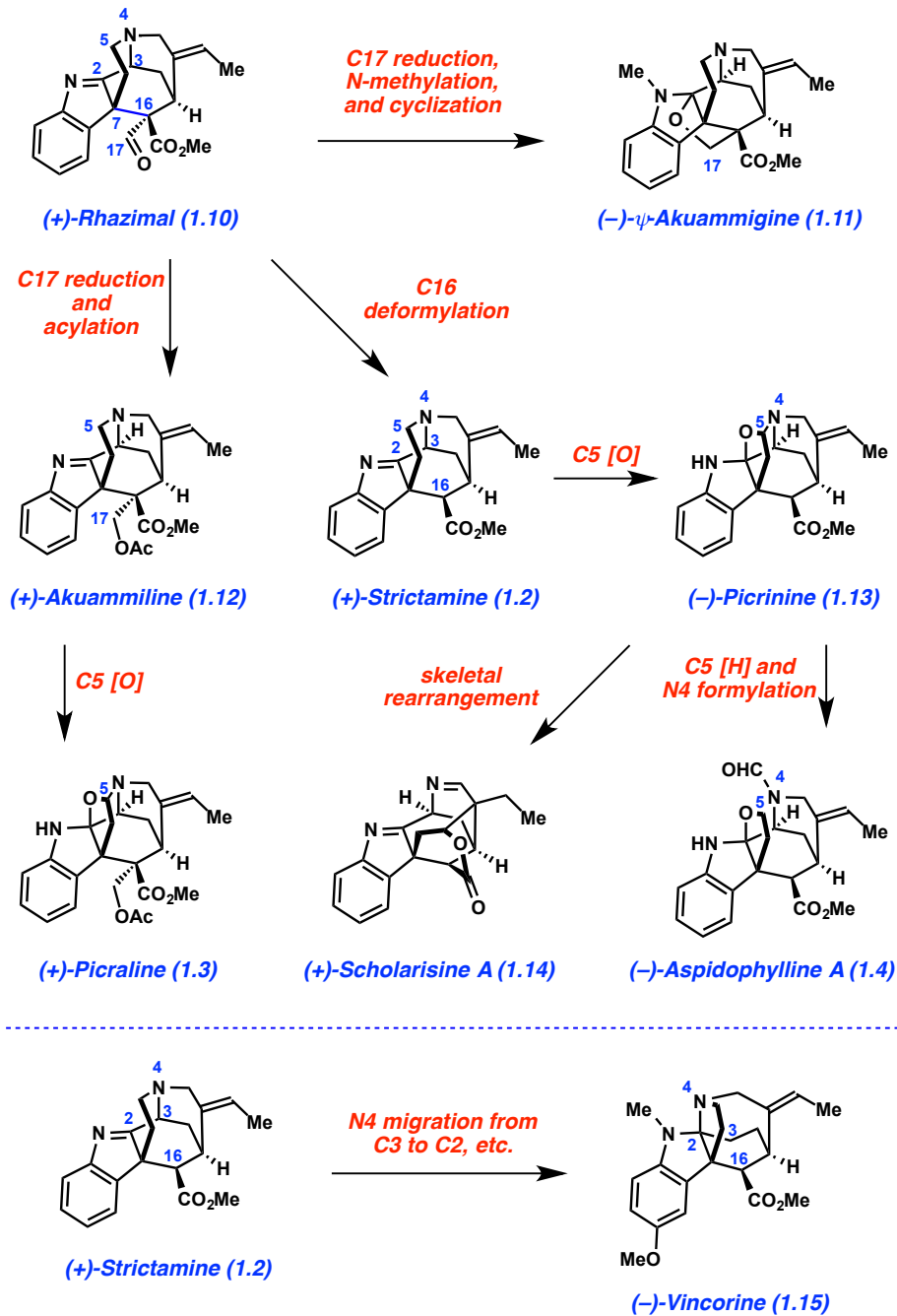
Figure 1.2 Proposed biosynthesis of several monoterpene indole alkaloid classes.



The polycyclic natural product rhazimal (**1.10**) is thought to serve as a molecular platform to access to all the other akuammiline family members through redox transformations, acylations, alkylations or skeletal migrations (Scheme 1.1). For example, pseudoakuammigine (**1.11**)^[12] is thought to arise from aldehyde reduction, *N*-methylation, and tetrahydrofuran ring formation from **1.10**. Alternatively, akuammiline (**1.12**),¹² the namesake of the family, forms from reduction and acylation of the C17 carbonyl. Strictamine (**1.2**), on the other hand, forms from C16 deformylation.⁵ Oxidation of akuammiline (**1.12**) at C5 would provide picraline

(**1.3**),^{7,7b} while the analogous transformation from **1.2** would yield picrinine (**1.13**).¹³ Both scholarisine A (**1.14**) and aspidophylline A (**1.4**) are believed to arise from picrinine (**1.13**). Aspidophylline A (**1.4**)⁹ could be generated by reduction at C5 and N4 formylation, whereas scholarisine A (**1.14**) is proposed to come from a redox isomerization and skeletal reconfiguration.¹⁴ Finally, the pyrrolidinoindoline scaffold of vincorine (**1.15**)¹⁵ is thought to stem from strictamine (**1.2**) via N4 migration from C3 to C2.⁵

Scheme 1.1 Divergent biosynthetic relationship of the akuammiline alkaloids.



Research concerning the akuammilines has historically focused on isolation and pharmacological studies^{1a} with relatively less emphasis on synthetic chemistry. However, synthetic studies by Dolby in the 1970's brought some attention to the akuammilines and

provided some noteworthy lessons on synthetic strategies for accessing these challenging natural products.¹⁶ Since then, many research groups have reported promising strategies toward the akuammilines, including those of Sakai,¹⁷ Toupet,¹⁸ Bosch,¹⁹ Takemoto,²⁰ Higuchi,²¹ Shi,²² and Zhu.²³

Although many akuammiline alkaloids have yet to succumb to laboratory synthesis, synthetic efforts spanning the past 6 years have led to the completed total synthesis of four daunting akuammilines: vincorine (**1.15**),^{24,25,26} aspidophylline A (**1.4**),^{27,28,29} picrinine (**1.13**),³⁰ and scholarisine A (**1.14**).^{31,32} Although the synthetic routes towards these alkaloids contain a variety of creative elements, one unifying theme is their utilization of innovative cascade reactions to elegantly and efficiently forge their intricate architectures. This chapter provides a perspective on the key transformations that construct multiple chemical bonds in one process, and how these cascades have fueled achievements in akuammiline total synthesis. Additionally, other important bond formations are highlighted, specifically those that played instrumental roles in enabling the completed syntheses.

1.3 Total Syntheses of Vincorine

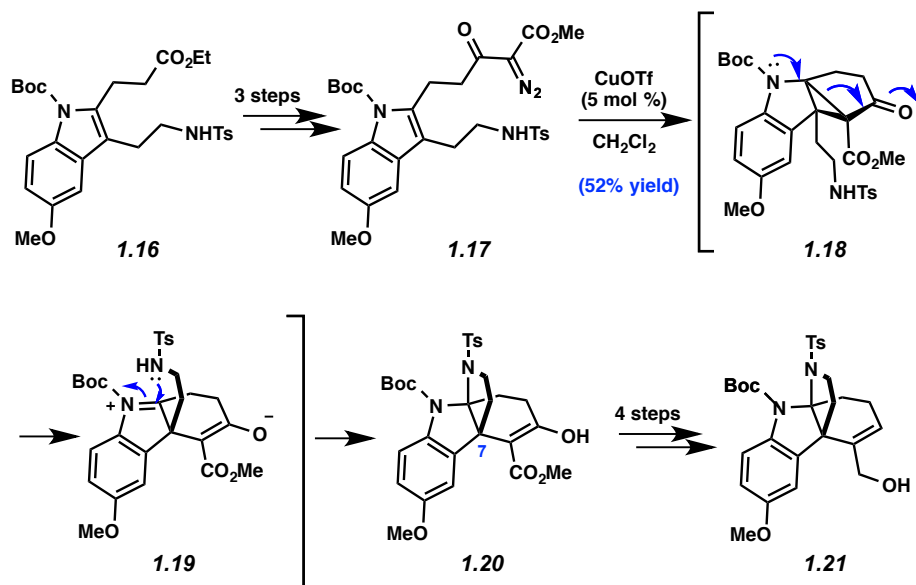
(-)-Vincorine (**1.15**, Scheme 1.1) was first isolated in 1962 from *Vinca minor* by Šefčovič and co-workers.¹⁵ As mentioned above, this alkaloid contains a pyrrolidinoindoline core that arises from a nitrogen migration within the parent akuammiline architecture. This migration results in a pentacyclic scaffold that includes one seven-membered ring and four contiguous stereocenters, one of which is quaternary. This section highlights the three completed total syntheses of **1.15** that have been reported to date by the groups of Qin,²⁴ Ma,²⁵ and MacMillan.²⁶

1.3.1 Qin's Cyclopropanation Approach

The first breakthrough in the total synthesis of akuammilines came from Qin and co-workers, who reported the total synthesis of (\pm)-vincorine (**1.15**) in 2009.²⁴ The Qin group targeted two key challenges: assembly of the cyclohexyl-fused pyrrolidinoindoline framework and construction of the seven-membered ring. To address the former difficulty, Qin and co-workers employed an elegant cyclopropanation/fragmentation cascade sequence, which had earlier proven useful in their synthesis of the *strychnos* alkaloid minfiensine.³³

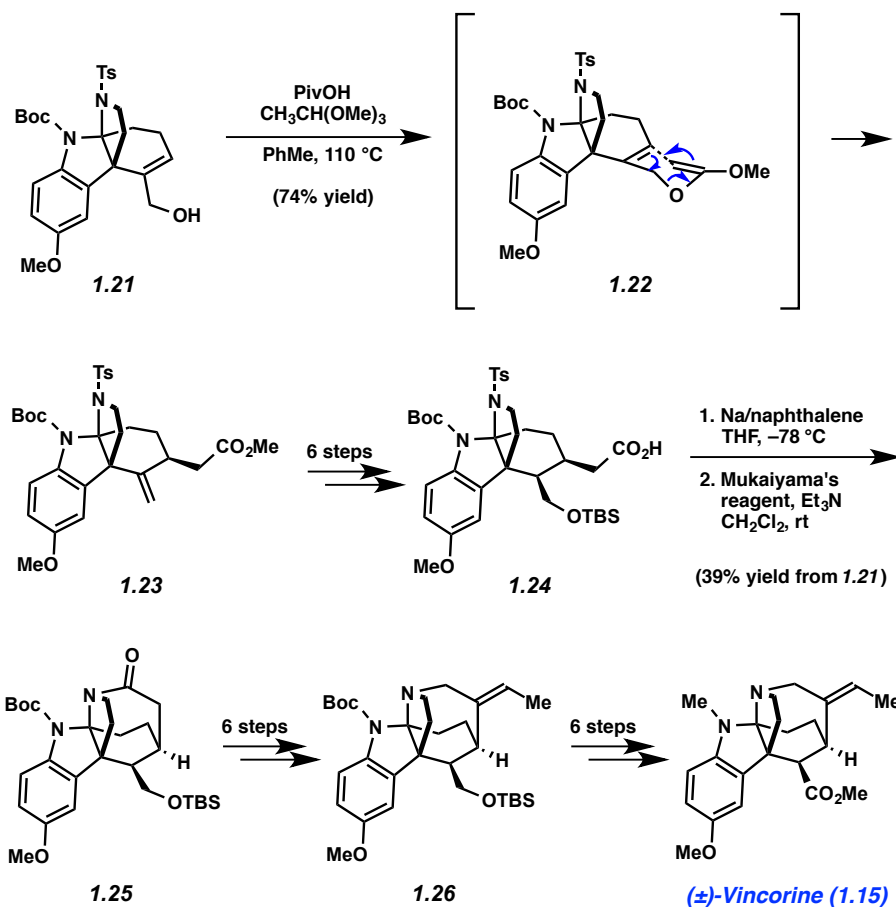
As depicted in Scheme 1.2, a three-step sequence was used to convert ester **1.16**, a readily available intermediate,³⁴ to α -diazoester **1.17**, the substrate for the key cascade reaction. Using 5 mol% of copper(I) triflate, α -diazoester **1.17** underwent the desired cyclopropanation/fragmentation sequence to furnish tetracycle **1.20** in 52% yield. The transformation is thought to proceed by initial cyclopropanation of the indole moiety. Subsequent fragmentation of the cyclopropane (transition structure **1.18**) to the corresponding indoleninium species presumably occurs rapidly by virtue of the indoline nitrogen. Subsequent trapping by the tosyl-protected amine (transition structure **1.19**) then delivers the tetracyclic product. Notably, this cascade reaction concisely builds one carbon–nitrogen bond and one carbon–carbon bond. Moreover, the key C7 quaternary stereocenter is introduced, in addition to the pyrrolidinoindoline scaffold. From tetracycle **1.20**, four steps were used to access allylic alcohol **1.21**.

Scheme 1.2 Qin's key cyclopropanation step to construct **1.21**.



An abbreviated sequence illustrating the endgame to Qin's synthesis of (\pm)-vincorine (**1.15**) is shown in Scheme 1.3. Upon treatment with pivalic acid and trimethyl orthoacetate, alcohol **1.21** was converted into ester **1.23** in a 74% yield of the desired diastereomer, via a Johnson–Claisen rearrangement (transition structure **1.22**).³⁵ Ester **1.23** was elaborated in six steps to acid **1.24**, an important precursor towards constructing the natural product's seven-membered ring. The tosyl protecting group on the fused pyrrolidine was removed with Na/naphthalene, which set the stage for amide bond formation using Mukaiyama's reagent. Impressively, amide **1.25** was accessed in 39% yield from alcohol **1.21** (nine steps). Further manipulation provided silyl ether **1.26** over six steps, which included introduction of the exocyclic olefin. A final six-step sequence was used to convert silyl ether **1.26** to (\pm)-vincorine (**1.15**) via deprotection and redox manipulations of the alcohol, and a deprotection and *N*-methylation of the indole nitrogen.

Scheme 1.3 Qin's synthetic endgame and completion of (\pm)-vincorine (**1.15**).



Qin's synthesis of (\pm)-vincorine (**1.15**) proceeded in 31 steps from known intermediate **1.16**, in roughly 1% overall yield. Of note, this was the first reported total synthesis of any akuammiline alkaloid, which marked a major achievement in the field. Qin's approach relied on intermediate tetracycle **1.20**, which was synthesized using a copper-catalyzed cyclopropanation/fragmentation cascade. This sequence built an important quaternary center, part of the compound's distinct fused pyrrolidinoindoline scaffold. Qin's efforts toward (\pm)-vincorine (**1.15**) also served to reveal the many challenges associated with assembling the natural product's core, such as constructing the seven-membered ring of the natural product. These

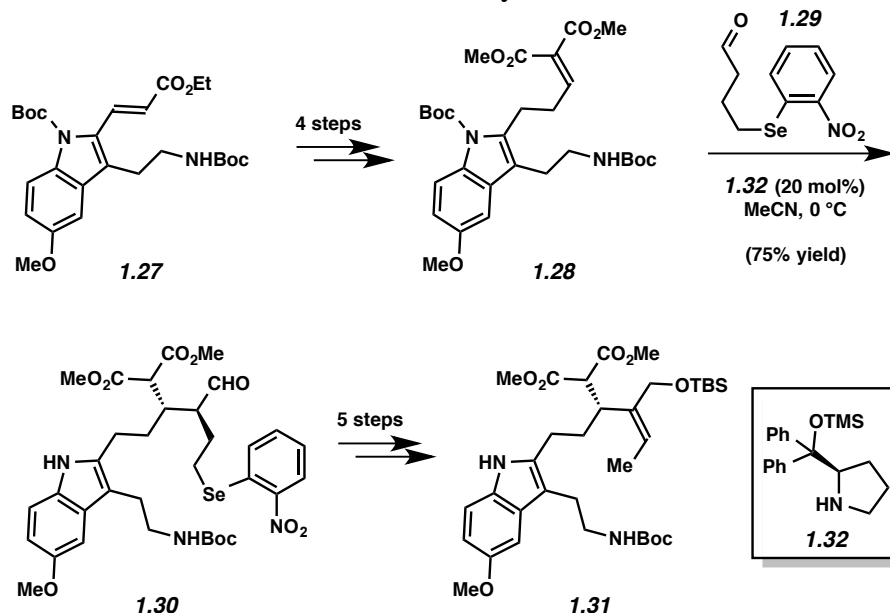
seminal studies provided significant groundwork for future syntheses of vincorine (**1.15**) and other akuammiline alkaloids.

1.3.2 Ma's Oxidative Coupling Approach

In 2012, Ma and co-workers reported the first enantioselective synthesis of (–)-vincorine (**1.15**).²⁵ Similar to the approach of Qin, Ma elected to forge the pyrrolidinoindoline scaffold early in the synthesis. Ma's approach utilizes a bioinspired intramolecular oxidative coupling to introduce all of the requisite carbon atoms of the natural product, prior to building the seven-membered ring. It should be noted that the Ma laboratory had previously developed a similar oxidative coupling strategy for their enantioselective synthesis of communesin F.³⁶

Ma's synthesis of the key oxidative cyclization precursor, diester **1.31**, is summarized in Scheme 1.4. α,β -Unsaturated ester **1.27**, an intermediate readily accessed from tryptophan, was elaborated to malonate **1.28** in four steps. Toward installing the ethylidene unit, the Ma laboratory implemented an organocatalyzed enantioselective Michael addition of **1.29** using a proline-derived catalyst on the basis of precedent.³⁷ Although both aldehyde **1.29** and malonate **1.28** were both more complex than substrates reported in the literature, the desired coupling proceeded smoothly to deliver selenide **1.30** in 75% yield as a 5:1 diastereomeric mixture. Selenide **1.30** was then converted to the oxidative intramolecular coupling substrate **1.31** over a five-step sequence.

Scheme 1.4 Ma's enantioselective synthesis of intermediate **1.31**.

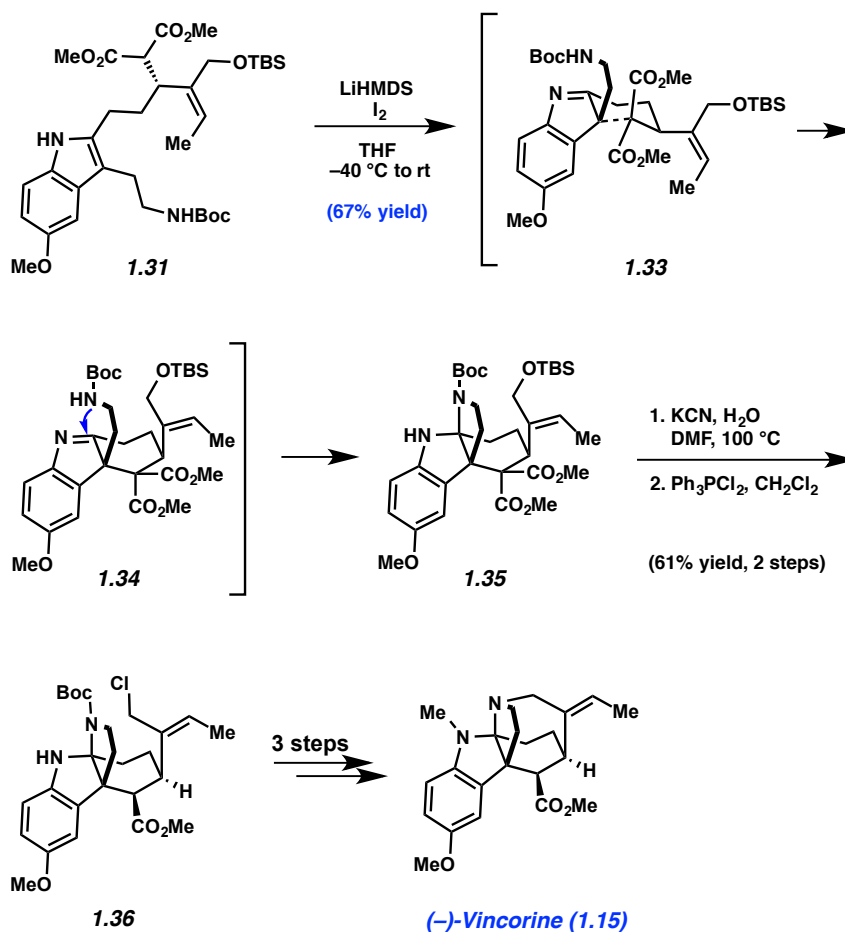


Having established an efficient synthesis of diester **1.31**, the focus turned to forming the fused pyrrolidinoindoline core of the natural product. As shown in Scheme 1.5, diester **1.31** underwent oxidative cyclization in the presence of two equivalents of lithium hexamethyldisilazide (LiHMDS) and a solution of iodine to give indoline **1.35**. This key cascade sequence presumably proceeds through formation of tricyclic indolenine intermediate, followed by subsequent trapping by the Boc-protected amine (see transition structure **1.34**). The stereochemical outcome of this transformation can be attributed to the chair-like transition structure **1.33** shown in Scheme 1.5. In this orientation, the axial ester avoids repulsive interactions with the indole moiety, thus resulting in the desired stereochemical outcome. It should be noted that initial attempts at $-78\text{ }^{\circ}\text{C}$ gave minor amounts of the desired indoline **1.35**, but when the reaction was started at $-40\text{ }^{\circ}\text{C}$ and allowed to warm to room temperature, the yield improved to an impressive 67%. Starting the reaction at a higher temperature did not improve the yield. It should also be noted that the use of other oxidants such as Fe(III) salts, Cu(II) salts, or

N-iodosuccinimide in place of iodine,³⁸ had detrimental effects on the reaction. Nonetheless, this bioinspired cascade transformation resulted in the construction of the key C7 quaternary center and three of the natural product's four stereogenic centers. In addition, the oxidative coupling was highly diastereoselective, translating the stereoselectivity of the organocatalyzed Michael addition into the enantioenriched pyrrolidinoindoline product.

To complete the total synthesis, Krapcho decarboxylation³⁹ of diester **1.35**, followed by treatment with triphenylphosphine dichloride⁴⁰ delivered alkyl chloride **1.36** in 61% yield over two steps. This intermediate was then quickly elaborated to (–)-vincorine (**1.15**) after a final three-step sequence involving deprotection, cyclization to forge the seven-membered ring, and methylation.

Scheme 1.5 Ma's oxidative cyclization and completion of (–)-vincorine (**1.15**).



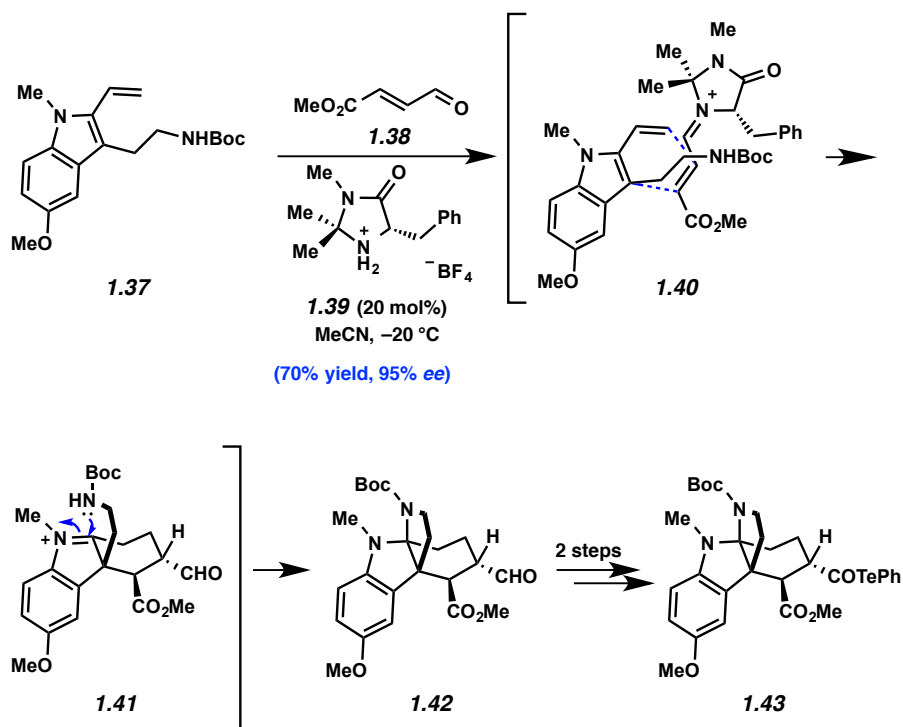
Ma's total synthesis of (–)-vincorine (**1.15**) stands as the first asymmetric route to this complex natural product. A key feature of the synthesis is the use of an oxidative cyclization to construct the quaternary center of **1.15** and two of its complex rings. Of note, this cascade also builds the compound's carbon framework, which greatly facilitated late-stage transformations. Ma's approach to (–)-vincorine (**1.15**) proceeds in 18 steps from commercially available starting materials in a striking overall yield of 5%.

1.3.3 MacMillan's Organocatalytic Approach

Most recently, the MacMillan laboratory successfully completed a concise enantioselective total synthesis of (–)-vincorine (**1.15**).²⁶ Similar to the overall bond construction strategy pursued by the Qin and Ma laboratories, MacMillan opted to first assemble the pyrrolidinoindoline framework of the natural product, before building the seven-membered ring. However, in the interest of creating a general strategy toward (–)-vincorine (**1.15**) and related natural products, MacMillan and co-workers designed an enantioselective organocatalytic Diels–Alder/iminium ion cyclization cascade sequence⁴¹ to construct the fused pyrrolidinoindoline tetracyclic core, which, in turn, enabled the efficient introduction of the seven-membered ring.

The details of the key cascade reaction are presented in Scheme 1.6. Vinyl tryptamine **1.37**, a readily accessible intermediate from 5-methoxy-*N'*-Boc tryptamine, was combined with enal **1.38** and treated with catalyst **1.39** at –20 °C to afford tetracycle **1.42** in 70% yield and 95% *ee*. It is proposed that the activated iminium species approaches the vinyl tryptamine as depicted in transition structure **1.40** in an *endo* fashion with the facial selectivity controlled by the catalyst's steric environment. Following tandem catalyst dissociation and acid-promoted protonation, an indoleninium is formed. Trapping of this ion by the tethered carbamate (see transition structure **1.41**) afforded the tetracyclic product **1.42**. It should be emphasized that this remarkable cascade reaction establishes the relative and absolute configuration of four stereocenters, three of which reside in the natural products' architecture. From there, tetracycle **1.42** was transformed to telluride **1.43** over two steps in preparation of constructing the seven-membered ring.

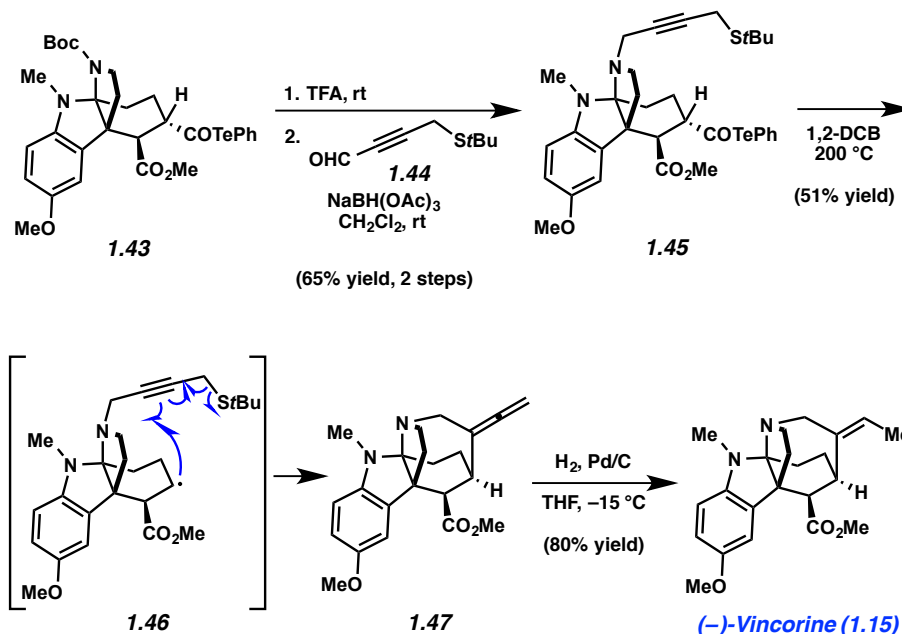
Scheme 1.6 MacMillan's key cascade transformation.



The elaboration of telluride **1.43** to the natural product is depicted in Scheme 1.7. Removal of the *N*-Boc group was effected with TFA and the resultant pyrrolidine nitrogen was alkylated under reductive amination conditions with aldehyde **1.44** to furnish **1.45** in 65% yield over two steps. Upon heating this substrate to $200\text{ }^{\circ}\text{C}$ for 10 h, the desired 7-*exo*-dig cyclization (see transition structure **1.46**) took place, furnishing the exocyclic allene product **1.47**.⁴² The authors propose that homolysis of the C–Te bond leads to extrusion of carbon monoxide and formation of a putative secondary radical. This radical is then poised to undergo the desired cyclization with the pendant π -acceptor to form the final ring system of the natural product. The authors noted that the corresponding transformation was less effective using other radical precursors, such as thiohydroxamic acids and acyl selenides, under a variety of radical initiation conditions. Nonetheless, the successful conversion of **1.43** to **1.45** represents the first example of

an acyl telluride being used as an alkyl radical precursor, and provides a bold and creative solution to the formation of the challenging seven-membered ring. With intermediate **1.47** in hand, selective hydrogenation of the allene terminus delivered (–)-vincorine (**1.15**) in 80% yield.

Scheme 1.7 MacMillan’s radical cyclization and completion of (–)-vincorine (**1.15**).



MacMillan’s synthesis of (–)-vincorine, which is just nine steps beginning from commercially available starting materials, is the most concise route to **1.15** reported to date. Furthermore, it proceeds in the highest overall yield, which is an impressive 9%. The brevity of the synthesis can be attributed to the elegant cascade reaction employed: the enantioselective organocatalytic Diels–Alder/iminium ion cyclization, which generates almost all of the natural product’s framework with control of relative and absolute stereochemistry. This reaction is a testament to the power of asymmetric organocatalysis for the generation of high molecular complexity in a single synthetic step from achiral starting materials.

1.4 Total Syntheses of Aspidophylline A and Picrinine

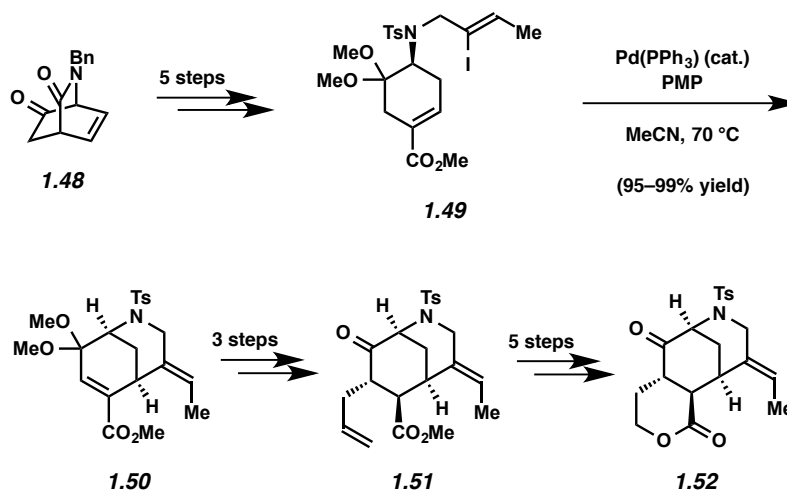
The akuammiline alkaloids aspidophylline A (**1.4**) and picrinine (**1.13**) were isolated in 2007⁹ and 1965,²⁷ respectively (Scheme 1.1). Aspidophylline A (**1.4**) was found to reverse drug resistance in cancer cells, while picrinine (**1.13**) has been shown to have mild analgesic activity.^[43] Each natural product contains a furoindoline motif embedded within a polycyclic framework. Additionally, both compounds contain multiple stereogenic centers, including quaternary centers at C7, thus rendering them daunting synthetic targets. This section includes a summary of total syntheses of aspidophylline A (**1.4**) reported by Garg,²⁷ Zhu,²⁸ and Ma,²⁹ as well as the total synthesis of picrinine (**1.13**).³⁰

1.4.1 Garg's Interrupted Fischer Approach

In 2011, the Garg laboratory reported the first synthesis of aspidophylline A (**1.4**), which was carried out in racemic form.²⁷ Central to their strategy for building the pentacyclic framework of the natural product was the construction of the fused indoline moiety through an interrupted Fischer indolization cascade reaction.⁴⁴ Of note, the authors were able to execute this challenging approach at a late stage in the total synthesis.

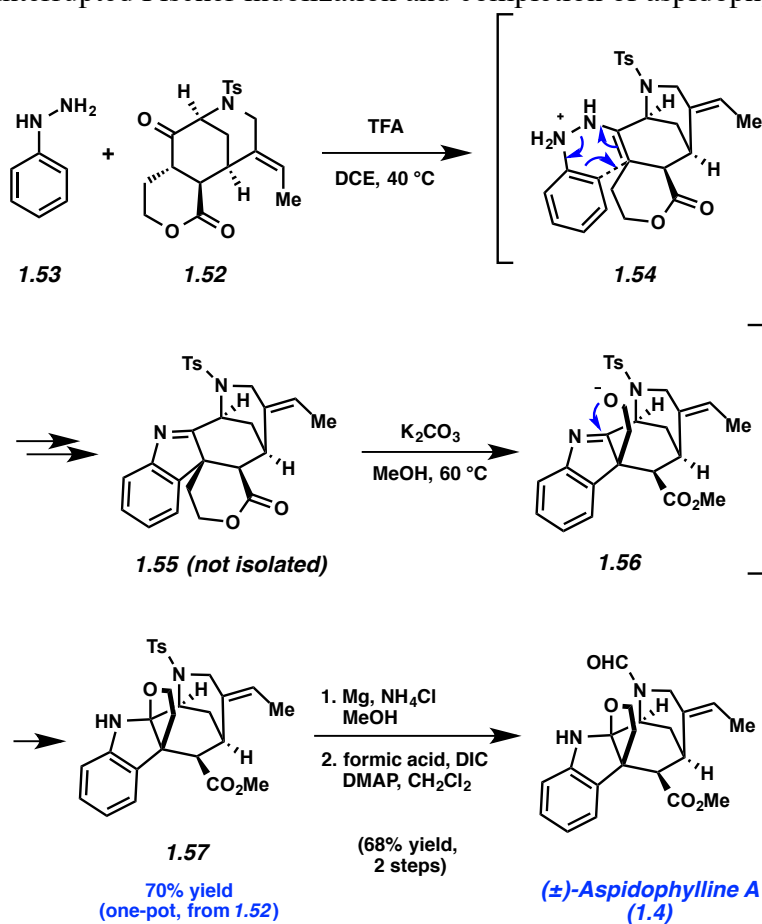
The synthesis of the substrate for the aforementioned cascade reaction is illustrated in Scheme 1.8. [2.2.2]-bicyclic lactam **1.48** was elaborated over five steps to vinyl iodide **1.49**, which, upon treatment with palladium (0) and pentamethylpiperidine, cleanly underwent a regioselective Heck cyclization⁴⁵ to forge the [3.3.1]-azabicyclic and furnish **1.50** in excellent yield. Next, in a series of transformations, [3.3.1]-azabicyclic **1.50** was converted to hydroxy ester **1.51** in three steps, which was subsequently carried forward to tricyclic lactone **1.52** in five steps.

Scheme 1.8 Garg's synthesis of lactone **1.52**.



As previously mentioned, tricyclic lactone **1.52** was identified as a suitable substrate for the key intended interrupted Fischer indolization cascade reaction, the details of which are shown in Scheme 1.9. Tricyclic lactone **1.52** was treated with phenylhydrazine (**1.53**) and trifluoroacetic acid in dichloroethane at 40 °C. The resulting ene-hydrazine underwent a charge-accelerated [3,3]-sigmatropic rearrangement (see transition structure **1.54**) and subsequent ammonia extrusion to furnish indolenine **1.55**. This intermediate was not isolated, but rather was subjected to base-promoted methanolysis to generate an alkoxide intermediate. In situ cyclization (see transition structure **1.56**) gave **1.57** in 70% yield, which contains the pentacyclic framework of (±)-aspidothylline A (**1.4**). Notably, this cascade reaction assembles two new C–heteroatom bonds, one new C–C bond, and one quaternary center, and also proceeds with complete diastereoselectivity. Following construction of pentacycle **1.57**, removal of the tosyl protecting group and *N*-formylation delivered (±)-aspidothylline A (**1.4**).

Scheme 1.9 Interrupted Fischer indolization and completion of aspidophylline A (**1.4**).



Garg's synthesis of (±)-aspidophylline A (**1.4**) marked the second total synthesis of any akuammiline alkaloid, preceded only by Qin's synthesis of (±)-vincorine (**1.15**). The synthesis proceeds in 7.5% overall yield, and requires 20 steps from commercially available starting materials. In particular, the hallmark of the synthesis is the use of the interrupted Fischer indolization cascade at a late stage to assemble the compound's complex pentacyclic architecture and introduce two stereogenic centers. This late-stage reaction demonstrates the efficiency of cascade reactions for swiftly generating and manipulating high molecular complexity, while also highlighting the virtues of the venerable Fischer indolization reaction.

1.4.2 Garg's Synthesis of Picrinine

The details of this synthesis are the main subject matter of Chapters 2 and 3 of this dissertation. An account of Garg's synthetic efforts towards picrinine (**1.13**) can be found in these respective sections.

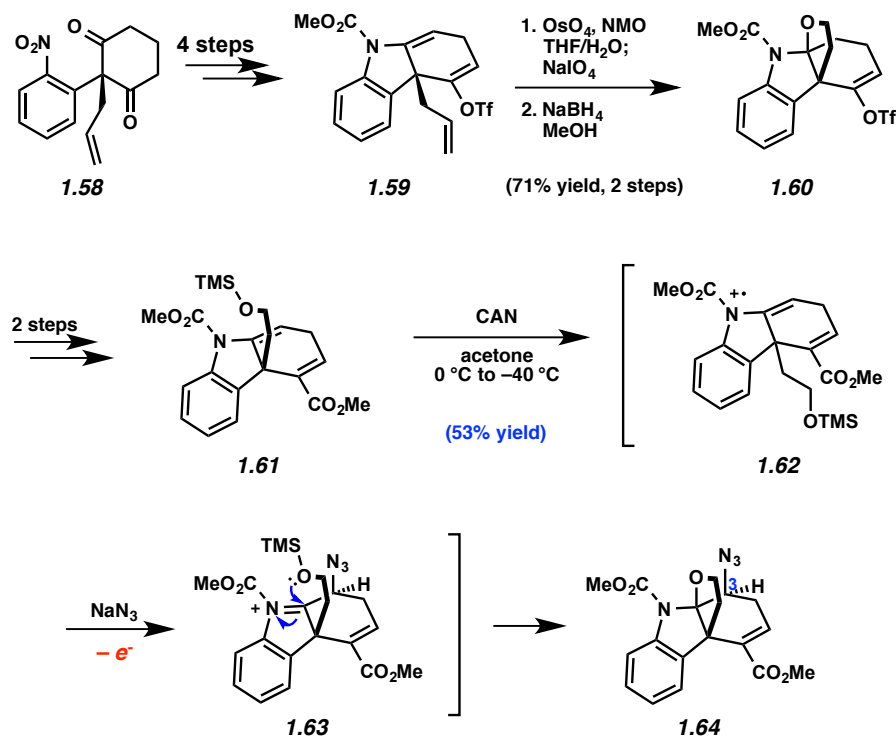
1.4.3 Zhu's Oxidative Azidoalkoxylation Approach

Earlier this year, Zhu and co-workers reported the second synthesis of (\pm)-aspidophylline A (**1.4**).²⁸ Zhu's synthesis hinged upon an oxidative azidoalkoxylation reaction⁴⁶ to install N2 of the alkaloid's scaffold while concurrently establishing the furoindoline moiety.⁴⁷ This contrasted with Garg's strategy described earlier, where installation of the [3.3.1]-azabicyclic was accomplished early in the synthesis, followed by late-stage introduction of the furoindoline.

As shown in Scheme 1.10, Zhu's synthesis commenced from readily available cyclohexanedione **1.58**,⁴⁸ which was elaborated to tricycle **1.59** through a triflation,⁴⁹ reduction,⁵⁰ and carbamoylation sequence. Next, chemoselective oxidation of the terminal olefin with osmium tetroxide and sodium periodate,⁵¹ followed by sodium borohydride reduction, provided furoindoline **1.60** in 71% yield over two steps. This intermediate was then elaborated to silyl ether **1.61**, the substrate for the key oxidative cyclization cascade. In the event, treatment of silyl ether **1.61** with ceric ammonium nitrate and sodium azide in acetone delivered azidofuroindoline **1.64** in 53% yield. Mechanistically, it is thought that ceric ammonium nitrate serves as a mild oxidant to first promote single electron transfer and putatively form radical cation **1.62**. Then, this radical cation is trapped by azide, with tandem loss of another electron, to afford an indoleninium species, which undergoes in situ cyclization (see transition structure **1.63**). This umpolung cascade transformation efficiently forges the tetracyclic furoindoline core of the

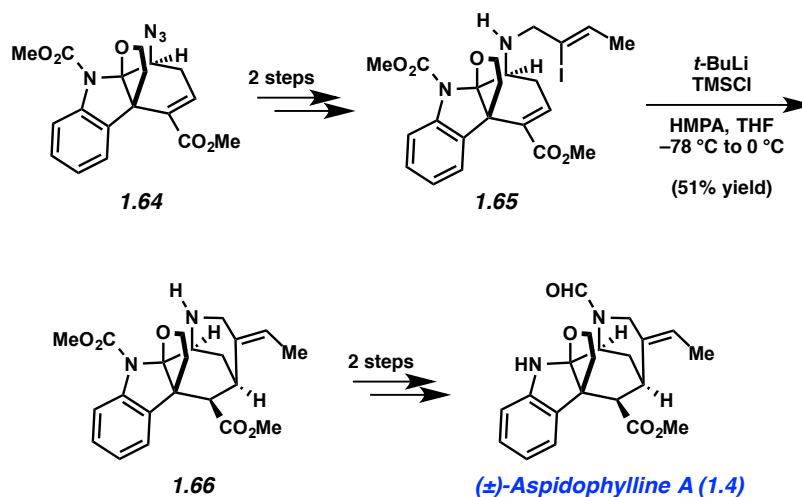
natural product. Additionally, it successfully installs three contiguous stereocenters and the important nitrogen substituent at C3 of the natural product.

Scheme 1.10 Zhu's oxidative key azidoalkoxylation transformation.



The remainder of Zhu's synthesis is depicted in Scheme 1.11. In a two-step azide reduction and alkylation sequence,⁵² furoindoline **1.64** was elaborated to iodide **1.65**. Iodide **1.65** was the utilized as the substrate for a challenging intramolecular Michael addition into the embedded enoate. After much optimization, the authors found that treatment of **1.65** with *t*-BuLi and TMSCl in HMPA and THF at low temperature delivered adduct **1.66** in 51% yield, thus forging the pentacyclic scaffold of the natural product.⁵³ Subsequent formylation and cleavage of the methyl carbamate delivered (\pm)-aspidophylline A (**1.4**).

Scheme 1.11 Zhu's completion of (\pm)-aspidothylline A (**1.4**).



Zhu's impressive total synthesis of (\pm)-**1.4** proceeds in just 14 steps from known cyclohexanedione **1.58**. The key oxidative azidoalkoxylation cascade reaction employed in the synthesis provides an elegant means to construct the natural product's densely substituted cyclohexane ring. Additionally, Zhu's swift approach demonstrates the enabling power of umpolung reactivity as a functionalization strategy in complex molecule synthesis.

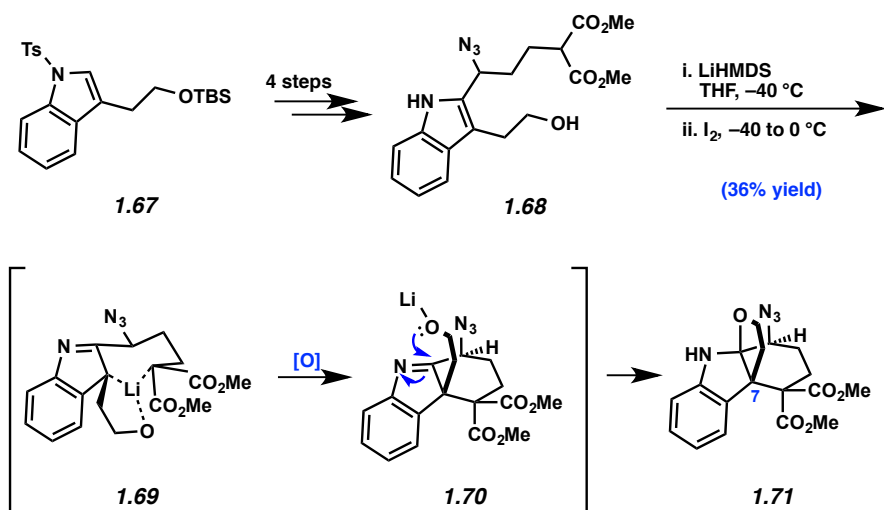
1.4.4 Ma's Oxidative Coupling Approach

Very recently, Ma and co-workers were also successful in completing a total synthesis of (\pm)-aspidothylline A (**1.4**).²⁹ Similar to their completed synthesis of (–)-vincorine (**1.15**), the authors sought to employ an intramolecular oxidative coupling³⁶ to build the core tetracyclic furoindoline scaffold of the natural product. Then, analogous to the overall strategy executed by Zhu, Ma envisioned construction of the piperidine ring through a late-stage cyclization strategy.

The synthesis began by elaborating indole **1.67** to azide **1.68**, which was the substrate for the key intermolecular oxidative coupling cascade reaction (Scheme 1.12). Although the

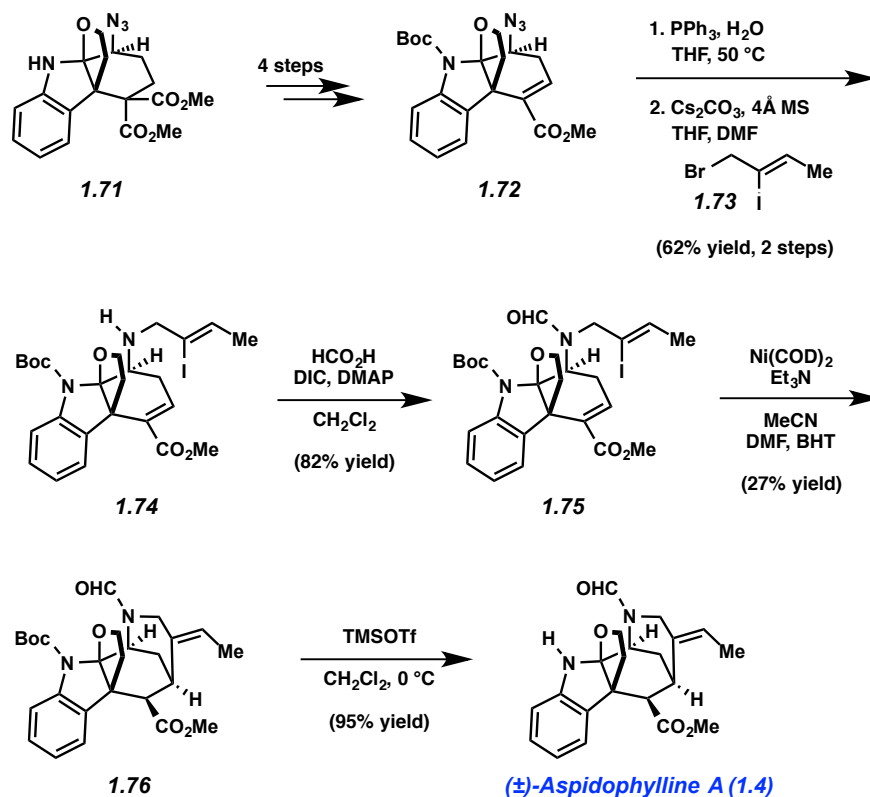
substrate for this coupling appeared less complex than the coupling substrate in the authors' synthesis of vincorine, the transformation proved to be quite challenging.⁵⁴ After optimization, it was discovered that treatment of **1.68** with LHMDS in THF at $-40\text{ }^{\circ}\text{C}$ promoted formation of the putative lithium complex **1.69**. Quenching with iodine and warming to $0\text{ }^{\circ}\text{C}$ led to oxidative C–C bond formation, thus furnishing an indolenine intermediate. In turn, this underwent in situ imine trapping (see transition structure **1.70**) to deliver furoindoline **1.71** in 36% yield. Ma and co-workers noted that the addition of additives to this reaction, such as HMPA, resulted mostly in oxidative coupling of the diester to the indole nitrogen, presumably as a result of HMPA disrupting the formation of complex **1.69**. Although the oxidative coupling was not as high yielding as the analogous reaction in Ma's vincorine synthesis, the transformation is quite impressive in that it provides the furoindoline scaffold of the natural product, with three contiguous stereocenters including the quaternary center at C7.

Scheme 1.12 Ma's key oxidative coupling to forge furoindoline **1.71**.



Ma's synthetic endgame is shown in Scheme 1.13. Furoindoline **1.71** was converted to tetracyclic enoate **1.72** through a protection, decarboxylation, and oxidation sequence. Similar to the approach taken by Zhu, vinyl iodide **1.74** was synthesized from enoate **1.72** in two steps including Staudinger reduction and alkylation with bromide **1.73**. Next, formylation of the secondary nitrogen with formic acid and *N,N'*-diisopropylcarbodiimide delivered formamide **1.75**. Following this acylation event, cyclization of the iodide with the pendant enoate was mediated by Ni(COD)₂ in the presence of triethylamine and BHT to deliver pentacycle **1.76** in 27% yield.⁵⁵ Following this difficult cyclization, cleavage of the Boc group was achieved in nearly quantitative yield to afford (±)-aspidothylline A (**1.4**).

Scheme 1.13 Ma's completion of (±)-aspidothylline A (**1.4**).



Ma's total synthesis of (\pm)-aspidophylline A (**1.4**) requires only 15 steps. Critical to the brevity of the synthesis is the use of an innovative intramolecular oxidative cascade coupling to rapidly assemble the furoindoline core of the natural product. This unique strategy, along with the concise construction of the piperidine ring, provides useful synthetic tools that should prove useful in assembling other complex molecules.

1.5 Total Syntheses of Scholarisine A

The natural product scholarisine A (**1.14**) is one of the most recently discovered akuammilines. Reported in 2008, Luo and co-workers isolated **1.14** from the tree *Alstonia scholaris*.¹⁴ Scholarisine A (**1.14**) contains a rearranged akuammiline skeleton with six fused rings and six stereogenic centers, including two quaternary centers. In addition, its unusual [2.2.2]-bicyclic lactone moiety provides a unique synthetic challenge in akuammiline alkaloid total synthesis. The valiant efforts of the Smith³¹ and Snyder³² laboratories have recently led to two completed total syntheses, both of which harness the power of cascade reactions to access **1.14**.

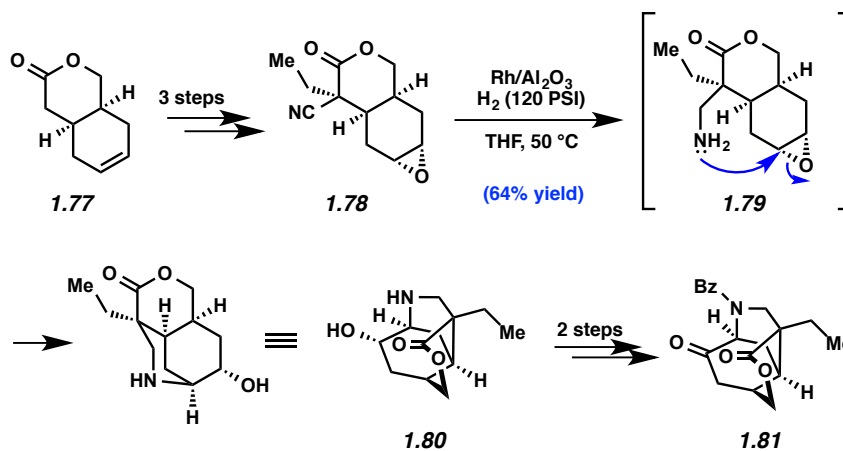
1.5.1 Smith's Reductive Cyclization Approach

In 2012, the Smith laboratory reported the first total synthesis of (+)-scholarisine A (**1.14**).³¹ Their route relied on the use of a reductive cyclization cascade to introduce three rings of the natural product. In addition, the authors utilized a late-stage Fischer indolization reaction to install the indole nucleus en route to forging the [2.2.2]-bicyclic lactone of the natural product.

The synthesis of ketone **1.81** is depicted in Scheme 1.14. Lactone **1.77**, a known compound synthesized from commercially available cis-4-cyclohexene-1,2-dicarboxylic

anhydride,⁵⁶ was elaborated to nitrile **1.78** in three steps. Upon treatment of **1.78** with H₂ and rhodium on alumina, the desired reductive cyclization cascade occurred to deliver tricyclic amine **1.80** in 64% yield. This cascade sequence presumably proceeds via reduction of the nitrile,⁵⁷ followed by intramolecular epoxide opening by the resulting amine.⁵⁸ Of note, the authors observed that this cyclization is the first of its kind and, importantly, forges the [3.3.1]-bicyclic moiety contained within the natural product's structure. In addition, the opening of the epoxide elegantly provided a secondary alcohol functional group handle that could be used to later install the indole nucleus. The authors performed two additional steps to convert amine **1.80** to ketone **1.81**, which involved amine protection and alcohol oxidation.

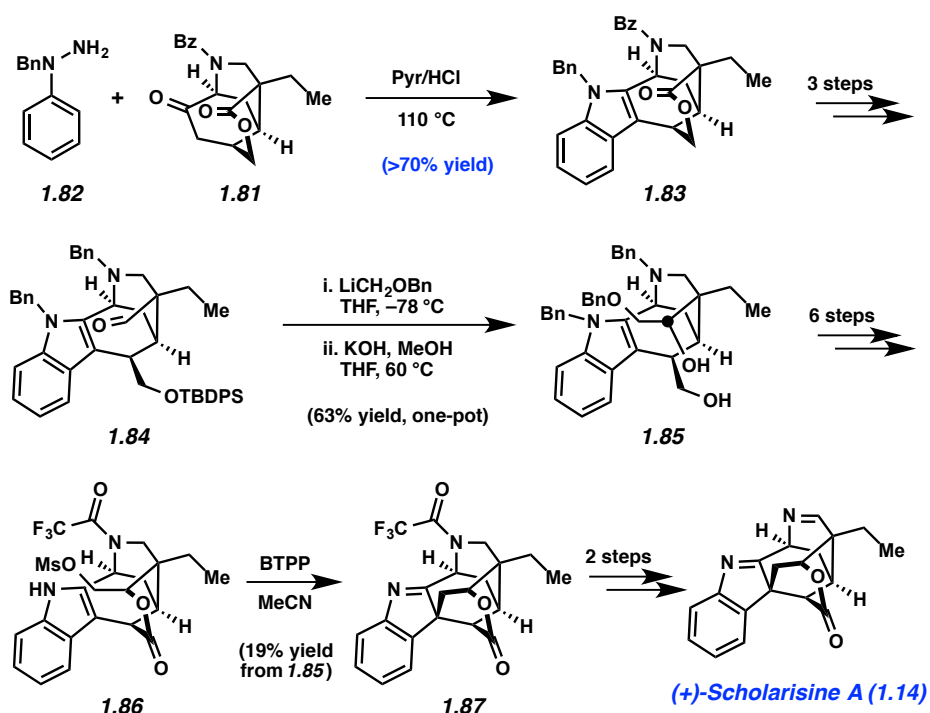
Scheme 1.14 Smith's key reductive cyclization cascade reaction.



The remainder of Smith's synthetic efforts are highlighted in Scheme 1.15. Treatment of ketone **1.81** with benzyl protected phenylhydrazine (**1.82**) and HCl in pyridine⁵⁹ facilitated the key Fischer indolization to provide indole **1.83** in 70% yield. Of note, indole **1.83** possesses most of the scholarisine A framework. A three-step sequence was used to elaborate indole **1.83** to aldehyde **1.84**, which, in turn, was treated with in situ-generated benzyloxy-methyl lithium.⁶⁰

Subsequent base-mediated desilylation in the same pot afforded diol **1.85**. Diol **1.85** was carried forward to mesylate **1.86** over six steps and subjected to *tert*-butyliminotri(pyrrolidino)-phosphorane (BTPP).⁶¹ This resulted in cyclization to provide indolenine **1.87** in 19% yield from diol **1.85**. Indolenine **1.87** was quickly elaborated to (+)-scholarisine A (**1.14**) using a two-step sequence.

Scheme 1.15 Smith's completion of (+)-scholarisine A (**1.14**).



Smith's elegant synthesis of (+)-scholarisine A (**1.14**) marked the first asymmetric synthesis of an akuammiline alkaloid. The longest linear reaction sequence to arrive at the intricate natural product structure is just 20 steps from known lactone **1.77**. A major highlight of the synthesis is Smith's use of a reductive cyclization cascade of nitrile **1.78** to smoothly construct the [3.3.1]-bicycle of the natural product. This key reaction provided the groundwork

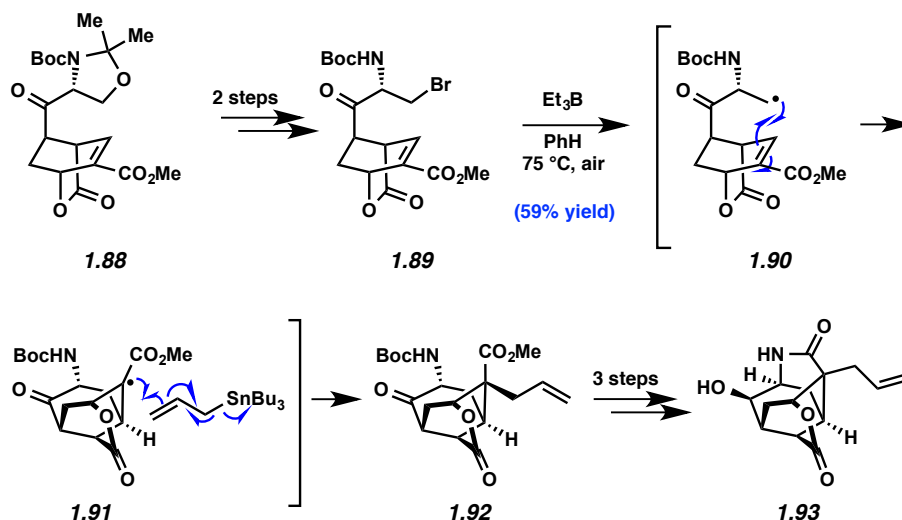
for the late-stage efforts, thus illustrating the importance of cascade reactions not solely for generating complexity, but also for providing properly functionalized synthetic intermediates for subsequent manipulations.

1.5.2 Snyder's Radical Functionalization Approach

The Snyder laboratory reported the most recent synthesis of (+)-scholarisine A (**1.14**) in 2013.³² Their strategy differed greatly from that of Smith's and relied heavily on radical cascade processes to forge the natural product's polycyclic skeleton. In particular, two cascade reactions were utilized to construct the two quaternary centers and, in turn, the important indolenine moiety.

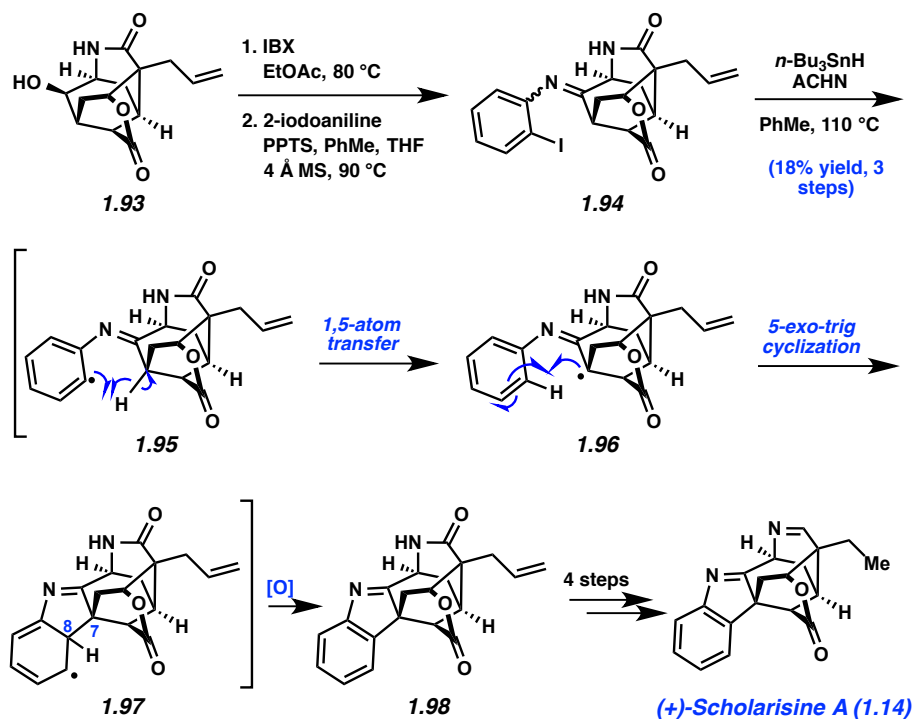
Shown in Scheme 1.16 is the key radical cascade used to construct tetracyclic lactam **1.93**. Starting from bicyclic lactone **1.88**, the substrate for the radical cascade (**1.89**) was synthesized in two steps via an acetonide hydrolysis⁶² and bromination sequence. Subsequent treatment of **1.89** with triethyl borane in the presence of air at 75 °C promoted homolysis of the carbon bromine bond which putatively revealed a primary radical.⁶³ This radical then underwent a 6-exo-trig cyclization (see transition structure **1.90**) resulting in tertiary radical compound **1.91**, which was trapped in situ with allyltributylstannane to give tricycle **1.92** with full diastereoselectivity. Notably, this cyclization/trapping cascade sequence forged two key carbon-carbon bonds with remarkable stereocontrol, and allowed for swift access to the natural product's core. This tricyclic intermediate was further elaborated over three steps to lactam **1.93** through a redox epimerization of the nitrogen substituent and intramolecular amide formation.

Scheme 1.16 Snyder's radical cyclization/Keck allylation cascade.



The construction of tetracyclic lactam **1.93** allowed for the second radical cascade to be executed en route to **1.14**, as shown in Scheme 1.17. First, oxidation of the secondary alcohol gave the corresponding ketone. Subsequent condensation with 2-iodoaniline provided imine **1.94** as a mixture of geometrical isomers. Upon heating **1.94** with tributylstannane and 1,1'-azobis(cyclohexane-carbonitrile) in toluene, the authors obtained indolenine **1.98**⁶⁴ (18% over the three steps from lactam **1.93**). The transformation is thought to proceed by initial homolysis of the C–I bond to give an aryl radical. 1,5-hydrogen atom transfer (see transition structure **1.95**) then yields an isomeric bridgehead radical intermediate. 5-exo-trig homolytic aromatic substitution on the pendant aryl ring, as suggested in transition structure **1.96**, would then forge the C7–C8 linkage and deliver intermediate **1.97**. Oxidation of the cyclohexadienyl radical provides indolenine **1.98**. This key synthetic intermediate was then used to complete the synthesis (+)-scholarisine A (**1.14**).

Scheme 1.17 Snyder's radical C–H activation and completion of (+)-scholarisine A (**1.14**).



Snyder's approach to (+)-scholarisine A (**1.14**) is currently the most concise approach to this complex alkaloid (14 steps). The synthesis was enabled by the daring use of two challenging radical cascades, which highlights their importance and utility in building complex molecular architectures.

1.6 Conclusions

In summary, the akuammiline alkaloid natural products have been the subject of many recent synthetic endeavors, despite being known for many decades. Their intricate structures, along with their promising biological activities, have made them attractive targets amongst the chemical community. Various approaches towards making these natural products have been reported, of which the successful routes are highlighted herein. These successful routes have

utilized cascade reactions to construct the cores of these compounds, demonstrating that these innovative techniques are useful for the construction of exceedingly complex structural manifolds. The collective efforts of the many laboratories involved in this area have not only provided a solid groundwork for making other akuammilines and their derivatives, but has also set the stage for using modern cascade reactions in the synthesis of other intricate molecular scaffolds.

1.7 References

- (1) (a) Ramírez, A.; García–Rubio, S. *Curr. Med. Chem.* **2003**, *10*, 1891–1915. (b) Eckermann, R.; Gaich, T. *Synthesis* **2013**, *45*, 2813–2823.
- (2) Baliga, M. S. *Chin. J. Integr. Med.* **2012**, 1–14.
- (3) Gorup-Besanez, v. *Justus Liebigs Ann. Chem.* **1875**, *176*, 88–89.
- (4) Jagetia, G. C.; Baliga, M. S.; Venkatesh, P.; Ulloor, J. N.; Mantena, S. K.; Genebriera, J.; Mathuram, V. *J. Pharm. Pharmacol.* **2005**, *57*, 1213–1219.
- (5) Schnoes, H.; Biemann, K.; Mokry, J.; Kompis, I.; Chatterjee, A.; Ganguli, G. *J. Org. Chem.* **1966**, *31*, 1641–1642.
- (6) Yuanyuan, H.; Xuelin, C.; Liqiang, W.; Binfeng, C.; Linyi, D.; Xiaodong, L.; Gang, B.; Wenyan, G. *J. Chromatogr. B* **2012**, *908*, 98–104.
- (7) For initial isolation, see: (a) Thomas, A. F. D. Phil. Thesis, Oxford, England, 1954. (b) Subsequent Isolation: Britten, A. Z.; Smith, G. F. *J. Chem. Soc.* **1963**, 3850–3854.

- (8) (a) Arai, H.; Hirasawa, Y.; Rahman, A.; Kusumawati, I.; Zaini, N. C.; Sato, S.; Aoyama, C.; Takeo, J.; Morita, H. *Bioorg. Med. Chem.* **2010**, *18*, 2152–2158. (b) Meng, W.; Ellsworth, B. A.; Nirschl, A. A.; McCann, J.; Patel, M.; Girotra, R. N.; Wu, G.; Sher, P. M.; Morrison, E. P.; Biller, S. A.; Zahler, R.; Deshpande, P. P.; Pullockaran, A.; Hagan, D. L.; Morgan, N.; Taylor, J. R.; Obermeier, M. T.; Humphreys, W. G.; Khanna, A.; Discenza, L.; Robertson, J. G.; Wang, A.; Han, S.; Wetterau, J. R.; Janovitz, E. B.; Flint, O. P.; Whaley, J. M.; W. N. Washburn, *J. Med. Chem.* **2008**, *51*, 1145–1149.
- (9) Subramanian, G.; Hiraku, O.; Hayashi, M.; Koyano, T.; Komiyama, K.; Kam, T.-S. *J. Nat. Prod.* **2007**, *70*, 1783–1789.
- (10) (a) Battersby, A. R.; Thompson, M.; Glüsenkamp, K.-H.; Tietze, L.-F. *Chem. Ber.* **1981**, *114*, 3430–3438. (b) Battersby, A. R.; Westcott, N. D.; Glüsenkamp, K.-H.; Tietze, L.-F. *Chem. Ber.* **1981**, *114*, 3439–3447. (c) Scott, A. I. *Acc. Chem. Res.* **1970**, *3*, 151–157. (d) Stöckigt, J.; Barleben, L.; Panjekar, S.; Loris, E. A. *Plant Physiol. Biochem.* **2008**, *46*, 340–355.
- (11) Ahmad, Y.; Fatima, K.; Le Quesne, P. W.; Atta-Ur-Rahman *Phytochemistry* **1983**, *22*, 1017–1019.
- (12) (a) Henry, T. A.; *J. Chem. Soc.* **1932**, 2759–2768. (b) Olivier, L.; Lévy, J.; Le Men, J.; Janot, M. M.; Budzikiewicz, H.; Djerassi, C. *Bull. Soc. Chim. Fr.* **1965**, 868–876.
- (13) Chatterjee, A.; Mukherjee, B.; Ray, A. B.; Das, B. *Tetrahedron Lett.* **1965**, *6*, 3633–3637.
- (14) Cai, X.-H.; Tan, Q.-G.; Liu, Y.-P.; Feng, T.; Du, Z.-Z.; Li, W.-Q.; Luo, X.-D. *Org. Lett.* **2008**, *10*, 577–580.

- (15) Mokřý, J.; Dúbravková, L.; Šefčovič, P. *Experientia* **1962**, *18*, 564–565.
- (16) (a) Dolby, L. J.; Esfandiari, Z. *J. Org. Chem.* **1972**, *37*, 43–46. (b) Dolby, L. J.; Nelson, S. J. *J. Org. Chem.* **1973**, *38*, 2882–2887.
- (17) Hoike, T.; Takayama, H.; Sakai, S. *Chem. Pharm. Bull.* **1991**, *39*, 1677–1681.
- (18) Lévy, J.; Sapi, J.; Laronze, J.-Y.; Royer, D.; Toupet, L. *Synlett* **1992**, 601–602.
- (19) Bennasar, M.-L.; Zulaica, E.; Ramrez, A.; Bosch, J. *J. Org. Chem.* **1996**, *61*, 1239–1251.
- (20) Yasui, Y.; Kinugawab, T.; Takemoto, Y. *Chem. Commun.* **2009**, 4275–4277.
- (21) Watanabe, T.; Kato, N.; Umezawa, N.; Higuchi, T. *Chem. Eur. J.* **2013**, *19*, 4255–4261.
- (22) Li, Q.; Li, G.; Ma, S.; Feng, P.; Shi, Y. *Org. Lett.* **2013**, *15*, 2601–2603.
- (23) Ren, W.; Tappin, N.; Wang, Q.; Zhu, J. *Synlett* **2013**, 1941–1944.
- (24) Zhang, M.; Huang, X.; Shen, L.; Qin, Y. *J. Am. Chem. Soc.* **2009**, *131*, 6013–6020.
- (25) Zi, W.; Xie, W.; Ma, D. *J. Am. Chem. Soc.* **2012**, *134*, 9126–9129.
- (26) Horning, B. D.; MacMillan, D. W. C. *J. Am. Chem. Soc.* **2013**, *135*, 6442–6445.
- (27) Zu, L.; Boal, B. W.; Garg, N. K. *J. Am. Chem. Soc.* **2011**, *133*, 8877–8879.
- (28) Ren, W.; Wang, Q.; Zhu, J. *Angew. Chem., Int. Ed.* **2014**, *53*, 1818–1821.
- (29) Teng, M.; Zi, W.; Ma, D. *Angew. Chem., Int. Ed.* **2014**, *53*, 1814–1817.
- (30) Smith, J. M.; Moreno, J.; Boal, B. W.; Garg, N. K. *J. Am. Chem. Soc.* **2014**, *136*, 4504–4507.

- (31) (a) Adams, G. L.; Carroll, P. J.; Smith, A. B. *J. Am. Chem. Soc.* **2012**, *134*, 4037–4040. (b) Adams, G. L.; Carroll, P. J.; Smith, A. B. *J. Am. Chem. Soc.* **2013**, *135*, 519–528.
- (32) Smith, M. W.; Snyder, S. A. *J. Am. Chem. Soc.* **2013**, *135*, 12964–12967.
- (33) (a) He, B.; Song, H.; Y. Du, Y. Qin, *J. Org. Chem.* **2009**, *74*, 298–304. (b) J. Yang, H. Wu, L. Shen, Y. Qin, *J. Am. Chem. Soc.* **2007**, *129*, 13794–13795. (c) Song, H.; Yang, J.; Chen, W.; Qin, Y. *Org. Lett.* **2006**, *8*, 6011–6014. (d) Yang, J.; Song, H.; Xiao, X.; Wang, J.; Qin, Y. *Org. Lett.* **2006**, *8*, 2187–2190.
- (34) Vercauteren, J.; Lavaud, C.; Lévy, J.; Massiot, G. *J. Org. Chem.* **1984**, *49*, 2278–2279.
- (35) (a) Schlama, T.; Baati, R.; Gouverneur, V.; Valleix, A.; Falck, J. R.; Mioskowski, C. *Angew. Chem., Int. Ed.* **1998**, *37*, 2085–2087. (b) Ng, F. W.; Lin, H.; Danishefsky, S. J. *J. Am. Chem. Soc.* **2002**, *124*, 9812–9824. (c) Birman, V. B.; S. J. Danishefsky, *J. Am. Chem. Soc.* **2002**, *124*, 2080–2081. (d) Kim, D.; Lee, J.; Shim, P. J.; Lim, J. I.; Jo, H.; Kim, S. *J. Org. Chem.* **2002**, *67*, 764–771. (e) Shigeyama, T.; Katakawa, K.; Kogure, N.; Kitajima, M.; Takayama, H. *Org. Lett.* **2007**, *9*, 4069–4072.
- (36) (a) Zuo, Z.; Xie, W.; Ma, D. *J. Am. Chem. Soc.* **2010**, *132*, 13226–13228. (b) Zuo, Z.; Ma, D. *Angew. Chem., Int. Ed.* **2011**, *50*, 12008–12011.
- (37) (a) Zhao, G.-L.; Vesely, J.; Sun, J.; Christensen, K. E.; Bonneau, C.; Córdova, A. *Adv. Synth. Catal.* **2008**, *350*, 657–661. (b) Wen, L.; Shen, Q.; Lu, L. *Org. Lett.* **2010**, *12*, 4655–4657. (c) Chowdhury, R.; Ghosh, S. K. *Tetrahedron: Asymmetry* **2010**, *21*, 2696–2702.

- (38) (a) Baran, P. S.; Richter, J. M. *J. Am. Chem. Soc.* **2004**, *126*, 7450–7451. (b) Baran, P. S.; Richter, J. M. *J. Am. Chem. Soc.* **2005**, *127*, 15394–15396. (c) Baran, P. S.; Guerrero, C. A.; Ambhaikar, N. B.; Hafensteiner, B. D. *Angew. Chem., Int. Ed.* **2005**, *44*, 606–609.
- (39) Krapcho, A. P.; Weimaster, J. F.; Eldridge, J. M.; Jahngen, Jr., E. G. E.; Lovey, A. J.; Stephens, W. P. *J. Org. Chem.* **1978**, *43*, 138–147.
- (40) Aizpurua, J. M.; Cossio, F. P.; Palomo, C. *J. Org. Chem.* **1986**, *51*, 4941–4943.
- (41) (a) Jones, S. B.; Simmons, B.; MacMillan, D. W. C. *J. Am. Chem. Soc.* **2009**, *131*, 13606–13607. (b) Jones, S. B.; Simmons, B.; Mastracchio, A.; MacMillan, D. W. C. *Nature* **2011**, *475*, 183–188.
- (42) Chen, C.; Crich, D.; Papadatos, A. *J. Am. Chem. Soc.* **1992**, *114*, 8313–8314.
- (43) Shang, J.-H.; Cai, X.-H.; Feng, T.; Zhao, Y.-L.; Wang, J.-K.; Zhang, L.-Y.; Yan, M.; Luo, X.-D. *J. Ethnopharmacol.* **2010**, *129*, 174–181.
- (44) (a) Boal, B. W.; Schammel, A. W.; Garg, N. K. *Org. Lett.* **2009**, *11*, 3458–3461. (b) Schammel, A. W.; Boal, B. W.; Zu, L.; Mesganaw, T.; Garg, N. K. *Tetrahedron* **2010**, *66*, 4687–4695. (c) Çelebi-Ölçüm, N.; Boal, B. W.; Hutters, A. D.; Garg, N. K.; Houk, K. N. *J. Am. Chem. Soc.* **2011**, *133*, 5752–5755. (d) Schammel, A. W.; Chiou, G.; Garg, N. K. *J. Org. Chem.* **2012**, *77*, 725–728. (e) Schammel, A. W.; Chiou, G.; Garg, N. K. *Org. Lett.* **2012**, *14*, 4556–4559.
- (45) (a) Rawal, V. H.; Michoud, C.; Monestel, R. F. *J. Am. Chem. Soc.* **1993**, *115*, 3030–3031. (b) Rawal, V. H.; Iwasa, S. *J. Org. Chem.* **1994**, *59*, 2685–2686. (c) Martin, D. B. C.; Vanderwal, C. D. *J. Am. Chem. Soc.* **2009**, *131*, 3472–3473.

- (46) For examples of oxidative azidoalkoxylation, see: (a) Chavan, S. P.; Subbarao, Y. T.; *Tetrahedron Lett.* **1999**, *40*, 5073–5074. (b) Norton Matos, M. R. P.; Alfonso, C. A. M.; Batey, R. A. *Tetrahedron Lett.* **2001**, *42*, 7007–7010. (c) Le Corre, L.; Kizirian, J.-C.; Levraud, C.; Boucher, J.-L.; Bonnet, V.; Dhimane, H. *Org. Biomol. Chem.* **2008**, *6*, 3388–3398.
- (47) Li, Q.; Li, G.; Ma, S.; Feng, P.; Shi, Y. *Org. Lett.* **2013**, *15*, 2601–2603.
- (48) Solé, D.; Bosch, J.; Bonjoch, J. *Tetrahedron* **1996**, *52*, 4013–4028.
- (49) Mi, Y.; Schreiber, J. V.; Corey, E. J. *J. Am. Chem. Soc.* **2002**, *124*, 11290–11291.
- (50) Kozmin, S. A.; Iwama, T.; Huang, Y.; Rawal, V. H. *J. Am. Chem. Soc.* **2002**, *124*, 4628–4641.
- (51) Trost, B. M.; Pissot-Soldermann, C.; Chen, I.; Schroeder, G. M. *J. Am. Chem. Soc.* **2004**, *126*, 4480–4481.
- (52) Sirasani, G.; Andrade, R. B. *Org. Lett.* **2011**, *13*, 4736–4737.
- (53) (a) Cooke, Jr., M. P.; Widener, R. K. *J. Org. Chem.* **1987**, *52*, 1381–1396. (b) Piers, E.; Harrison, C. L.; Zetina-Rocha, C. *Org. Lett.* **2001**, *3*, 3245–3247. (c) Dieter, R. K.; Oba, G.; Chandupatla, K. R.; Topping, C. M.; Lu, K.; Watson, R. T. *J. Org. Chem.* **2004**, *69*, 3076–3086. (d) Martin, D. B. C.; Vanderwal, C. D. *Chem. Sci.* **2011**, *2*, 649–651. (e) Martin, D. B. C.; Nguyen, L. Q.; Vanderwal, C. D. *J. Org. Chem.* **2012**, *77*, 17–46.
- (54) Zhu and co-workers attempted a similar type of oxidative coupling in efforts towards strictamine, see ref. 23.

- (55) (a) Solé, D.; Cancho, Y.; Llebaria, A.; Moretó, J. M.; Delgado, A. *J. Am. Chem. Soc.* **1994**, *116*, 12133–12134. (b) Bonjoch, J.; Solé, D.; Bosch, J. *J. Am. Chem. Soc.* **1995**, *117*, 11017–11018. (c) Solé, D.; Bonjoch, J.; Bosch, J. *J. Org. Chem.* **1996**, *61*, 4194–4195. (d) Bonjoch, J.; Solé, D.; García-Rubio, S.; Bosch, J. *J. Am. Chem. Soc.* **1997**, *119*, 7230–7240. (e) Ma, J.; Yin, W.; Zhou, H.; Cook, J. M. *Org. Lett.* **2007**, *9*, 3491–3494. (f) Yu, F.; Cheng, B.; Zhai, H. *Org. Lett.* **2011**, *13*, 5782–5783.
- (56) (a) Danieli, B.; Lesma, G.; Mauro, M.; Palmisano, G.; Passarella, D. *J. Org. Chem.* **1995**, *60*, 2506–2513. (b) Danieli, B.; Lesma, G.; Mauro, M.; Palmisano, G.; Passarella, D. *Tetrahedron* **1994**, *50*, 8837–8852. (c) Danieli, B.; Lesma, G.; Mauro, M.; G. Palmisano, D. Passarella *Tetrahedron: Asymmetry* **1990**, *1*, 793–800. For a modified procedure to access lactone **1.77** on gram scale, see reference 31b.
- (57) Freifelder, M. *J. Am. Chem. Soc.* **1960**, *82*, 2386–2389.
- (58) Schultz, R. J.; Staas, W. H.; Spurlock, L. A. *J. Org. Chem.* **1973**, *38*, 3091–3093.
- (59) Welch, W. M. *Synthesis* **1977**, 645–646.
- (60) Still, W. C. *J. Am. Chem. Soc.* **1978**, *100*, 1481–1487.
- (61) Schwesinger, R.; Willaredt, J.; Schlemper, H.; Keller, M.; Schmitt, D.; Fritz, H. *Chem. Ber.* **1994**, *127*, 2435–2454.
- (62) Yonezawa, Y.; Tani, N.; Shin, C.-G. *Heterocycles* **2005**, *65*, 95–105.
- (63) For use of Et₃B as a radical initiator, see: (a) Reddy, L. R.; Fournier, J.-F.; Reddy, B. V. S.; Corey, E. J. *J. Am. Chem. Soc.* **2005**, *127*, 8974–8976. (b) Lambert, T. H.; Danishefsky, S. J. *J. Am. Chem. Soc.* **2006**, *128*, 426–427.

(64) For examples of radical cyclizations to form indole derivatives, see: (a) Beckwith, A. L.; Storey, J. M. D. *J. Chem. Soc., Chem. Comm.* **1995**, 977–978. (b) Beckwith, A. L.; Bowry, V. W.; Bowman, W. R.; Mann, E.; Parr, J.; Storey, J. M. D. *Angew. Chem., Int. Ed.* **2004**, *43*, 95–98. (c) Jia, Y.-X.; Kündig, E. P. *Angew. Chem., Int. Ed.* **2009**, *48*, 1636–1639.

CHAPTER TWO

First-Generation Approach to the Total Synthesis of Picrinine

2.1 Abstract

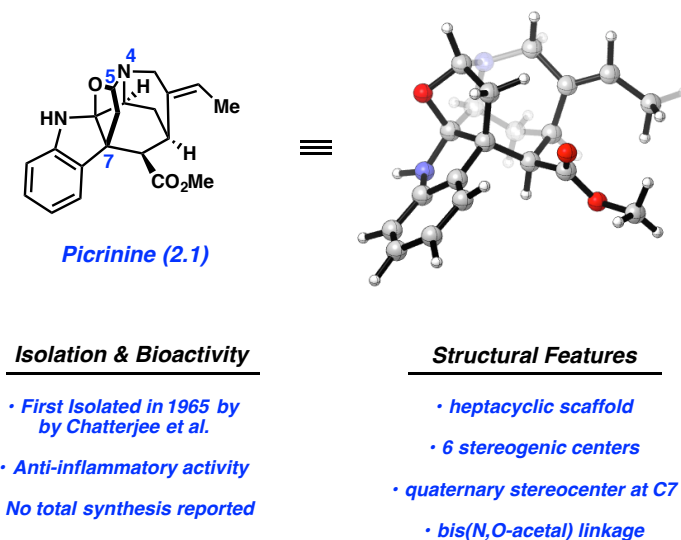
Picrinine, which is a member of the akuammiline family of alkaloids, was first isolated in 1965 from the leaves of *Alstonia scholaris*. The natural product possesses a daunting polycyclic skeleton that contains a furanoindoline, a bridged [3.3.1]-azabicyclic, two *N,O*-acetal linkages, and six stereogenic centers. These structural features render picrinine a challenging and attractive target for total synthesis. This Chapter describes our initial approach to synthesize this daunting target, with a Fischer indolization reaction being a key strategic transformation towards accessing the skeleton of the natural product. Additionally, efforts to circumvent the synthetic roadblocks en route to picrinine are described, along with our first-generation late-stage efforts towards completing its synthesis.

2.2 Introduction

The plant *Alstonia scholaris*, also known as the Dita Bark Tree, has been a rich source of alkaloid natural products for close to a century. In fact, extracts from its bark, leaves, seeds, fruitpods, flowers, and roots have been used in traditional folk medicines to treat various ailments in humans and livestock.¹ Amongst the alkaloids found in *Alstonia scholaris*, picrinine (**2.1**) is one of the major constituents that was first isolated and structurally elucidated in 1965 by Chatterjee and coworkers (Figure 2.1).² Following its isolation, an X-ray crystal structure of **2.1**

was obtained, which highlights the densely functionalized, cage-like structure of the natural product.³ Structural features of **2.1** include a fused furanoindoline framework, a [3.3.1]-azabicyclic, and a highly functionalized cyclohexyl unit that bears five of the natural product's six stereocenters. The C7 stereocenter is quaternary and presents a notable synthetic challenge. The remaining stereocenter is at C5, which is a part of the bis-(*N,O*-acetal) moiety that links the furanoindoline to N4 of the piperidine ring. Picrinine (**2.1**) has shown *in vitro* anti-inflammatory activity via inhibition of the 5-lipoxygenase enzyme.⁴ Moreover, **2.1** is a major constituent of the leaf extracts of *Alstonia scholaris* that have been approved for clinical trials in China due to their antitussive and antiasthmatic properties.⁵

Figure 2.1 Picrinine (**2.1**) and 3D representation from X-ray structure.



Picrinine (**2.1**) belongs to a larger family of alkaloids called the akuammilines.⁶ Over 30 akuammilines have been isolated over the past 90 years and their sources, much like *Alstonia*

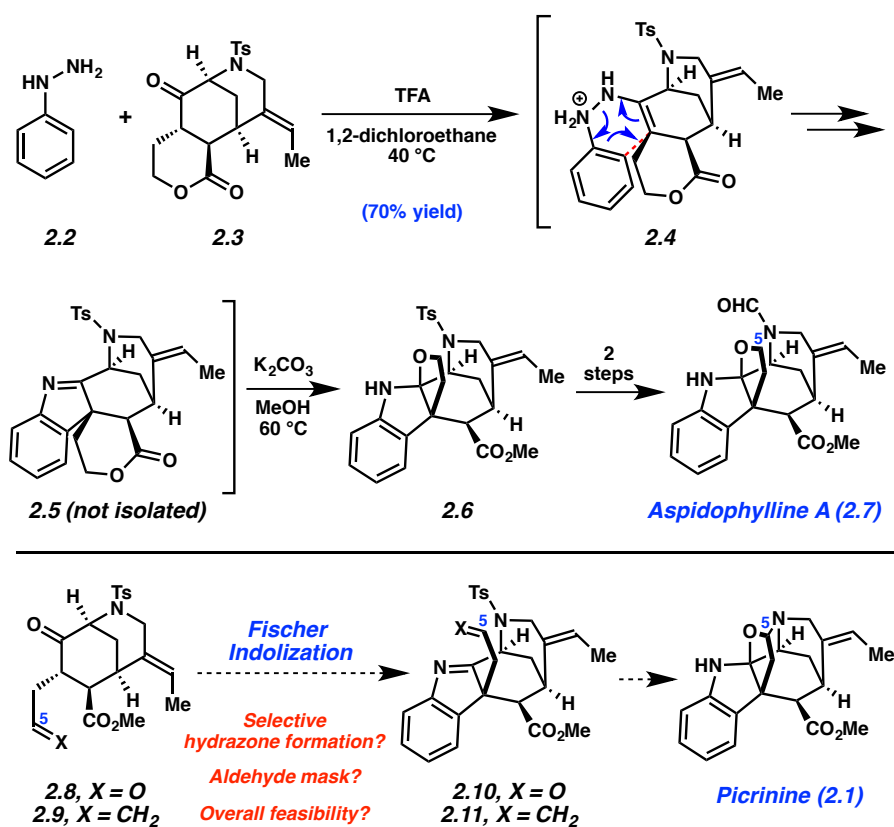
scholaris, have served as traditional ailment remedies across the Eastern Hemisphere. Biological testing of the akuammilines has revealed promising activities for combating illnesses that are viral, plasmodial, and cancerous.^{4a} An overview of these alkaloids is presented in Chapter 1.

This chapter describes a first-generation effort to achieve the first total synthesis of picrinine (**2.1**).⁷ The approaches described herein were inspired by our laboratory's prior total synthesis of aspidophylline A (**2.7**).⁸ Central to our synthetic approach to **2.7** was the key interrupted Fischer indolization reaction shown in Figure 2.2.⁹ Phenylhydrazine (**2.2**) was reacted with ketolactone **2.3** in the presence of trifluoroacetic acid (TFA) in 1,2-dichloroethane (DCE) at 40 °C to first give a hydrazone intermediate. Following tautomerization, charge-accelerated [3,3]-sigmatropic rearrangement (see transition structure **2.4**), and subsequent loss of ammonia, intermediate indolenine **2.5** was obtained. Removal of the volatiles, followed by the addition of K₂CO₃ and methanol, promoted lactone cleavage and spontaneous cyclization to build the pentacyclic furanoindoline product **2.6** in 70% yield. This process occurred with complete diastereoselectivity. Further elaboration through two additional steps provided the natural product (**2.7**), thus completing its first total synthesis.

We envisioned a similarly attractive strategy in our approach to picrinine (**2.1**) as suggested in Figure 2.2. Ideally, we sought to utilize interrupted Fischer indolization substrate **2.8** to access the core of the natural product, but foresaw challenges in achieving selective hydrazone formation of the ketone in the presence of the C5 aldehyde en route to **2.10**. The use of an alkene as an aldehyde mask presented a viable workaround, and led to the design of substrate **2.9**.¹⁰ After the Fischer indolization of **2.9** to furnish **2.11**, the alkene would be oxidatively cleaved at a late stage to access the correct C5 aldehyde oxidation state found in the natural product.^{8,11} Finally, the viability of the Fischer indolization reaction was a notable

concern considering the substrate's complexity, its differences compared to ketolactone **2.3** used in the synthesis of aspidophylline A (**2.7**),⁸ and our prior experiences with challenging Fischer indolizations of related substrates.¹²

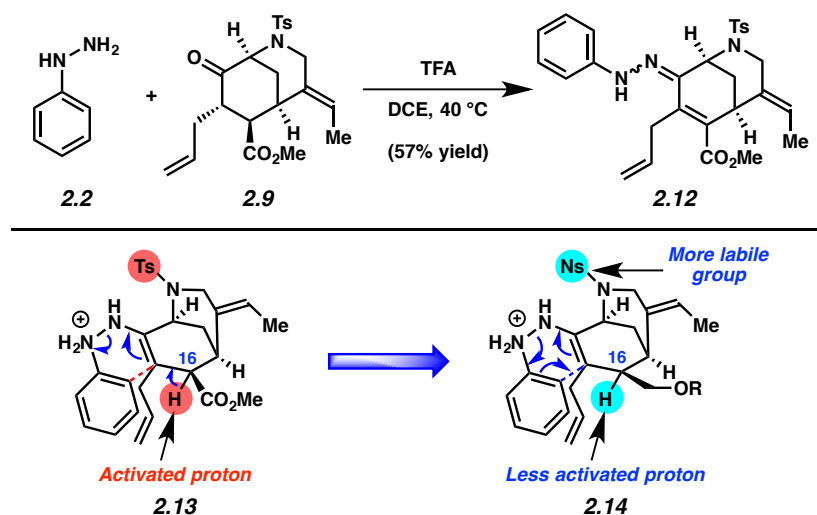
Figure 2.2. Summary of total synthesis of aspidophylline A (**2.7**) and initial synthetic plan for picrinine (**2.1**) utilizing the key Fischer indolization reaction.



2.3 Initial Forays and First Generation Retrosynthetic Analysis

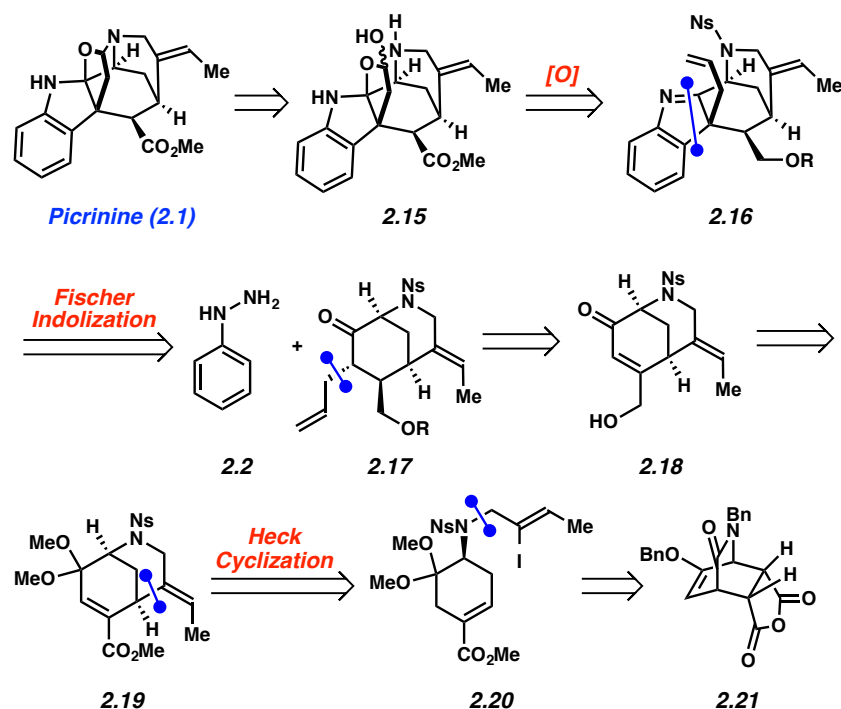
Based on the synthetic plan mentioned above, we tested the Fischer indolization of ketone **2.9**, a known intermediate from our prior synthesis of aspidophylline A (Figure 2.3).⁸ Upon treatment of **2.9** with phenylhydrazine (**2.2**) under the same Fischer indolization conditions used for the aspidophylline A (**2.7**) synthesis, none of the desired product (**2.11**) was observed, with only oxidized hydrazone derivative **2.12** forming as the major product in 57% yield. When the reaction was studied with different acid sources and/or temperatures, the same outcome was obtained. Similarly, attempts to rigorously exclude molecular oxygen from the reaction mixture also led to the formation of **2.12**. We hypothesized that the putatively formed ene-hydrazine **2.13** was prone to deprotonation at C16, and that the deprotonation would ultimately result in N–N bond cleavage. Such N–N bond cleavage processes have been observed in Fischer indolizations and studied by Houk and coworkers.¹³ Following this formal oxidation event (i.e., deprotonation and N–N bond cleavage), excess hydrazine in the reaction mixture could condense on the ketone to give the observed product **2.12**. As the desired [3,3]-sigmatropic rearrangement was presumably being outcompeted by this unproductive reaction pathway, we sought to design an alternate Fischer indolization substrate. It was hypothesized that by converting the exocyclic ester to a protected alcohol derivative, the undesired N–N bond cleavage might be suppressed due to the reduced acidity of the C16 proton (see structure **2.14**). Consequently, the desired [3,3]-sigmatropic rearrangement could be rendered the predominant reaction pathway. Additionally, we opted to switch the nitrogen protecting group from tosyl to the more labile nosyl group in order to facilitate removal at a late stage in the synthesis.¹⁴

Figure 2.3 Unsuccessful Fischer indolization of **2.9** and design of new substrate.



With the key elements and modifications of our design plans established, we devised the retrosynthetic analysis of **2.1** shown in Scheme 2.1. It was envisioned that the natural product could arise from the spontaneous cyclization of an intermediate such as **2.15**, which would result from oxidation and deprotection of indolenine **2.16**. In turn, indolenine **2.16** would arise from a late-stage Fischer indolization of phenylhydrazine (**2.2**) and ketone **2.17**.¹⁵ Ketone **2.17** would be derived from enone **2.18**, an intermediate that could be accessed from enoate **2.19**. This bicyclic enoate would arise by Heck cyclization of vinyl iodide **2.20**.^{16,17} Finally, the Heck cyclization substrate (**2.20**) would be derived from the known bicyclic lactam **2.21**,¹⁸ which can be readily prepared from commercially available starting materials.

Scheme 2.1 Initial retrosynthetic plan for the total synthesis of picrinine (**2.1**).

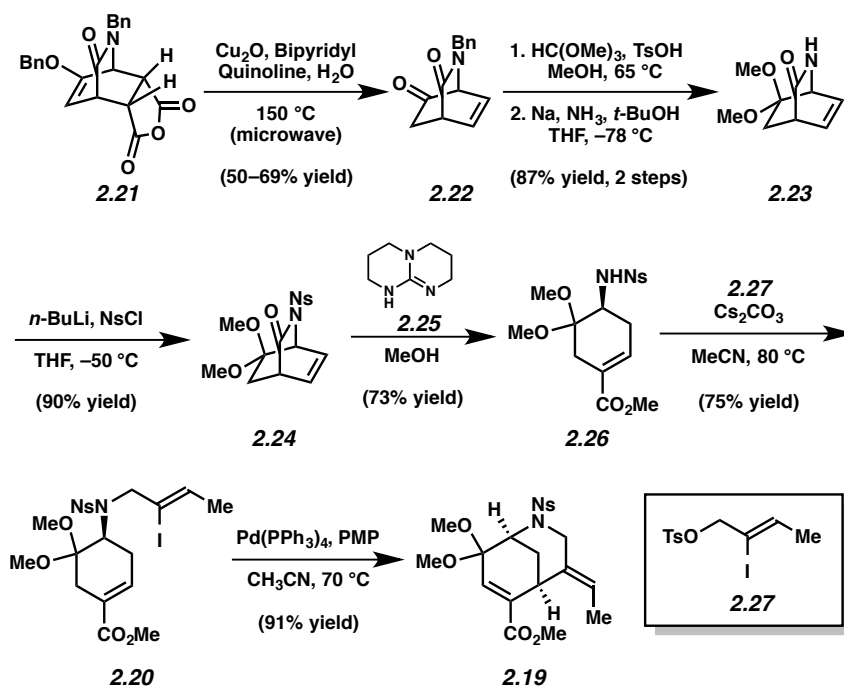


2.4 Synthesis of [3.3.1]-Azabicycle and Elaboration to Substrate 2.30

Our first goal was to assemble the [3.3.1]-azabicyclic core of the natural product using the Heck cyclization strategy mentioned earlier. Our synthesis of the desired bicyclic enoate **2.19** is depicted in Scheme 2.2. We were first able to access >20 g quantities of the starting tricyclic lactam **2.21** from a known Diels–Alder protocol.¹⁸ This intermediate was then subjected to a mixture of copper (I) oxide in water and quinoline under microwave irradiation to promote an oxidative bis(decarboxylation) reaction.¹⁹ This transformation gave ketone **2.22** in 50–69% yield, although yields were lower and less consistent if the reaction was run above 40 mg scale. To facilitate material throughput, we employed an automated microwave reactor to prepare gram

quantities of **2.22**.²⁰ Next, a two step sequence involving ketalization and debenzoylation afforded bicyclic lactam **2.23** in excellent yield. Bicycle **2.23** was then protected as the 2-nitrobenzenesulfonamide upon treatment with *n*-BuLi at low temperature, followed by quenching with NsCl to give **2.24**. We next sought to achieve methanolysis of the lactam with olefin transposition, but this transformation proved challenging. Typical cleavage conditions utilizing K₂CO₃ and methanol resulted in low yields of enoate **2.26**, in addition to substantial nonspecific decomposition. After surveying a number of bases to effect methanolysis, it was found that utilizing 1,5,7-triazabicyclo[4.4.0]dec-5-ene (TBD) (**2.25**) in methanol²¹ was most effective and delivered enoate **2.26** in 73% yield. Following methanolysis, alkylation with tosylate **2.27**²² in the presence of Cs₂CO₃ at elevated temperature provided vinyl iodide **2.20**, the substrate for the key Heck cyclization. Following inspiration from the groups of Rawal and Vanderwal,¹⁶ iodide **2.20** was exposed to Pd(PPh₃)₄ (5 mol%) in the presence of 1,2,2,6,6-pentamethylpiperidine (PMP) at 70 °C in acetonitrile to furnish **2.19** in 91% yield. Notably, this transformation efficiently constructed the important [3.3.1]-azabicyclic product.

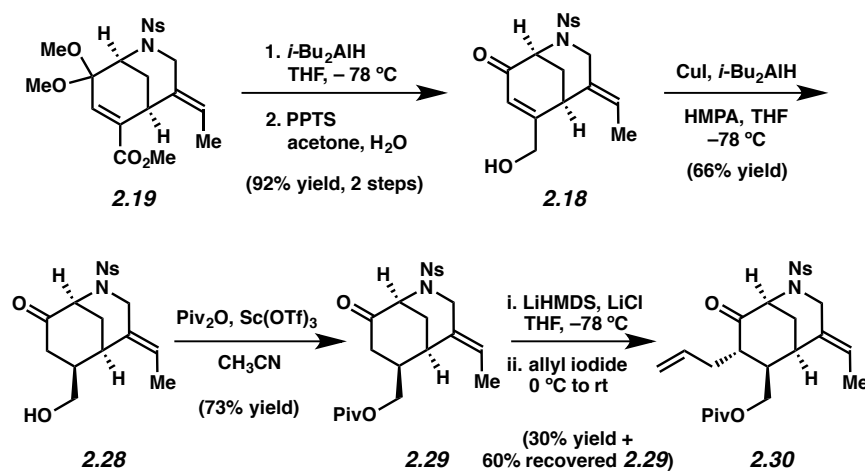
Scheme 2.2 Synthesis of [3.3.1]-azabicycle **2.19**.



With enoate **2.19** in hand, we were poised to complete the synthesis of the desired Fischer indolization substrate **2.30** (Scheme 2.3). Reduction of the enoate, followed by acid-promoted cleavage of the dimethylketal with pyridinium *p*-toluenesulfonate (PPTS), gave enone **2.18** in 92% yield over two steps. Enone **2.18** was then subjected to a conjugate reduction protocol, which proceeded with complete diastereoselectivity to give ketone **2.28** in 66% yield.²³ The primary alcohol was then protected as the corresponding pivalate ester to give **2.29**. To access Fischer indolization substrate **2.30**, it would be necessary to introduce an allyl substituent. Thus, ketone **2.29** was treated with lithium hexamethyldisilazide (LiHMDS) and quenched with allyl iodide to afford the desired product, albeit in modest yield. The addition of various additives (HMPA, DMPU, etc.) did not improve the reaction yield. Furthermore, this challenging alkylation was hampered by the low reactivity of the enolate at low temperatures and the

propensity for double alkylation to occur at warmer temperatures. As a result, our optimal procedure involves stopping the reaction in a manner that allows for the recovery of ketone **2.29** (60% recovered yield) and material recycling. Nonetheless, the aforementioned sequence provided adequate quantities of **2.30** to test the pivotal Fischer indolization reaction.

Scheme 2.3 Synthesis of Fischer indolization substrate **2.30**.

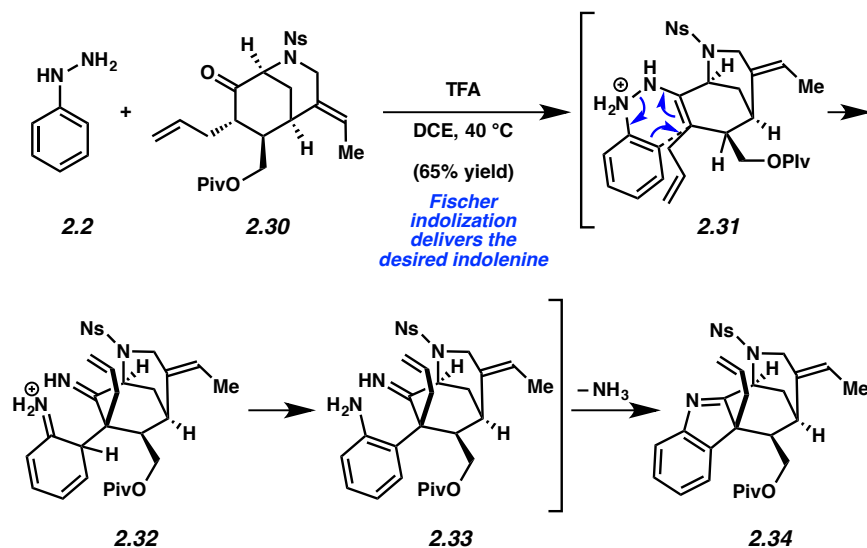


2.5 Fischer Indolization and Unsuccessful Late-State Studies

With ketone **2.30** in hand, we attempted the key Fischer indolization (Scheme 2.4). Gratifyingly, upon exposure of substrate **2.30** to phenylhydrazine (**2.2**) and TFA in DCE at 40 °C, we observed clean conversion to indolenine **2.34** in 65% yield. Of note, the undesired oxidation observed in our earlier studies (see Figure 2.3) was not seen. Based on this result, we concluded that the putative ene-hydrazine underwent the desired [3,3]-sigmatropic rearrangement (see transition structure **2.31**) to form intermediate **2.32** instead of undergoing N–N bond cleavage. Following tautomerization of **2.32**, intermediate **2.33** presumably cyclizes with

loss of ammonia to deliver the desired indolenine **2.34**. It is worth noting that the Fischer indolization of ketone **2.30** is more sluggish compared to the corresponding reaction of lactone **2.3** (see Figure 2.2) used in the aspidophylline A (**2.7**) synthesis (24 h vs 16 h).⁸ We attribute this difference to the presence of the freely rotating allyl group in **2.30**, which provides additional steric encumbrance in the [3,3]-sigmatropic rearrangement step. Nonetheless, the successful Fischer indolization of substrate **2.30** to give tetracyclic indolenine **2.34** validated our hypothesis that by the judicious modification of substrate, we could suppress the undesired formal oxidation pathway and promote the critical [3,3]-sigmatropic rearrangement process.

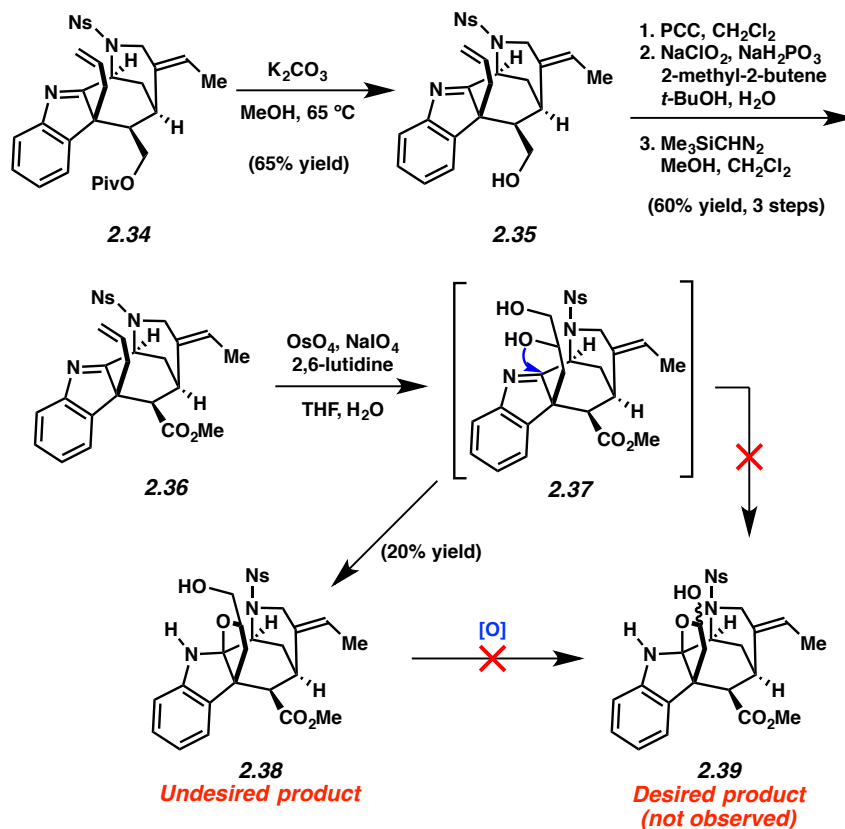
Scheme 2.4 Successful Fischer indolization of ketone **2.30**.



With most of the carbon framework of the natural product intact, we set our sights on completing the synthesis of picrinine (**2.1**) (Scheme 2.5). Our first goal was to introduce the methyl ester, which was achieved in four operations. First, deprotection of the alcohol occurred

smoothly using a standard methanolysis procedure to give **2.35**. Subsequent PCC oxidation and Lindgren oxidation with NaClO₂ in the presence of 2-methyl-2-butene gave an intermediate carboxylic acid. Methylation using trimethylsilyldiazomethane afforded ester **2.36** in 38% yield over the three steps.²⁴ At this point, all that remained was to implement a chemoselective oxidative cleavage of the terminal olefin²⁵ and to remove the sulfonamide protecting group. Upon treatment of ester **2.36** with aqueous osmium tetroxide in the presence of NaIO₄ and 2,6-lutidine, selective oxidation occurred to putatively give diol **2.37**. However, instead of undergoing the desired oxidative C–C bond cleavage to deliver lactol **2.39**, cyclization took place to give furanoindoline **2.38**. Considerable efforts were undertaken to effect the desired oxidative cleavage of **2.38**; however, the formation of **2.39** was never observed.²⁶ Thus, despite the excitement of having circumvented the problems associated with the key Fischer indolization in this particular synthetic approach to picrinine (**2.1**), further modification of our synthetic plan would be required in order to access the natural product.

Scheme 2.5 Unsuccessful attempts to elaborate Fischer indolization product **2.34**.



2.6 Conclusions

Although unsuccessful, our first-generation synthetic efforts towards picrinine were valuable in understanding various aspects of our synthetic approach. First, with regard to the Fischer indolization reaction, subtle structural effects of the substrate have an enormous effect on the course of the reaction. Through a probe of our mechanistic hypothesis, the design of an altered substrate (**2.30**) resulted in a successful construction of the C7 quaternary center as well as supported our rationalization for the initially undesired reactivity of **2.9**. The undesired

cyclization observed in the late-stage oxidation of **2.36** should be considered in moving forward towards successful construction of picrinine (**2.1**).

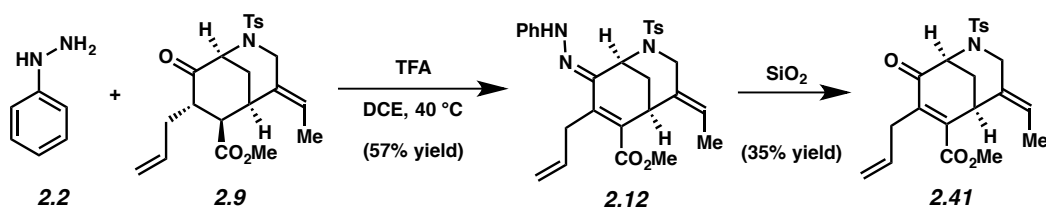
2.7 Experimental Section

2.7.1 Materials and Methods

Unless stated otherwise, reactions were conducted in flame-dried glassware under an atmosphere of nitrogen using anhydrous solvents (either freshly distilled or passed through activated alumina columns). *n*-Butyllithium (*n*-BuLi), 1,5,7-triazabicyclo[4.4.0]dec-5-ene, 1,2,2,6,6-pentamethylpiperidine (PMP), diisobutyl-aluminum hydride (*i*-Bu₂AlH), pyridinium *p*-toluenesulfonate (PPTS), pivaloic anhydride (Piv₂O), scandium (III) triflate [Sc(OTf)₃], lithium hexamethyldisilazide (LiHMDS), allyl iodide, sodium chlorite (NaClO₂), 2-methyl-2-butene, and 2,6-lutidine were obtained from Sigma–Aldrich. Tetrakis(triphenylphosphine)palladium [Pd(PPh₃)₄], copper iodide (CuI), and osmium tetroxide (OsO₄) were obtained from Strem. Trifluoroacetic acid (TFA) and monobasic sodium phosphate (NaH₂PO₄) were obtained from Fischer. Phenylhydrazine (**2.2**) and pyridinium chlorochromate (PCC) were obtained from Acros. In addition, phenylhydrazine (**2.2**) was purified by flash chromatography (4:1 hexanes:EtOAc) prior to use. Sodium periodate (NaIO₄) was obtained from Alfa-Aesar. 2-Nitrobenzenesulfonyl chloride (NsCl) and trimethylsilyldiazomethane (TMSCHN₂) were obtained from TCI. Potassium carbonate (K₂CO₃) was obtained from EMD. Acetic acid (AcOH) was obtained from JT Baker. Unless stated otherwise, reactions were performed at room temperature (approximately 23 °C). Microwave reactions were conducted on a Discover microwave reactor from CEM with an automated Explorer sample changer. Thin-layer

chromatography (TLC) was conducted with EMD gel 60 F254 pre-coated plates (0.25 mm) and visualized using a combination of UV, anisaldehyde, and iodine staining. SiliCycle silica gel 60 (particle size 0.040–0.063 mm) was used for flash column chromatography. ^1H NMR spectra were recorded on Bruker spectrometers (500 and 600 MHz). Data for ^1H spectra are reported as follows: chemical shift (δ ppm), multiplicity, coupling constant (Hz), integration and are referenced to the residual solvent peak 7.26 ppm for CDCl_3 . ^{13}C NMR spectra are reported in terms of chemical shift (at 125 MHz) and are referenced to the residual solvent peak 77.16 ppm for CDCl_3 . IR spectra were recorded on a Perkin-Elmer 100 spectrometer and are reported in terms of frequency absorption (cm^{-1}). Uncorrected melting points were measured using a Mel-Temp II melting point apparatus with a Fluke 50S thermocouple and a Digimelt MPA160 melting point apparatus. High-resolution mass spectra were obtained from the UC Irvine and UCLA Mass Spectrometry Facilities.

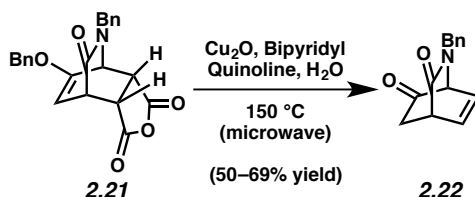
2.7.2 Experimental Procedures



Hydrazone 2.12 and Enone 2.41. To a solution of ketone **2.9** (5.0 mg, 0.012 mmol) in 1,2-dichloroethane (DCE) (0.5 mL) was added phenylhydrazine (**2.2**) (1.8 μL , 0.018 mmol) and trifluoroacetic acid (TFA) (5.0 μL , 0.060 mmol). The reaction mixture was heated to 40 °C. After 24 h, the reaction was diluted with EtOAc (5 mL) and poured into a solution of saturated aqueous NaHCO_3 (10 mL). The layers were separated, and the aqueous layer was extracted with

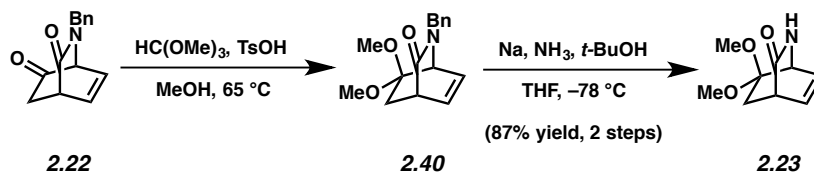
EtOAc (3 x 15 mL). The combined organic layers were dried over MgSO₄, filtered, and evaporated under reduced pressure. Hydrazone **2.12** was the major product in the crude reaction mixture (3.5 mg, 57% crude yield). The crude residue was purified via preparative TLC (2:1 hexanes:EtOAc → 1:2 hexanes:EtOAc) to afford enone **2.41** (1 mg, 20% yield) as an orange oil.

Hydrazone **2.12**: *R_f* 0.55 (2:1 hexanes:EtOAc); ¹H NMR (500 MHz, CDCl₃): δ 9.58 (s, 1H), 7.79 (d, *J* = 8.3, 2H), 7.37–7.30 (m, 6H), 6.99 (tt, *J* = 7.2, 1.4, 1H), 6.01 (m, 1H), 5.49 (q, *J* = 6.9, 1H), 5.20 (dq, *J* = 17.1, 1.7, 1H), 5.03 (dq, *J* = 10.1, 1.7, 1H), 4.94 (t, *J* = 2.9, 1H), 4.18 (d, *J* = 16.0, 1H), 3.92–3.85 (m, *J* = 3H), 3.80 (dd, *J* = 13.4, 6.5, 1H), 3.77 (s, 3H), 2.49 (s, 3H), 1.70–1.62 (m, 4H), 1.17 (dt, *J* = 12.9, 3.2, 1H); **Enone 2.41**: *R_f* 0.70 (1:2 hexanes:EtOAc); ¹H NMR (500 MHz, CDCl₃): δ 7.67 (d, *J* = 8.3, 2H), 7.27 (d, *J* = 8.3, 2H), 5.65 (q, *J* = 6.9, 1H), 5.27 (m, 1H), 4.78 (dq, *J* = 17.1, 1.7, 1H), 4.71 (dq, *J* = 10.1, 1.7, 1H), 4.55 (t, *J* = 3.3, 1H), 4.14 (d, *J* = 13.6, 1H), 3.98 (t, *J* = 3.2, 1H), 3.77 (s, 3H), 3.50 (dt, *J* = 13.6, 2.0, 1H), 3.09 (dd, *J* = 13.8, 6.7, 1H), 2.99 (dd, *J* = 13.8, 6.7, 1H), 2.41 (s, 3H), 2.34 (dt, *J* = 13.1, 3.3, 1H), 2.11 (dt, *J* = 13.1, 3.2, 1H), 1.69 (dd, *J* = 6.9, 1.9, 3H); ¹³C NMR (125 MHz, CDCl₃): δ 192.9, 167.2, 144.3, 143.6, 140.8, 135.4, 134.1, 129.5, 128.8, 128.2, 124.5, 116.5, 56.0, 52.5, 46.7, 33.9, 33.1, 30.5, 21.7, 12.9; IR (film): 2923, 2853, 1723, 1786, 1456, 1350, 1248, 1219, 1163, 1096; HRMS–ESI (*m/z*) [M + H]⁺ calcd for C₂₂H₂₆NO₅S⁺, 416.15262; found 416.15044.



Alkene 2.22. To a solution of anhydride **2.21** (40 mg, .103 mmol), copper oxide (32 mg, .226 mmol), and bipyridyl (18 mg, .113 mmol) in quinoline (1.0 mL) was added deionized H₂O (20

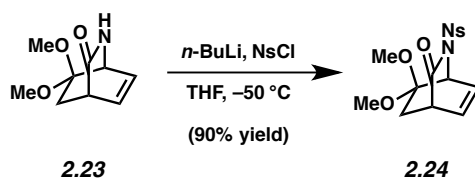
μL , 1.03 mmol). The reaction was heated to 150 °C for 25 min in the microwave reactor. The reaction was poured into a 1 M HCl aqueous solution (15 mL) and extracted with CH_2Cl_2 (3 X 10 mL). The organic layers were combined, dried over Na_2SO_4 , and evaporated under reduced pressure. The resulting residue was purified by flash chromatography (2:1 \rightarrow 1:1 hexanes:EtOAc) to afford alkene **2.22** (15.6 mg, 69% yield) as an orange oil. Alkene **22**: R_f 0.2 (1:1 hexanes:EtOAc); ^1H NMR (500 MHz, CDCl_3): δ 7.39–7.31 (m, 3H), 7.21–7.16 (m, 2H), 6.73 (ddd, $J = 9, 6, 1.5$, 1H), 6.47 (d, $J = 9, 6, 2$ 1H), 4.89 (d, $J = 15$, 1H), 4.33 (d, $J = 15$, 1H), 4.18(dd, $J = 6, 2$, 1H), 3.80 (ddd, $J = 5, 3, 2.5$, 1H), 2.45 (dd, $J = 18, 2.5$, 1H), 2.16 (dd, $J = 18, 3$, 1H); ^{13}C NMR (125 MHz, CDCl_3): δ 200.2, 170.5, 136.9, 135.7, 129.1, 128.7, 127.9, 64.8, 48.6, 44.6, 32.0; IR (film): 3467, 3031, 2923, 1736, 1671, 1445, 1419, 1240, 1156; HRMS-ESI (m/z) [$\text{M} + \text{Na}$] $^+$ calcd for $\text{C}_{14}\text{H}_{13}\text{NO}_2$, 250.0844; found 250.0845.



Amide 2.23. To a solution of alkene **2.22** (2.04 g, 8.99 mmol) and trimethoxymethane (20.0 mL, 182.8 mmol) in methanol (80 mL) was added 4-methylbenzenesulfonic acid monohydrate (*p*-TsOH) (855 mg, 4.50 mmol). The reaction was heated to reflux. After 14 h, the reaction mixture was cooled to rt, excess methanol was removed under reduced pressure, and the reaction was poured into a sat. aq. NaHCO_3 solution (200 mL). The solution was diluted with CH_2Cl_2 (50 mL) and the layers were separated. The aqueous layer was extracted with CH_2Cl_2 (3 x 50 mL). The organic layers were combined, dried over Na_2SO_4 , and evaporated under reduced pressure. The resulting residue was purified by flash chromatography (2:1 \rightarrow 1:1 hexanes:EtOAc) to afford

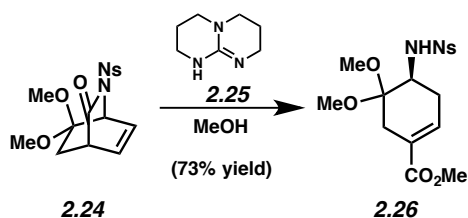
ketal **2.40** (2.42 g, 99% yield) as an orange oil. R_f 0.2 (1:1 hexanes:EtOAc); $^1\text{H NMR}$ (500 MHz, CDCl_3): δ 7.32–7.25 (m, 3H), 7.12 (d, $J = 7.5$, 2H), 6.44 (dd, $J = 7, 6$, 1H), 6.29 (dd, $J = 7, 5.5$, 1H), 4.01 (d, $J = 5.5$, 1H), 3.90 (d, $J = 15.5$, 1H), 3.49–3.47 (m, 1H), 3.20 (s, 3H), 3.13 (s, 3H), 2.15 (dd, $J = 13, 1.5$, 1H), 1.64 (dd, $J = 13, 2.5$, 1H).

To a solution of sodium metal (786 mg, 34.2 mmol) in NH_3 (30 mL) was added a solution of ketal **2.40** (3.11 g, 11.4 mmol) and *tert*-butanol (0.2 mL, 3.45 mmol) in THF (40 mL) at -78 °C. After 30 min, the reaction mixture was quenched with a solution of sat. aq. NH_4Cl (15 mL) at -78 °C. The reaction was warmed to rt and poured into brine (20 mL). The solution was diluted with EtOAc (50 mL) and the layers were separated. The aqueous layer was extracted with EtOAc (3 x 50 mL). The organic layers were combined, dried over MgSO_4 , and evaporated under reduced pressure. The resulting residue was purified by flash chromatography (100:0 \rightarrow 90:10 CH_2Cl_2 :MeOH) to afford amide **2.23** (1.84 g, 88% yield) as a beige solid. Amide **2.23**: R_f 0.1 (1:1 hexanes:EtOAc); $^1\text{H NMR}$ (500 MHz, CDCl_3): δ 7.41 (s, 1H), 6.48 (s, 2H), 4.27 (s, 1H), 3.33 (s, 1H), 3.28 (s, 3H), 3.22 (s, 3H), 1.72 (d, $J = 12.5$, 1H), 1.29 (d, $J = 12.5$, 1H); $^{13}\text{C NMR}$ (125 MHz, CDCl_3): δ 176.4, 132.7, 131.8, 106.9, 53.3, 49.1, 49.0, 44.3, 34.1; IR (film): 3242, 2946, 1683, 1638, 1618, 1451, 1131, 1063; HRMS-ESI (m/z) [$\text{M} + \text{Na}$] $^+$ calcd for $\text{C}_9\text{H}_{13}\text{NO}_3\text{Na}$, 206.0793; found 206.0796.



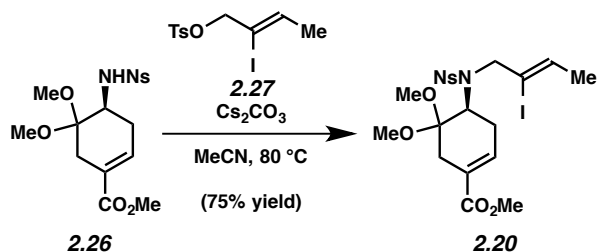
Bicyclic Lactam 2.24. To a solution of amide **2.23** (0.900 g, 4.92 mmol) in THF (117 mL) was added a solution of *n*-butyllithium (*n*-BuLi) (2.7 mL, 2.46 M in hexanes) at -50 °C. The solution

was stirred for 30 min, and then a solution of 2-nitrobenzenesulfonyl chloride (NsCl) (1.634 g, 7.38 mmol) in THF (8 mL) was added. After stirring for 30 min at $-50\text{ }^{\circ}\text{C}$, the reaction was quenched by the addition of a solution of saturated aqueous NH_4Cl (10 mL) and warmed to room temperature. The reaction was then poured into brine (50 mL) and extracted with CH_2Cl_2 (3 x 100 mL). The combined organic layers were dried over MgSO_4 , filtered, and evaporated under reduced pressure. The resulting residue was purified via flash chromatography (2:1 hexanes:EtOAc) to afford lactam **2.24** (1.630 g, 90% yield) as a white solid. Lactam **2.24**: mp: 154–156 $^{\circ}\text{C}$; R_f 0.52 (3:1 benzene:EtOAc); ^1H NMR (500 MHz, CDCl_3): δ 8.48 (m, 1H), 7.76–7.72 (m, 3H), 6.74 (ddd, $J = 7.6, 6.0, 1.6$, 1H), 6.33 (ddd, $J = 7.7, 6.2, 1.6$, 1H), 5.25 (dd, $J = 6.0, 1.7$, 1H), 3.39 (s, 3H), 3.37 (m, 1H), 3.27 (s, 3H), 2.10 (dd, $J = 13.2, 2.6$, 1H), 1.85 (dd, 13.2, 3.2, 1H); ^{13}C NMR (125 MHz, CDCl_3): δ 170.8, 148.0, 134.8, 134.6, 133.3, 132.3, 132.2, 130.6, 124.6, 105.5, 58.2, 49.8, 49.6, 45.2, 33.4; IR (film): 3102, 2950, 2839, 1726, 1541, 1441, 1367, 1264, 1229, 1177, 1135, 1117, 1092, 1061, 1040; HRMS–ESI (m/z) $[\text{M} + \text{H}]^+$ calcd for $\text{C}_{15}\text{H}_{17}\text{N}_2\text{O}_7\text{S}^+$, 369.07510; found 369.07382.



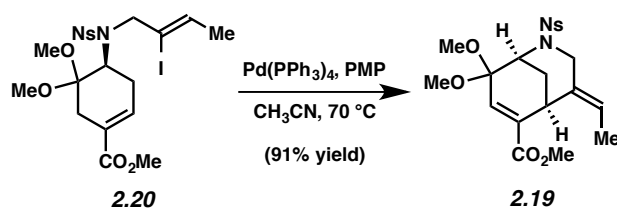
Enoate 2.26. To a solution of lactam **2.24** (1.630 g, 4.43 mmol) in MeOH (70 mL) was added 1,5,7-triazabicyclo[4.4.0]dec-5-ene (**2.25**) (0.739 g, 5.31 mmol) at room temperature. After 1 h, the reaction was diluted with EtOAc (50 mL) and poured into a solution of saturated aqueous NH_4Cl (75 mL). The layers were separated, and the aqueous layer was extracted with EtOAc (3 x 75 mL). The combined organic layers were dried over MgSO_4 , filtered, and evaporated under

reduced pressure. The resulting residue was purified via flash chromatography (2:1 hexanes:EtOAc) to afford enoate **2.26** (1.292 g, 73% yield) as a colorless oil. Enoate **2.26**: R_f 0.47 (3:1 benzene:EtOAc); $^1\text{H NMR}$ (500 MHz, CDCl_3): δ 8.16 (dd, $J = 7.6, 1.9$, 1H), 7.91 (m, 1H), 7.75 (m, 2H), 6.68 (s, 1H), 5.58 (d, $J = 7.0$, 1H), 3.81 (m, 1H), 3.74 (s, 3H), 3.11 (s, 3H), 2.89 (s, 3H), 2.69 (d, $J = 18.3$, 1H), 2.60 (br. s, 2H), 2.35 (dq, $J = 18.3, 2.3$, 1H); $^{13}\text{C NMR}$ (125 MHz, CDCl_3): δ 166.5, 147.8, 135.9, 135.1, 133.4, 132.9, 131.1, 127.0, 125.5, 99.4, 52.1, 51.5, 48.6, 48.1, 31.5, 29.4; IR (film): 3298, 3098, 2951, 2836, 1714, 1541, 1438, 1362, 1263, 1166, 1126, 1081, 1061; HRMS–ESI (m/z) $[\text{M} - \text{H}]^-$ calcd for $\text{C}_{16}\text{H}_{19}\text{N}_2\text{O}_8\text{S}^-$, 399.08676; found 399.08626.



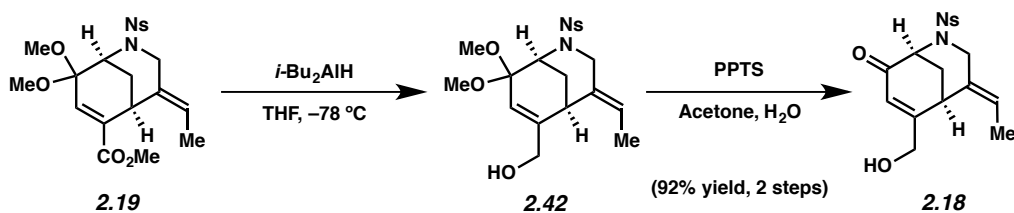
Iodide 2.20. To a solution of enoate **2.26** (0.349 g, 0.983 mmol) in MeCN (9.8 mL) was added tosylate **2.27** (1.300 g, 3.83 mmol)²⁷ and Cs_2CO_3 (0.417 g, 1.28 mmol). The reaction mixture was heated to 80 °C. After 3.5 h, the reaction was cooled to room temperature and the solvent was removed under reduced pressure. The residue was redissolved in CH_2Cl_2 (50 mL) and poured into a solution of saturated aqueous NH_4Cl (50 mL). The layers were separated, and the aqueous layer was extracted with CH_2Cl_2 (3 x 50 mL). The combined organic layers were dried over MgSO_4 , filtered, and evaporated under reduced pressure. The resulting residue was purified via flash chromatography (4:1 hexanes:EtOAc \rightarrow 2:1 hexanes:EtOAc) to afford iodide **2.20** (0.393 g, 75% yield) as a pale yellow oil. Iodide **2.20**: R_f 0.44 (2:1 hexanes:EtOAc); $^1\text{H NMR}$ (500

MHz, CDCl₃): δ 7.96 (dd, *J* = 7.8, 1.3, 1H), 7.69–7.59 (m, 3H), 6.97 (m, 1H), 6.01 (qt, *J* = 6.4, 1.4, 1H), 4.47 (dt, *J* = 16.9, 1.4, 1H), 4.42 (t, *J* = 6.92, 1H), 4.37 (dt, *J* = 16.9, 1.7, 1H), 3.75 (s, 3H), 3.30 (s, 3H), 3.24 (s, 3H), 2.89–2.79 (m, 2H), 2.74 (m, 1H), 2.60 (dq, *J* = 18.1, 2.6, 1H), 1.62 (dt, *J* = 6.4, 1.2, 3H); ¹³C NMR (125 MHz, CDCl₃): δ 166.8, 147.9, 138.7, 135.5, 134.0, 133.3, 132.4, 131.5, 126.7, 124.4, 106.0, 100.0, 57.4, 56.6, 52.1, 51.0, 49.5, 30.8, 30.2, 22.0; IR (film): 2950, 2838, 1713, 1657, 1543, 1437, 1372, 1266, 1163, 1125, 1077; HRMS–ESI (*m/z*) [M + H]⁺ calcd for C₂₀H₂₆N₂O₈S⁺, 581.04491; found 581.04118.



Enoate 2.19. In the glovebox, tetrakis(triphenylphosphine)palladium [Pd(PPh₃)₄] was added to a 500 mL round-bottom flask. The flask was removed from the glovebox, and a solution of iodide **2.20** (0.843 g, 1.45 mmol) in MeCN (104 mL) was added, followed by 1,2,2,6,6-pentamethylpiperidine (PMP) (0.676 g, 4.36 mmol). The reaction mixture was sparged with N₂ for 10 min, and heated to 70 °C. After 16 h, the reaction mixture was cooled to room temperature and the solvent was removed under reduced pressure. The residue was redissolved in CH₂Cl₂ (40 mL) and poured into H₂O (40 mL). The layers were separated, and the aqueous layer was extracted with CH₂Cl₂ (3 x 40 mL). The combined organic layers were dried over MgSO₄, filtered, and evaporated under reduced pressure. The resulting residue was purified via flash chromatography (4:1 hexanes:EtOAc → 2:1 hexanes:EtOAc) to afford enoate **2.19** (0.597 g, 91% yield) as a pale yellow oil. Enoate **2.19**: R_f 0.44 (2:1 hexanes:EtOAc); ¹H NMR (500 MHz, CDCl₃): δ 8.04 (d, *J* = 7.5, 1H), 7.64 (m, 3H), 7.02 (s, 1H), 5.40 (q, *J* = 6.7, 1H), 4.40 (s, 1H),

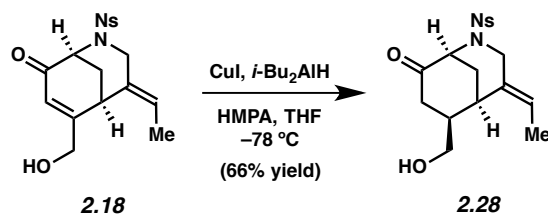
3.92 (d, $J = 14.8$, 1H), 3.86 (d, $J = 14.8$, 1H), 3.83 (t, $J = 2.8$, 1H), 3.73 (s, 3H), 3.28 (s, 3H), 3.27 (s, 3H), 2.06 (dt, $J = 13.1$, 2.8, 1H), 1.79 (dt, $J = 13.1$, 2.8, 1H), 1.67 (d, $J = 6.7$, 3H); ^{13}C NMR (125 MHz, CDCl_3): δ 166.0, 148.1, 135.9, 134.5, 134.3, 133.3, 131.4, 131.1, 130.1, 124.2, 123.1, 96.3, 52.4, 52.2, 49.4, 49.3, 47.4, 30.7, 30.4, 12.8; IR (film): 2950, 2857, 1720, 1543, 1438, 1372, 1356, 1248, 1163, 1123, 1076, 1042; HRMS–ESI (m/z) $[\text{M} + \text{H}]^+$ calcd for $\text{C}_{20}\text{H}_{25}\text{N}_2\text{O}_8\text{S}^+$, 453.13261; found 453.12936.



Enone 2.18. To a solution of enoate **2.19** (0.560 g, 1.24 mmol) in THF (8.3 mL) was added diisobutylaluminum hydride (*i*-Bu₂AlH) (4.95 mL, 1M in hexanes) at -78 °C. After 4 h, the reaction was quenched with a solution of saturated aqueous NH₄Cl (10 mL) and warmed to room temperature. The mixture was then poured into a solution of saturated aqueous sodium potassium tartrate (Rochelle's salt) (10 mL) and stirred vigorously for 30 min. The mixture was extracted with EtOAc (3 x 50 mL) and the organic layers were combined, dried over MgSO₄, filtered, and evaporated under reduced pressure afforded alcohol **2.42**, which was used in the subsequent step without further purification.

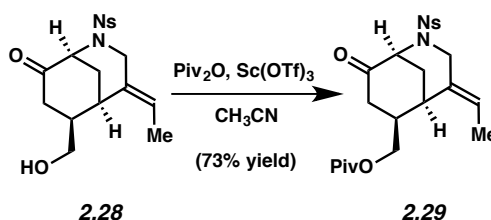
To a solution of alcohol **2.42** (0.526 g, 1.24 mmol) in acetone (13.6 mL) and H₂O (0.7 mL) was added pyridinium *p*-toluenesulfonate (PPTS) (0.062 g, 0.248 mmol). The reaction mixture was heated to 40 °C. After 1.5 h, the reaction was poured into a solution of saturated aqueous NH₄Cl (10 mL) and the mixture was extracted with EtOAc (3 x 40 mL). The combined organic layers were dried over MgSO₄, filtered, and evaporated under reduced pressure. The

resulting residue was purified via flash chromatography (1:2 hexanes:EtOAc) to afford enone **2.18** (0.431 g, 92% yield, 2 steps) as a colorless foam. Enone **2.18**: R_f 0.34 (1:2 hexanes:EtOAc); ^1H NMR (500 MHz, CDCl_3): δ 8.14 (dd, $J = 2.0, 7.3$, 1H), 7.70 (m, 2H), 7.61 (dd, $J = 2.0, 7.4$, 1H), 6.28 (s, 1H), 5.68 (q, $J = 7.0$, 1H), 4.44 (br. s, 1H), 4.33 (d, $J = 17.4$, 1H), 4.20 (d, $J = 15.2$, 2H), 3.86 (dt, $J = 2.2, 14.5$, 1H), 3.56 (t, $J = 3.2$, 1H), 2.31 (dt, $J = 13.2, 3.4$, 1H), 2.20 (dt, $J = 13.2, 3.0$, 1H), 1.74 (dd, $J = 1.9, 6.8$, 3H); ^{13}C NMR (125 MHz, CDCl_3): δ 192.7, 165.2, 148.2, 133.8, 133.4, 132.0, 131.9, 129.7, 124.3, 124.11, 124.10, 63.5, 56.7, 47.4, 34.1, 32.4, 13.0; IR (film): 3432, 2926, 1676, 1542, 1440, 1370, 1281, 1164, 1127, 1073; HRMS–ESI (m/z) [$M + \text{H}$] $^+$ calcd for $\text{C}_{17}\text{H}_{19}\text{N}_2\text{O}_6\text{S}^+$, 379.09583; found 379.09474.



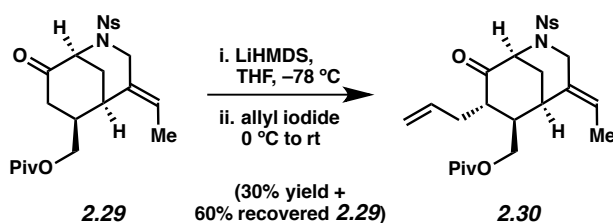
Hydroxyketone 2.28. To a solution of copper iodide (CuI) (0.500 g, 2.62 mmol) in hexamethylphosphoramide (HMPA) (1mL) and THF (8 mL) was added diisobutylaluminum hydride ($i\text{-Bu}_2\text{AlH}$) (5.24 mL, 1 M in hexanes) at $-78\text{ }^\circ\text{C}$. The solution was stirred for 30 min at which point a solution of enone **2.18** (0.395 g, 1.05 mmol) in THF (3 mL) was added at $-78\text{ }^\circ\text{C}$. After 2 h, the reaction was quenched with a solution of saturated aqueous NH_4Cl (10 mL) and allowed to warm to room temperature. The mixture was filtered over a pad of celite and washed with EtOAc (5 x 30 mL). The mixture was then poured into a solution of saturated aqueous sodium potassium tartrate (Rochelle's salt) (100 mL) and stirred vigorously for 30 min. The layers were separated and the aqueous layer was extracted with EtOAc (3 x 100 mL). The combined organic layers were dried over MgSO_4 , filtered, and evaporated under reduced

pressure. The resulting residue was purified via flash chromatography (2:1 hexanes:EtOAc → 1:1 hexanes:EtOAc) to afford hydroxyketone **2.28** (0.261 g, 66% yield) as a colorless foam. Hydroxyketone **2.28**: R_f 0.12 (1:2 hexanes:EtOAc); $^1\text{H NMR}$ (500 MHz, CDCl_3): δ 8.08 (m, 1H), 7.71 (m, 2H), 7.63 (m, 1H), 5.72 (q, $J = 7.0$, 1H), 4.27 (d, $J = 14.8$, 1H), 4.26 (app. s, 1H), 4.13 (dt, $J = 14.8$, 2.1, 1H), 3.55 (m, 2H), 3.20 (q, $J = 3.1$, 1H), 2.56 (d, $J = 13.2$, 1H), 2.30 (m, 2H), 2.19 (dt, $J = 14.0$, 3.6, 1H), 2.01 (dt, $J = 14.0$, 3.0, 1H), 1.74 (dd, $J = 7.0$, 1.8, 3H); $^{13}\text{C NMR}$ (125 MHz, CDCl_3): δ 205.3, 134.2, 134.1, 132.3, 132.2, 132.0, 130.8, 124.6, 124.3, 65.3, 59.0, 50.1, 44.2, 41.8, 33.9, 29.6, 13.1; IR (film): 3472, 2924, 1717, 1542, 1440, 1370, 1248, 1165, 1073, 1033; HRMS–ESI (m/z) [$\text{M} + \text{H}$] $^+$ calcd for $\text{C}_{17}\text{H}_{21}\text{N}_2\text{O}_6\text{S}^+$, 381.11148; found 381.10923.



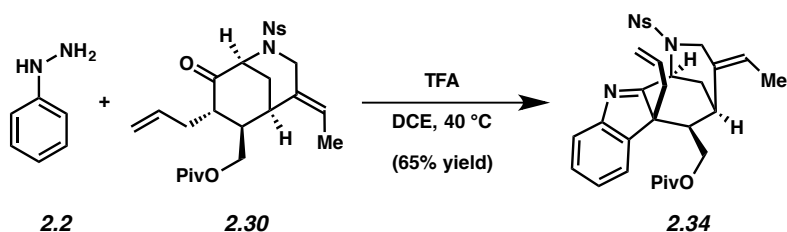
Pivaloate 2.29. To a solution of ketone **2.28** (59 mg, 0.16 mmol) in MeCN (1 mL) was added pivalic anhydride (Piv_2O) (86 mg, 0.47 mmol) and scandium triflate [$\text{Sc}(\text{OTf})_3$] (8.0 mg, 0.016 mmol). After 10 min, the solvent was removed under reduced pressure. The resulting residue was redissolved in CH_2Cl_2 (20 mL) and poured into a solution of saturated aqueous NH_4Cl (10 mL). The layers were separated, and the aqueous layer was extracted with CH_2Cl_2 (3 x 30 mL). The combined organic layers were dried over MgSO_4 , filtered, and evaporated under reduced pressure. The resulting residue was purified via flash chromatography (5:1 hexanes:EtOAc → 1:1 hexanes:EtOAc) to afford pivaloate **2.29** (54 mg, 73% yield) as a colorless foam. Pivaloate **2.29**: R_f 0.62 (3:2 hexanes:EtOAc); $^1\text{H NMR}$ (500 MHz, CDCl_3): δ 8.08 (m, 1H), 7.71 (m, 2H), 7.64 (m, 1H), 5.73 (q, $J = 6.95$, 1H), 4.27 (m, 2H), 4.15 (dt, $J = 15.2$, 2.2, 1H), 3.98 (dd, $J = 11.2$,

6.9, 1H), 3.91 (dd, $J = 11.2, 6.5$, 1H), 3.12 (app. q, $J = 3.6$, 1H), 2.58 (dd, $J = 15.9, 5.9$, 1H) 2.46 (m, 1H), 2.32 (dd, $J = 15.9, 12.9$, 1H), 2.20 (dt, $J = 14.0, 3.6$, 1H), 2.02 (dt, $J = 14.0, 3.1$, 1H), 1.68 (dd, $J = 6.9, 1.7$, 3H), 1.18 (s, 9H); ^{13}C NMR (125 MHz, CDCl_3): (19 of 20 observed) δ 204.4, 178.4, 148.1, 134.1, 132.2, 132.0, 129.8, 124.9, 124.3, 66.2, 58.7, 49.9, 42.0, 41.1, 38.9, 33.7, 29.8, 27.3, 13.2; IR (film): 2959, 2928, 1721, 1543, 1367, 1282, 1164, 1128; HRMS–ESI (m/z) $[\text{M} + \text{H}]^+$ calcd for $\text{C}_{22}\text{H}_{29}\text{N}_2\text{O}_7\text{S}^+$, 465.16900; found 465.16831.



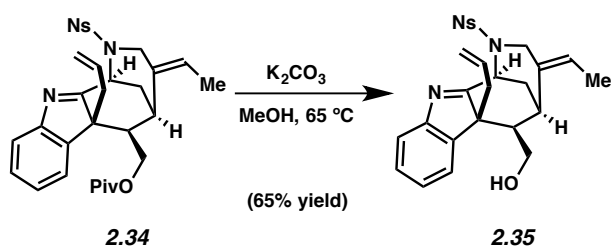
Ketone 2.30. To a solution of pivaloate **2.29** (78 mg, 0.167 mmol) in THF (2 mL) was added a solution of lithium hexamethyldisilazide (LHMDS) (0.028 g, 0.167 mmol) in THF (1.3 mL) at $-78\text{ }^\circ\text{C}$. After 30 min, the solution was warmed to $0\text{ }^\circ\text{C}$ and stirred for 1 h. Allyl iodide ($15.2\text{ }\mu\text{L}$, 0.167 mmol) was then added at $0\text{ }^\circ\text{C}$ and the reaction mixture was allowed to warm to room temperature. After 3 h, the reaction mixture was poured into a solution of saturated aqueous NH_4Cl (10 mL). The layers were separated, and the aqueous layer was extracted with CH_2Cl_2 (3 x 20 mL). The combined organic layers were dried over MgSO_4 , filtered, and evaporated under reduced pressure. The resulting residue was purified via flash chromatography (4:1 hexanes:EtOAc \rightarrow 2:1 hexanes:EtOAc) to afford ketone **2.30** (25 mg, 30% yield) as a colorless foam and recovered pivaloate **2.29** (47 mg, 60% yield). Ketone **2.30**: R_f 0.68 (3:2 hexanes:EtOAc); ^1H NMR (500 MHz, CDCl_3): δ 8.07 (m, 1H), 7.70 (m, 2H), 7.61 (m, 2H), 5.69 (q, $J = 6.6$, 1H), 5.58 (m, 1H), 4.98 (dq, $J = 17.2, 1.5$, 1H), 4.95 (d, $J = 10.2$, 1H), 4.31 (t, $J = 3.3$, 1H), 4.30 (d, $J = 14.5$, 1H), 4.21 (dt, $J = 14.5, 2.2$, 1H), 4.20 (dd, $J = 11.5, 2.4$, 1H), 3.94 (dd, $J =$

11.5, 7.3, 1H), 3.17 (app. q, $J = 3.4$, 1H), 2.57 (ddd, $J = 12.1, 6.4, 3.2$, 1H), 2.45 (dq, $J = 14.5, 1.6$, 1H), 2.30 (m, 1H), 2.20, (m, 1H), 2.14 (dt, $J = 14.0, 3.6$, 1H), 1.97 (dt, $J = 14.0, 3.1$, 1H), 1.68 (dd, $J = 6.9, 1.9$, 3H), 1.19 (s, 9H); ^{13}C NMR (125 MHz, CDCl_3): δ 205.7, 178.4, 148.1, 135.0, 134.1, 132.24, 132.20, 132.0, 130.6, 124.4, 124.2, 117.6, 64.7, 59.1, 50.3, 49.1, 44.9, 38.9, 33.8, 31.5, 31.1, 27.3, 13.0; IR (film): 3077, 2974, 1721, 1545, 1370, 1283, 1165, 1071; HRMS–ESI (m/z) [$M + H$] $^+$ calcd for $\text{C}_{25}\text{H}_{33}\text{N}_2\text{O}_7\text{S}^+$, 505.20030; found 505.20001.



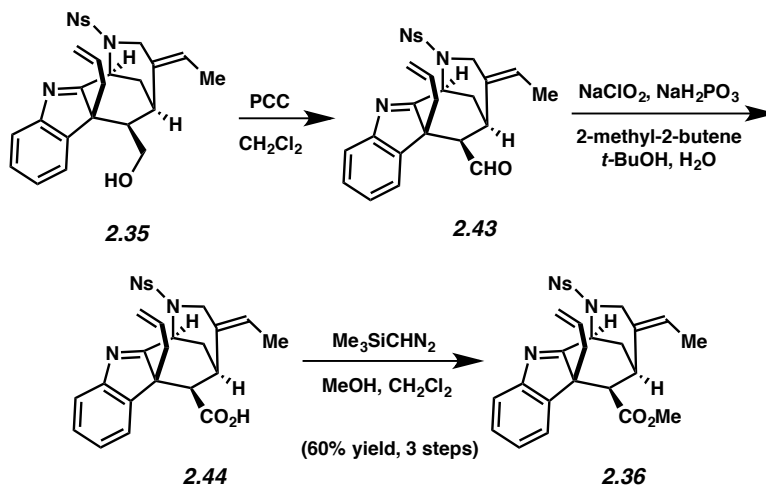
Indolenine 2.34. To a solution of ketone **2.30** (14 mg, 0.028 mmol) in 1,2-dichloroethane (DCE) (0.5 mL) was added phenylhydrazine (**2.2**) (16.4 μL , 0.17 mmol) and trifluoroacetic acid (TFA) (43 μL , 0.56 mmol). The reaction mixture was heated to 40 $^\circ\text{C}$. After 24 h, the reaction was diluted with EtOAc (5 mL) and poured into a solution of saturated aqueous NaHCO_3 (10 mL). The layers were separate, and the aqueous layer was extracted with EtOAc (3 x 15 mL). The combined organic layers were dried over MgSO_4 , filtered, and evaporated under reduced pressure. The resulting residue was purified via flash chromatography (2:1 hexanes:EtOAc \rightarrow 1:2 hexanes:EtOAc) to afford indolenine **2.34** (11 mg, 65% yield) as an orange oil. Indolenine **2.34**: R_f 0.70 (1:2 hexanes:EtOAc); ^1H NMR (500 MHz, CDCl_3): δ 8.17 (m, 1H), 7.74 (m, 2H), 7.68 (d, $J = 7.7$, 1H), 7.63 (m, 1H), 7.45 (d, $J = 7.4$, 1H), 7.36 (td, $J = 7.7, 1.1$, 1H), 7.27 (td, $J = 7.4, 1.1$, 1H), 5.80 (q, $J = 7.2$, 1H), 5.25 (t, $J = 3.2$, 1H), 5.10 (m, 1H), 4.83 (dd, $J = 11.3, 2.5$, 1H), 4.71 (d, $J = 16.8$, 1H), 4.62 (d, $J = 10.1$, 1H), 4.43 (d, $J = 15.1$, 1H), 4.22 (t, $J = 11.2$, 1H), 4.05 (dt, $J = 15.1, 2.6$, 1H), 3.21 (s, 1H), 3.11 (dd, $J = 14.0, 4.6$, 1H), 2.50 (dd, $J = 14.0, 8.9$, 1H),

2.46 (dt, $J = 14.0, 3.6$, 1H), 1.85 (dt, $J = 14.0, 3.0$, 1H), 1.74 (dd, $J = 7.0, 1.9$, 1H), 1.68 (dt, $J = 11.1, 3.0$, 1H), 1.17 (s, 9H); ^{13}C NMR (125 MHz, CDCl_3): δ 183.3, 178.3, 154.1, 148.9, 143.3, 134.1, 131.9, 131.82, 131.77, 131.6, 131.3, 128.4, 126.1, 125.1, 124.3, 123.6, 121.8, 118.4, 62.7, 61.4, 54.8, 51.8, 47.7, 38.9, 36.0, 35.2, 29.0, 27.4, 13.9; IR (film): 2975, 1727, 1545, 1480, 1456, 1441, 1371, 1282, 1164, 1074; HRMS–ESI (m/z) $[\text{M} + \text{H}]^+$ calcd for $\text{C}_{31}\text{H}_{36}\text{N}_3\text{O}_6\text{S}^+$, 578.23193; found 578.23111.



Alcohol 2.35. To a solution of indolenine **2.34** (15 mg, 0.026 mmol) in MeOH (2 mL) was added potassium carbonate (K_2CO_3) (20 mg, 0.14 mmol). The reaction mixture was heated to 65 °C. After 4 h, the reaction was diluted with EtOAc (10 mL), poured into a solution of aqueous NaHSO_4 (10 mL, 0.5 M). The layers were separated, and the aqueous layer was extracted with EtOAc (3 x 10 mL). The combined organic layers were dried over MgSO_4 , filtered, and evaporated under reduced pressure. The resulting residue was purified via flash chromatography (1:3 hexanes:EtOAc) to afford alcohol **2.35** (8 mg, 65% yield) as colorless oil. Alcohol **2.35**: R_f 0.21 (1:2 hexanes:EtOAc); ^1H NMR (500 MHz, CDCl_3): δ 8.15 (m, 1H), 7.72 (m, 2H), 7.67 (d, $J = 7.6$, 1H), 7.61 (m, 1H), 7.38 (d, $J = 7.6$, 1H), 7.35 (dt, $J = 7.6, 1.2$, 1H), 7.23 (dt, $J = 7.6, 1.2$, 1H), 5.78 (q, $J = 7.1$, 1H), 5.23 (t, $J = 3.4$, 1H), 5.10 (m, 1H), 4.70 (d, $J = 16.7$, 1H), 4.61 (d, $J = 10.2$, 1H), 4.41 (d, $J = 15.1$, 1H), 4.07–3.95 (m, 2H), 3.37 (br. s, 1H), 3.10 (ddt, $J = 14.1, 4.8, 1.5$, 1H), 2.43 (m, 2H), 1.88 (dd, $J = 7.1, 2.1$, 3H), 1.82 (dt, $J = 14.1, 3.1$, 1H), 1.48 (dt, $J = 10.4, 3.3$, 1H), 1.36 (dd, $J = 6.4, 3.3$, 1H); ^{13}C NMR (125 MHz, CDCl_3): δ 184.1, 154.2, 148.9, 143.7,

134.0, 132.3, 131.8, 131.7, 131.6, 131.3, 128.3, 125.7, 125.2, 124.2, 123.6, 121.8, 118.2, 61.9, 60.6, 55.9, 55.0, 47.8, 35.9, 35.5, 28.2, 14.3; IR (film): 3422, 3070, 2924, 2840, 1542, 1441, 1371, 1173, 1127, 1074; HRMS–ESI (m/z) [$M + H$]⁺ calcd for C₂₆H₂₈N₃O₅S⁺, 494.17442; found 494.17214.

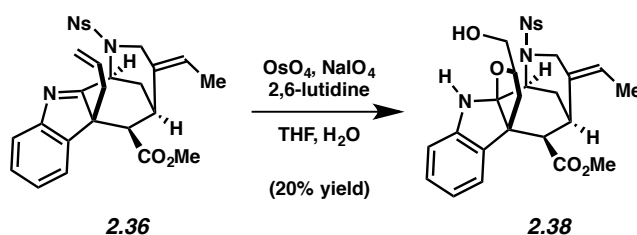


Ester 2.36. To a solution of alcohol **2.35** (4 mg, 0.008 mmol) in CH₂Cl₂ (0.30 mL) was added pyridinium chlorochromate (PCC) (6 mg, 0.028 mmol). After 1 h, celite (0.5 g) was added followed by Et₂O (3 mL). The heterogeneous mixture was filtered over a pad of basic alumina and celite and washed with EtOAc (20 mL). Evaporation of the filtrate under reduced pressure afforded a crude residue of aldehyde **2.43** which was used in the subsequent step without further purification.

To a solution of crude aldehyde **2.43** (4 mg) and 2-methyl-2-butene (0.10 mL) in *t*-BuOH (0.150 mL) at 0 °C was added a solution of sodium chlorite (NaClO₂) (4 mg, 0.040 mmol) and monobasic sodium phosphate (NaH₂PO₄) (6 mg, 0.047 mmol) in H₂O (0.150 mL). After 15 min, the reaction mixture was quenched with AcOH (0.25 mL), diluted with EtOAc (mL), and poured into a brine solution (4 mL). The layers were separated, and the aqueous layer was extracted with

EtOAc (3 x 5 mL). The combined organic layers were dried over MgSO₄, filtered, and evaporated under reduced pressure. The crude residue of acid **2.44** was used in the subsequent step without purification.

To a solution of acid **2.44** (4 mg) in MeOH (0.15 mL) and CH₂Cl₂ (0.25 mL) was added trimethylsilyldiazomethane (Me₃SiCHN₂) (5 μL, 2 M in hexanes). After 15 min, the reaction mixture was quenched with acetic acid (AcOH) (0.25 mL) and concentrated under reduced pressure. The crude residue was purified by preparative TLC (1:1 hexanes:EtOAc) to afford ester **2.36** (2.5 mg, 60% yield over 3 steps) as a colorless oil. Ester **2.36**: R_f 0.42 (1:1 hexanes:EtOAc); ¹H NMR (500 MHz, CDCl₃): 8.19–8.13 (m, 1H), 7.77–7.68 (m, 2H), 7.65 (d, *J* = 7.7, 1H), 7.63–7.60 (m, 1H), 7.35 (d, *J* = 7.5, 1H), 7.33 (t, *J* = 7.7, 1H), 7.21 (t, *J* = 7.5, 1H), 5.76 (q, *J* = 7.2, 1H), 5.29 (t, *J* = 3.1, 1H), 5.13–5.00 (m, 1H), 4.72 (d, *J* = 17.2, 1H), 4.58 (d, *J* = 10.2, 1H), 4.41 (d, *J* = 15.1, 1H), 4.00 (d, *J* = 15.1, 1H), 3.74 (s, 3H), 3.64 (dd, *J* = 14.4, 9.4, 1H), 3.54 (br s, 1H), 3.31 (dd, *J* = 14.4, 4.9, 1H), 2.47 (dt, *J* = 13.9, 3.4, 1H), 2.16 (d, *J* = 3.0, 1H), 1.85 (dt, *J* = 13.9, 3.41, 1H), 1.61 (d, *J* = 7.9, 3H).



Furanoindoline 2.38. To a solution of ester **2.36** (6 mg, 0.012 mmol) in THF (0.40 mL) and H₂O (0.20 mL) was added 2,6-lutidine (5.4 μL, 0.046 mmol) and sodium periodate (NaIO₄) (10 mg, 0.046 mmol) followed by aqueous osmium tetroxide (OsO₄) (25 μL, 0.079 M in H₂O). After 16 h, the reaction was poured into a brine solution (5 mL) and the mixture was extracted with EtOAc (3 x 10 mL). The combined organic layers were dried over MgSO₄, filtered and

evaporated under reduced pressure. The resulting residue was purified via preparative TLC (1:1 hexanes:EtOAc) to afford furanoindoline **2.38** (1.3 mg, 20% yield) as a colorless oil. Furanoindoline **2.38**: R_f 0.45 (1:1 hexanes:EtOAc); ^1H NMR (500 MHz, CDCl_3): δ 8.16 (m, 1H), 7.72 (m, 3H), 7.14 (d, $J = 7.3$, 1H), 7.07 (t, $J = 8.0$, 1H), 6.75 (t, $J = 7.3$, 1H), 6.61 (d, $J = 8.0$, 1H), 5.35 (q, $J = 6.8$, 1H), 4.52 (s, 1H), 4.44 (t, $J = 3.0$, 1H), 4.30 (d, $J = 14.6$, 1H), 4.02 (d, $J = 13.1$, 1H), 3.77 (d, $J = 11.1$, 1H), 3.71 (s, 3H), 3.46 (d, $J = 14.6$, 1H), 3.45 (d, $J = 12.4$, 1H), 3.28 (m, 1H), 3.10 (d, $J = 5.1$, 1H), 3.02 (t, $J = 12.2$, 1H), 2.31 (dd, $J = 13.1, 4.1$, 1H), 2.04 (dt, $J = 13.7, 3.7$, 1H), 2.01 (dt, $J = 13.7, 2.8$, 1H), 1.54 (d, $J = 6.8$, 3H); ^{13}C NMR (125 MHz, CDCl_3): δ 172.0, 147.8, 146.7, 137.0, 133.8, 133.2, 132.2, 132.0, 129.7, 128.6, 125.2, 125.0, 123.3, 119.9, 108.6, 100.7, 80.5, 61.6, 54.7, 54.6, 54.2, 51.8, 48.7, 37.6, 30.4, 30.0, 12.9; IR (film): 3372, 2917, 2849, 2338, 1734, 1608, 1541, 1472, 1319, 1155, 1100; HRMS–ESI (m/z) [$\text{M} + \text{H}$] $^+$ calcd for $\text{C}_{27}\text{H}_{28}\text{N}_3\text{O}_5\text{S}^+$, 556.1748; found 556.1754.

2.8 References

- (1) Baliga, M. S. *Chin. J. Integr. Med.* **2012**, DOI: 10.1007/s11655-011-0947-0.
- (2) Chatterjee, A.; Mukherjee, B.; Ray, A. B.; Das, B. *Tetrahedron Lett.* **1965**, *6*, 3633–3637.
- (3) For X-ray structure of **2.1**, see: (a) Ghosh, R.; Roychowdhury, P.; Chattopadhyay, D.; Iitaka, Y. *Acta Crystallogr.* **1988**, *C44*, 2151–2154. (b) The 3D representation was prepared from the X-ray data of **5** using CYLview. For CYLview, see: (c) Legault, C. Y. CYLview, 1.0b; Université de Sherbrooke: Québec, Montreal, Canada, 2009; <http://www.cylview.org>.
- (4) Shang, J.-H.; Cai, X.-H.; Feng, T.; Zhao, Y.-L.; Wang, J.-K.; Zhang, L.-Y.; Yan, M.; Luo, X.-D. *J. Ethnopharmacol.* **2010**, *129*, 174–181.

- (5) Shang, J.-H.; Cai, X.-H.; Zhao, Y.-L.; Feng, T.; Luo, X.-D. *J. Ethnopharmacol.* **2010**, *129*, 293–298.
- (6) For reviews on the akuammiline alkaloids, see: (a) Ramírez, A.; García–Rubio, S. *Curr. Med. Chem.* **2003**, *10*, 1891–1915. (b) Eckermann, R.; Gaich, T. *Synthesis* **2013**, *45*, 2813–2823. (c) Smith, J. M.; Moreno, J.; Boal, B. W.; Garg, N. K. *Angew. Chem., Int. Ed.* **2015**, *54*, 400–412.
- (7) Smith, J. M.; Moreno, J.; Boal, B. W.; Garg, N. K. *J. Am. Chem. Soc.* **2014**, *136*, 4504–4507.
- (8) Zu, L.; Boal, B. W.; Garg, N. K. *J. Am. Chem. Soc.* **2011**, *133*, 8877–8879.
- (9) For the classic Fischer indole synthesis, see: (a) Fischer, E.; Jourdan, F. *Ber.* **1883**, *16*, 2241–2245. (b) Fischer, E.; Hess, O. *Ber.* **1884**, *17*, 559–568.
- (10) For related examples, see: (a) Boal, B. W.; Schammel, A. W.; Garg, N. K. *Org. Lett.* **2009**, *11*, 3458–3461. (b) Schammel, A. W.; Boal, B. W.; Zu, L.; Mesganaw, T.; Garg, N. K. *Tetrahedron* **2010**, *66*, 4687–4695. (c) Schammel, A. W.; Chiou, G.; Garg, N. K. *J. Org. Chem.* **2012**, *77*, 725–728. (d) Schammel, A. W.; Chiou, G.; Garg, N. K. *Org. Lett.* **2012**, *14*, 4556–4559. (e) Bunders, C.; Cavanaugh, J.; Melander, C. *Org. Biomol. Chem.* **2011**, *9*, 5476–5481.
- (11) Liu, P.; Wang, J.; Zhang, J.; Qiu, F. G. *Org. Lett.* **2011**, *13*, 6426–6428.
- (12) Zu, L.; Boal, B. W.; Garg, N. K., unpublished results.
- (13) For a study on N–N bond cleavage in Fischer indolization reactions, see: Çelebi-Ölçüm, N.; Boal, B. W.; Hutters, A. D.; Garg, N. K.; Houk, K. N. *J. Am. Chem. Soc.* **2011**, *133*, 5752–5755.
- (14) For a review on the nosyl protecting group, see: Kan, T.; Fukuyama, T. *Chem. Commun.* **2004**, 353–359.
- (15) For examples of the Fischer indolization being employed in late-stage total synthesis of complex alkaloids, see ref 8 in addition to the following: (a) Ban, Y.; Sato, Y.; Inoue, I.; Nagai, M.; Oishi, T.; Terashima, M.; Yonemitsu, O.; Kanaoka, Y. *Tetrahedron Lett.* **1965**, *6*,

2261–2268. (b) Ueda, H.; Satoh, H.; Matsumoto, K.; Sugimoto, K.; Fukuyama, T.; Tokuyama, H. *Angew. Chem., Int. Ed.* **2009**, *48*, 7600–7603. (c) Satoh, H.; Ueda, H.; Tokuyama, H. *Tetrahedron* **2013**, *69*, 89–95.

(16) For reviews of the Heck reaction, see: (a) Dounay, A. B.; Overman, L. E. *Chem. Rev.* **2003**, *103*, 2945–2964. (b) Beletskaya, I. P.; Cheprakov, A. V. *Chem. Rev.* **2000**, *100*, 3009–3066. (c) Amatore, C.; Jutand, A. *J. Organomet. Chem.* **1999**, *576*, 254–278. (d) Heravi, M. M.; Hashemi, E.; Ghobadi, N. *Curr. Org. Chem.* **2013**, *17*, 2192–2224.

(17) For the use of the Heck reaction in the synthesis of *Strychnos* alkaloids, see: (a) Rawal, V. H.; Michoud, C.; Monestel, R. F. *J. Am. Chem. Soc.* **1993**, *115*, 3030–3031. (b) Rawal, V. H.; Iwasa, S. *J. Org. Chem.* **1994**, *59*, 2685–2686. (c) Martin, D. B. C.; Vanderwal, C. D. *J. Am. Chem. Soc.* **2009**, *131*, 3472–3473.

(18) Herdeis, C.; Hartke, C. *Heterocycles* **1989**, *29*, 287–296.

(19) (a) Fessner, W. D.; Sedelmeier, G.; Spurr, P. R.; Rihs, G.; Prinzbach, H. *J. Am. Chem. Soc.* **1987**, *109*, 4626–4642. (b) Snow, R. A.; Degenhardt, C. R.; Paquette, L. A. *Tetrahedron Lett.* **1976**, *17*, 4447–4450.

(20) See Materials and Methods for microwave reactor details.

(21) For an example of aminolysis using TBD, see: Sabot, C.; Kumar, K. A.; Meunier, S.; Mioskowski, C. *Tetrahedron Lett.* **2007**, *48*, 3863–3866.

(22) Rawal, V. H.; Michoud, C. *Tetrahedron Lett.* **1991**, *32*, 1695–1698.

(23) Nagata, H.; Kawamura, M.; Ogasawara, K. *Synthesis* **2000**, *13*, 1825–1834.

(24) Kraus, G. A.; Roth, B. *J. Org. Chem.* **1980**, *45*, 4825–4830.

(25) Sabahi, A.; Novikov, A.; Rainier, J. D. *Angew. Chem., Int. Ed.* **2006**, *45*, 4317–4320.

(26) Hypervalent iodine reagents such as $\text{PhI}(\text{OAc})_2$ and periodic acid were ineffective for this transformation.

(27) Rawal, V. H.; Michoud, C. *Tetrahedron Lett.* **1991**, 32, 1695–1698.

APPENDIX ONE

Spectra Relevant to Chapter Two:

First-Generation Approach to the Total Synthesis of Picrinine

Current Data Parameters
 NAME zls-copper
 EXPNO 2
 PROCNO 1

F2 - Acquisition Parameters
 Date 20110308
 Time 11:48
 INSTRUM avx500
 PROBHD 5 mm broadband
 PULPROG zg30
 TD 65536
 SOLVENT CDCl3
 NS 8
 DS 0
 SWH 10000.000 Hz
 FIDRES 0.152588 Hz
 AQ 3.2768500 sec
 RG 1024
 DW 50.000 usec
 DE 71.43 usec
 TE 300.0 K
 D1 2.00000000 sec
 P1 11.00 usec
 SFO1 500.1330008 MHz
 NUCLEUS 1H

F2 - Processing parameters
 SI 32768
 SF 500.1300182 MHz
 WDW EM
 SSB 0
 LB 0.30 Hz
 GB 0
 PC 1.00

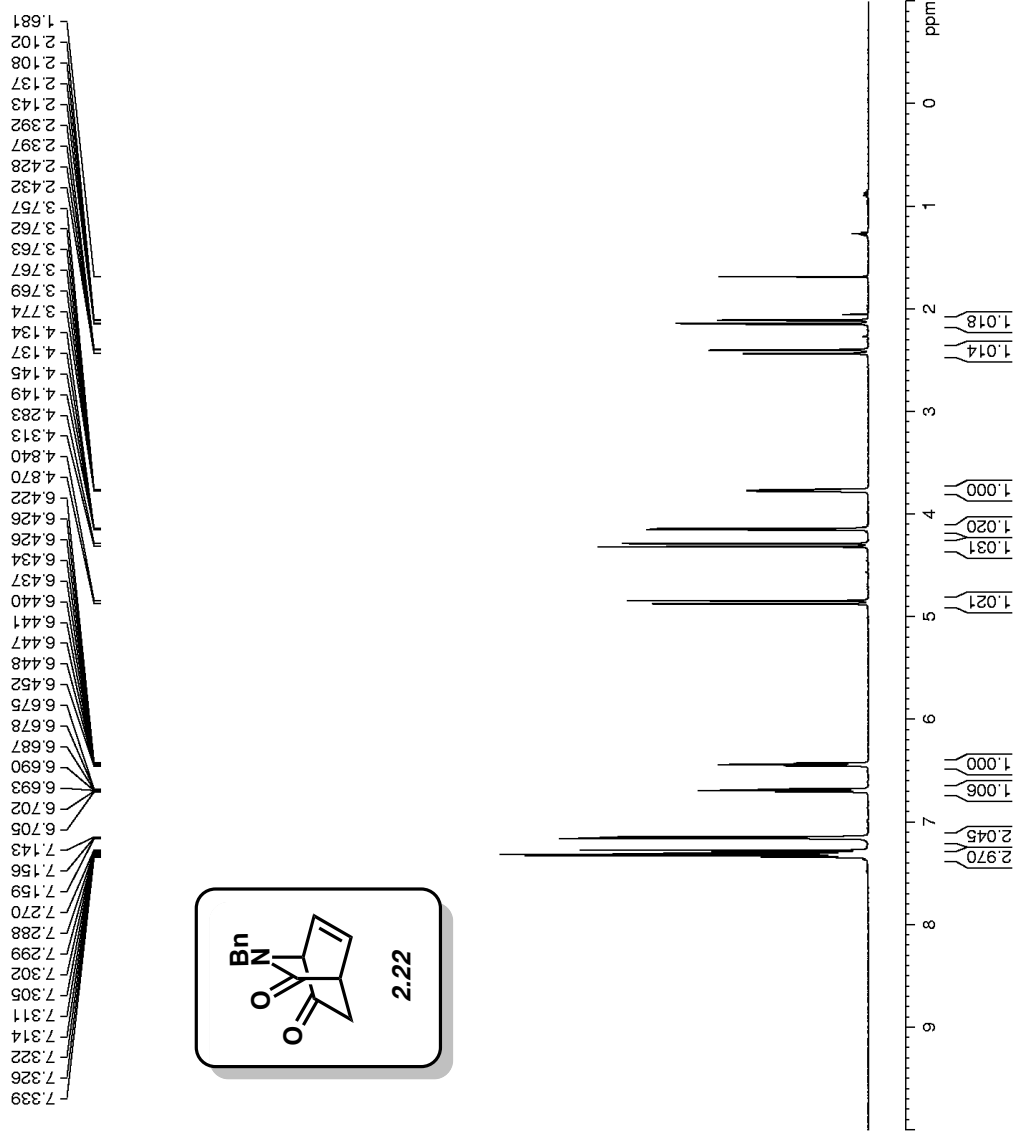


Figure A1.1 ^1H NMR (500 MHz, CDCl_3) of compound 2.22.

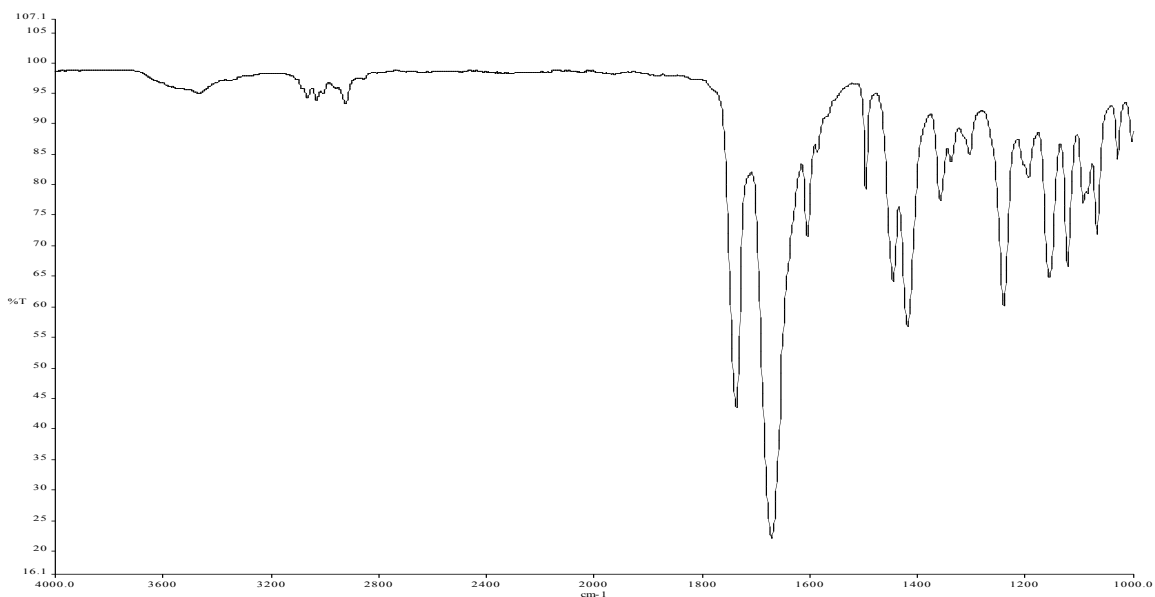


Figure A1.2 Infrared spectrum of compound **2.22**.

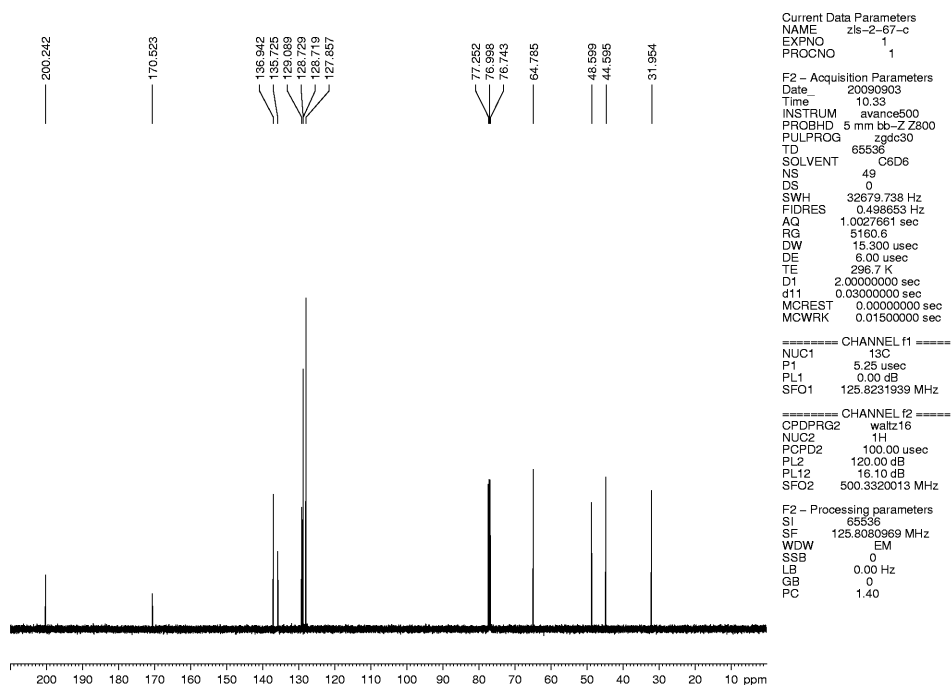


Figure A1.3 ^{13}C NMR (125 MHz, CDCl_3) of compound **2.22**.

Current Data Parameters
 NAME zls-2-206
 EXPNO 1
 PROCNO 1
 F2 - Acquisition Parameters
 Date_ 20100115
 Time 16.32
 INSTRUM ark500
 PROBHD 5 mm broadband
 PULPROG zg30
 TD 65536
 SOLVENT CDCl3
 NS 8
 DS 0
 SWH 10000.000 Hz
 FIDRES 0.152588 Hz
 AQ 3.2768500 sec
 RG 360
 DW 50.000 usec
 DE 71.43 usec
 TE 300.0 K
 D1 2.00000000 sec
 P1 11.00 usec
 SFO1 500.1330008 MHz
 NUCLEUS 1H
 F2 - Processing parameters
 SI 32768
 SF 500.1300186 MHz
 WDW EM
 SSB 0
 LB 0.30 Hz
 GB 0
 PC 1.00

1.917
1.892
1.700
1.675

3.179
3.242
3.295

4.235
4.229

6.444
6.451

7.368
7.270

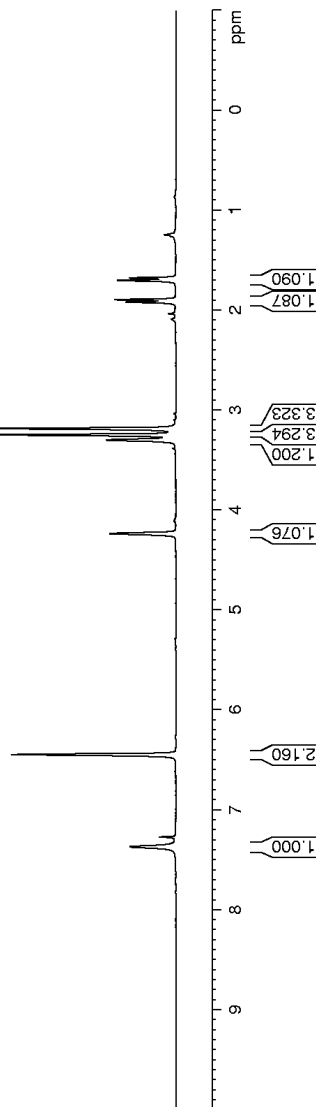
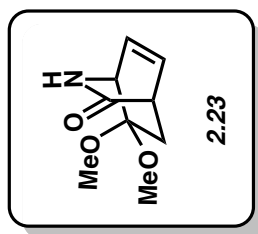


Figure A1.4 ¹H NMR (500 MHz, CDCl₃) of compound 2.23.

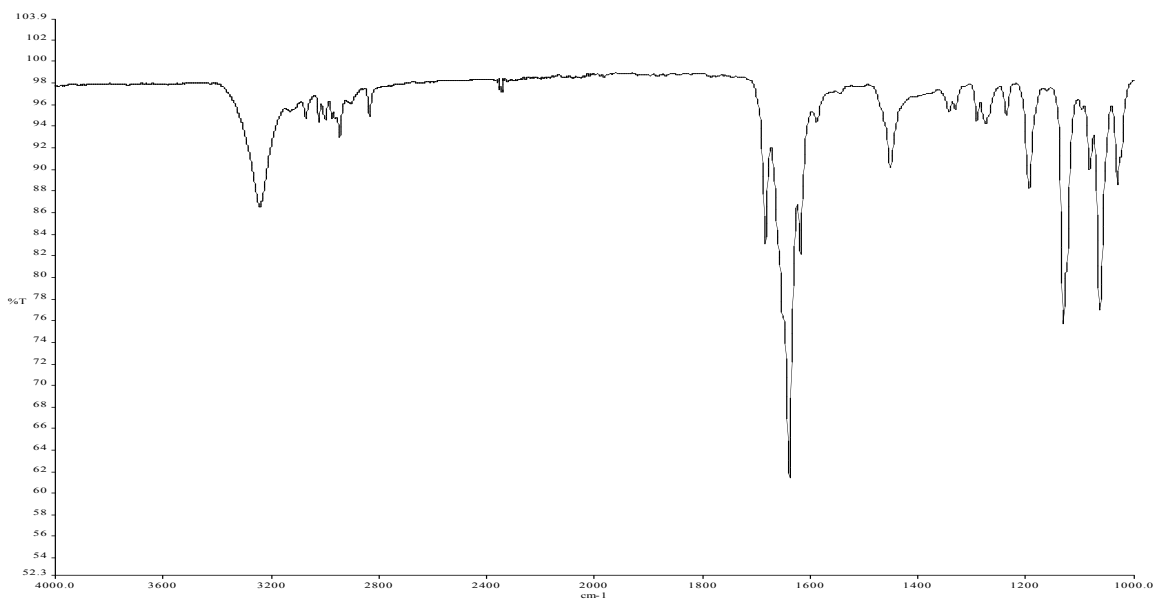


Figure A1.5 Infrared spectrum of compound **2.23**.

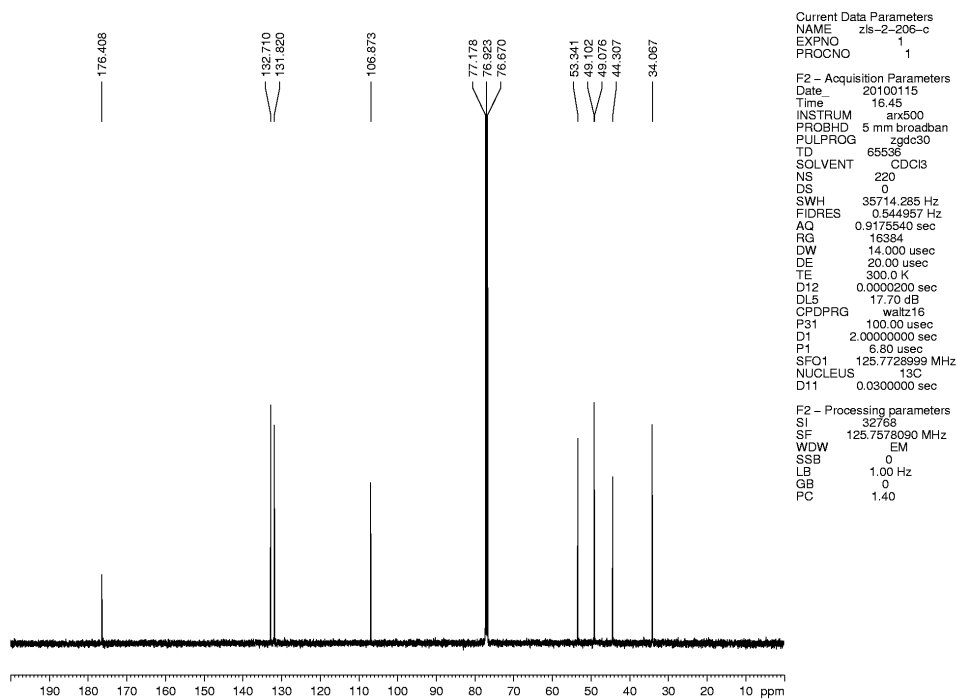


Figure A1.6 ^{13}C NMR (125 MHz, CDCl_3) of compound **2.23**.

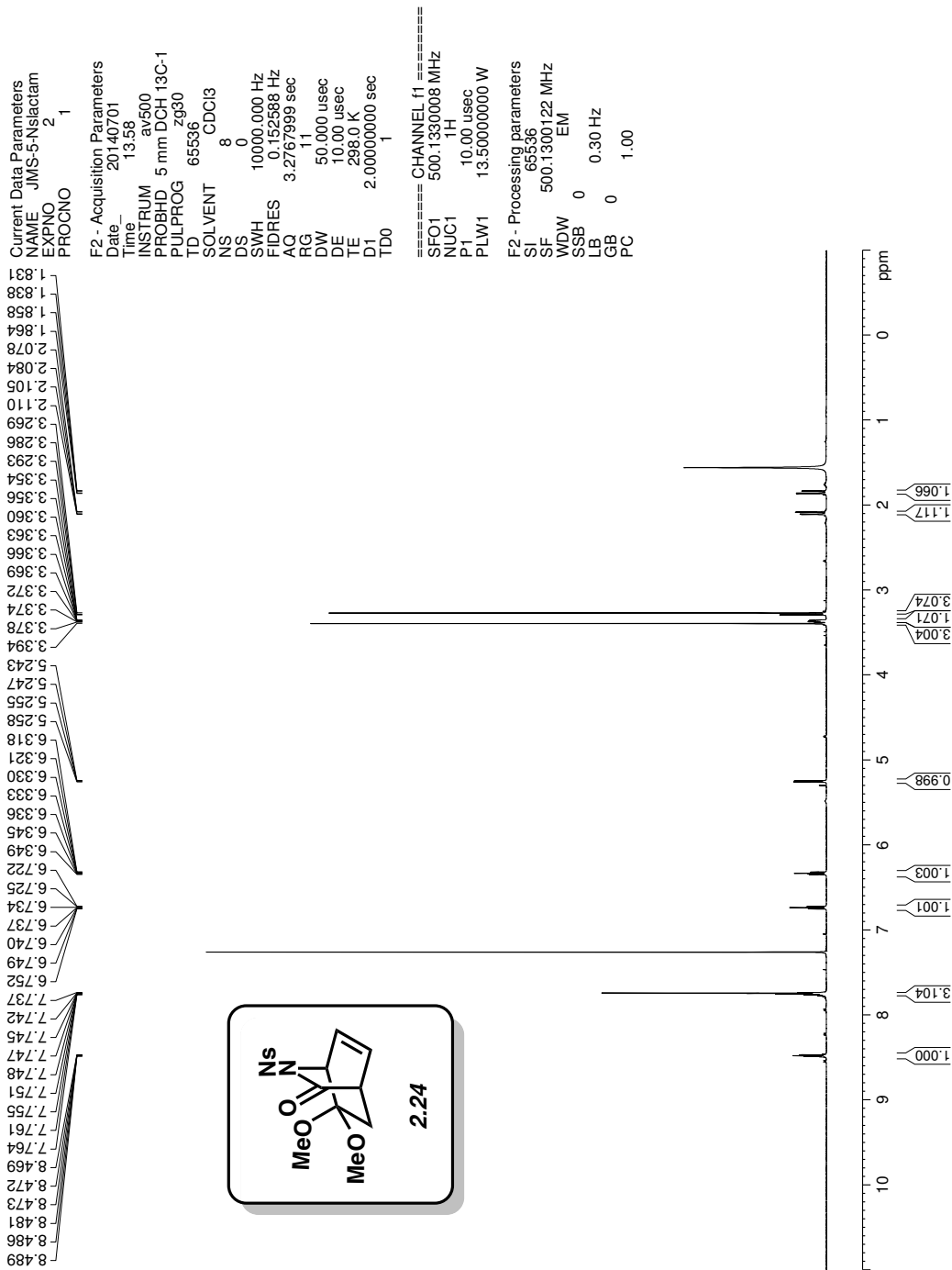


Figure A1.7 ¹H NMR (500 MHz, CDCl₃) of compound 2.24.

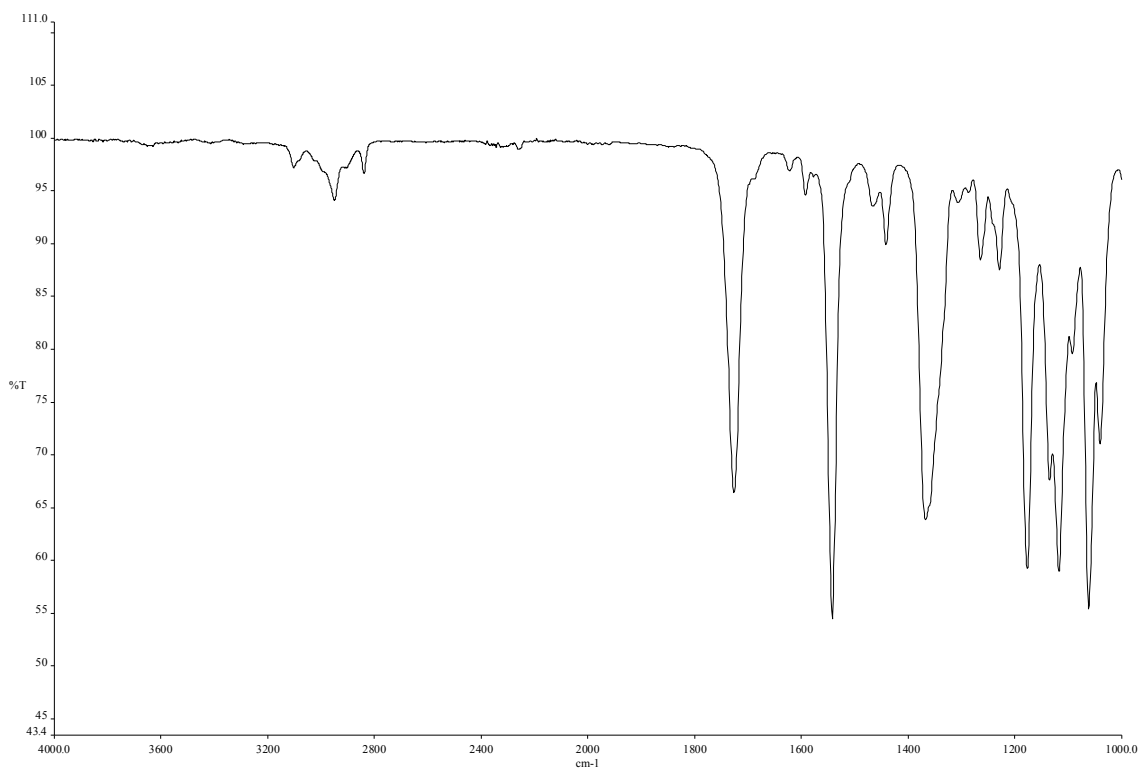


Figure A1.8 Infrared spectrum of compound **2.24**.

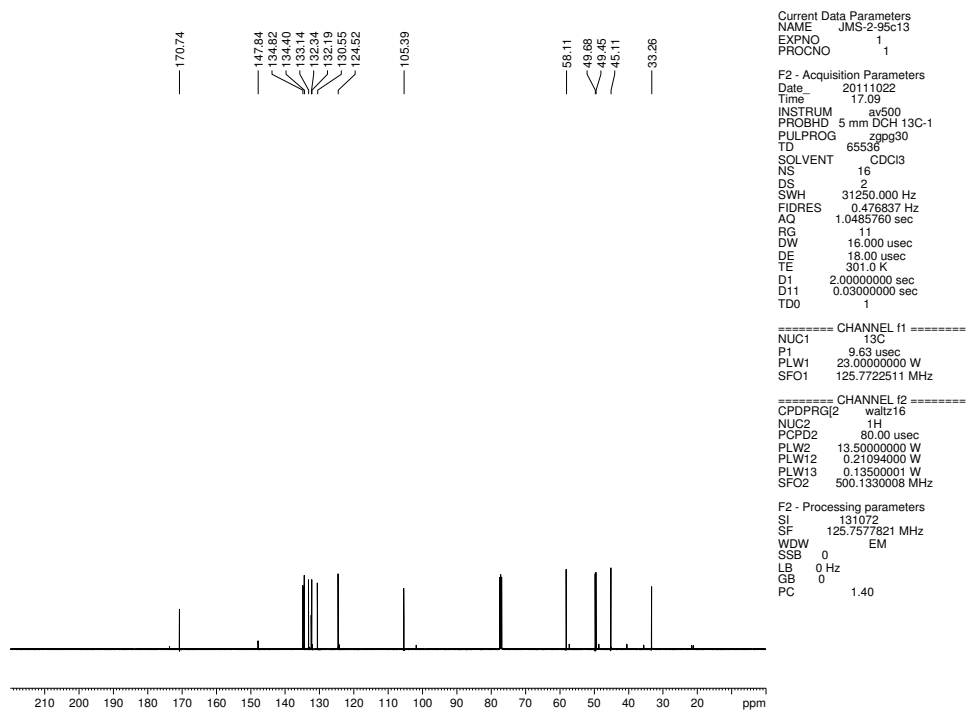


Figure A1.9 ^{13}C NMR (125 MHz, CDCl_3) of compound **2.24**.

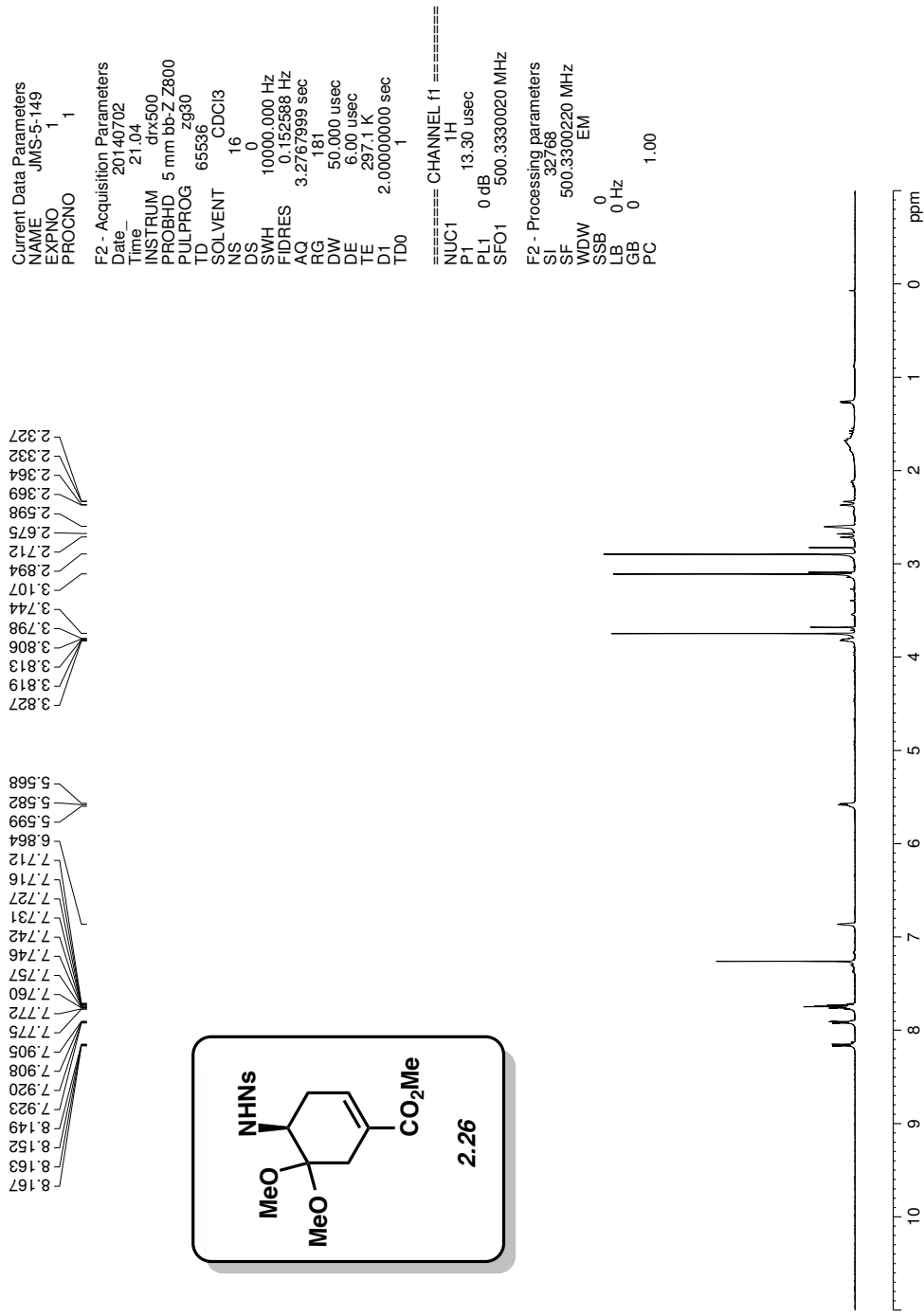


Figure A1.10 ¹H NMR (500 MHz, CDCl₃) of compound 2.26.

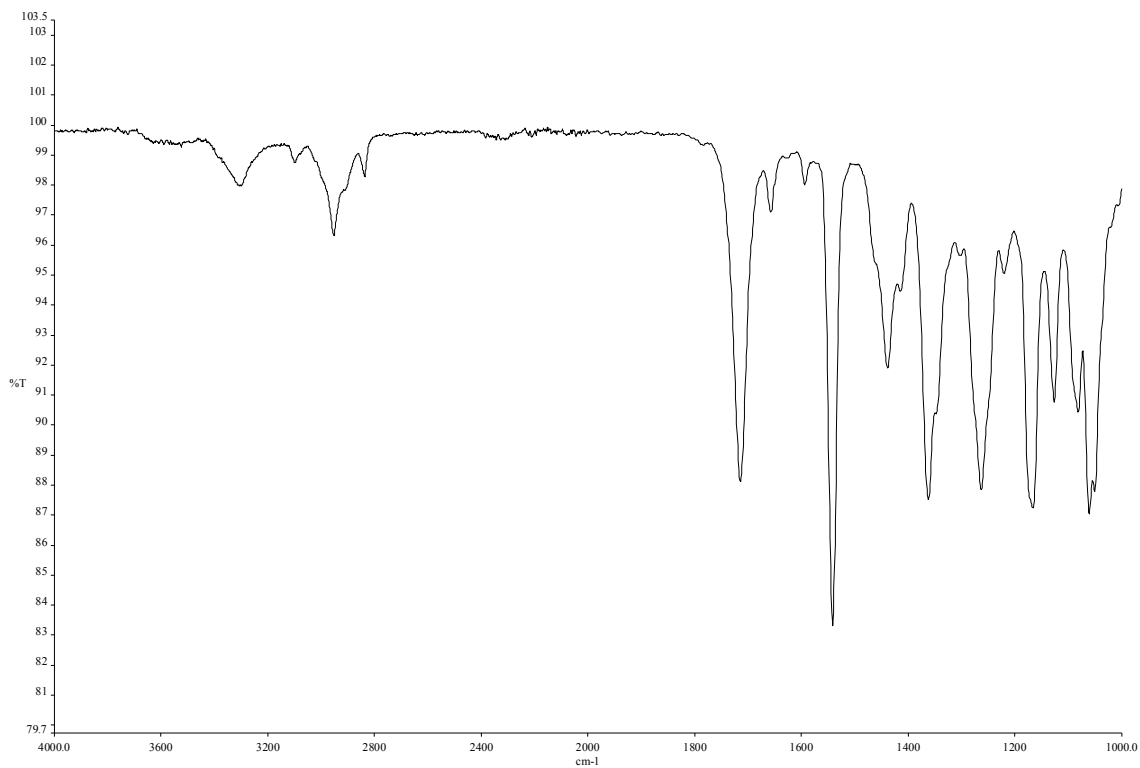


Figure A1.11 Infrared spectrum of compound 2.26.

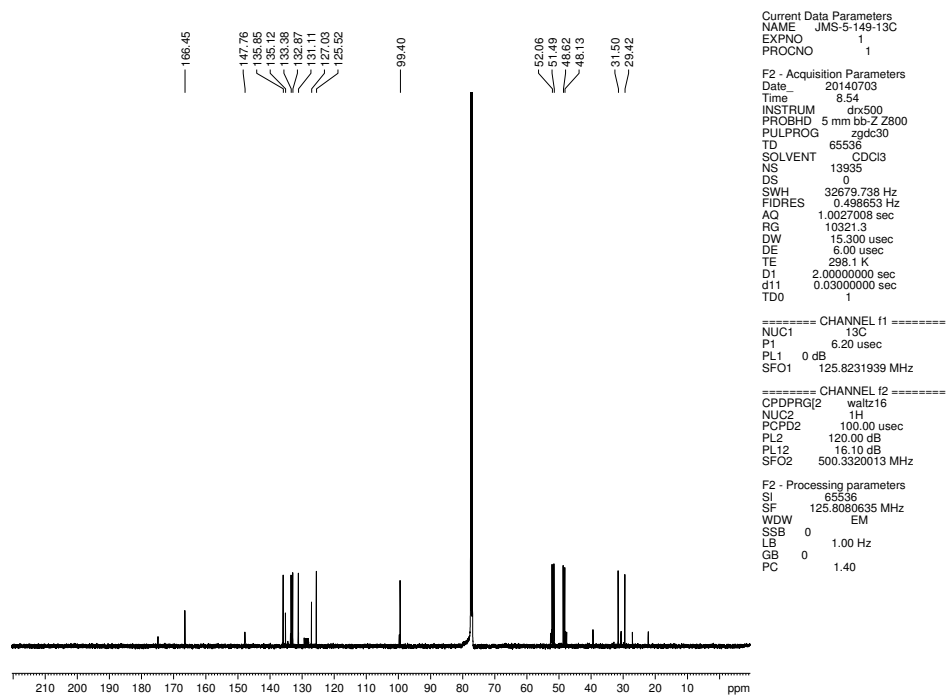


Figure A1.12 ^{13}C NMR (125 MHz, CDCl_3) of compound 2.26.

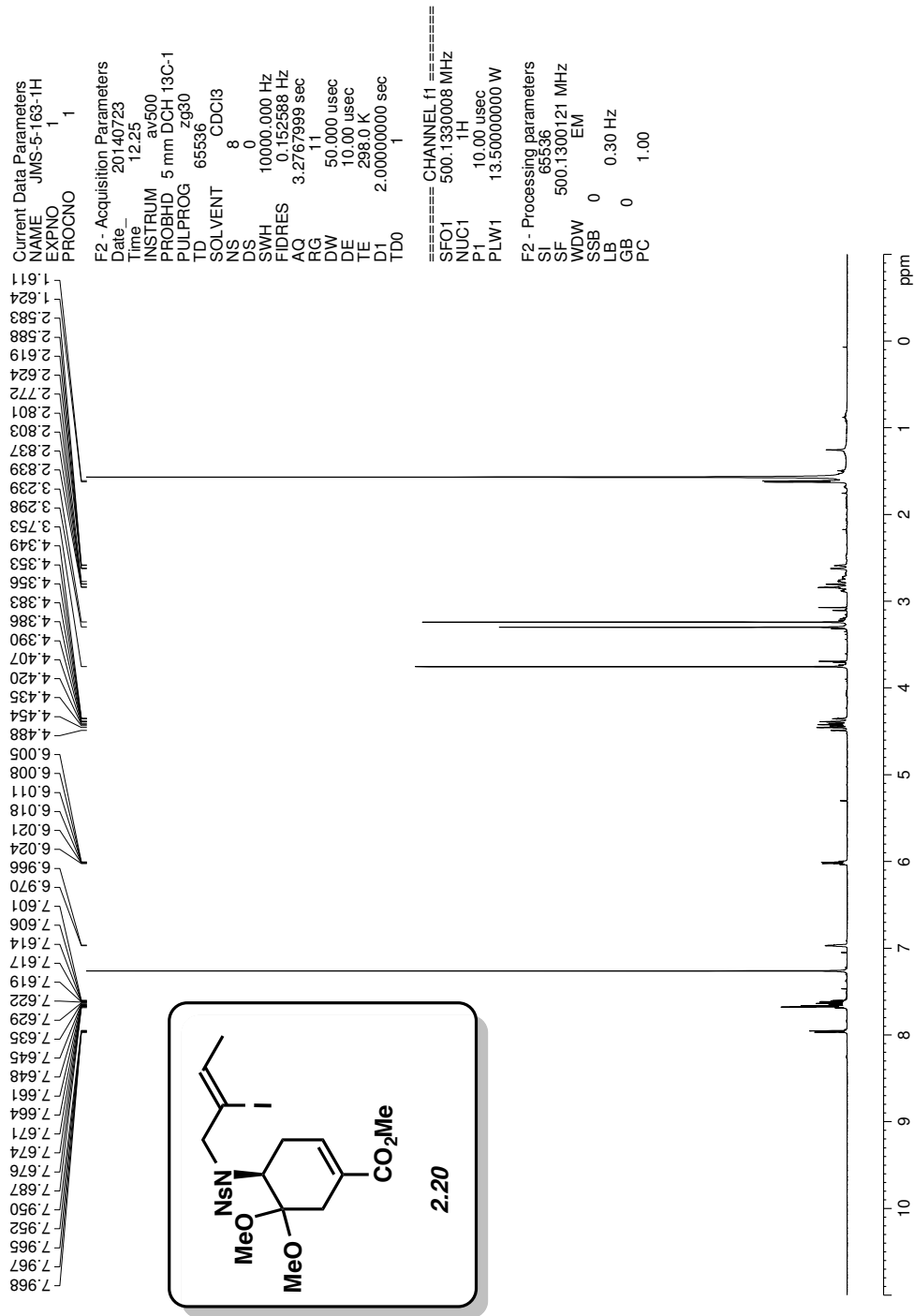


Figure A1.13 ¹H NMR (500 MHz, CDCl₃) of compound 2.20.

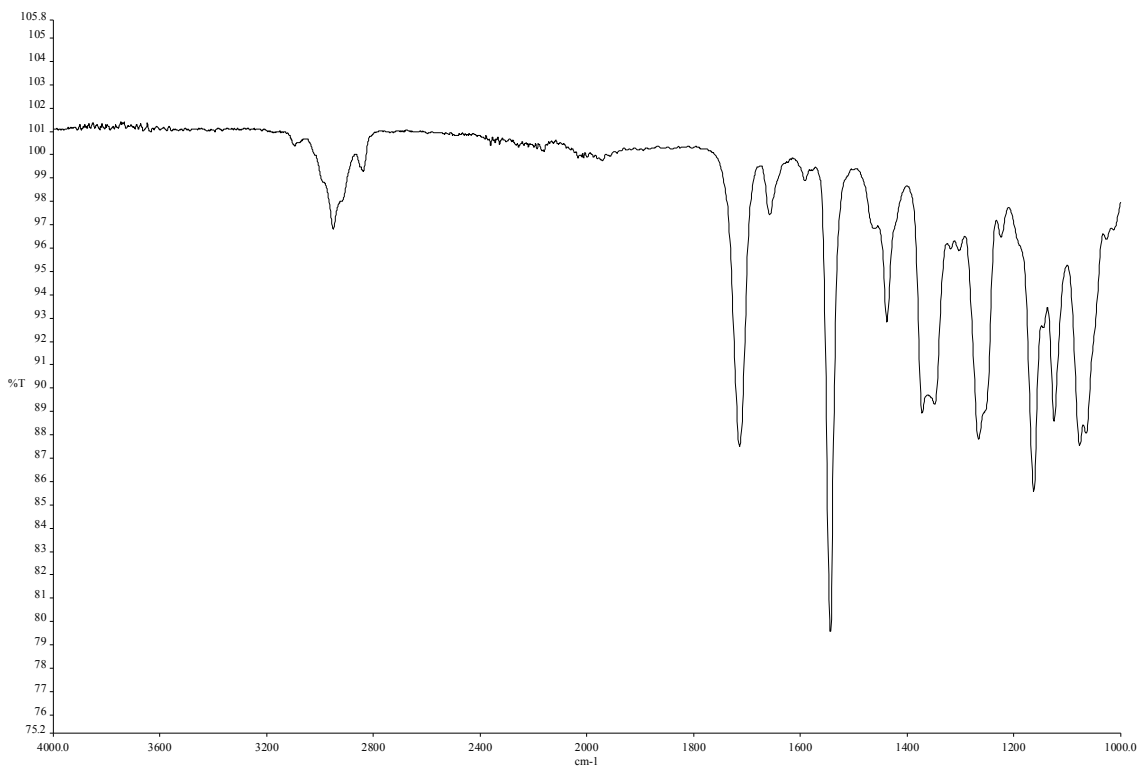


Figure A1.14 Infrared spectrum of compound **2.20**.

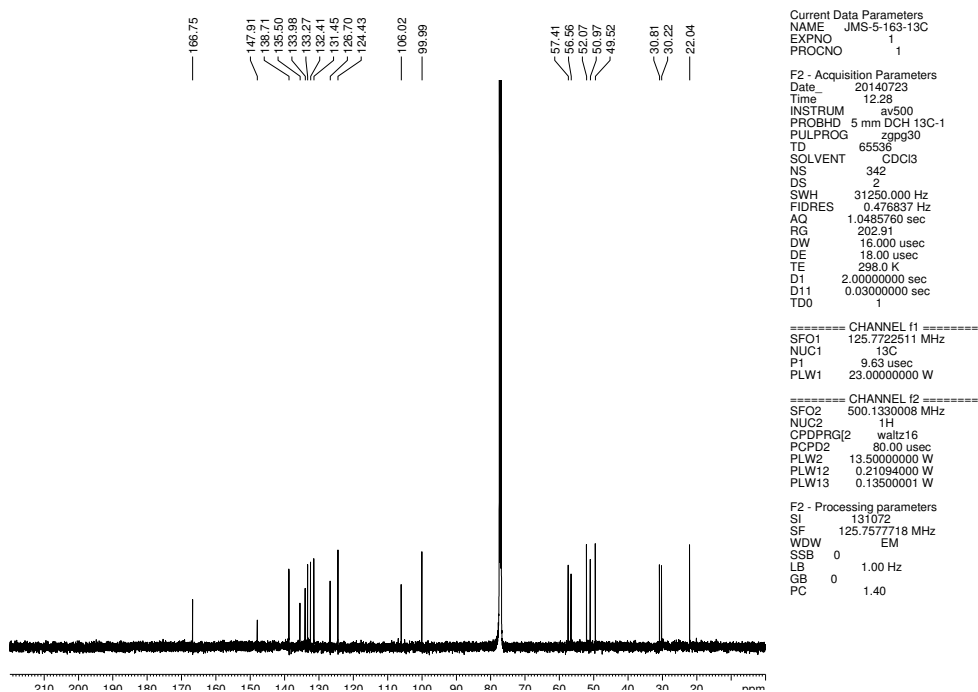


Figure A1.15 ^{13}C NMR (125 MHz, CDCl_3) of compound **2.20**

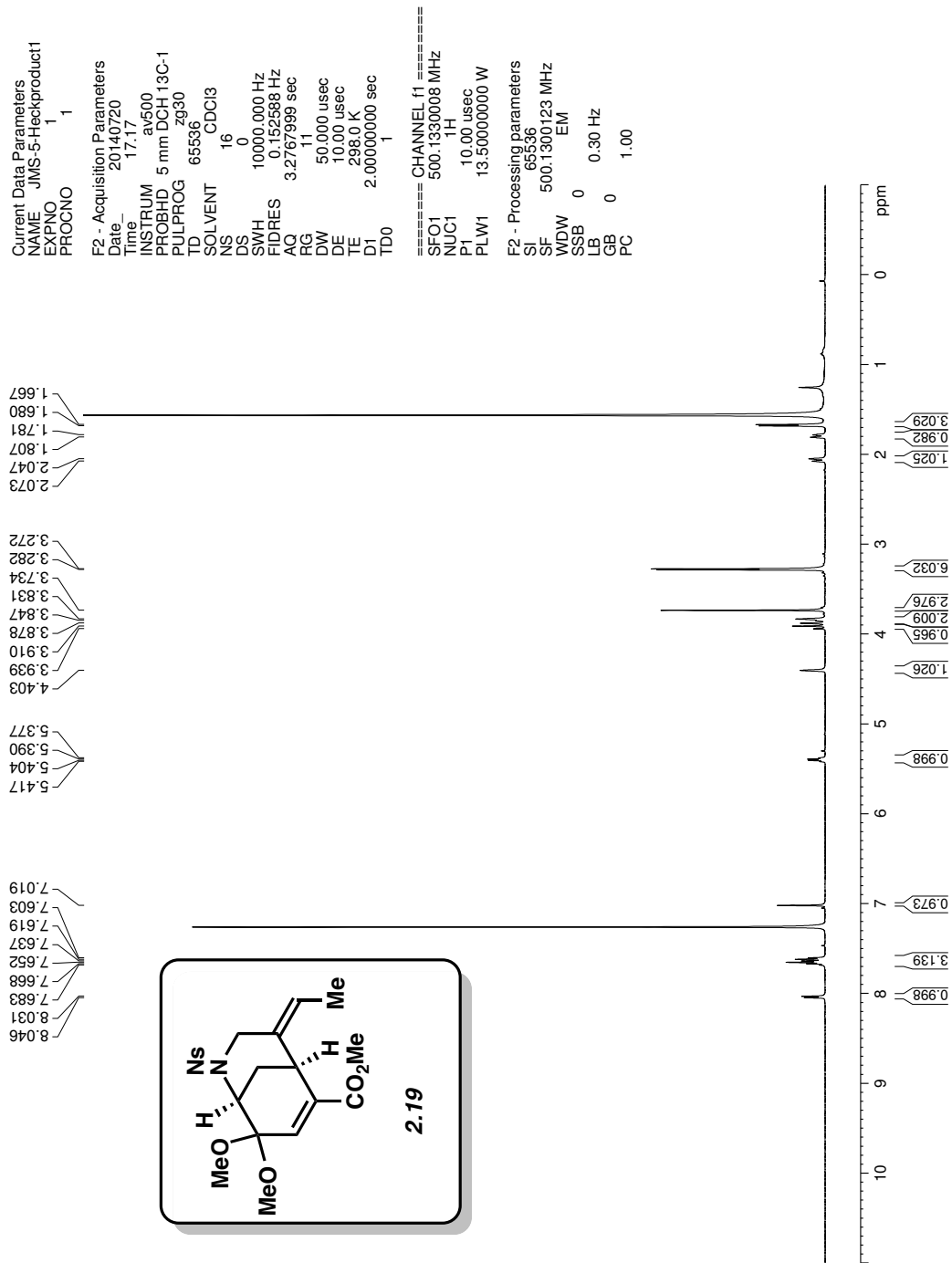


Figure A1.16 ¹H NMR (500 MHz, CDCl₃) of compound 2.19.

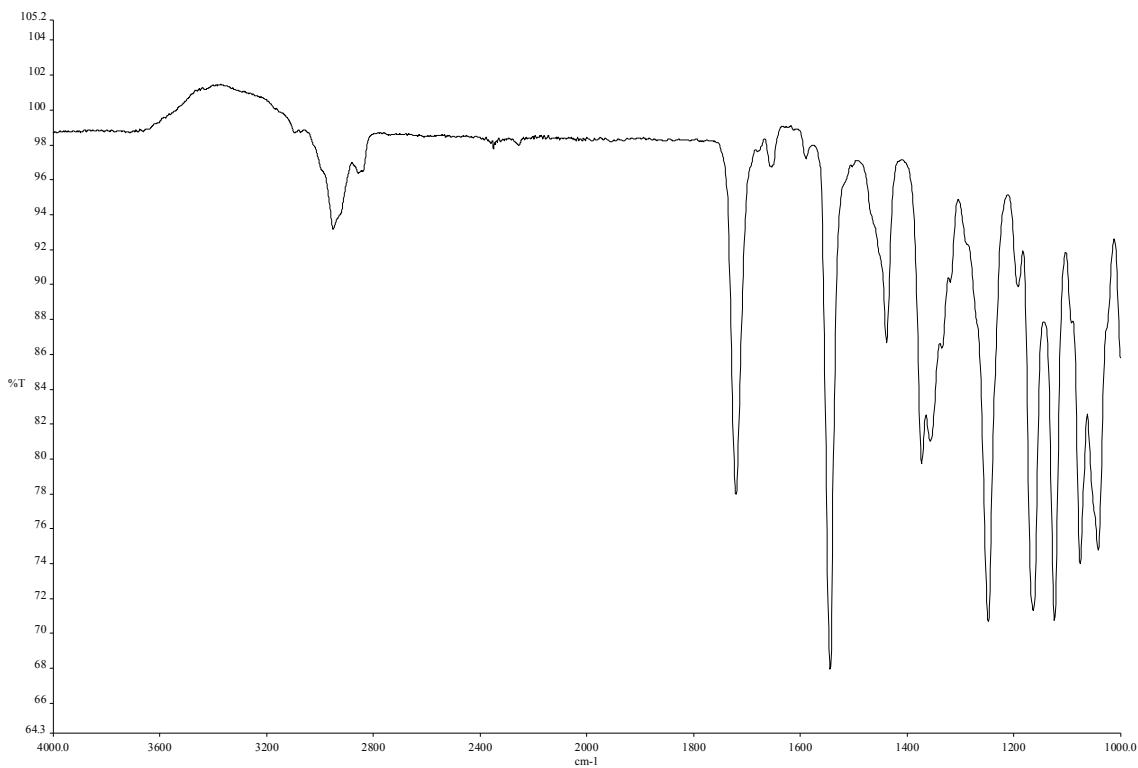


Figure A1.17 Infrared spectrum of compound **2.19**.

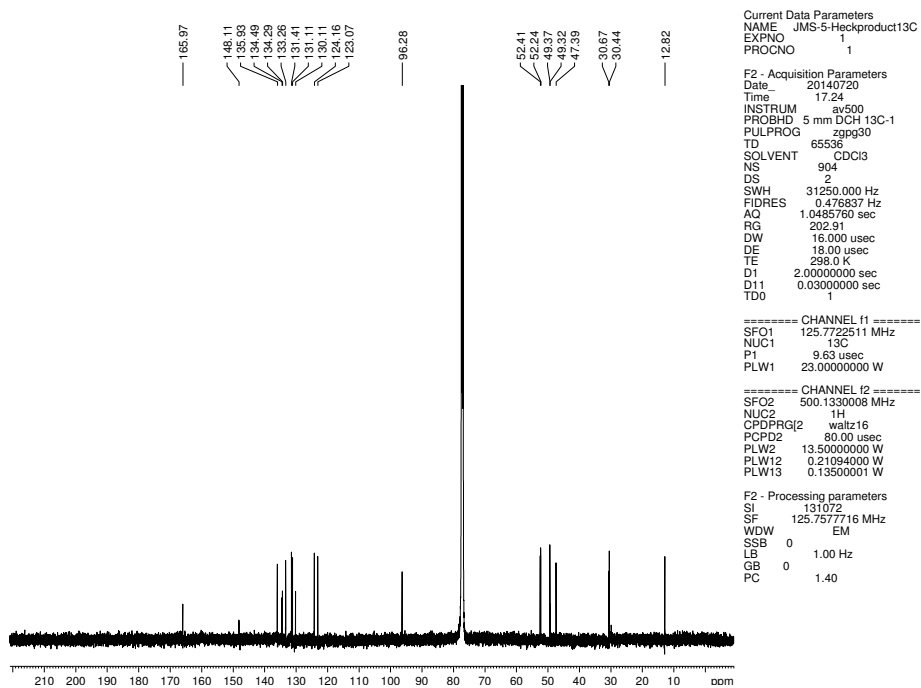


Figure A1.18 ^{13}C NMR (125 MHz, CDCl_3) of compound **2.19**.

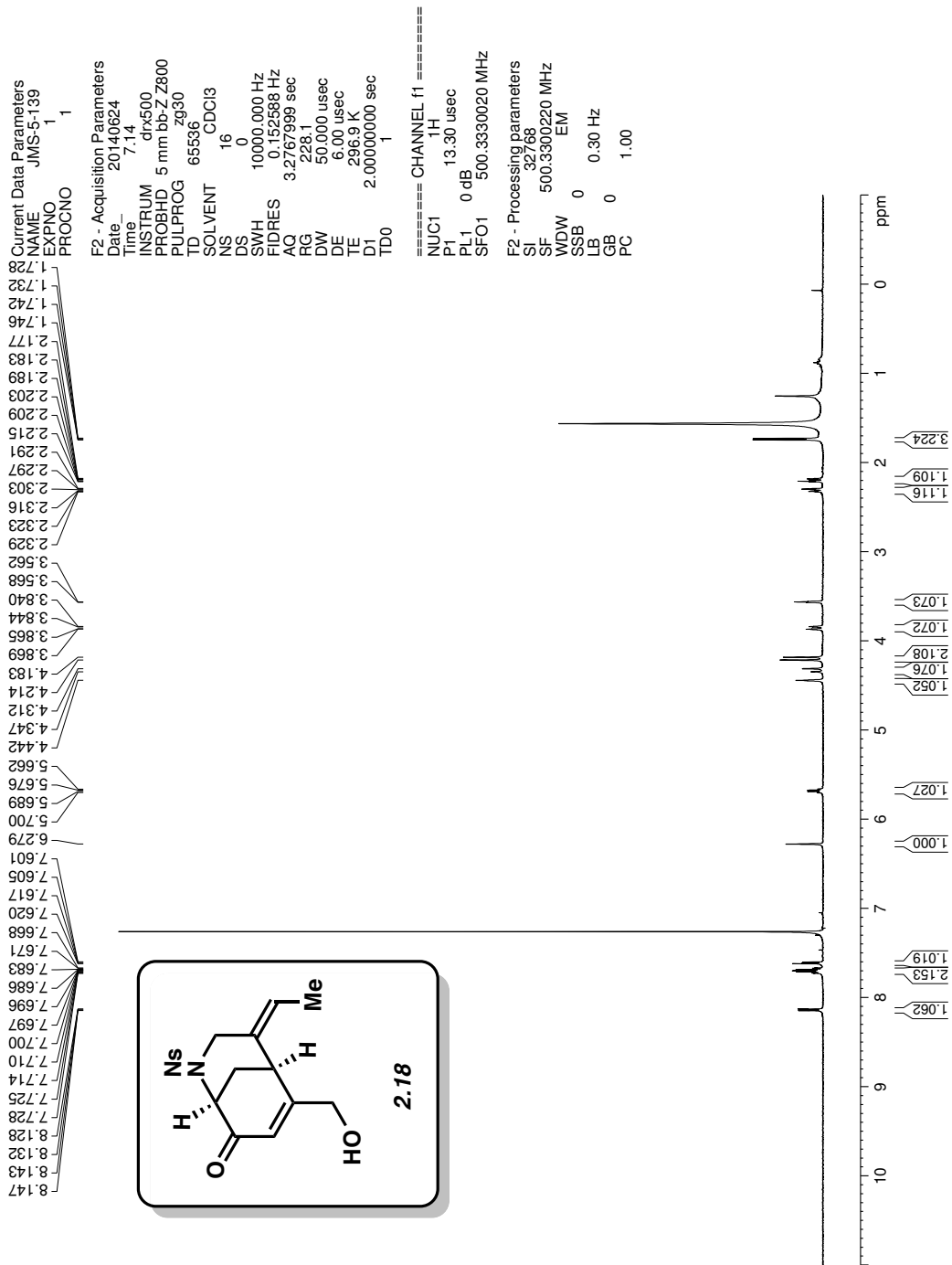


Figure A1.19 ¹H NMR (500 MHz, CDCl₃) of compound 2.18.

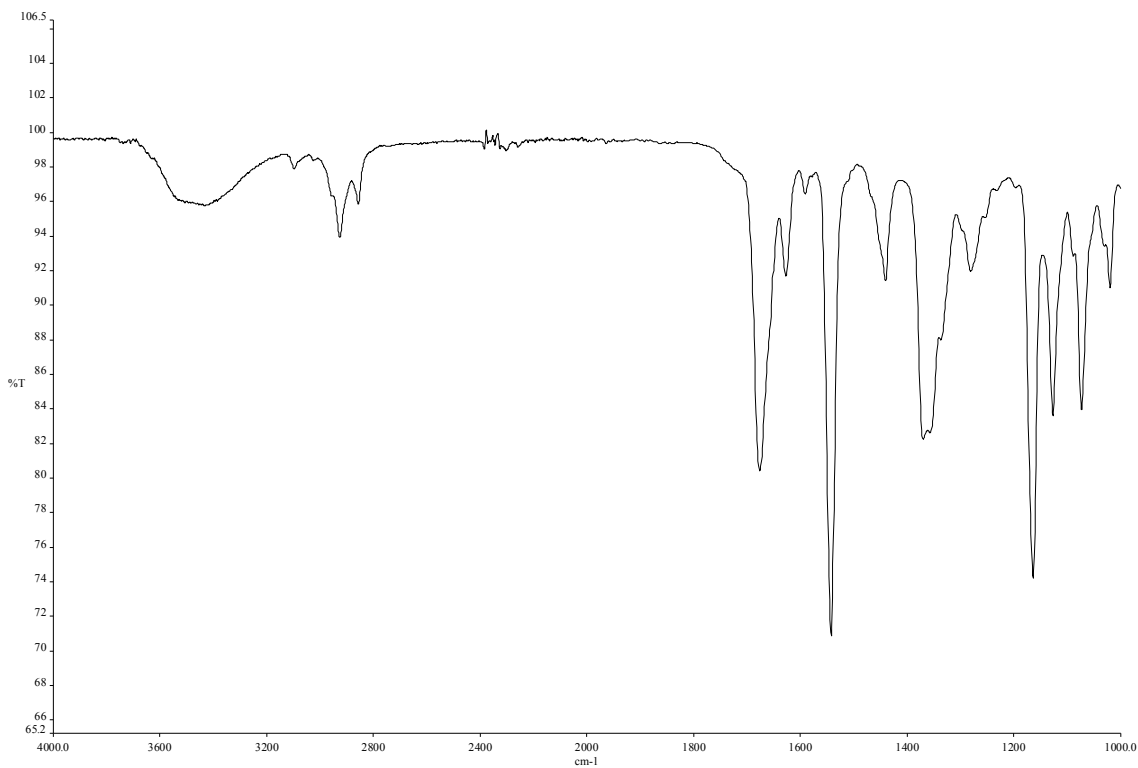


Figure A1.20 Infrared spectrum of compound **2.18**.

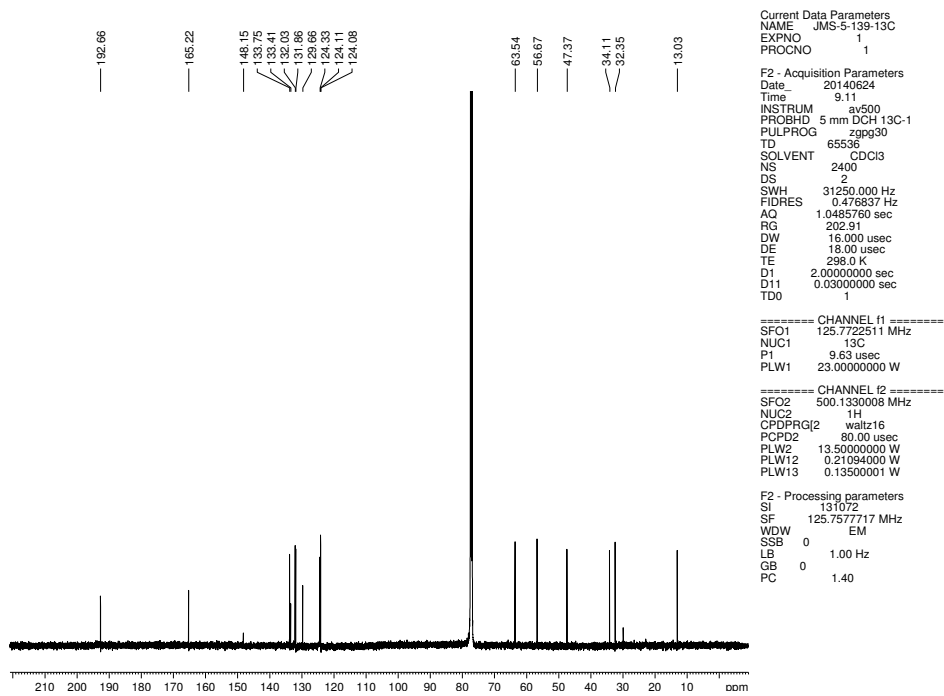


Figure A1.21 ^{13}C NMR (125 MHz, CDCl_3) of compound **2.18**.

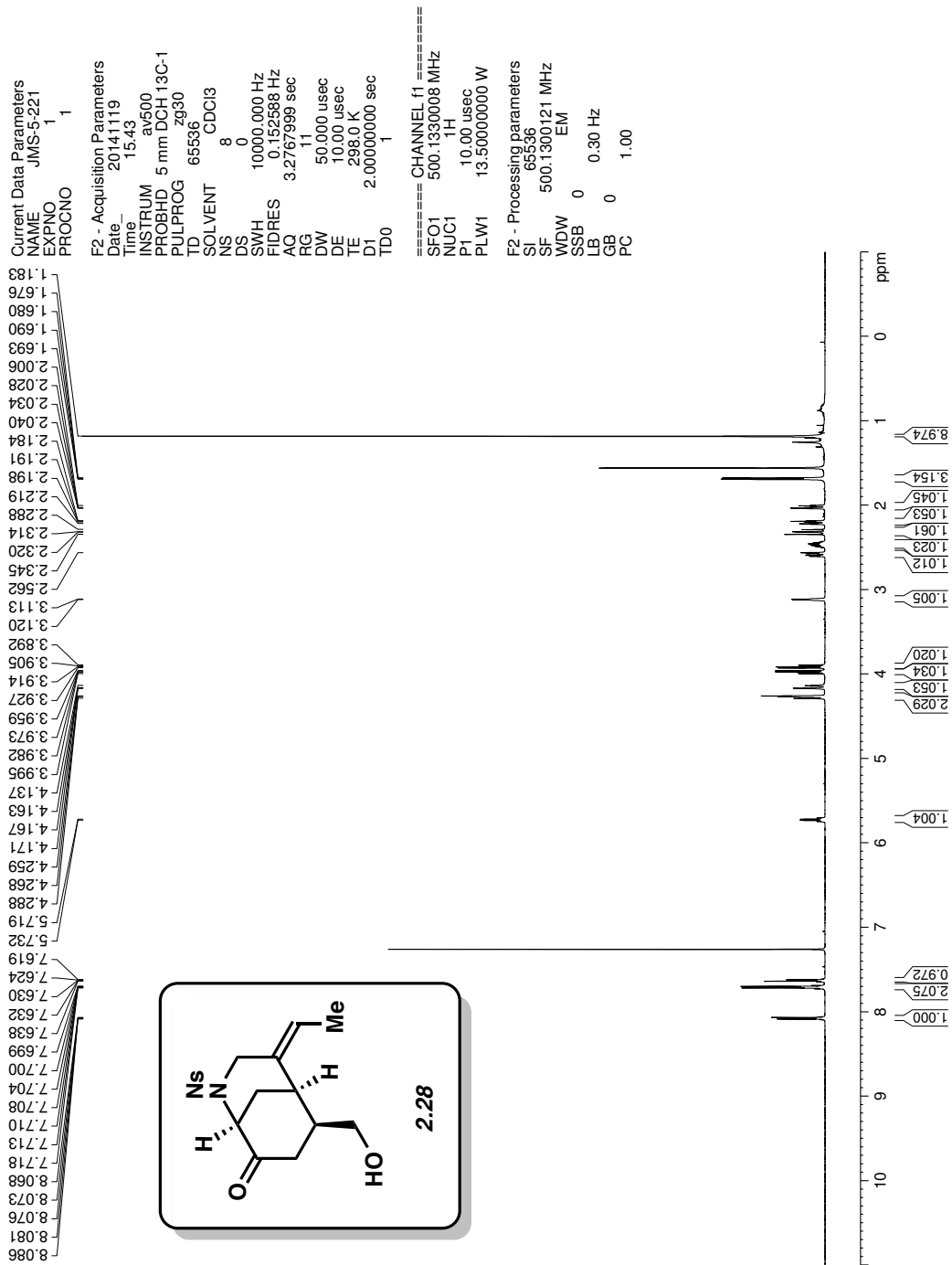


Figure A1.22 ¹H NMR (500 MHz, CDCl₃) of compound 2.28.

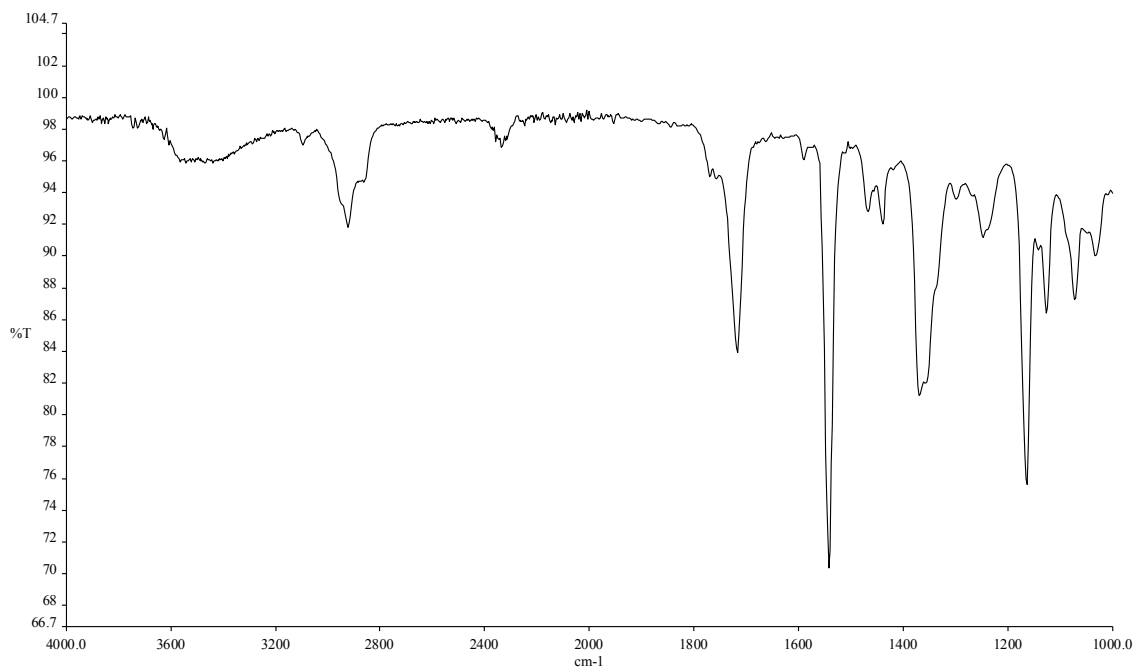


Figure A1.23 Infrared spectrum of compound **2.28**.

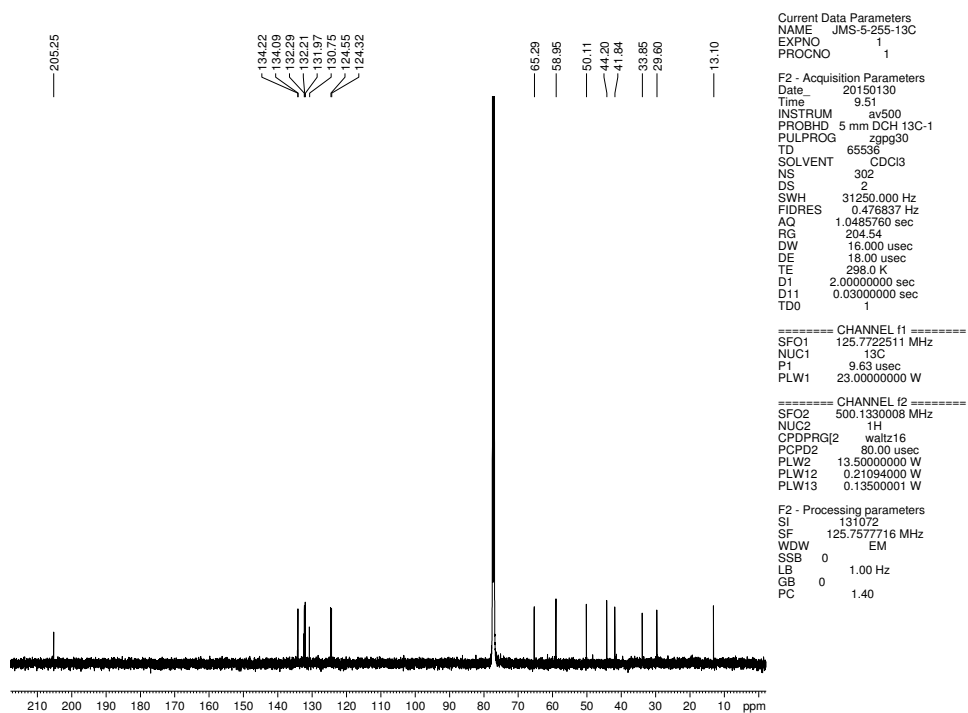


Figure A1.24 ^{13}C NMR (125 MHz, CDCl_3) of compound **2.28**.

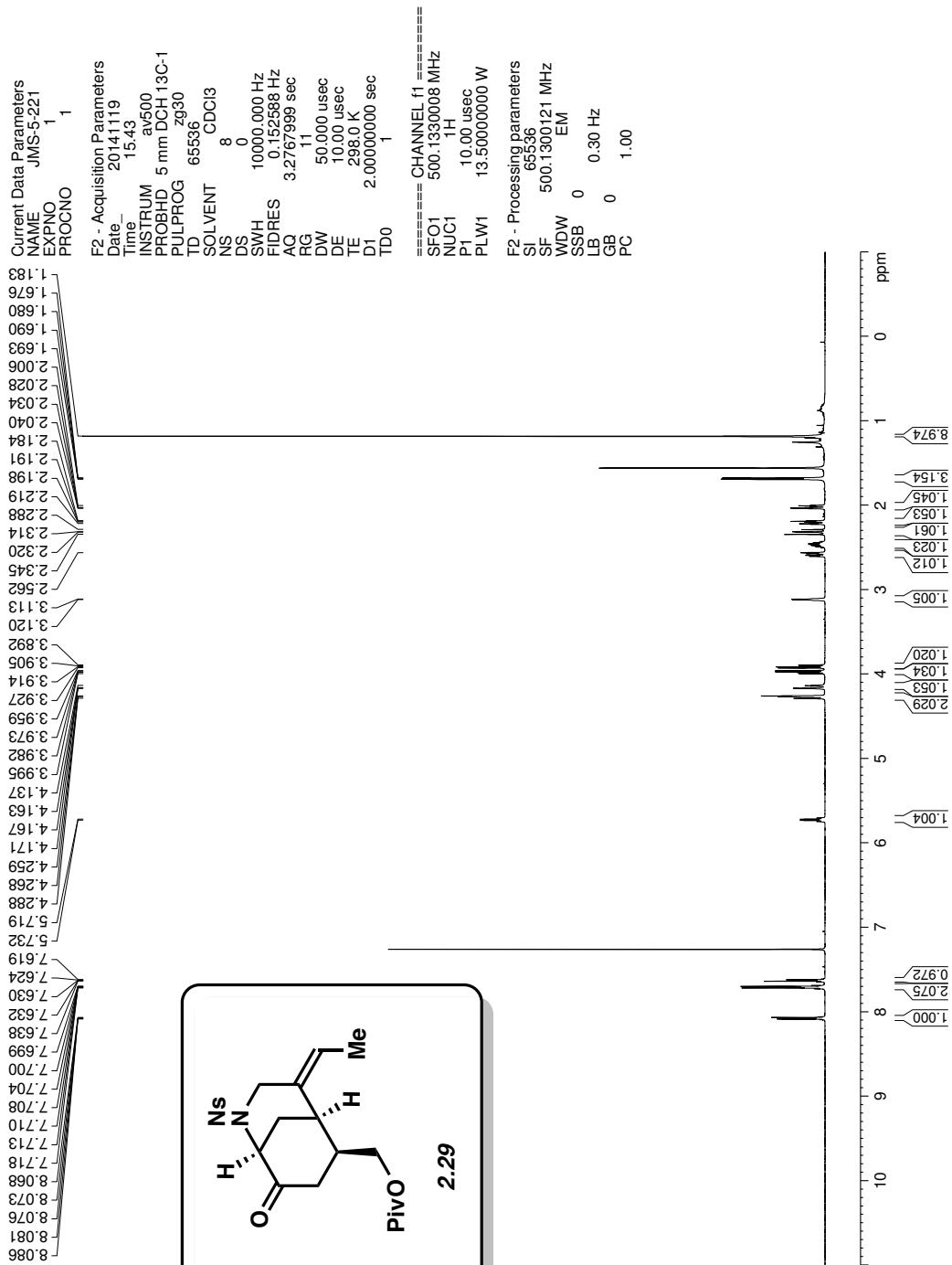


Figure A1.25 ¹H NMR (500 MHz, CDCl₃) of compound 2.29.

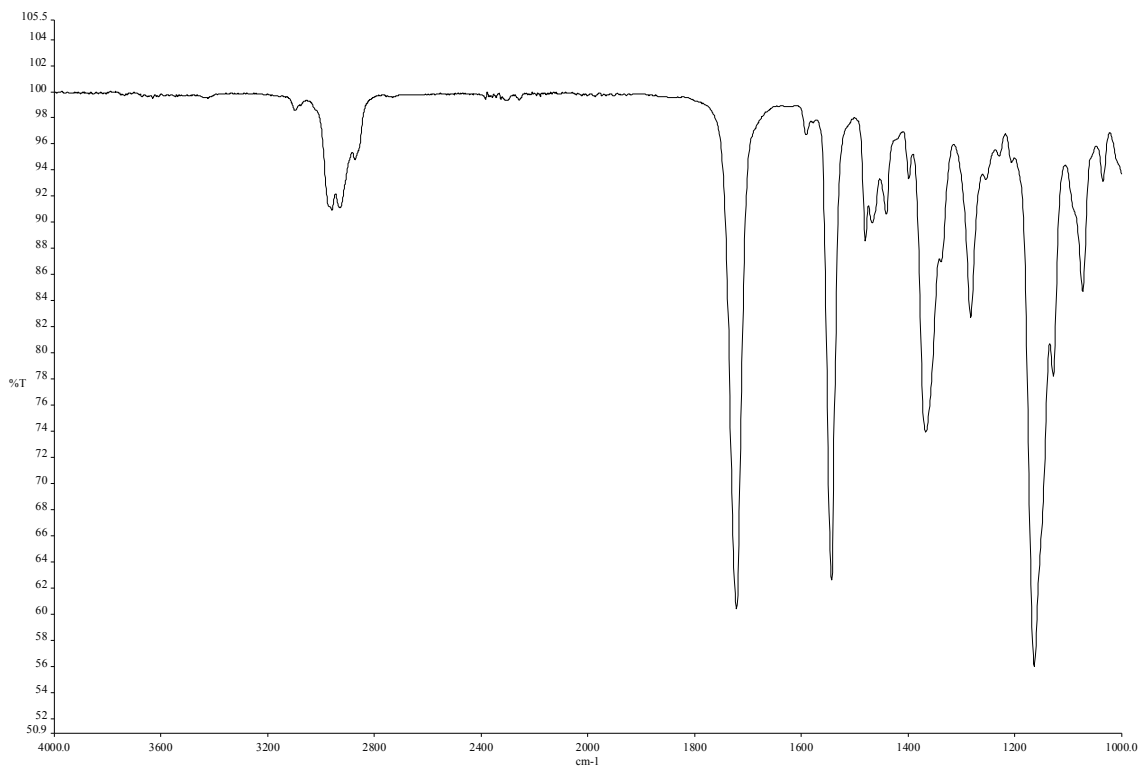


Figure A1.26 Infrared spectrum of compound **2.29**.

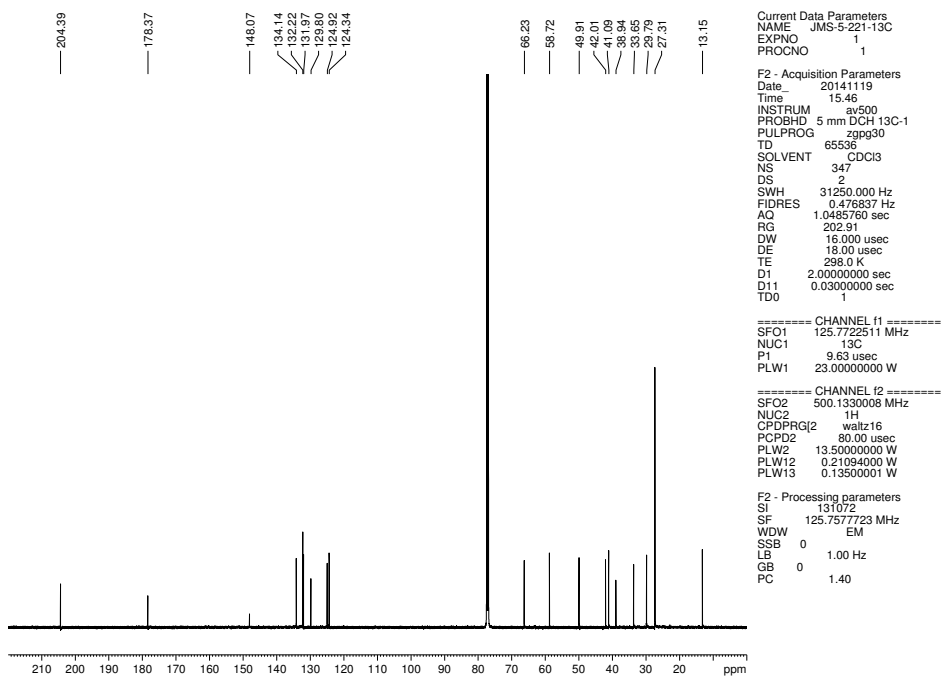


Figure A1.27 ^{13}C NMR (125 MHz, CDCl_3) of compound **2.29**

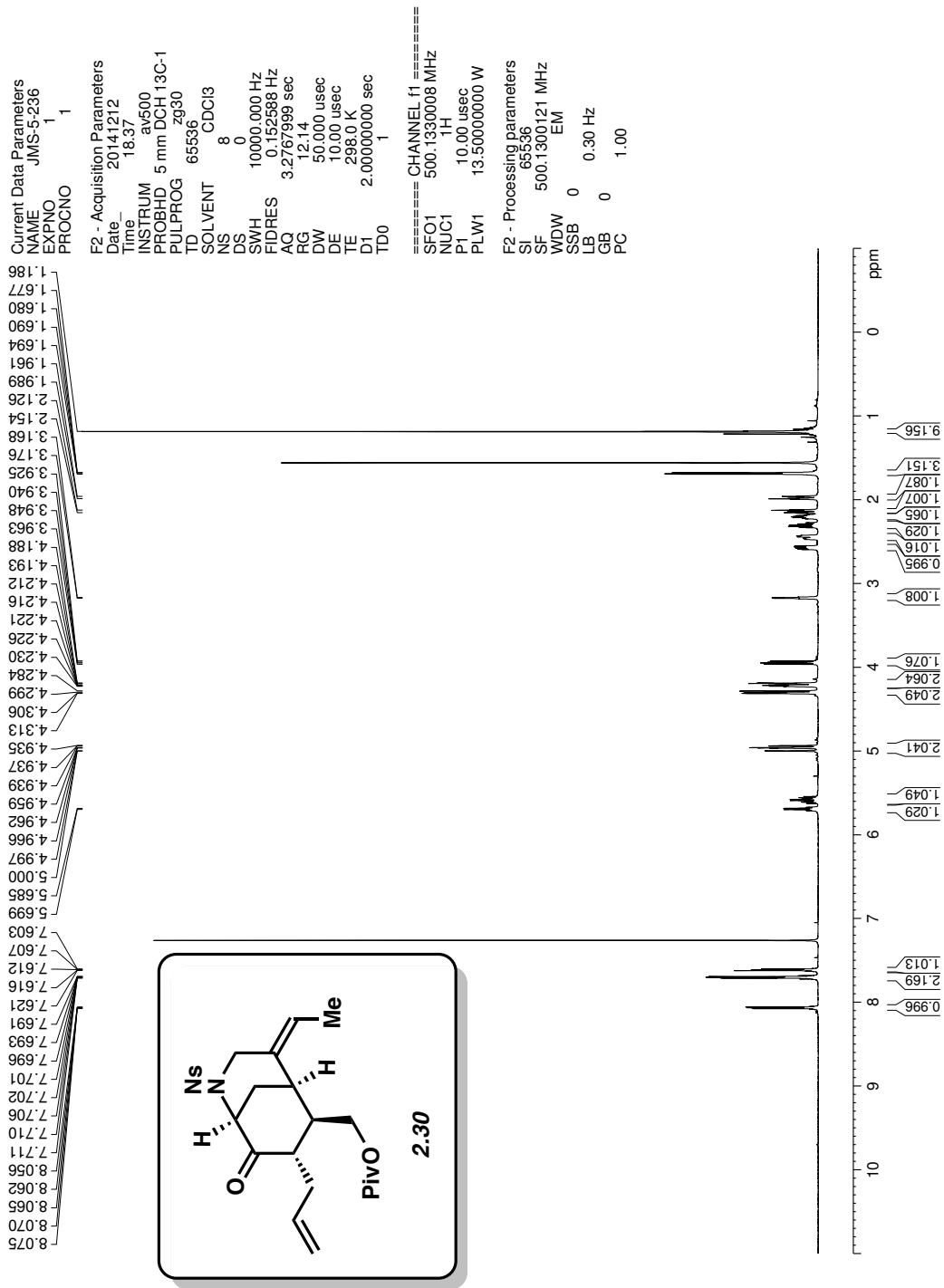


Figure A1.28 ¹H NMR (500 MHz, CDCl₃) of compound 2.30.

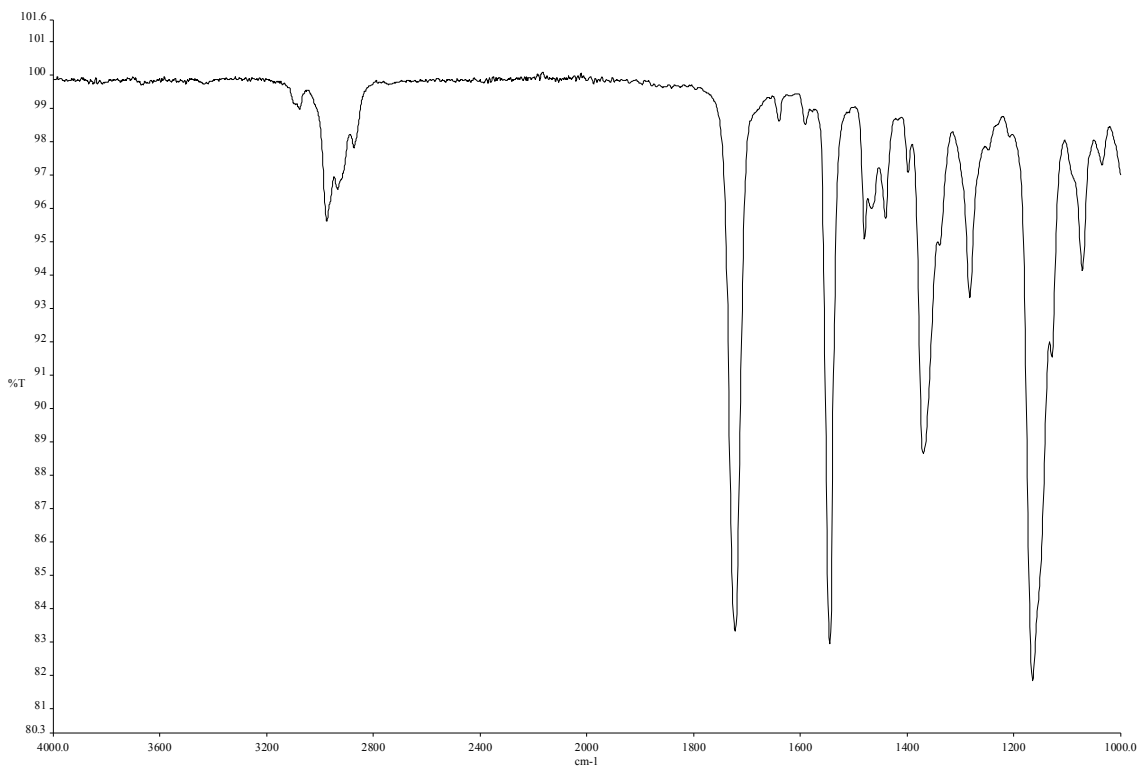


Figure A1.29 Infrared spectrum of compound **2.30**.

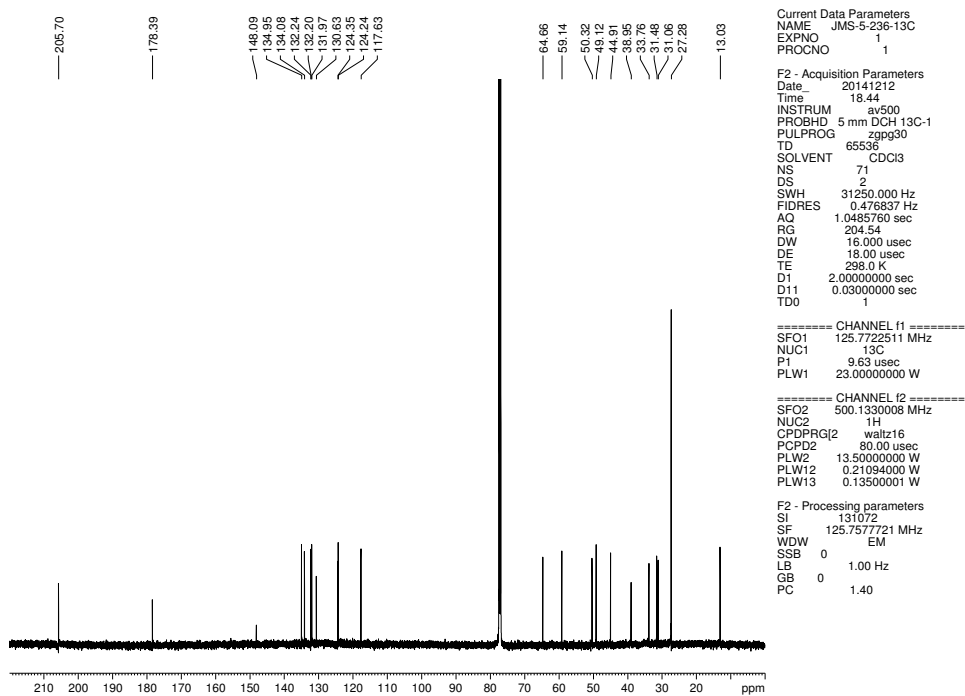


Figure A1.30 ^{13}C NMR (125 MHz, CDCl_3) of compound **2.30**.

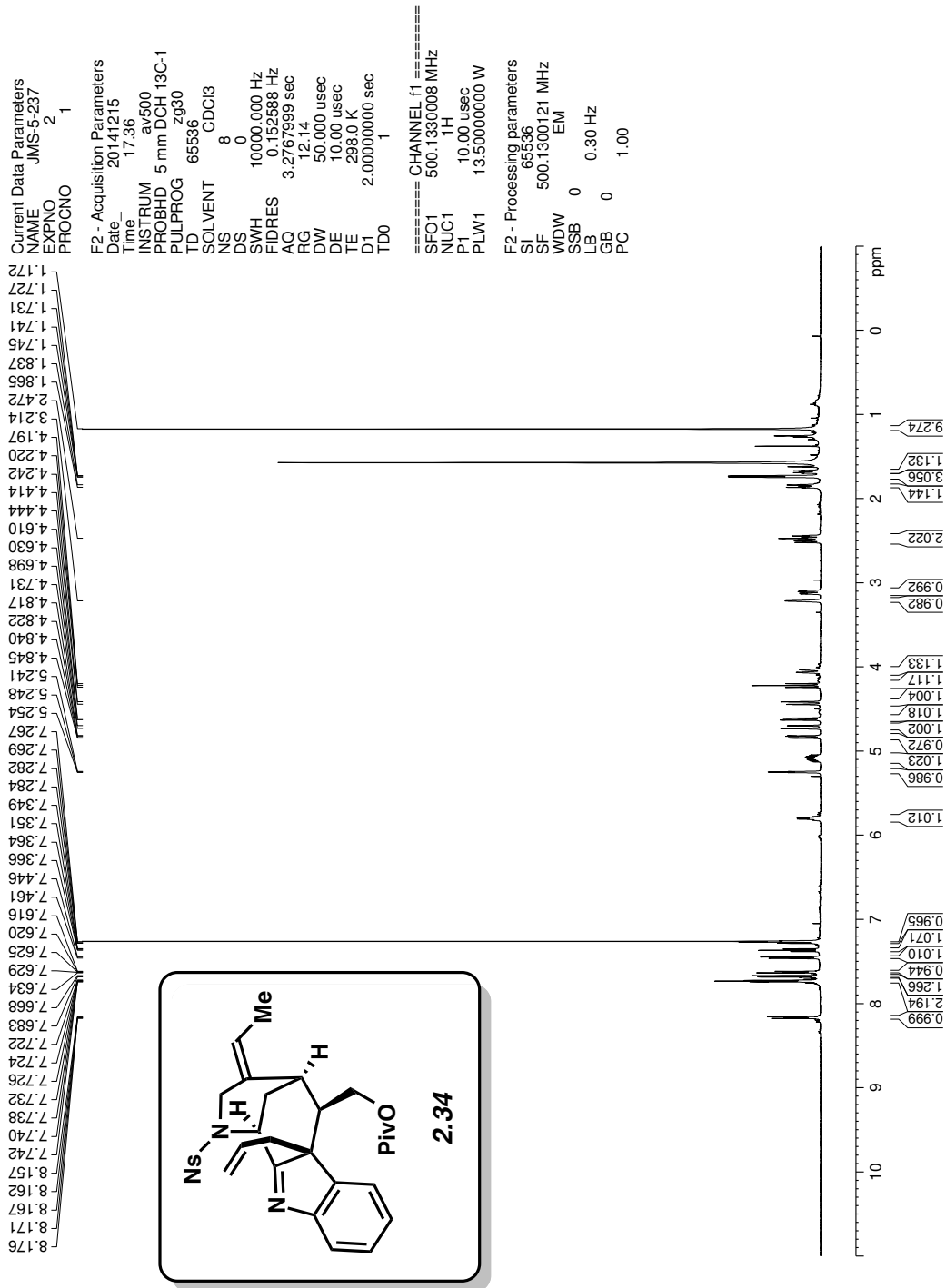


Figure A1.31 ¹H NMR (500 MHz, CDCl₃) of compound 2.34.

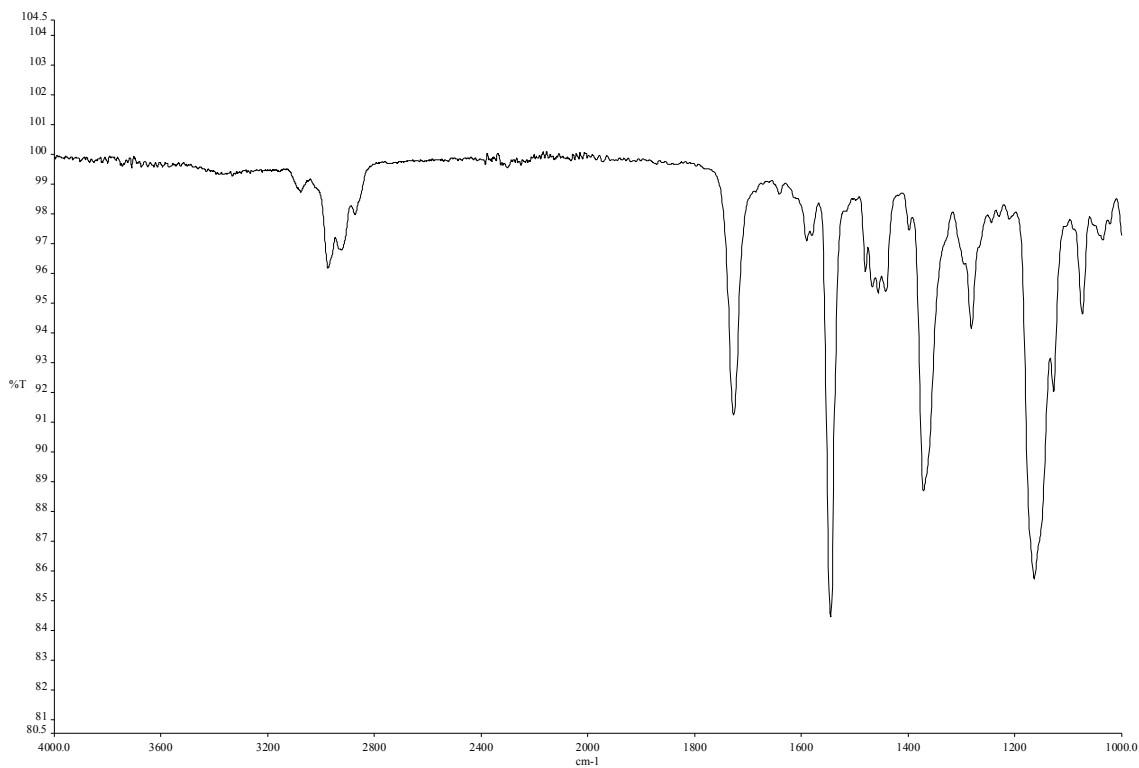


Figure A1.32 Infrared spectrum of compound **2.34**.

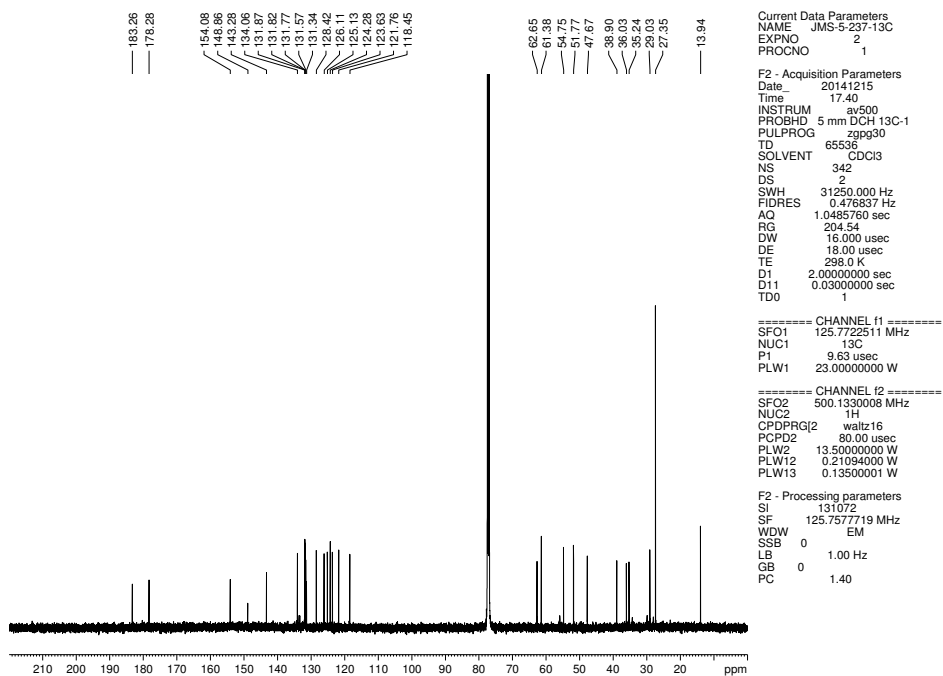


Figure A1.33 ^{13}C NMR (125 MHz, CDCl_3) of compound **2.34**.

Current Data Parameters
 NAME JMS-5-indolaminealcohol
 EXPNO 1
 PROCNO 1

F2 - Acquisition Parameters

Date_ 20150205
 Time 11.50
 INSTRUM av500
 PROBHD 5 mm DCH 13C-1
 PULPROG zg30
 TD 65536
 SOLVENT CDCl3
 NS 8
 DS 0
 SWH 1000.000 Hz
 FIDRES 0.152568 Hz
 AQ 3.2767999 sec
 RG 12.14
 DW 50.000 usec
 DE 10.00 usec
 TE 298.0 K
 D1 2.00000000 sec
 TD0 1

==== CHANNEL f1 =====

SFO1 500.130008 MHz
 NUC1 1H
 P1 10.00 usec
 PLW1 13.50000000 W

F2 - Processing parameters

SI 65536
 SF 500.1300124 MHz
 WDW EM
 SSB 0
 LB 0
 GB 0
 PC 1.00

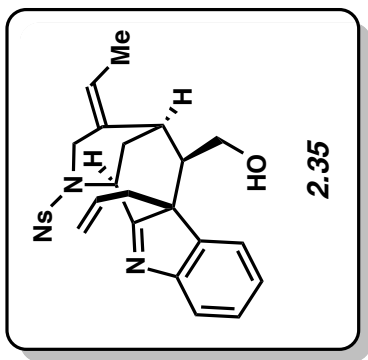
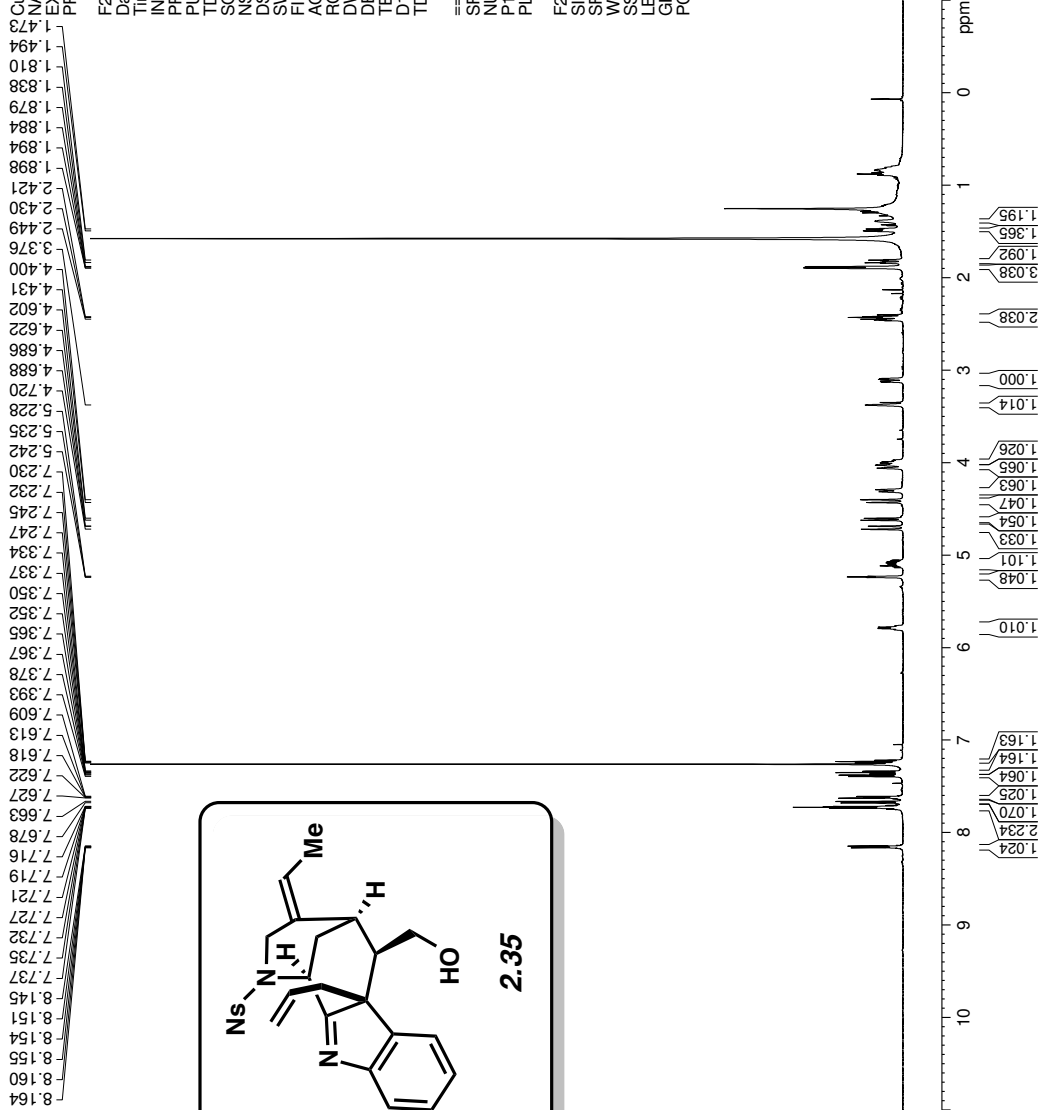


Figure A1.34 ¹H NMR (500 MHz, CDCl₃) of compound 2.35.

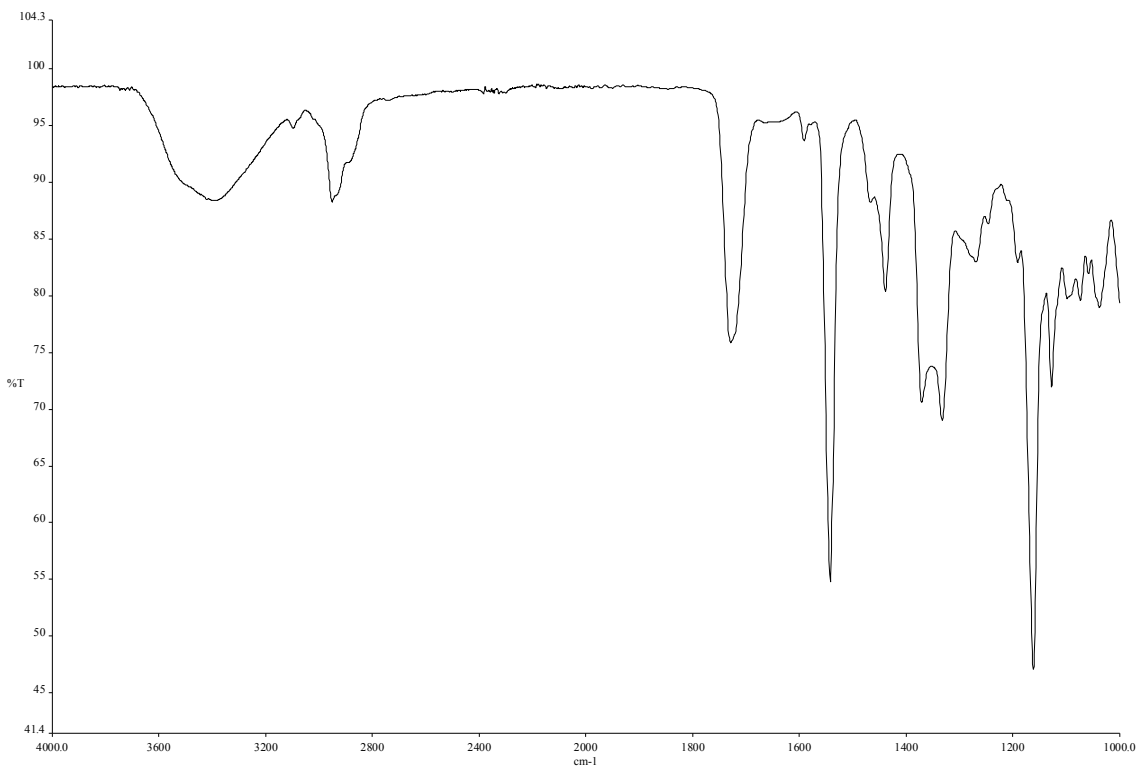


Figure A1.35 Infrared spectrum of compound **2.35**.

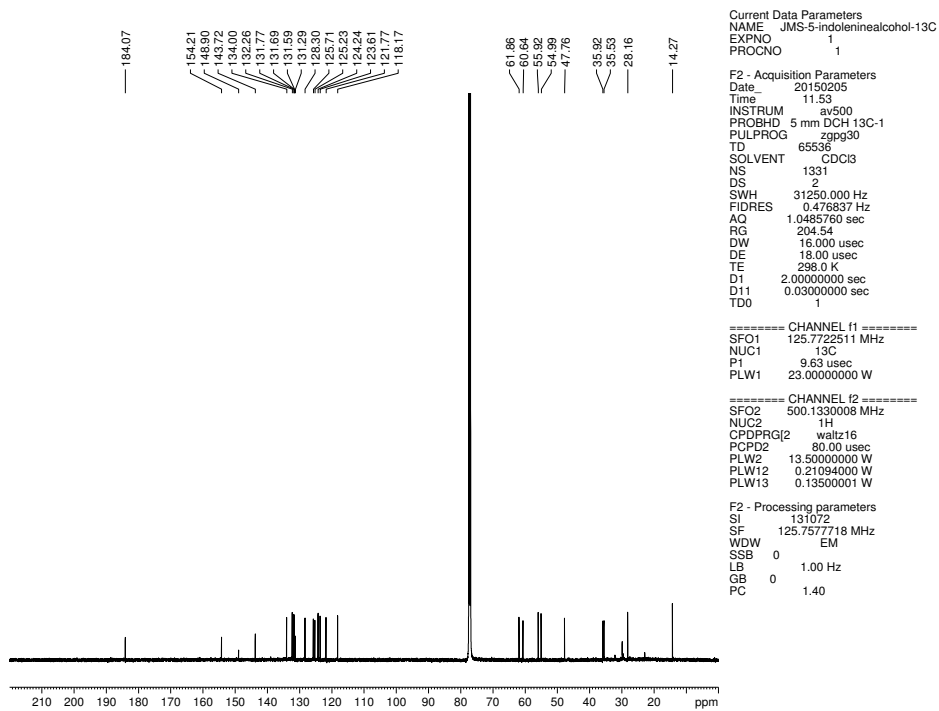


Figure A1.36 ¹³C NMR (125 MHz, CDCl₃) of compound **2.35**.

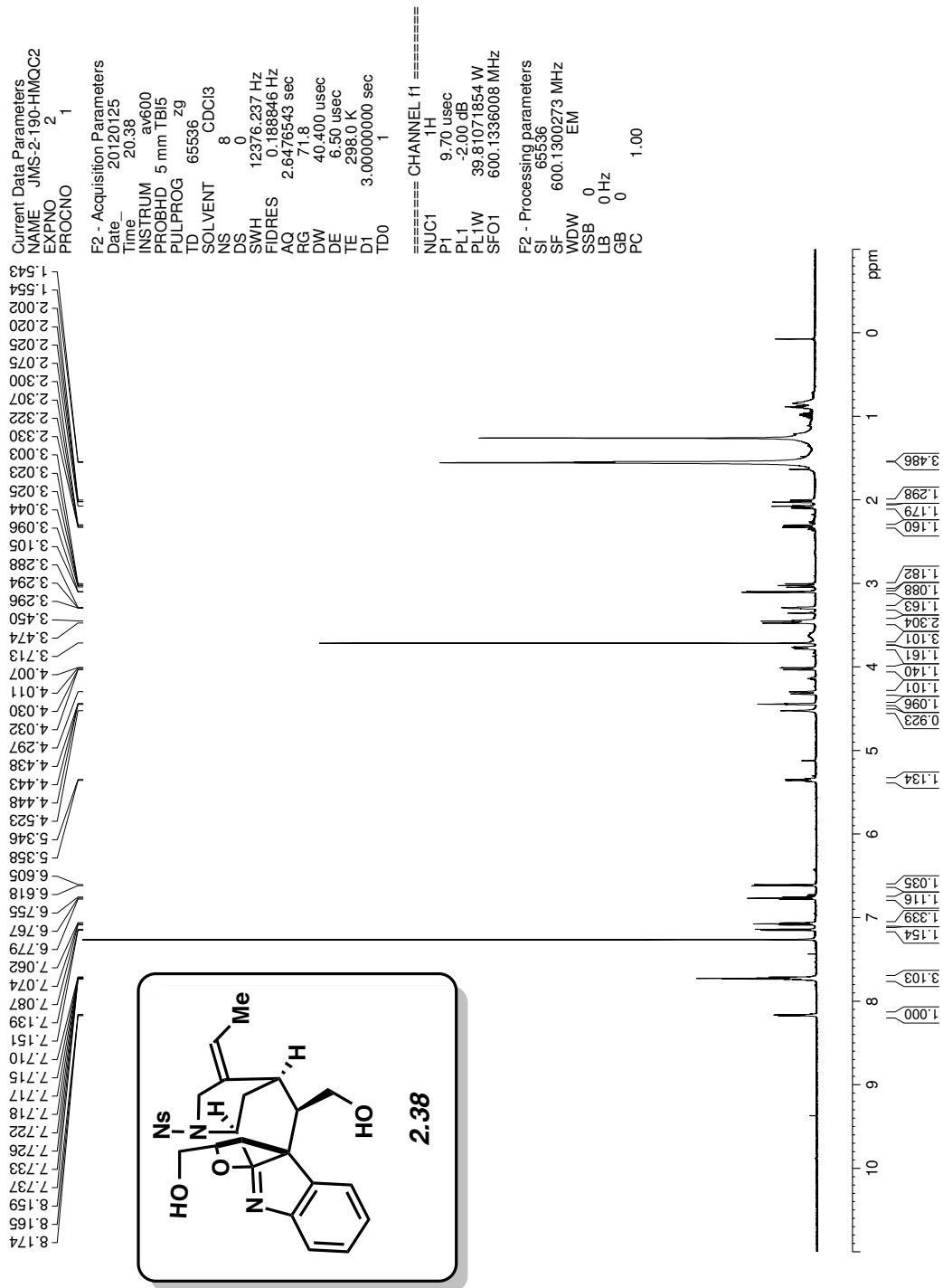


Figure A1.37 ¹H NMR (500 MHz, CDCl₃) of compound 2.38.

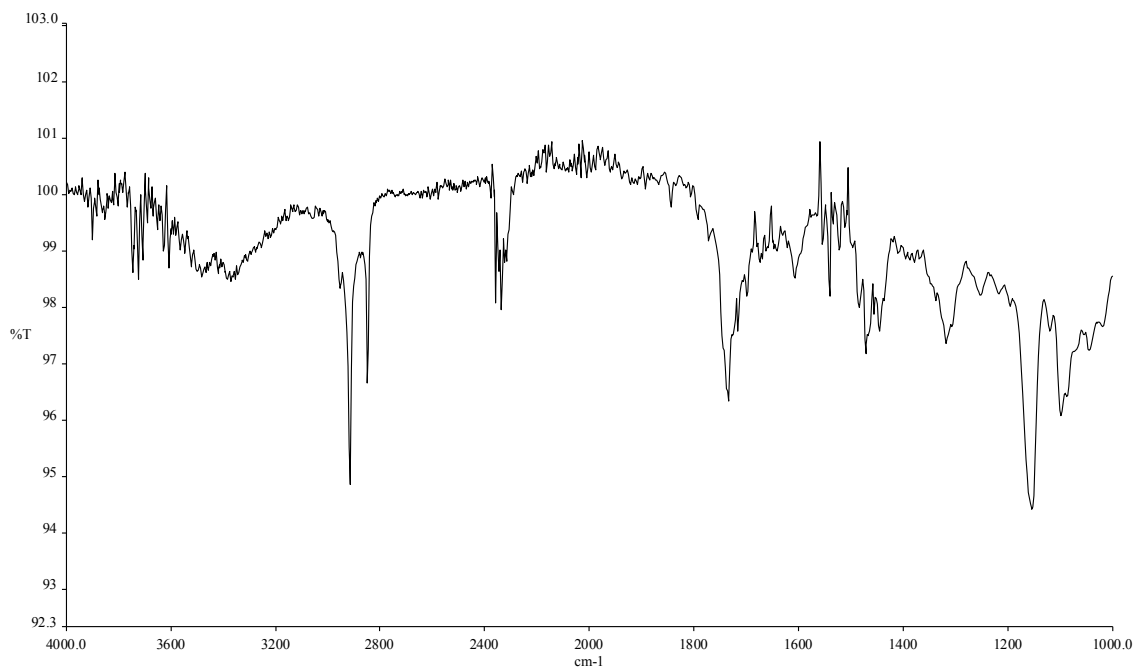


Figure A1.38 Infrared spectrum of compound **2.38**.

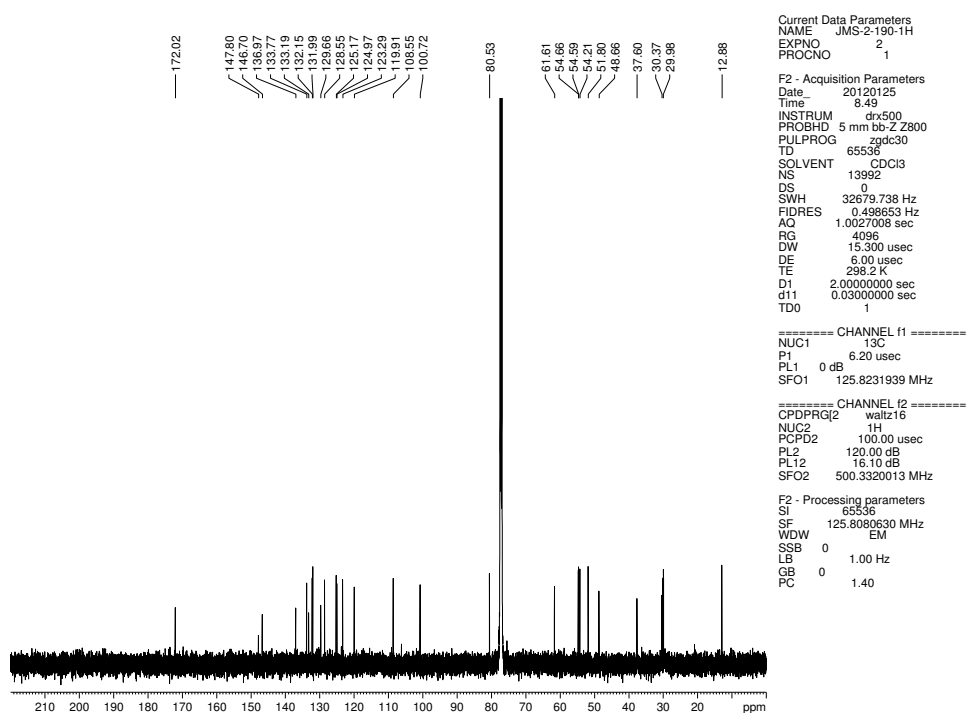


Figure A1.39 ^{13}C NMR (125 MHz, CDCl_3) of compound **2.38**.

CHAPTER THREE

Second-Generation Approach and Total Synthesis of Picrinine

3.1 Abstract

This chapter describes a second-generation approach to the akuammiline alkaloid picrinine. Central to the success of our approach is the use of a Fischer indolization reaction a cyclopentene-containing substrate to circumvent the previously encountered roadblocks. Additionally, a more concise and scalable synthetic strategy towards building the natural product scaffold is detailed, which ultimately fueled a thorough investigation of late-stage chemistry. Furthermore, we describe various roadblocks encountered in our experimental efforts are described, which were successfully overcome to complete the total synthesis.

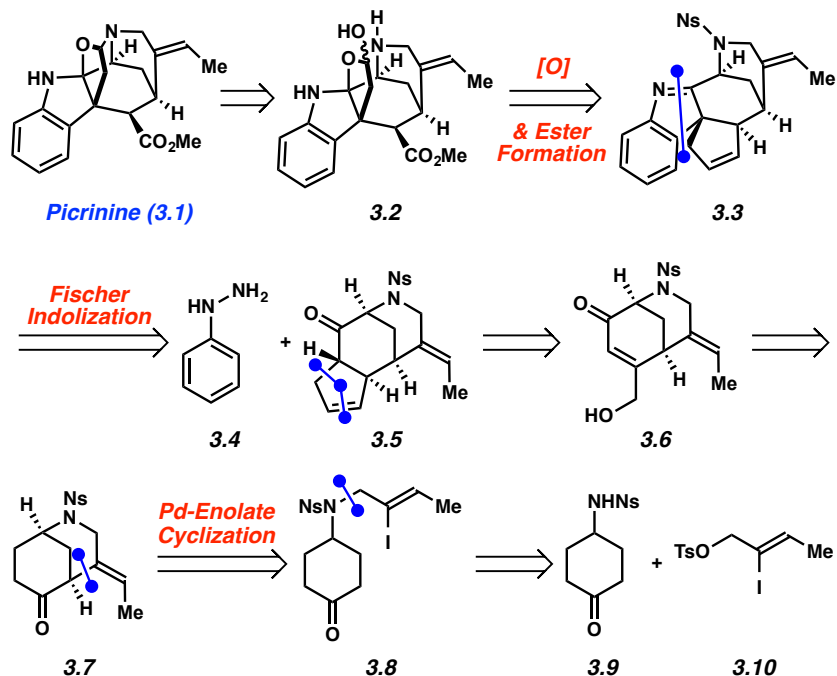
3.2 Introduction

As described in Chapter 2, our initial route to picrinine (**3.1**) were met with many setbacks. Among these difficulties was that the route provided inefficient material throughput due to scale limitations. This impediment provided for little faculty in the investigation of the final synthetic manipulations. Thus, we were prompted to devise a new, concise, and efficient strategy that allowed for scalability, while addressing the strategic hurdles encountered in the later stages of our first-generation route.

3.3 Second-Generation Retrosynthetic Analysis

Our second-generation retrosynthetic analysis of **3.1** is shown in Scheme 3.1. Identical to our first strategy, we envisioned picrinine (**3.1**) arising from cyclization of the penultimate lactol **3.2**. However, we now sought to access this lactol from indolenine **3.3**, which bears a cyclopentene moiety. The cyclopentene would serve as a “tethered” variant of the previously problematic allyl sidechain (see chapter 2). Specifically, we envisaged that the oxidative cleavage of cyclopentene **3.3**¹ would not be hampered by cyclization of the presumed diol intermediate due to geometric constraints; accordingly, C–C bond cleavage could occur. Indolenine **3.3** would be derived from late-stage Fischer indolization of phenylhydrazine (**3.4**) and ketone **3.5**, the latter of which would be derived from enone **3.6**. Although we previously had been able to access **3.6** (see Chapter 2, Scheme 2.3), our route was significantly hampered by poor material throughput. Thus, we took the opportunity to design a new and scalable synthetic route to this key intermediate. We envisioned that enone **3.6** could be accessed from bicyclic ketone **3.7**,² the product of an intramolecular Pd-catalyzed enolate coupling of vinyl iodide **3.8**. Finally, the iodide would be prepared from readily available fragments cyclohexanone **3.9** and tosylate **3.10**.

Scheme 3.1 Revised retrosynthetic analysis of picrinine (**3.1**).

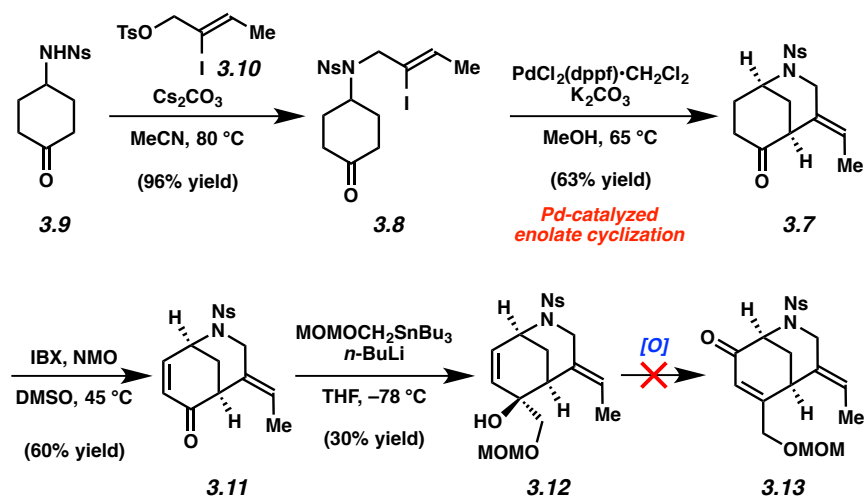


3.4 Development of a Synthetic Route to Access Fischer Indolization Substrate 3.5

Scheme 3.2 shows the successful synthesis of bicyclic ketone **3.7** and our initial attempt to elaborate it further. Starting with cyclohexanone **3.9**,³ alkylation with tosylate **3.10**⁴ in the presence of Cs_2CO_3 provided vinyl iodide **3.8** in excellent yield. When treated with $\text{PdCl}_2(\text{dppf})\cdot\text{CH}_2\text{Cl}_2$ (20 mol%) and K_2CO_3 in methanol at 65 °C, iodide **3.8** underwent efficient conversion to bicyclic ketone **3.7** in 63% yield.⁵ This transformation was performed on multigram scale and allowed access to the important [3.3.1]-azabicyclic in just two steps from **3.9**, which was a notable improvement compared to our earlier approach to assembling the azabicyclic (see Chapter 2, Scheme 2.2). With ketone **3.7** in hand, IBX oxidation provided enone

3.11 in 60% yield.⁶ Enone **3.11** was treated with a preformed MOM-protected alkyllithium species at low temperature to give tertiary allylic alcohol **3.12**, albeit in low yield.⁷ Unfortunately, all attempts to oxidatively rearrange allylic alcohol **3.12** to enone **3.13** were unsuccessful. The use of various Cr (VI)⁸ reagents, hypervalent iodine reagents,⁹ or *N*-oxoammonium salts¹⁰ was ineffective, and largely resulted in the recovery of starting material or decomposition. Attempts to isomerize the allylic alcohol without oxidation were also unsuccessful. We surmise that the difficulties encountered in our attempts to manipulate **3.12** are due to the tertiary alcohol being extremely sterically hindered.

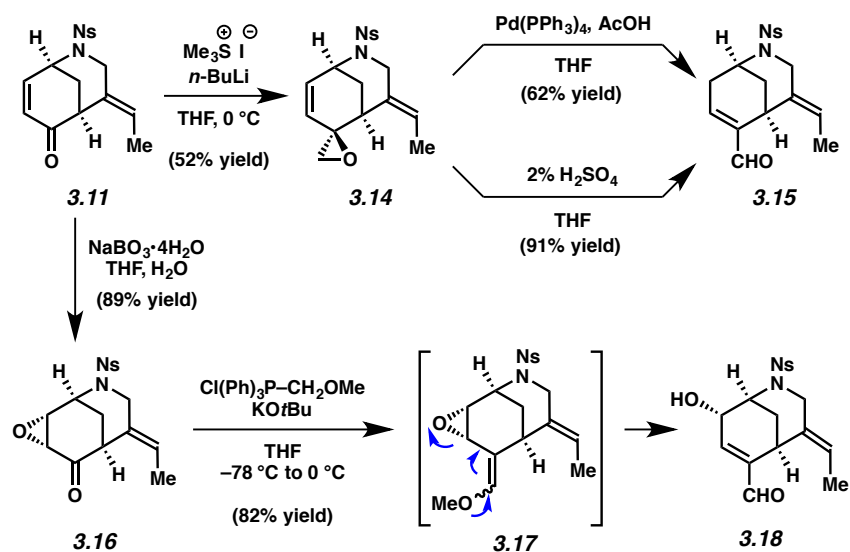
Scheme 3.2 Assembly of the [3.3.1]-azabicycle and attempted elaboration to enone **3.13**.



To side step our inability to utilize allylic alcohol **3.12**, we pursued the epoxidation/fragmentation sequence shown in Scheme 3.3. First, enone **3.11** was exposed to a Corey-Chaykovsky homologation with a preformed sulfur ylide to produce spiroepoxide **3.14**.¹¹ With the goal of introducing oxygenation through an $\text{S}_{\text{N}}2'$ -type substitution process, epoxide

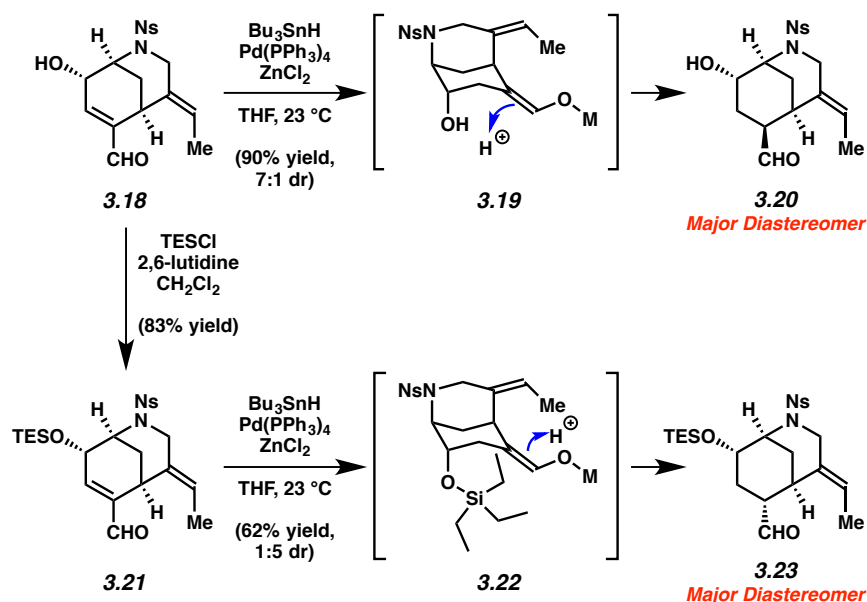
3.14 was treated with $\text{Pd}(\text{PPh}_3)_4$ in the presence of AcOH .¹² However, the only product obtained was enal **3.15**, which presumably arises by initial formation of a π -allylpalladium complex and subsequent β -hydride elimination and tautomerization. A second effort to open epoxide **3.14** was attempted using dilute sulfuric acid,¹³ but this also delivered the undesired enal **3.15**. In an alternate strategy, we returned to enone **3.11** and performed an oxidation using sodium perborate tetrahydrate in THF and water,¹⁴ which furnished epoxide **3.16** in 89% yield. This epoxide was subsequently treated with methylmethoxytriphenylphosphonium chloride in the presence of base to furnish enal **3.18** in 82% yield.¹⁵ Presumably this transformation proceeds via Wittig olefination **3.15** and spontaneous epoxide fragmentation and hydrolysis (see transition structure **3.17**). Using this sequence, gram quantities of enal **3.18** were accessible.

Scheme 3.3 Approaches to homologate and oxidize enone **3.11**.



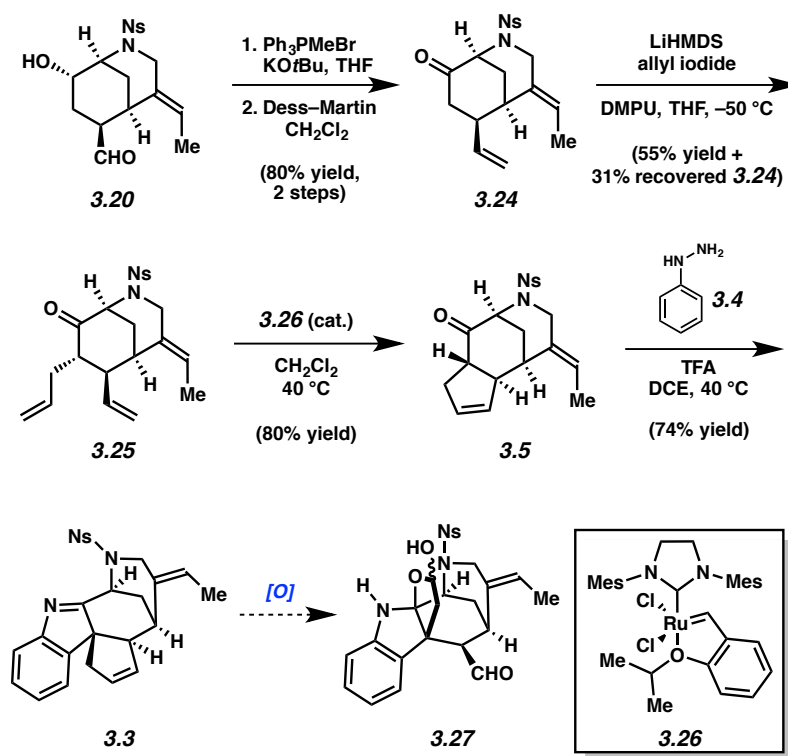
En route to the desired Fischer indolization substrate, we sought to perform a conjugate reduction of the enal (Scheme 3.4). Our initial attempts involved treatment of enal **3.18** with a number of copper¹⁶ or rhodium-based reducing agents,¹⁷ however these efforts were ineffective. Hypothesizing that the secondary alcohol was problematic, we silyl protected it to give **3.21** in 83% yield. Reduction of **3.21** in the presence of Pd(PPh₃)₄, Bu₃SnH, and ZnCl₂ in THF¹⁸ proceeded in 62% yield, although with poor diastereoselectivity (dr = 1:5), favoring the undesired epimer **3.23**. The diastereoselectivity of this process is thought to be governed by the bulky triethylsilyl ether, which sterically hinders protonation (see **3.22**).¹⁹ Although further attempts to reduce **3.18** were also unsuccessful, we found that treatment of unprotected enal **3.18** under the Pd-catalyzed reduction conditions gave the desired hydroxyaldehyde **3.20** in 90% yield (dr = 7:1). The favorable selectivity presumably arises from protonation of the intermediate enolate on the sterically more accessible face of the [3.3.1]-azabicycle (see **3.19**).

Scheme 3.4 Diastereoselective reduction of enal **3.18**.



As shown in Scheme 3.5, aldehyde **3.20** could be readily elaborated to the desired Fischer indolization substrate. Wittig olefination of the aldehyde, followed by oxidation of the secondary alcohol with Dess–Martin periodinane, afforded ketone **3.24** in 80% over two steps. Next, allylic alkylation of **3.24** with allyl iodide in the presence of strong base and *N,N'*-dimethylpropyleneurea (DMPU) furnished **3.25** in 55% yield, along with 31% recovered ketone **3.24**. To arrive at the desired Fischer indolization substrate, **3.25** was treated with the Grubbs–Hoveyda 2nd Generation catalyst (**3.26**) in CH₂Cl₂ at reflux to give cyclopentene **3.5** in good yield.²⁰ It is worth noting that epimerization was not observed in this reaction and the *trans*-hydrindenone product (**3.5**) was the only product observed. To our delight, reaction of ketone **3.5** with phenylhydrazine (**3.4**) and TFA delivered indolenine **3.3** in 74% yield via late-stage Fischer indolization. Of note, only a single diastereomer was observed in this complexity-generating step. The transformation required only 2 h, which compares favorably to our earlier Fischer indolization studies. It is hypothesized that the rigid nature of the substrate is responsible for the facile nature of the [3,3]-sigmatropic rearrangement. Nonetheless, our ability to access **3.3** marked a critical juncture in our synthetic efforts, as we expected that oxidative cleavage of the cyclopentene could lead to assembly of the important furanoindoline motif present in the natural product.

Scheme 3.5 Synthesis of cyclopentene **3.5** and Fischer indolization.



3.5 Failed Oxidation and Modification of Synthetic Route

Our excitement in having accessed Fischer indolization product **3.3** was quickly thwarted by our inability to oxidatively cleave the cyclopentene ring. Figure 3.1 summarizes a variety of reaction conditions were tested as a means to selectively oxidize the endocyclic olefin. Each of these efforts resulted in the recovery of starting material or substantial nonspecific decomposition of substrate **3.3**. Osmium-,^{21–22} along with ruthenium-²³ and manganese-based oxidations,²⁴ were deemed ineffective. Similarly, attempted epoxidation with *m*-CPBA or direct oxidative cleavage using ozonolysis conditions resulted in decomposition of the starting material.

Figure 3.1 Attempted olefin oxidation of indolenine substrate **3.3**.

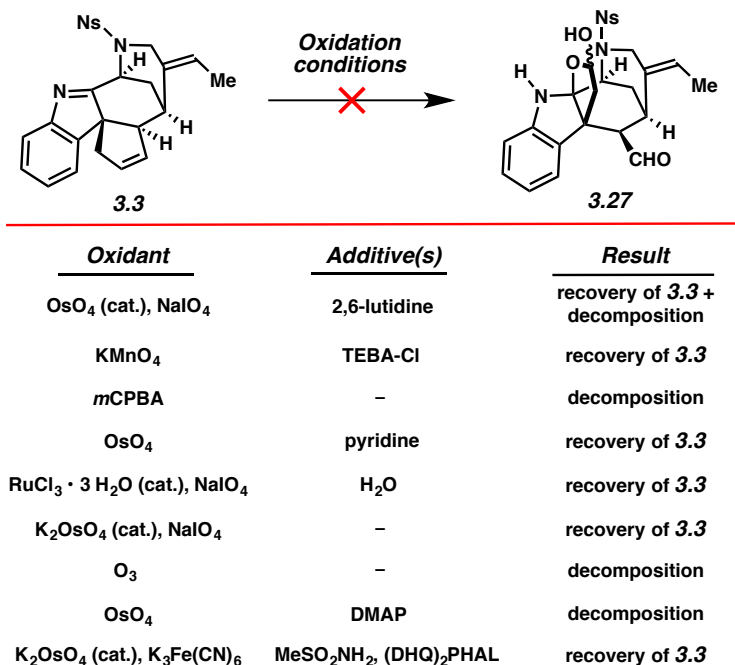
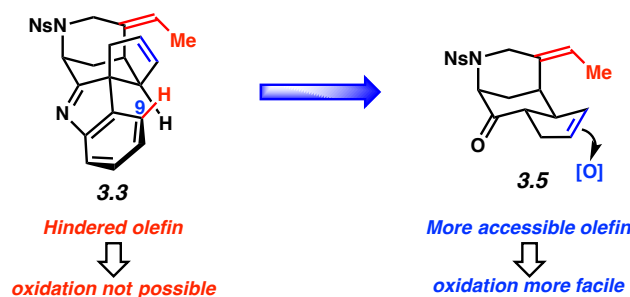


Figure 3.2 suggests a reasonable hypothesis for the difficulties we experienced in attempting to oxidatively cleave cyclopentene **3.3**. A three-dimensional depiction of **3.3** shows that approach to the olefin is severely obstructed on both faces. On one hand, the proximal ethylidene moiety blocks approach of an oxidant, whereas approach to the other face is impeded by the hydrogen at C9. As a workaround, we considered performing the oxidative functionalization of cyclopentene **3.5** prior to performing the Fischer indolization step. Although the ethylidene similarly blocks approach of one face of the olefin in **3.5**, the other face appeared accessible for oxidation to occur.

Figure 3.2 Hypothesis for oxidation difficulties and revision of strategy.



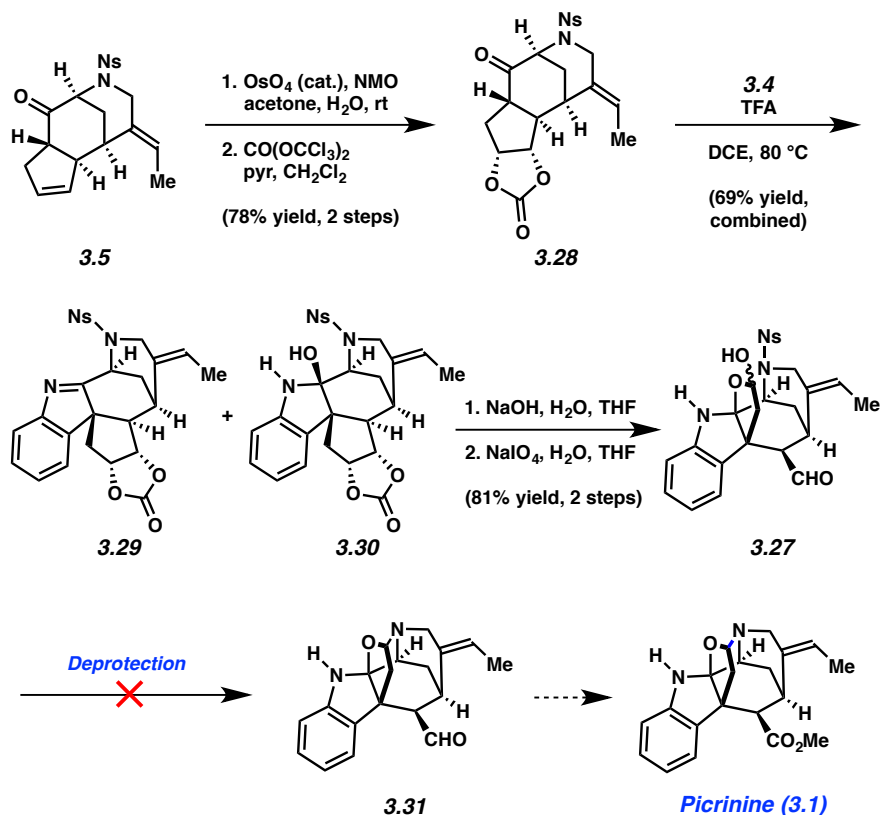
3.6 Earlier Oxidation, Successful Fischer indolization, and Late-Stage Challenges

Our efforts to carry out the revised endgame strategy are depicted in Scheme 3.6. First, chemo- and diastereoselective Upjohn dihydroxylation²⁵ of the *trans*-hydrindenone **3.5**, followed by protection of the resultant diol as the cyclic carbonate,²⁶ gave tetracyclic intermediate **3.28** in 78% yield over 2 steps. The success of this sequence validated our hypothesis shown in Figure 3.2 and allowed us to attempt the key Fischer indolization step. Treatment of **3.28** with phenylhydrazine (**3.4**) and TFA at 80 °C in DCE gave a mixture of two products in a combined yield of 69%. After careful separation and 2D-NMR analysis of each compound in C₆D₆, the two products were identified as indolenine **3.29** and hydrate **3.30**.²⁷ These compounds could be taken forward as an inconsequential mixture. It is worth noting that the Fischer indolization of substrate **3.28** is one of the most complex examples in the literature to date.²⁸

The next late-stage maneuver involved revealing the diol moiety and performing oxidative cleavage. This was achieved by treating the mixture of **3.29** and **3.30** with NaOH,²⁹ followed by exposure of the intermediate diol to NaIO₄. The resulting lactol, **3.27**, was obtained in 81% yield over 2 steps.³⁰ Thus, by installing oxidation prior to the Fischer indolization, our problematic

oxidation of cyclopentene **3.3** (see Figures 3.1 and 3.2) had been successfully circumvented. Having synthesized lactol **3.27**, all that remained was conversion of the exocyclic aldehyde to a methyl ester, cleavage of the sulfonamide, and construction of the *N,O*-acetal. In our first efforts, we attempted to cleave the sulfonamide group using thiol-based denosylation conditions.³¹ Unfortunately, these attempts led to the formation of multiple products that proved difficult to isolate. To facilitate purification, the deprotection of **3.27** was tried using a resin-bound thiol (MetSThiol) in the presence of Cs₂CO₃.³² Although it appeared that cleavage of the nosyl protecting group had occurred,³³ we regrettably did not detect formation of the desired product **3.31**. Thus, our efforts to access the natural product (**3.1**) had again been foiled.

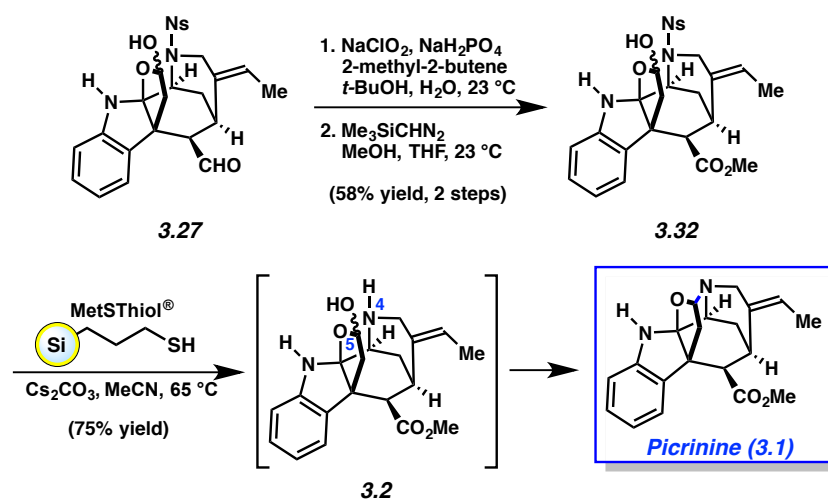
Scheme 3.6 Synthesis of lactol **3.27** and failed late-stage *N,O*-acetal formation.



3.7 Completion of the Total Synthesis of Picrinine (3.1)

With limited options available, we decided to change the order of late-stage transformations by introducing the ester prior to denosylation (Scheme 3.7). Toward this end, Lindgren oxidation of **3.27** gave an intermediate carboxylic acid, which was methylated with trimethylsilyldiazomethane to afford ester **3.32** in 58% yield over 2 steps.³⁴ This delicate oxidation is noteworthy in that it occurred without any competitive oxidation of the lactol. With ester **3.32** in hand, we attempted the nosyl removal using the solid-supported conditions mentioned previously. Much to our pleasure, picrinine (**3.1**) was obtained as the sole product.³⁵ It is likely that the smooth formation of **3.1** occurs via cyclization of intermediate **3.2** due to the constrained proximity of N4 and C5. Our synthetic sample of picrinine (**3.1**) was found to be identical to a natural sample.³⁶

Scheme 3.7 Completion of the total synthesis of picrinine (**3.1**).



3.8 Conclusion

In conclusion, we have developed the first total synthesis of the daunting, polycyclic akuammiline alkaloid picrinine (**3.1**). Challenges from our first-generation approach prompted us to develop a revised synthesis of the [3.3.1]-azabicyclic core of the natural product, which proved far more robust and scalable compared to our initial route. In turn, efficient access to the azabicyclic core permitted late-stage studies and the design and testing of substrates for late-stage Fischer indolization reactions. In fact, the substrates utilized in our synthetic forays toward picrinine represent some of the most complex examples of Fischer indolizations to date. It is hoped that the lessons learned in the course of our total synthesis of **3.1** will help guide synthetic studies pertaining to akuammilines and other classes of complex indole alkaloids.

3.9 Experimental Section

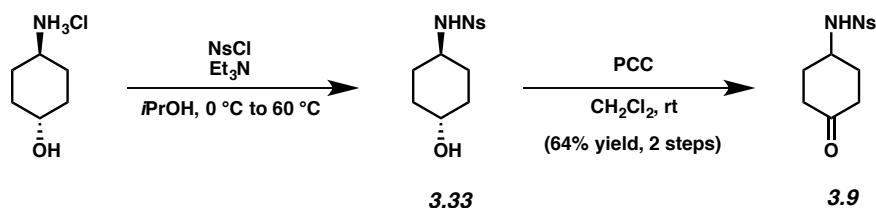
3.9.1 Materials and Methods

Unless stated otherwise, reactions were conducted in flame-dried glassware under an atmosphere of nitrogen using anhydrous solvents (either freshly distilled or passed through activated alumina columns). 2-Iodoxybenzoic acid (IBX)³⁷ and Dess–Martin periodinane³⁸ were prepared from known literature procedures. *trans*-4-Aminocyclohexanol•HCl, pyridinium chlorochromate (PCC), potassium *tert*-butoxide (KO*t*-Bu), lithium hexamethyldisilazide (LHMDS), sodium chlorite, 2-methyl-2-butene, *N*-methylmorpholine-*N*-oxide (NMO), triphosgene, methoxymethyltriphosponium chloride, methyltriphosponium bromide, tributyltin hydride, trimethylsulfonium iodide (Me₃SI), *n*-butyllithium (*n*-BuLi), 2,6-lutidine, and allyl iodide were

obtained from Sigma–Aldrich. Osmium tetroxide, bis(diphenylphosphino)ferrocene-palladium(II) dichloride dichloromethane adduct $[\text{PdCl}_2(\text{dppf})\cdot\text{CH}_2\text{Cl}_2]$, palladium diacetate $[\text{Pd}(\text{OAc})_2]$, tetrakis(triphenylphosphine)palladium $[\text{Pd}(\text{PPh}_3)_4]$, and zinc chloride (ZnCl_2) were obtained from Strem. Triethylsilylchloride (TESCl) was obtained from Oakwood. Sodium perborate and trifluoroacetic acid were obtained from Fischer. Phenylhydrazine was obtained from Acros and purified by flash chromatography (4:1 hexanes:EtOAc). The Hoveyda–Grubbs second-generation catalyst was obtained from Materia. Sodium periodate and cesium carbonate were obtained from Alfa-Aesar. 2-Nitrobenzenesulfonyl chloride (NsCl) and trimethylsilyldiazomethane were obtained from TCI. Solid supported thiol-resin (MetSThiol[®]) was obtained from SiliCycle (Product # R51030B). 1,3-dimethyl-3,4,5,6-tetrahydro-2(1H)-pyrimidinone (DMPU) was obtained from Aldrich and distilled from calcium hydride before use. Unless stated otherwise, reactions were performed at room temperature (approximately 23 °C). Thin-layer chromatography (TLC) was conducted with EMD gel 60 F254 pre-coated plates (0.25 mm) and visualized using a combination of UV, anisaldehyde, and iodine staining. SiliCycle silica gel 60 (particle size 0.040–0.063 mm) was used for flash column chromatography. ¹H NMR spectra were recorded on Bruker spectrometers (300 and 500 MHz). Data for ¹H spectra are reported as follows: chemical shift (δ ppm), multiplicity, coupling constant (Hz), integration and are referenced to the residual solvent peak 7.26 ppm for CDCl_3 and 7.16 ppm for C_6D_6 . ¹³C NMR spectra are reported in terms of chemical shift (at 125 MHz) and are referenced to the residual solvent peak 77.16 ppm for CDCl_3 , and 128.06 for C_6D_6 . IR spectra were recorded on a Perkin-Elmer 100 spectrometer and are reported in terms of frequency absorption (cm^{-1}). Uncorrected melting points were measured using a Mel-Temp II melting point apparatus with a Fluke 50S thermocouple and a Digimelt MPA160 melting point apparatus. High-resolution mass

spectra were obtained from the UC Irvine and UCLA Mass Spectrometry Facilities.

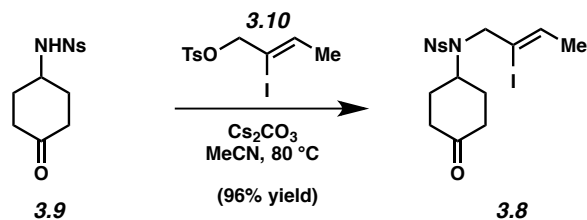
3.9.2 Experimental Procedures



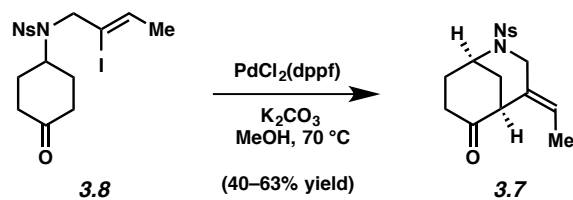
Nosyl Ketone 3.9. To a solution of *trans*-4-aminocyclohexanol•HCl (10.0 g, 66.0 mmol) in isopropyl alcohol (120 mL) was added 2-nitrobenzenesulfonyl chloride (14.6 g, 66.0 mmol) and triethylamine (36.7 mL, 263.8 mmol) at 0 °C. The mixture was heated to 60 °C and after 2 h, the reaction was filtered and the filtrate was concentrated under reduced pressure. The resulting residue was dissolved in EtOAc (200 mL) and washed successively with 0.5 M HCl (50 mL) and H₂O (100 mL). The aqueous layer was extracted with EtOAc (50 mL) and the organic layers were combined, dried over MgSO₄, and evaporated under reduced pressure to afford the crude product **3.33**. This residue was used in the subsequent step without further purification.

To a solution of pyridinium chlorochromate (26.0 g, 120.9 mmol) and celite (9.5 g) in CH₂Cl₂ (202 mL) was added **3.33** at room temperature. After 12 h, the reaction was diluted with Et₂O (300 mL), filtered over a pad of layered celite, alumina, and sand, and washed with EtOAc (1 L). The filtrate was concentrated under reduced pressure to afford nosyl ketone **3.9** (12.5 g, 64% yield, 2 steps) as a beige solid. Nosyl ketone **3.9**: mp: 145–147 °C; R_f 0.25 (1:1 hexanes:EtOAc); ¹H NMR (500 MHz, CDCl₃): δ 8.21 (m, 1H), 7.90 (m, 1H), 7.78 (m, 2H), 5.41 (d, *J* = 7.0), 3.79 (m, 1H), 2.47–2.32 (m, 4H), 2.12 (m, 2H), 1.86 (m, 2H); ¹³C NMR (125 MHz, CDCl₃): δ 208.6, 148.1, 134.5, 134.0, 133.2, 130.9, 125.7, 51.1, 38.5, 32.6; IR (film) 3305, 2952,

1710, 1538, 1443, 1343, 1163; HRMS–ESI (m/z) [$M + H$]⁺ calcd for C₁₂H₁₅N₂O₅S⁺, 299.06962; found 299.06911.

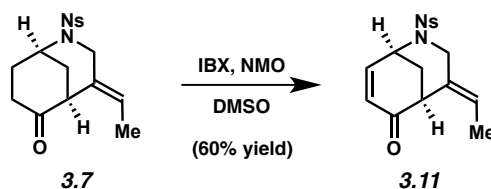


Iodide 3.8. To a suspension of ketone **3.9** (15.0 g, 50.3 mmol) and cesium carbonate (24.6 g, 75.5 mmol) in MeCN (250 mL) was added tosylate **3.10**³⁹ (21.3 g, 60.5 mmol). The reaction was refluxed at 80 °C. After 1.5 h, the reaction was cooled to room temperature and excess MeCN was removed under reduced pressure. The residue was poured into deionized water (100 mL) and the resulting mixture was diluted with CH₂Cl₂ (250 mL). The layers were separated and the aqueous layer was extracted with CH₂Cl₂ (3 x 100 mL). The organic layers were combined, dried over MgSO₄, and evaporated under reduced pressure. The resulting residue was purified via flash chromatography (1.5:1 hexanes:EtOAc) to afford iodide **3.8** (23.1 g, 96% yield) as a yellow solid. Iodide **3.8**: mp: 58–61 °C; R_f 0.53 (1:1 hexanes:EtOAc); ¹H NMR (500 MHz, CDCl₃): δ 8.02–8.00 (m, 1H), 7.75–7.65 (m, 3H), 6.00 (qt, $J = 6.4, 1.3$, 1H), 4.42 (tt, $J = 12.1, 3.6$, 1H), 4.20 (t, $J = 1.3$, 2H), 2.51 (, $J = 14.6, 6$, 2H), 2.42 (dt, $J = 14.6, 2.4$, 2H), 2.23–2.17 (m, 2H), 1.89 (qd, $J = 12.8, 4.7$, 2H), 1.66 (dt, $J = 6.4, 1.3$, 3H); ¹³C NMR (125 MHz, CDCl₃): δ 208.8, 147.9, 134.4, 134.2, 133.9, 131.8 (2 carbons), 124.6, 105.3, 56.5, 55.8, 40.1, 30.6, 22.0; IR (film): 2957, 1716, 1541, 1369, 1345, 1160; HRMS–ESI (m/z) [$M + Na$]⁺ calcd for C₁₆H₁₉IN₂O₅SNa⁺, 500.9952; found 500.9960.

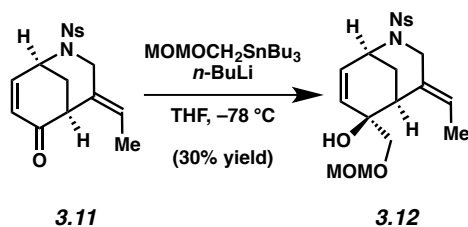


Ketone 3.7. A solution of iodide **3.8** (500 mg, 1.05 mmol) in MeOH (20 mL) was cooled to -100 °C. After stirring for 5 min, the solution was put under vacuum. After 5 additional min of stirring, the reaction was sparged with N_2 for 10 min, followed by the addition of 1,1'-bis(diphenylphosphino)ferrocene-palladium(II)dichloride dichloromethane adduct (171 mg, 0.209 mmol) and potassium carbonate (570 mg, 4.18 mmol) (Note: The variable amount of oxygen present in the reaction can alter the yield, thus rigorous deoxygenation is required). The cooling bath was removed from the reaction and continued to be degassed while warming up to room temperature, at which point the reaction was refluxed at 70 °C. After 45 min, the reaction was cooled to room temperature and the excess MeOH was removed under reduced pressure. The resulting residue was diluted with deionized water (100 mL) and CH_2Cl_2 (100 mL). The layers were separated and the aqueous layer was extracted with CH_2Cl_2 (2 x 100 mL). The organic layers were combined, dried over Na_2SO_4 , and evaporated under reduced pressure. The resulting residue was purified via flash chromatography (1.5:1 hexanes:EtOAc) to afford ketone **3.7** (195 mg, 53% yield) as a brown solid. Ketone **3.7**: mp: 125 – 129 °C; R_f 0.29 (1:1 hexanes:EtOAc); ^1H NMR (300 MHz, CDCl_3): δ 8.07–8.03 (m, 1H), 7.77–7.68 (m, 2H), 7.67–7.60 (m, 1H), 5.68 (q, $J = 7.0$, 1H), 4.30 (t, $J = 5.8$, 1H), 4.15 (d, $J = 13.9$, 1H), 3.90 (dt, $J = 13.9$, 0.9, 1H), 3.49 (br. s, 1H), 2.90–2.79 (m, 1H), 2.33–2.24 (m, 2H), 2.03 (dt, $J = 14.1$, 2.7, 1H), 1.97–1.85 (m, 1H), 1.61 (dt, $J = 7.0$, 0.9, 3H); ^{13}C NMR (125 MHz, CDCl_3): δ 208.1, 148.5, 134.0, 132.0, 131.8, 131.3, 128.8, 126.6, 124.4, 49.0, 48.2, 46.7, 35.0, 32.9, 31.4, 13.2; IR (film):

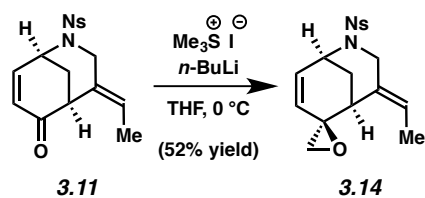
2956, 1713, 1543, 1373, 1164; HRMS–ESI (m/z) $[M + Na]^+$ calcd for $C_{16}H_{18}N_2O_5SNa^+$, 373.0829; found 373.0836.



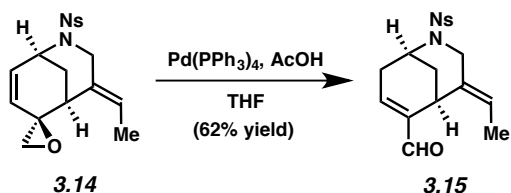
Enone 3.11. To a dram vial charged with IBX (0.128 g, 0.457 mmol) and NMO (0.056 g, 0.476 mmol) was added DMSO (0.5 mL). The mixture was stirred for 10 min at room temperature at which point a solution of ketone **3.7** (0.050 g, 0.143 mmol) in DMSO (0.64 mL) was added and the reaction was heated to 45 °C. After 20 h, the reaction was cooled to room temperature and washed with a 5% aq. NaHCO_3 solution (2 mL) and extracted with Et_2O (4 x 20 mL). The organic layers were combined, dried over MgSO_4 , and evaporated under reduced pressure. The resulting residue was purified via flash chromatography (1.5:1 hexanes:EtOAc) to afford enone **3.11** (0.030 g, 60% yield) as a white solid. Enone **3.11**: mp: 122.5–124 °C; R_f 0.48 (1.5:1 hexanes:EtOAc); ^1H NMR (500 MHz, CDCl_3): δ 8.08 (dd, $J = 7.4, 2, 1\text{H}$), 7.67–7.67 (m, 3H), 6.85 (ddd, $J = 10.0, 6.1, 1.8, 1\text{H}$), 6.26 (dd, $J = 10.0, 1.1$), 5.58 (q, $J = 7.2, 1\text{H}$), 4.74 (dt $J = 6.1, 3.1, 1\text{H}$), 4.00 (d, $J = 14.7, 1\text{H}$), 3.85 (dt, $J = 14.7, 2.1, 1\text{H}$), 3.67 (t, $J = 3.0, 1\text{H}$), 2.36 (dt, $J = 13.1, 3.1, 1\text{H}$), 2.05 (m, 1H), 1.73 (dd, $J = 6.8, 2.1, 3\text{H}$); ^{13}C NMR (125 MHz, CDCl_3): δ 197.2, 147.9, 142.3, 134.0, 133.2, 133.1, 132.1, 131.0, 128.0, 124.9, 124.7, 47.6, 47.1, 44.2, 32.8, 12.9; IR (film): 2925, 1686, 1542, 1370, 1165 cm^{-1} ; HRMS–ESI (m/z) $[M + Na]^+$ calcd for $C_{16}H_{16}N_2O_5SNa^+$, 371.0677; found 371.0672.



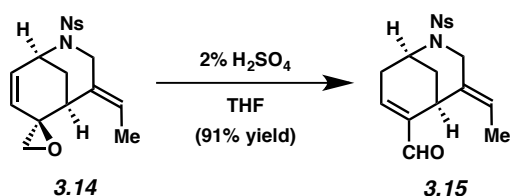
Alcohol 3.12. To a solution of $\text{CH}_3\text{OCH}_2\text{OCH}_2\text{SnBu}_3$ (39 mg, 0.11 mmol)⁴⁰ in THF (1 mL) was added a solution of *n*-butyllithium (*n*-BuLi) (0.046 mL, 2.05 M in hexanes) at $-78\text{ }^\circ\text{C}$. The reaction mixture was stirred for 20 min, at which point a solution of enone **3.11** (25 mg, 0.072 mmol) in THF (1 mL) was added dropwise over 1 min at $-78\text{ }^\circ\text{C}$. After 1 h, the reaction mixture was quenched with a solution of saturated aqueous NH_4Cl (3 mL) and allowed to warm to room temperature. The layers were separated, and the aqueous layer was extracted with EtOAc (4 x 10 mL). The combined organic layers were dried over MgSO_4 , filtered, and evaporated under reduced pressure. The resulting residue was purified via flash chromatography (2:1 hexanes:EtOAc) to afford alcohol **3.12** (9 mg, 30% yield) as a pale yellow oil. Alcohol **3.12**: R_f 0.28 (2:1 hexanes:EtOAc); $^1\text{H NMR}$ (500 MHz, CDCl_3): δ 8.02 (m, 1H), 7.68 (m, 2H), 7.62, (m, 1H), 5.86 (dd, $J = 10.0, 1.3$, 1H), 5.73 (ddd, $J = 10.0, 5.7, 1.3$, 1H), 5.66 (q, $J = 6.9$, 1H), 4.68–4.48 (m, 3H), 3.97 (d, $J = 14.1$, 1H), 3.90 (dt, $J = 14.1, 2.0$, 1H), 3.58 (d, $J = 10.4$, 1H), 3.48 (d, $J = 10.4$, 1H), 3.38 (s, 3H), 3.23 (t, $J = 3.8$, 1H), 2.49 (s, 1H), 1.99 (dt, $J = 13.4, 3.0$, 1H), 1.82 (dt, $J = 13.4, 3.4$, 1H), 1.66 (dd, $J = 6.9, 2.0$, 3H); $^{13}\text{C NMR}$ (125 MHz, CDCl_3): δ 148.0, 136.2, 133.7, 133.6, 131.8, 131.2, 130.8, 125.6, 124.8, 124.4, 97.3, 72.8, 71.5, 55.7, 47.9, 47.7, 35.0, 30.9, 12.9; IR (film): 3526, 2931, 1543, 1442, 1372, 1352, 1213, 1164, 1108, 1036; HRMS–ESI (m/z) $[\text{M} + \text{H}]^+$ calcd for $\text{C}_{19}\text{H}_{25}\text{N}_2\text{O}_7\text{S}^+$, 425.13770; found 425.13565.



Epoxide 3.14. To a suspension of trimethylsulfonium iodide ($\text{Me}_3\text{S}^+\text{I}^-$) (39 mg, 0.19 mmol) in THF (1 mL) was added *n*-butyllithium (*n*-BuLi) (65 μL , 2.65 M in hexanes) at 0 $^\circ\text{C}$. After 5 min, a solution of enone **3.11** (56 mg, 0.16 mmol) in THF (0.6 mL) was added dropwise over 1 min at 0 $^\circ\text{C}$. After 30 min, the reaction was warmed to room temperature and poured into a brine solution (3 mL). The layers were separated, and the aqueous layer was extracted with EtOAc (3 x 10 mL). The combined organic layers were dried over MgSO_4 , filtered, and evaporated under reduced pressure. The resulting residue was purified via flash chromatography (2:1 hexanes:EtOAc) to afford epoxide **3.14** (30 mg, 52% yield) as a pale yellow oil. Epoxide **3.14**: R_f 0.58 (2:1 hexanes:EtOAc); ^1H NMR (500 MHz, CDCl_3): δ 8.04 (m, 1H), 7.69 (m, 2H), 7.63 (m, 1H), 5.94 (ddd, $J = 1.5, 5.9, 9.9$, 1H), 5.56 (q, $J = 6.8, 12$), 5.55 (dd, $J = 1.2, 9.9$, 1H), 4.61 (dt, $J = 3.0, 5.9$, 1H), 4.00 (m, 2H), 2.96 (d, $J = 5.2$, 1H), 2.85 (d, $J = 5.2$, 1H), 2.73 (br. s, 1H), 2.16 (dt, $J = 3.1, 12.9$, 1H), 1.99 (ddt, $J = 1.6, 3.4, 12.9$, 1H), 1.56 (dd, $J = 1.5, 6.3$, 3H); ^{13}C NMR (125 MHz, CDCl_3): δ 148.0, 135.8, 133.6, 133.7, 131.9, 131.0, 130.8, 129.1, 124.4, 123.5, 58.3, 56.4, 47.6, 47.3, 34.9, 32.3, 12.7; IR (film): 2924, 1543, 1440, 1372, 1165, 1127, 1075; HRMS–ESI (m/z) [$\text{M} + \text{H}$] $^+$ calcd for $\text{C}_{17}\text{H}_{19}\text{N}_2\text{O}_5\text{S}^+$, 363.10090; found 369.10024.

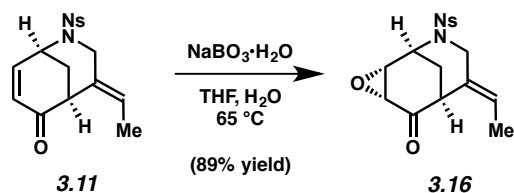


Enal 3.15. To a solution of tetrakis(triphenylphosphine)palladium [Pd(PPh₃)₄] (1 mg, 0.00030 mmol) and acetic acid (AcOH) (2 μL, 0.033 mmol) in THF (0.25 mL) was added a solution of epoxide **3.14** (0.011 g, 0.030 mmol) dropwise over 1 min. After 30 min, the reaction was filtered over a plug of SiO₂, washed with EtOAc (25 mL) and the filtrate was concentrated under reduced pressure. The resulting residue was purified via preparative TLC (2:1 hexanes:EtOAc) to afford enal **3.15** (7 mg, 62% yield) as a colorless oil.

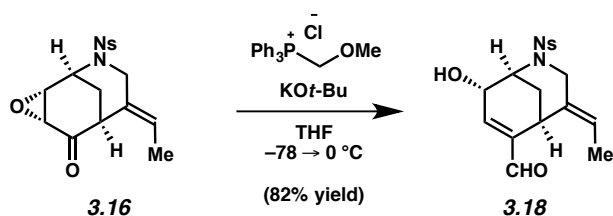


Enal 3.15. To a solution of epoxide **3.14** (11 mg, 0.030 mmol) in THF (0.30 mL) was added an aqueous solution of sulfuric acid (H₂SO₄) (0.2 mL, 2% w/w). After 5 min, the reaction mixture was diluted with EtOAc (5 mL) and poured into a solution of saturated aqueous NaHCO₃ (5 mL). The layers were separated and the aqueous layer was extracted with EtOAc (3 x 10 mL). The combined organic layers were dried over MgSO₄, filtered, and evaporated under reduced pressure. The resulting residue was purified via flash chromatography (2:1 hexanes:EtOAc) to afford enal **3.15** (10 mg, 91% yield) as a colorless oil. Enal **3.15**: R_f 0.38 (2:1 hexanes:EtOAc); ¹H NMR (500 MHz, CDCl₃): δ 9.37 (s, 1H), 8.05 (m, 1H), 7.74–7.63 (m, 3H), 6.91 (t, *J* = 3.7, 1H), 5.43 (q, *J* = 6.9, 1H), 4.45 (br. s, 1H), 3.96 (br. s, 1H), 3.85 (d, *J* = 14.3, 1H), 3.71 (d, *J* = 14.3, 1H), 2.82 (ddd, *J* = 3.4, 5.9, 21.5, 1H), 2.59 (dd, *J* = 3.9, 21.5, 1H), 1.92 (dt, *J* = 3.4, 12.8, 1H), 1.78 (dd, *J* = 1.8, 6.8, 3H), 1.69 (dt, *J* = 3.1, 12.8, 1H); ¹³C NMR (125 MHz, CDCl₃): δ 191.8, 149.1, 148.0, 142.5, 133.7, 133.6, 131.9, 131.0, 130.7, 124.5, 122.7, 48.0, 47.0, 33.2, 30.9,

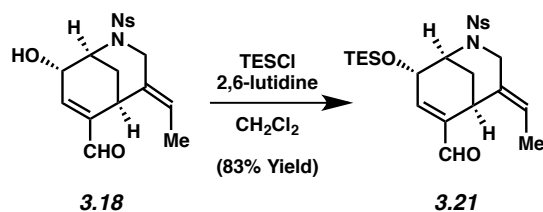
26.6, 12.9; IR (film): 2923, 1682, 1542, 1440, 1371, 1340, 1164, 1126, 1081; HRMS–ESI (m/z) $[M + H]^+$ calcd for $C_{17}H_{19}N_2O_5S^+$, 363.10090; found 363.10022.



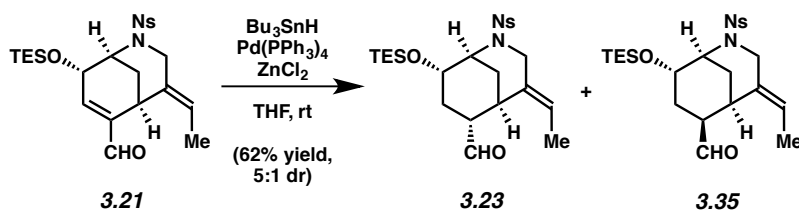
Epoxide 3.16. To two individual, but identical solutions of enone **3.11** (422 mg, 1.21 mmol) in 1:1 THF: H_2O (4 mL) was added sodium perborate monohydrate (375 mg, 3.76 mmol). Each reaction was heated to $65\text{ }^\circ\text{C}$. After stirring for 12 h, each reaction was cooled to room temperature and poured into deionized water (150 mL) and diluted with EtOAc (150 mL). The layers were separated and the aqueous layer was extracted with EtOAc (2 x 150 mL). The organic layers from both reactions were combined, dried over $MgSO_4$, and evaporated under reduced pressure. The combined residue was purified via flash chromatography (2:1 hexanes:EtOAc) to afford epoxide **3.16** (785 mg, 89% yield) as a yellow solid. Epoxide **3.16**: mp: $147\text{--}149\text{ }^\circ\text{C}$; R_f 0.45 (1:1 hexanes:EtOAc); 1H NMR (500 MHz, $CDCl_3$): δ 8.13–8.11 (m, 1H), 7.77–7.69 (m, 3H), 5.60 (q, $J = 6.9$, 1H), 4.72 (q, $J = 2.9$, 1H), 4.06 (d, $J = 15.1$, 1H), 3.97 (dt, $J = 15.1$, 1.8), 3.62 (t, $J = 3.2$, 1H), 3.52 (t, $J = 2.7$, 1H), 3.38 (d, $J = 3.2$, 1H), 2.33 (dt, $J = 13.7$, 2.9, 1H), 1.71–1.68 (m, 4H); ^{13}C NMR (125 MHz, $CDCl_3$): δ 201.7, 147.8, 134.1, 133.0, 132.1, 131.0, 128.3, 125.1, 124.7, 54.2, 51.7, 48.4, 47.6, 42.0, 23.6, 12.8; IR (film): 2919, 1716, 1542, 1371, 1163; HRMS–ESI (m/z) $[M + Na]^+$ calcd for $C_{16}H_{16}N_2O_6SNa^+$, 387.0621; found 387.0630.



Enal 3.18. In a glovebox, a round-bottom flask was charged with methoxymethyl-triphenylphosphonium chloride (0.659 g, 1.93 mmol), and a dram vial was charged with potassium *tert*-butoxide (0.198 g, 1.76 mmol). The contents were removed from the glovebox, placed under N₂ pressure, and THF was added to the flask and vial (8 mL and 2 mL, respectively). The solution of methoxymethyltriphenylphosphonium chloride in THF was cooled to –78 °C and the solution of potassium *tert*-butoxide in THF was added dropwise over 1 min. The mixture was stirred at –78 °C for 30 min, at which point a solution of epoxide **3.16** (0.585 g, 1.60 mmol) in THF (6 mL) was added dropwise over 1 min. The reaction was warmed to 0 °C, and after stirring for 15 min, the reaction was quenched with a solution of sat. aq. NH₄Cl (15 mL). The resulting mixture was poured into deionized water (100 mL) and diluted with EtOAc (100 mL). The layers were separated and the aqueous layer was extracted with EtOAc (2 x 100 mL). The organic layers were combined, dried over MgSO₄, and evaporated under reduced pressure. The resulting residue was purified via flash chromatography (1:1 hexanes:EtOAc) to afford enal **3.18** (0.500 g, 82% yield) as a clear wax. Enal **3.18**: R_f 0.15 (1:1 hexanes: EtOAc); ¹H NMR (500 MHz, CDCl₃): δ 9.47 (s, 1H), 8.05 (dd, *J* = 1.7, 7.5, 1H), 7.76–7.65 (m, 3H), 6.86 (d, *J* = 3.8, 1H), 5.45 (q, *J* = 6.8, 1H), 4.42 (d, *J* = 2.7, 1H), 4.26 (s, 1H), 3.93 (s, 1H), 3.84 (d, *J* = 14.5, 1H), 3.60 (d, *J* = 14.5, 1H), 2.70 (s, 1H), 1.91 (dt, *J* = 13.3, 3.2), 1.81–1.73 (m, 4H); ¹³C NMR (125 MHz, CDCl₃): δ 192.3, 147.9, 146.7, 143.6, 133.9, 133.3, 132.1, 131.0, 129.4, 124.6, 123.5, 67.6, 55.1, 47.2, 27.1, 26.6, 12.9; IR (film): 3406, 2926, 2859, 1686, 1541, 1370, 1160, 1127; HRMS–ESI (*m/z*) [*M* – H][–] calcd for C₁₇H₁₇N₂O₆S[–], 377.0807; found 377.0821.



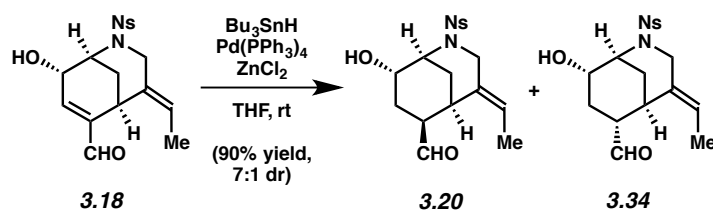
Enal 3.21. To a solution of enal **3.18** (25 mg, 0.066 mmol) in CH_2Cl_2 (1 mL) was added 2,6-lutidine (0.046 mL, 0.40 mmol) and chlorotriethylsilane (TESCl) (33 μL , 0.20 mmol). After stirring for 17 h, the reaction mixture was diluted with CH_2Cl_2 (5 mL) and poured into H_2O (5 mL). The layers were separated, and the aqueous layer was extracted with CH_2Cl_2 (2 x 10 mL). The combined organic layers were dried over MgSO_4 , filtered, and evaporated under reduced pressure. The resulting residue was purified via preparative TLC (1:1 hexanes:EtOAc) to afford enal **3.21** (27 mg, 83% yield) as a colorless oil. Enal **3.21**: R_f 0.31 (4:1 hexanes:EtOAc); ^1H NMR (500 MHz, CDCl_3): δ 9.44 (s, 1H), 8.06 (m, 1H), 7.73–7.65 (m, 3H), 6.75 (dd, $J = 4.0, 1.2$, 1H), 5.41 (q, $J = 6.7$, 1H), 4.41 (d, $J = 4.0$, 1H), 4.06 (br. s, 1H), 2.90 (t, $J = 2.9$, 1H), 3.81 (d, $J = 14.5$, 1H), 3.67 (dt, $J = 14.5, 1.9$, 1H), 1.95 (dt, $J = 13.0, 3.1$, 1H), 1.76 (dd, $J = 6.8, 1.9$, 3H), 1.66 (dt, $J = 13.0, 3.2$, 1H), 0.96 (t, $J = 8.1$, 9H), 0.66 (q, $J = 8.1$, 6H); ^{13}C NMR (125 MHz, CDCl_3): δ 192.6, 148.0 (2 carbons), 142.1, 133.8, 133.4, 131.9, 131.1, 129.7, 124.7, 122.9, 67.9, 55.1, 47.2, 27.1, 26.2, 12.8, 6.9, 4.7; IR (film): 2957, 2877, 1690, 1543, 1457, 1440, 1370, 1343, 1240, 1164, 1126, 1071, 1009; HRMS–ESI (m/z) $[\text{M} + \text{H}]^+$ calcd for $\text{C}_{23}\text{H}_{32}\text{N}_2\text{O}_6\text{SSi}^+$, 493.18231; found 493.17800.



Aldehyde 3.23 and Aldehyde 3.35. In the glovebox, a vial was charged with tetrakis(triphenylphosphine)palladium [Pd(PPh₃)₄] (2 mg, 0.0016 mmol) and zinc chloride (ZnCl₂) (17 mg, 0.125 mmol). The flask was removed from the glovebox, placed under N₂ pressure, and THF (1.5 mL) was added. To this solution was added a solution of enal **3.21** (27 mg, 0.054 mmol) in THF (1.2 mL). The resulting mixture was sparged with N₂ for 10 min, at which point tributyltin hydride (Bu₃SnH) (0.029 mL, 0.11 mmol) was added. After 20 h, the reaction mixture was diluted with EtOAc (10 mL) and poured into H₂O (10 mL). The layers were separated, and the aqueous layer was extracted with EtOAc (2 x 10 mL). The combined organic layers were dried over MgSO₄, filtered, and evaporated under reduced pressure. The resulting residue was purified via preparative TLC (18:1:1 benzene:Et₂O:CH₂Cl₂) to afford aldehyde **3.23** (14 mg, 52% yield) and aldehyde **3.35** (3 mg, 10% yield) as colorless oils. The stereochemical assignment of **3.23** and **3.35** were determined by analysis of ¹H NMR coupling constants. Aldehyde **3.23**: R_f 0.48 (2:1 hexanes:EtOAc); ¹H NMR (500 MHz, CDCl₃): δ 9.72 (s, 1H), 7.96 (m, 1H), 7.70 (m, 2H), 7.61 (m, 1H), 5.48 (q, *J* = 7.0, 1H), 4.14 (app. q, *J* = 3.1, 1H), 4.06 (d, *J* = 14.1, 1H), 3.75 (m, 2H), 3.36 (br. s, 1H), 2.35 (ddd, *J* = 14.8, 6.8, 2.5, 1H), 2.30 (dt, *J* = 14.2, 2.7, 1H), 2.25 (d, *J* = 6.8, 1H), 2.03 (d, *J* = 14.8, 1H), 1.57 (d, *J* = 7.0, 3H), 1.50 (dt, *J* = 14.2, 3.7, 1H), 0.96 (t, *J* = 8.1, 9H), 0.62 (q, *J* = 8.1, 6H); ¹³C NMR (125 MHz, CDCl₃): δ 202.6, 148.7, 134.4, 133.8, 131.61, 131.57, 131.2, 124.4, 121.9, 68.9, 54.3, 48.61, 48.60, 27.19, 27.17, 20.4, 13.2, 6.9, 4.7; IR (film): 2955, 2921, 2876, 1720, 1544, 1467, 1439, 1373, 1356, 1242, 1168, 1105, 1082, 1069; HRMS–ESI (*m/z*) [M + H]⁺ calcd for C₂₃H₃₄N₂O₆SSi⁺, 495.19796; found 495.19705.

Aldehyde **3.35**: R_f 0.48 (2:1 hexanes:EtOAc); ¹H NMR (500 MHz, CDCl₃): δ 9.64 (s, 1H), 8.04 (m, 1H), 7.69 (m, 3H), 5.45 (q, *J* = 6.9, 1H), 4.19 (app. q, *J* = 2.7, 1H), 4.13 (dt, *J* =

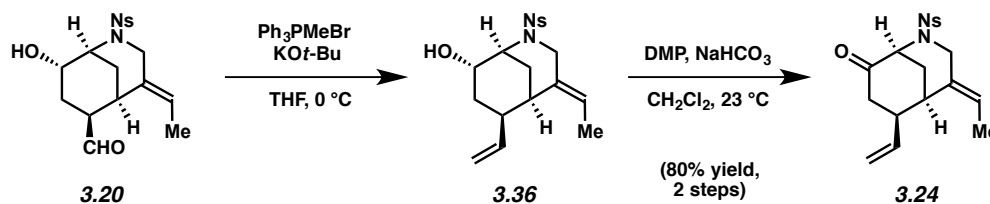
15.3, 2.4, 1H), 3.90 (d, $J = 15.3$, 1H), 3.85 (app. q, $J = 3.5$, 1H), 3.35 (app. q, $J = 3.5$, 1H), 3.02 (dt, $J = 12.7$, 4.4, 1H), 2.41 (dt, $J = 13.2$, 3.1, 1H), 2.10 (ddd, $J = 15.7$, 13.0, 3.4, 1H), 1.85 (dd, $J = 15.7$, 4.8, 1H), 1.60 (dd, $J = 6.9$, 1.6, 3H), 1.56 (dt, $J = 13.2$, 3.6, 1H), 0.95 (t, $J = 8.1$, 9H), 0.61 (q, $J = 8.1$, 6H); ^{13}C NMR (125 MHz, CDCl_3): δ 203.4, 148.1, 133.7, 133.0, 131.8, 131.3, 130.7, 124.7, 122.5, 68.5, 53.3, 49.7, 48.7, 29.0, 28.8, 26.7, 13.2, 7.0, 4.7; IR (film): 2955, 2920, 2876, 1723, 1543, 1459, 1440, 1369, 1243, 1164, 1127, 1099, 1067, 1045, 1006; HRMS–ESI (m/z) $[\text{M} + \text{H}]^+$ calcd for $\text{C}_{23}\text{H}_{34}\text{N}_2\text{O}_6\text{SSi}^+$, 495.19796; found 495.19642.



Aldehyde 3.20 and Aldehyde 3.34. In a glovebox, a round-bottom flask was charged with tetrakis(triphenylphosphine)palladium $[\text{Pd}(\text{PPh}_3)_4]$ (68.0 mg, 0.059 mmol) and zinc chloride (ZnCl_2) (370 mg, 2.71 mmol). The flask was removed from the glovebox, placed under N_2 pressure, and THF (11 mL) was added. To this solution was added a solution of enal **3.18** (430 mg, 1.17 mmol) in THF (11 mL). The resulting mixture was sparged with N_2 for 10 min, at which point tributyltin hydride (Bu_3SnH) (0.63 ml, 2.35 mmol) was added. After stirring for 12 h, the reaction was quenched with a solution of saturated aqueous NH_4Cl (30 mL). The resulting mixture was diluted with EtOAc (65 mL). The layers were separated and the aqueous layer was extracted with EtOAc (2 x 65 mL). The combined organic layers were washed with saturated aqueous NH_4Cl (30 mL), dried over MgSO_4 , filtered and evaporated under reduced pressure. The resulting residue was purified via flash chromatography (1.5:1 hexanes:EtOAc \rightarrow 1:1.5 hexanes:EtOAc) to afford aldehyde **3.20** (0.341 g, 79% yield) as a yellow solid and aldehyde

3.34 (0.049 g, 0.13 mmol) as a colorless foam. The stereochemical assignment of **3.20** and **3.34** were determined by analysis of ^1H NMR coupling constants. Aldehyde **3.20**: mp: 52–55 °C; R_f 0.12 (1:1 hexanes:EtOAc); ^1H NMR (500 MHz, CDCl_3): δ 9.60 (s, 1H), 8.06–8.04 (m, 1H), 7.73–7.68 (m, 2H), 7.77–7.64 (m, 1H), 5.46 (q, $J = 6.8$, 1H), 4.25 (br. s, 1H), 4.12 (dt, $J = 15.3$, 2.0, 1H), 4.03–4.01 (m, 1H), 3.92 (d, $J = 15.3$, 1H), 3.41–3.39 (m, 1H), 3.04 (dt, $J = 13.0$, 4.6, 1H), 2.41 (dt, $J = 13.3$, 3.0, 1H), 2.15 (ddd, $J = 15.9$, 13, 3.9, 1H), 1.97 (dd, $J = 15.9$, 4.6, 1H), 1.87 (d, $J = 3.4$, 1H), 1.64 (dt, $J = 13.3$, 3.4, 1H), 1.61 (dd, $J = 6.8$, 2.0, 3H); ^{13}C NMR (125 MHz, CDCl_3): δ 202.6, 147.9, 133.7, 132.7, 131.8, 131.1, 130.2, 124.5, 122.8, 67.9, 52.7, 49.7, 48.4, 28.8, 27.7, 26.8, 13.0; IR (film): 3432, 2924, 2851, 1720, 1542, 1371, 1164; HRMS–ESI (m/z) [$\text{M} + \text{H}$] $^+$ calcd for $\text{C}_{17}\text{H}_{21}\text{N}_2\text{O}_6\text{S}^+$, 381.11148; found 381.11309.

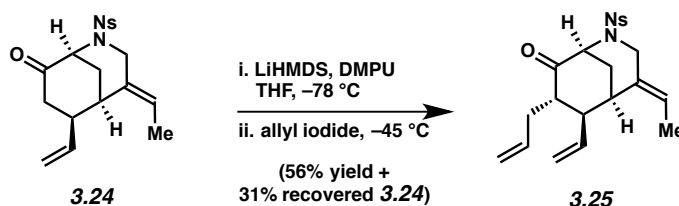
Aldehyde **3.34**. R_f 0.12 (1:1 hexanes:EtOAc); ^1H NMR (500 MHz, CDCl_3): δ 9.79 (s, 1H), 8.01 (m, 1H), 7.71 (m, 2H), 7.61 (m, 1H), 5.53 (q, $J = 6.9$, 1H), 4.16 (t, $J = 3.0$, 1H), 4.11 (d, $J = 14.2$, 1H), 3.88 (app. q, $J = 3.4$, 1H), 3.82 (d, $J = 14.2$, 1H), 3.35 (br. s, 1H), 2.45 (d, $J = 6.9$, 1H), 2.37 (d, $J = 4.1$, 1H), 2.30 (ddd, $J = 15.3$, 6.9, 3.2, 1H), 2.16 (dt, $J = 14.9$, 2.9, 1H), 2.13 (d, $J = 15.3$, 1H), 1.62 (d, $J = 6.9$, 3H), 1.55 (dt, $J = 14.9$, 3.8, 1H); ^{13}C NMR (125 MHz, CDCl_3): δ 203.7, 148.7, 134.0, 133.9, 131.7, 131.5, 131.3, 124.3, 122.4, 68.0, 53.8, 49.1, 48.6, 27.2, 25.5, 20.5, 13.2; IR (film): 3516, 2926, 2854, 1716, 1542, 1467, 1440, 1373, 1352, 1165, 1127, 1102, 1078, 1066; HRMS–ESI (m/z) [$\text{M} + \text{H}$] $^+$ calcd for $\text{C}_{17}\text{H}_{21}\text{N}_2\text{O}_6\text{S}^+$, 381.11148; found 381.11041.



Vinyl Ketone 3.24. In a glovebox, a dram vial was charged with potassium *tert*-butoxide (125 mg, 1.10 mmol). The vial was removed from the glovebox and placed under N₂ pressure. To a suspension of methyltriphenylphosphonium bromide (417 mg, 1.16 mmol) in THF (2 mL) at 0 °C was added a solution of the potassium *tert*-butoxide in THF (2 mL) dropwise over 1 min. The mixture was stirred at 0 °C for 30 min, at which point a solution of aldehyde **3.20** (200 mg, 0.526 mmol) in THF (8 mL) was added dropwise over 1 min. After 10 min of stirring at 0 °C, the reaction was quenched with acetone (6 mL) and deionized water (6 mL). The resulting mixture was diluted with EtOAc (50 mL). The layers were separated and the aqueous layer was extracted with EtOAc (2 x 50 mL). The organic layers were combined and dried over MgSO₄. Evaporation of the solvent under reduced pressure afforded vinyl alcohol **3.36**, which was used in the subsequent step without further purification.

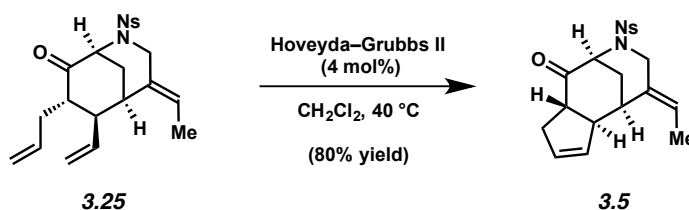
To a solution of crude vinyl alcohol **3.36** and sodium bicarbonate (420 mg, 4.96 mmol) in CH₂Cl₂ (5 mL) was added Dess–Martin Periodinane (631 mg, 1.49 mmol). After stirring for 1.5 h, the reaction mixture was quenched with a solution of sat. aq. NaHCO₃ (10 mL) and diluted with CH₂Cl₂ (65 mL). The layers were separated and the aqueous layer was extracted with CH₂Cl₂ (2 x 65 mL). The organic layers were combined, dried over MgSO₄, and evaporated under reduced pressure. The resulting residue was purified via flash chromatography (1.5:1 hexanes:EtOAc) to afford vinyl ketone **3.24** (159 mg, 80% yield, 2 steps) as a white solid. Vinyl ketone **3.24**: mp: 159–161 °C; R_f 0.47 (1:1 hexanes:EtOAc); ¹H NMR (500 MHz, CDCl₃): 8.08–8.06 (m, 1H), 7.76–7.68 (m, 2H), 7.64–7.62 (m, 1H), 5.75–5.66 (m, 2H), 5.07–5.02 (m, 2H), 4.26–4.17 (m, 3H), 3.07 (q, *J* = 3.6, 1H), 2.78 (dd, *J* = 12.2, 6.4, 1H), 2.54 (dd, *J* = 15.7, 12.4, 1H), 2.46 (dd, *J* = 15.7, 6.4, 1H), 2.20 (dt, *J* = 14.0, 3.6, 1H), 2.03 (dt, *J* = 14.0, 2.9, 1H), 1.63 (dq, *J* = 6.9, 1, 3H); ¹³C NMR (125 MHz, CDCl₃): δ 205.7, 148.1, 139.2, 134.1, 132.23, 132.20,

131.9, 130.2, 124.3, 124.0, 115.6, 58.7, 49.6, 46.6, 43.9, 33.6, 33.0, 13.5; IR (film): 2921, 2851, 1721, 1633, 1542, 1370, 1166; HRMS–ESI (m/z) $[M + H]^+$ calcd for $C_{18}H_{21}N_2O_5S^+$, 377.1166; found 377.11588.



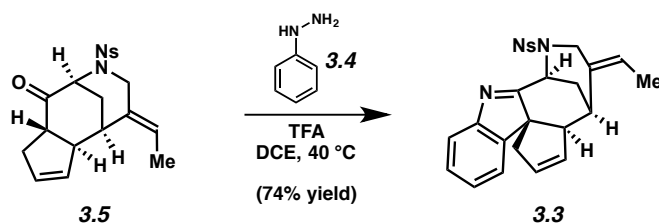
Allyl–vinyl Ketone 3.25. In a glovebox, a dram vial was charged with LiHMDS (129 mg, 0.77 mmol). The vial was removed from the glovebox, placed under N_2 pressure, and THF was added (4 mL). To a solution of ketone **3.24** (288 mg, 0.77 mmol) in THF (4 mL) at $-78\text{ }^\circ\text{C}$ was added the solution of LHMDS dropwise over 1 min. The resulting mixture was stirred for 20 min at $-78\text{ }^\circ\text{C}$, at which point DMPU (2 mL) was added. After 15 min of additional stirring at $-78\text{ }^\circ\text{C}$, a solution of allyl iodide (210 μL , 2.30 mmol) in THF (3 mL) was added and the reaction was subsequently warmed to $-45\text{ }^\circ\text{C}$. Following 1 h, an additional solution of allyl iodide (210 μL , 2.30 mmol) in THF (3 mL) was added at $-45\text{ }^\circ\text{C}$. Following 2 h, an additional solution of allyl iodide (210 μL , 2.30 mmol) in THF (3 mL) was added at $-45\text{ }^\circ\text{C}$. After 1 further h, the reaction was quenched with a solution of sat. aq. NH_4Cl (9 mL) and warmed to room temperature. The resulting mixture was poured into deionized water (6 mL) and diluted with EtOAc (75 mL). The layers were separated and the aqueous layer was extracted with EtOAc (2 x 75 mL). The organic layers were combined, dried over $MgSO_4$, and evaporated under reduced pressure. The resulting residue was purified via flash chromatography (4:1 hexanes:EtOAc \rightarrow 1:1.5 hexanes:EtOAc) to afford recovered vinyl–ketone **3.24** (88 mg, 31% yield) and allyl–vinyl ketone **3.25** (179 mg, 56% yield) as a clear oil. Allyl–vinyl ketone **3.25**: R_f 0.64 (1:1 hexanes:EtOAc); 1H NMR (500

MHz, CDCl₃): 8.07–8.02 (m, 1H), 7.72–7.67 (m, 2H), 7.64–7.59 (m, 1H), 5.69 (q, *J* = 7.0, 1H) 5.65–5.52 (m, 2H), 5.12–5.07 (m, 2H), 4.92–4.86 (m, 2H), 4.31 (dt, *J* = 15.1, 1.9, 1H), 4.26 (dt, *J* = 15.1, 1.2, 1H) 4.23 (dd, *J* = 4.0, 2.8, 1H), 3.05 (q, *J* = 3.4, 1H), 2.60 (ddd, *J* = 11.4, 7.1, 3.5, 1H), 2.46 (ddd, *J* = 12.7, 9.3, 4.6, 1H), 2.26–2.18 (m, 2H), 2.16 (ddd, *J* = 13.9, 4.0, 3.1, 1H), 2.00 (dt, *J* = 13.9, 3.1, 1H), 1.61 (dt, *J* = 7.0, 1.2, 3H); ¹³C NMR (125 MHz, CDCl₃): δ 206.9, 148.1, 138.8, 135.6, 134.0, 132.3, 132.1, 132.0, 130.4, 124.3, 123.9, 117.5, 116.8, 59.7, 52.4, 50.5, 49.4, 34.1, 33.9, 30.9, 13.6; IR (film): 2922, 1718, 1542, 1358, 1166; HRMS–ESI (*m/z*) [*M* + H]⁺ calcd for C₂₁H₂₅N₂O₅S⁺, 417.14787; found 417.14670.



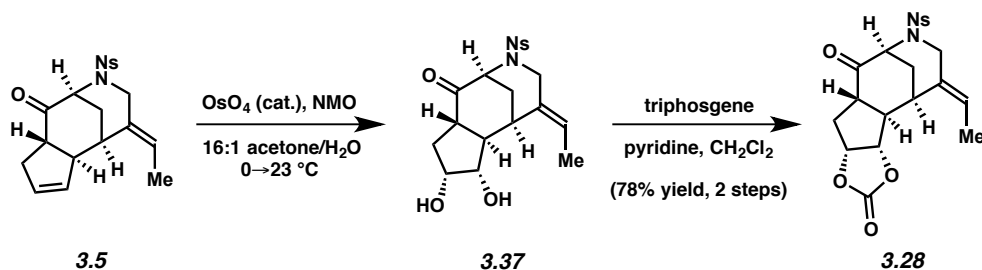
Cyclopentene 3.5. In a glovebox, a dram vial was charged with Hoveyda–Grubbs second generation catalyst (9.8 mg, 0.016 mmol). The vial was removed from the glovebox, placed under N₂ pressure, and CH₂Cl₂ (1 mL) was added. A solution of allyl vinyl ketone **3.25** (93 mg, 0.22 mmol) in CH₂Cl₂ (10 ml) was added to the solution of Hoveyda–Grubbs second generation catalyst. The resulting mixture was heated to 40 °C. After 24 h, the reaction was cooled to room temperature and directly purified by flash chromatography (1:5:1 hexanes:EtOAc) to afford cyclopentene **3.5** (69 mg, 80% yield) as a white solid. Cyclopentene **3.5**: mp: 144–147 °C; R_f 0.37 (1:1 hexanes:EtOAc); ¹H NMR (500 MHz, CDCl₃): 8.04–8.00 (m, 1H), 7.73–7.68 (m, 2H), 7.66–7.64 (m, 1H), 5.83–5.81 (m, 1H), 5.77–5.73 (m, 2H), 4.41 (d, *J* = 15.0, 1H), 4.09 (ddd, *J* = 15.0, 2.4, 1.2, 1H), 4.04 (dd, *J* = 4.1, 2.4, 1H), 3.53 (ddd, *J* = 17.5, 10.8, 6.8, 1H), 3.38 (br. s, 1H),

2.72–2.68 (m, 1H), 2.47–2.43 (m, 1H), 2.42–2.37 (m, 1H), 2.05–2.00 (m, 1H), 1.94 (dt, 14.3, 2.7, 1H), 1.69 (dd, 7.1, 2.4, 3H); ^{13}C NMR (125 MHz, CDCl_3): δ 207.9, 148.0, 134.0, 132.5, 132.02, 132.00, 131.9, 131.7, 131.5, 124.6, 124.3, 61.0, 60.3, 50.5, 48.4, 34.9, 31.6, 29.0, 14.9; IR (film): 2923, 2854, 1733, 1543, 373, 1166; HRMS–ESI (m/z) $[\text{M} + \text{H}]^+$ calcd for $\text{C}_{19}\text{H}_{21}\text{N}_2\text{O}_5\text{S}^+$, 389.11657; found 389.11773.



Indolenine 3.3. To a solution of cyclopentene **3.5** (6 mg, 0.015 mmol) in 1,2-dichloroethane (DCE) (0.40 mL) was added phenylhydrazine (**3.4**) (4.6 μL , 0.046 mmol), followed by trifluoroacetic acid (9.5 μL , 0.124 mmol). The reaction was heated to 40 °C. After 2.5 h, the reaction was cooled to room temperature and quenched with a solution of sat. aq. NaHCO_3 (10 mL). The resulting mixture was diluted with EtOAc (10 mL). The layers were separated and the aqueous layer was extracted with EtOAc (2 x 10 mL). The organic layers were combined, dried over MgSO_4 , and evaporated under reduced pressure. The resulting residue was purified by flash chromatography (2:1 hexanes:EtOAc \rightarrow 1:2 hexanes:EtOAc) to afford indolenine **3.3** (5.3 mg, 74% yield) as a brown solid. Indolenine **3.3**: mp: 98–101 °C; R_f 0.48 (3:1 EtOAc:hexanes); ^1H NMR (500 MHz, CDCl_3): δ 8.19–8.17 (m, 1H), 7.69–7.65 (m, 2H), 7.62–7.60 (m, 2H), 7.36 (d, $J = 7.5$, 1H), 7.31 (dt, $J = 7.6$, 1.0, 1H), 7.13 (dt, $J = 7.5$, 1.0, 1H), 6.05–6.03 (m, 1H), 5.96–5.94 (m, 1H), 5.62 (q, $J = 6.2$, 1H), 5.07 (dd, $J = 4.4$, 2.0, 1H), 4.29 (d, $J = 15.2$, 1H), 4.09 (dt, $J = 15.2$, 2, 1H), 3.10 (dq, $J = 17.0$, 2.4, 1H), 3.02 (m, 2H), 2.48 (ddd, $J = 14.0$, 4.4, 3, 1H), 2.17 (dd, $J = 17.0$, 2.4, 1H), 1.87 (dt, $J = 14.0$, 2.4, 1H), 1.61 (d, $J = 6.2$, 3H); ^{13}C NMR (125 MHz,

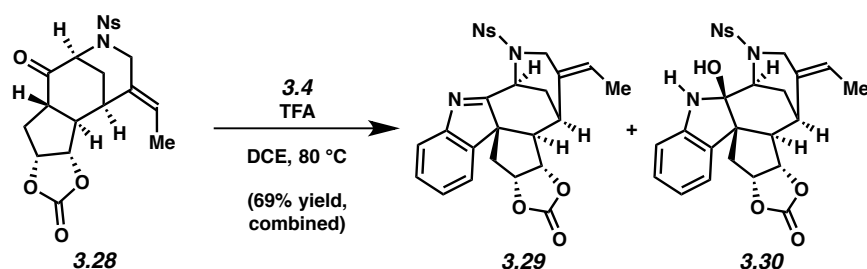
CDCl₃): δ 185.6, 152.8, 148.4, 148.3, 133.9, 132.7, 132.3, 132.1, 131.8 (2 carbons), 131.7, 128.0, 126.2, 124.2, 123.3, 120.89, 120.87, 62.2, 60.2, 54.7, 48.0, 40.7, 36.4, 31.6, 15.0; IR (film): 2920, 2851, 1544, 1440, 1358, 1169; HRMS–ESI (m/z) [$M + H$]⁺ calcd for C₂₅H₂₄N₃O₄S⁺, 462.1482, found 462.14698.



Carbonate 3.28. To a solution of cyclopentene **3.5** (27.2 mg, 0.070 mmol) in 16:1 acetone:H₂O (0.58 mL) was added a solution of *N*-methylmorpholine-*N*-oxide (8.6 mg, 0.0073 mmol) in acetone (0.82 mL). The solution was cooled to 0 °C. After stirring for 5 min, a solution of osmium tetroxide in water (45 μ L of a 20 mg /1 mL solution, 0.0036 mmol) was added. The reaction was stirred at 0 °C for one additional h before being warmed to room temperature. After 4 h, the reaction mixture was poured into deionized water (10 mL) and brine (5 mL) and the resulting mixture was diluted with EtOAc (15 mL). The layers were separated and the aqueous layer was extracted with EtOAc (2 x 15 mL). The organic layers were combined and dried over MgSO₄. Evaporation of the solvent under reduced pressure afforded diol **3.37**, which was used in the subsequent step without further purification.

To a solution of crude diol **3.37** (23 mg, 0.054 mmol) in CH₂Cl₂ (2.0 mL) and pyridine (0.20 mL) was added a solution of triphosgene (15.3 mg, 0.051 mmol) in CH₂Cl₂ (0.5 mL) dropwise. After stirring for 10 min, the volatiles were removed under reduced pressure and the resulting residue was purified by flash chromatography (1:1 hexanes:EtOAc \rightarrow 100% EtOAc) to afford carbonate **3.28** (24.5 mg, 78% yield, 2 steps) as a brown solid. Carbonate **3.28**: mp: 121–

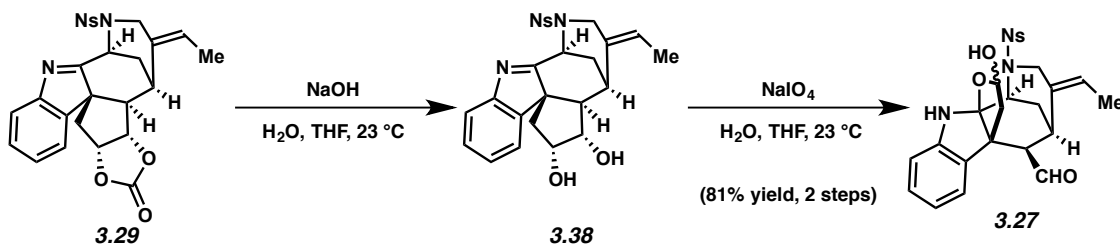
124 °C; R_f 0.23 (3:1 EtOAc:hexanes); $^1\text{H NMR}$ (500 MHz, CDCl_3): 8.06 (dd, $J = 7.3$, 2, 1H) 7.74 (m, 2H), 7.68 (dd, $J = 7.3$, 2, 1H), 5.69 (q, $J = 6.7$, 1H), 5.11 (dd, $J = 6$, 3.6, 1H), 5.07 (t, $J = 6.0$, 1H), 4.40 (dt, 15.5, 1.6, 1H), 4.25 (dd, $J = 4.2$, 2.4, 1H), 4.11 (dt, $J = 15.5$, 1.4, 1H), 3.41–3.38 (m, 2H), 2.26 (ddd, $J = 14.1$, 4.2, 3, 1H), 2.13 (dd, $J = 15.1$, 5.8, 1H), 2.00 (m, 1H), 1.94 (dt, $J = 14.1$, 3, 1H), 1.81 (dt, $J = 14.0$, 3.6, 1H), 1.73 (dt, $J = 6.7$, 1.4, 3H); $^{13}\text{C NMR}$ (125 MHz, CDCl_3): δ 205.3, 154.6, 148.1, 134.4, 132.3, 132.0, 131.5, 128.8, 125.1, 124.7, 81.3, 79.3, 59.9, 55.1, 48.5, 46.1, 35.9, 31.6, 29.5, 13.6; IR (film): 2923, 2851, 1799, 1730, 1543, 1373, 1167; HRMS–ESI (m/z) $[\text{M} + \text{H}]^+$ calcd for $\text{C}_{20}\text{H}_{21}\text{N}_2\text{O}_8\text{S}^+$, 449.10131, found 449.10056.



Indolenine 3.29 and Indoline 3.30. To a solution of carbonate **3.28** (14.7 mg, 0.033 mmol) in 1,2-dichloroethane (DCE) (1.1 mL) was added phenylhydrazine (**3.4**) (10 μL , 0.098 mmol), followed by trifluoroacetic acid (TFA) (20 μL , 0.26 mmol). The reaction was heated to 80 °C. After stirring for 2 h, the reaction mixture was cooled to room temperature and quenched with a solution of saturated aqueous NaHCO_3 (15 mL). The resulting mixture was diluted with EtOAc (15 mL). The layers were separated and the aqueous layer was extracted with EtOAc (2 x 15 mL). The combined organic layers were dried over MgSO_4 , filtered, and evaporated under reduced pressure. The resulting residue was purified via flash chromatography (2:1 hexanes:EtOAc \rightarrow 1:2 hexanes:EtOAc) to afford indolenine **3.29** and indoline **3.30** (12.0 mg, 69% yield) as a red oil. Indolenine **3.29**: R_f 0.39 (3:1 EtOAc:hexanes); $^1\text{H NMR}$ (500 MHz,

C_6D_6): 7.85 (dd, $J = 7.9, 1.3, 1H$), 7.69 (d, $J = 7.7, 1H$), 7.09 (dt, $J = 7.7, 1.0, 1H$), 6.89 (dt, $J = 7.5, 1.0, 1H$), 6.62 (dd, $J = 7.9, 1.3, 1H$), 6.57 (dt, $J = 7.7, 1.3, 1H$), 6.42 (dt, $J = 7.7, 1.3, 1H$), 6.24 (d, $J = 7.5, 1H$), 5.43 (dd, $J = 4.2, 2.7, 1H$), 5.29 (q, $J = 7.0, 1H$), 4.61 (dt, $J = 15.5, 2.4, 1H$), 4.38 (app. t, $J = 8.8, 1H$), 4.31–4.25 (m, 1H), 3.94 (dt, $J = 15.5, 1.2, 1H$), 2.78 (dd, $J = 15.3, 5.9, 1H$), 2.55 (quin, $J = 3.1, 1H$), 1.79 (ddd, $J = 13.8, 4.2, 3, 1H$), 1.72 (dd, $J = 7.0, 1.2, 3H$), 1.53 (m, 2H), 1.31 (dt, $J = 13.8, 3.1, 1H$); ^{13}C NMR (23 of 26 observed, 125 MHz, C_6D_6): δ 183.0, 154.3, 153.8, 148.4, 146.5, 133.4, 132.4, 131.7, 130.8, 126.2, 123.9, 122.3, 120.9, 80.7, 80.4, 61.8, 54.4, 53.4, 48.8, 38.5, 36.8, 28.2, 13.9; IR (film): 2923, 2851, 1802, 1543, 1373, 1166; HRMS–ESI (m/z) [$M + Na$] $^+$ calcd for $C_{26}H_{23}N_3O_7SNa^+$, 544.1149; found 544.1160.

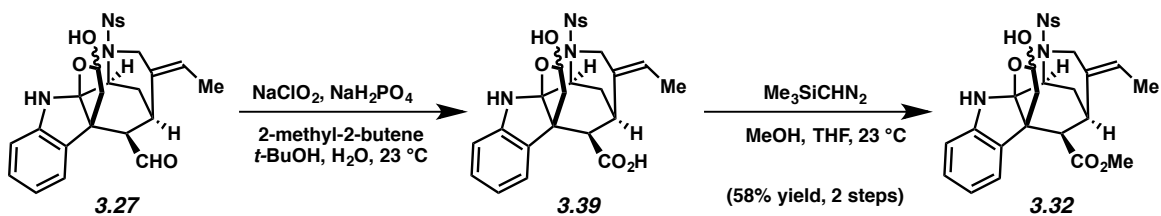
Indoline **3.30**: R_f 0.77 (3:1 EtOAc:hexanes); 1H NMR (500 MHz, C_6D_6): 7.71 (dd, $J = 7.9, 1.3, 1H$), 7.06 (td, $J = 7.6, 1.1, 1H$), 6.68–6.61 (m, 3H), 6.45 (td, $J = 7.7, 1.3, 1H$), 6.38 (d, $J = 7.6, 1H$), 6.1 (d, $J = 7.5, 1H$), 5.35 (q, $J = 7.7, 1H$), 4.39–4.34 (m, 3H), 4.23 (t, $J = 3.1, 1H$), 3.80 (d, $J = 15.4, 1H$), 3.09 (s, br, 1H), 3.05 (s, br, $J = 1H$), 2.90 (dd, $J = 16.0, 2.9, 1H$), 2.49 (dd, $J = 3.5, 3.0, 1H$), 2.17 (m, 1H), 1.91 (dt, $J = 13.4, 3.1, 1H$), 1.76 (dt, $J = 13.4, 3.5, 1H$), 1.55–1.53 (m, 1H) 1.65 (dd, $J = 7.7, 2.1, 3H$); ^{13}C NMR (500 MHz, C_6D_6): δ 154.7, 147.8, 145.1, 138.7, 133.3, 133.2, 131.5, 131.2, 129.4, 129.1, 127.5, 124.1, 121.4, 119.5, 109.9, 94.2, 81.1, 80.3, 55.7, 55.3, 53.7, 50.5, 37.1, 32.3, 27.2, 13.4; IR (film): 3475, 3359, 1803, 1731, 1599, 1542, 1372, 1163; HRMS–ESI (m/z) [$M + Na$] $^+$ calcd for $C_{26}H_{25}N_3O_8SNa^+$, 562.1255; found 562.1262.



Aldehyde 3.27. To a solution of indolenine **3.29** (9.0 mg, 0.017 mmol) in THF (0.17 mL) was added an aqueous solution of NaOH (0.5 N, 0.17 mL). After vigorous stirring for 45 min, the reaction mixture was poured into deionized water (10 mL) and the resulting mixture was diluted with EtOAc (10 mL). The layers were separated and the aqueous layer was extracted with EtOAc (2 x 10 mL). The organic layers were combined and dried over MgSO₄. Evaporation of the solvent under reduced pressure afforded diol **3.38**, which was used in the subsequent step without further purification.

To a solution of crude diol **3.38** in 1:1 THF:H₂O (0.34 mL) was added NaIO₄ (10.9 mg, 0.051 mmol). After stirring for 1.5 h, the reaction mixture was poured into deionized water (5 mL) and brine (5 mL), and the resulting mixture was diluted with EtOAc (10 mL). The layers were separated and the aqueous layer was extracted with EtOAc (2 x 10 mL). The organic layers were combined and dried over MgSO₄. The resulting residue was purified via flash chromatography (2:1 hexanes:EtOAc) to afford aldehyde **3.27** (7.1 mg, 81% yield) as an orange solid and as an inseparable mixture of diastereomers (2:1). These compounds were characterized as a mixture. Aldehyde **3.27**: mp: 145–148 °C; R_f 0.50 (1.5:1 EtOAc:hexanes); **3.27(major)**: ¹H NMR (500 MHz, C₆D₆): 9.27 (d, *J* = 0.6, 1H), 7.85 (dd, *J* = 8.0, 1.3, 1H), 7.23 (d, *J* = 7.4, 1H), 6.96 (dd, *J* = 7.7, 1.2, 1H), 6.78–6.67 (m, 3H), 6.53 (dt, *J* = 7.7, 1.4, 1H), 6.30 (d, *J* = 7.7, 1H), 5.30–5.24 (m, 1H), 4.96 (q, *J* = 7.0, 1H), 4.58 (app. s, 1H), 4.04 (s, 1H), 3.74 (app. d, 1H), 3.61 (dt, *J* = 15.2, 2.2, 1H), 2.75 (d, *J* = 14.4, 1H), 2.68–2.65 (m, 1H), 2.35 (dd, *J* = 14.4, 5.6, 1H), 1.96 (app. d, 1H), 1.89 (dt, *J* = 13.5, 3.8, 1H), 1.66 (d, *J* = 8.5, 1H), 1.63 (dt, *J* = 13.6, 2.9, 1H), 1.16 (dd, *J* = 7.0, 1.7, 3H); **3.27(minor)**: ¹H NMR (500 MHz, C₆D₆): 9.29 (d, *J* = 1.1, 1H), 7.78 (dd, *J* = 8.0, 1.3, 1H), 7.02 (dd, *J* = 7.7, 1.2, 1H), 6.78–6.67 (m, 3H), 6.64 (dt, *J* = 7.7, 1.3, 1H), 6.49 (dt, *J* = 7.7, 1.4, 1H), 6.35 (d, *J* = 7.7, 1H), 5.30–5.24 (m, 1H), 4.85 (q, *J* = 7.0, 1H), 4.58

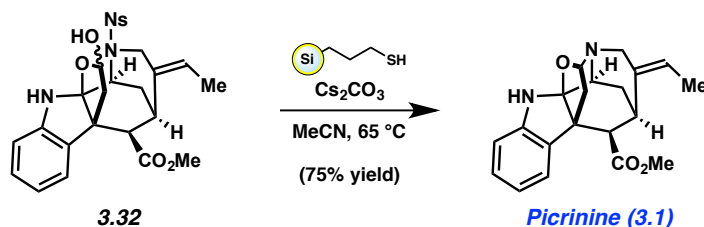
(app. s, 1H), 4.15 (dt, $J = 15.4, 2.3$, 1H), 3.74 (app. d, 1H), 3.71 (d, $J = 8.1$, 1H), 3.52 (d, $J = 15.4$, 1H), 3.03 (dd, $J = 13.7, 4.9$, 1H), 2.68–2.65 (m, 1H), 2.21 (dd, $J = 13.7, 7.6$, 1H), 2.00 (dd, $J = 13.5, 3.8$, 1H), 1.96 (app. d, 1H), 1.76 (dd, $J = 13.7, 2.9$, 1H), 1.14 (dd, $J = 7.0, 1.6$, 3H); ^{13}C NMR (125 MHz, CDCl_3): δ 201.1, 200.9, 148.1 (2 carbons), 145.8, 144.8, 136.7, 135.8, 133.8, 133.6, 133.5, 133.0, 132.4, 132.0, 131.7, 131.5, 129.23, 129.15, 129.12, 128.9, 125.3, 125.1, 124.9, 124.6, 124.1, 123.8, 120.8, 120.5, 110.4, 110.1, 104.0, 101.2, 101.0, 99.0, 77.4, 77.2, 76.9, 62.6, 61.8, 54.0, 53.8, 52.0, 51.3, 48.3, 48.2, 43.9, 43.8, 30.4, 30.1, 28.0 (2 carbons), 13.7, 13.6; IR (film): 3371, 2925, 2851, 1721, 1542, 1468, 1370, 1263, 1162; HRMS–ESI (m/z) $[\text{M} + \text{Na}]^+$ calcd for $\text{C}_{25}\text{H}_{25}\text{N}_3\text{O}_7\text{SNa}^+$, 534.1311; found 534.1324.



Ester 3.32. To a solution of aldehyde **3.27** (5.2 mg, 0.010 mmol) in *t*-BuOH (0.39 mL) and 2-methyl-2-butene (0.26 mL) at $0\text{ }^\circ\text{C}$ was added a solution of sodium chlorite (5.1 mg, 0.056 mmol) and monobasic sodium phosphate (7.9 mg, 0.066 mmol) in H_2O (0.39 mL). The reaction was allowed to warm to room temperature while stirring. After vigorous stirring for 1 h, the reaction mixture was poured into deionized water (10 mL) and the resulting mixture was diluted with EtOAc (10 mL). The layers were separated and the aqueous layer was extracted with EtOAc (2 x 10 mL). The organic layers were combined and dried over MgSO_4 . Evaporation of the solvent under reduced pressure afforded acid **3.39**, which was used in the subsequent step without further purification.

To a solution of crude acid **3.39** in 5:3 THF/MeOH (1.0 mL) was added trimethylsilyldiazomethane (20 μ L of a 0.6 M solution in hexanes, 0.012 mmol). After stirring for 30 min, the reaction mixture was poured into deionized water (10 mL) and the resulting mixture was diluted with CH₂Cl₂ (10 mL). The layers were separated and the aqueous layer was extracted with CH₂Cl₂ (2 x 10 mL). The organic layers were combined and dried over MgSO₄. The resulting residue was purified via flash chromatography (2:1 hexanes:EtOAc) to afford ester **3.32** (3.2 mg, 58% yield) as a brown solid and as an inseparable mixture of diastereomers (1.5:1). These compounds were characterized as a mixture. Ester **3.32**: mp: 78–82 °C; R_f 0.51 (1.5:1 EtOAc:hexanes); **3.32(major)**: ¹H NMR (26 of 27 observed, 500 MHz, CDCl₃): δ 8.11–8.07 (m, 1H), 7.74–7.72 (m, 1H), 7.70–7.64 (m, 2H), 7.16–7.08 (m, 2H), 6.81 (dt, $J = 7.5, 0.7$, 1H), 6.71 (d, $J = 7.8$, 1H), 5.55–5.46 (m, 1H), 5.29 (dd, $J = 8.7, 5.5$, 1H), 4.76 (s, 1H), 4.48–4.45 (m, 1H), 3.92 (dt, $J = 15.2, 2.1$, 1H), 3.85 (d, $J = 15.2$, 1H), 3.70 (s, 3H), 3.34–3.28 (m, 1H), 3.07–3.00 (m, 1H), 2.79 (d, $J = 4.5$, 1H), 2.74 (d, $J = 14.9$, 1H), 2.23–2.13 (m, 1H), 2.11–2.08 (app. t, $J = 3.3$, 1H), 1.56 (app. d, 3H); **3.32(minor)**: ¹H NMR (26 of 27 observed, 500 MHz, CDCl₃): δ 8.18–8.15 (m, 1H), 7.74–7.72 (m, 1H), 7.70–7.64 (m, 2H), 7.16–7.08 (m, 2H), 6.79 (dt, $J = 7.5, 0.7$, 1H), 6.67 (d, $J = 7.8$, 1H), 5.55–5.46 (m, 1H), 5.17–5.12 (m, 1H), 4.59 (s, 1H), 4.48–4.45 (m, 1H), 4.29 (dt, $J = 14.9, 2.0$, 1H), 3.68 (s, 3H), 3.34–3.28 (m, 1H), 3.07–3.00 (m, 1H), 2.77 (d, $J = 4.5$, 1H), 2.54 (dd, $J = 14.1, 7.8$, 1H), 2.23–2.13 (m, 1H), 2.11–2.08 (app. t, $J = 3.3$, 1H), 1.86 (d, $J = 9.0$, 1H), 1.56 (app. s, 3H); ¹³C NMR (125 MHz, CDCl₃): δ 172.02, 171.97, 148.2, 148.1, 145.9, 144.9, 136.8, 136.1, 133.8, 133.6, 133.5, 132.9, 132.6, 132.0, 131.69, 131.67, 129.1, 128.94, 128.90, 128.84, 125.8, 125.4, 124.9, 124.5, 123.4, 123.1, 120.7, 120.4, 110.7, 110.4, 103.9, 101.3, 101.1, 99.0, 54.5, 54.1, 53.8, 52.7, 51.92, 51.89, 51.84, 48.2, 48.1, 43.8, 43.7, 30.8, 30.5, 29.9, 29.8, 13.02, 12.99; IR (film): 3497, 3365, 2917, 2850, 1737, 1542,

1441, 1364, 1261, 1162; HRMS–ESI (m/z) $[M + H]^+$ calcd for $C_{26}H_{28}N_3O_8SH^+$, 542.15916; found 542.15948.



Picrinine (3.1). To a suspension of ester **3.32** (6.3 mg, 0.012 mmol) and cesium carbonate (11.4 mg, 0.035 mmol) in MeCN (0.39 mL) was added SiliaMetS[®] Thiol (35.0 mg, 0.047 mmol). The reaction was heated to 65 °C. After 1 h, the reaction was cooled to room temperature, and directly purified by flash chromatography (30:1 EtOAc:MeOH → 9:1 IPA:CH₂Cl₂) to afford picrinine **3.1** (2.9 mg, 75% yield) as a white solid. Spectral data for ¹H NMR for synthetic **3.1** was consistent with literature reports³⁶ and a natural sample of **3.1** obtained from Prof. T.-S. Kam (see comparison ¹H NMR spectra). Spectral data for ¹³C NMR for synthetic **3.1** was consistent with literature reports.³⁶ Picrinine (**3.1**): ¹H NMR (500 MHz, CDCl₃): δ 7.14 (d, $J = 7.5$, 1H), 7.09 (dt, $J = 7.7$, 1.3, 1H), 6.79 (dt, $J = 7.5$, 1.0, 1H), 6.76 (d, $J = 7.7$, 1H), 5.40 (q, $J = 7.0$, 1H), 4.82 (d, $J = 2.6$, 1H), 4.72 (s, 1H), 3.76 (dt, $J = 17.6$, 2.5, 1H), 3.65 (s, 3H), 3.59 (d, $J = 4.9$, 1H), 3.42 (d, $J = 13.7$, 1H) 3.28 (app. d, $J = 2.8$, 1H), 3.09 (d, $J = 17.0$, 1H), 2.44 (d, $J = 3.5$, 1H), 2.26 (dd, $J = 13.7$, 2.6, 1H), 2.15 (ddd, $J = 14.1$, 4.9, 3.5, 1H), 1.86 (dd, $J = 14.1$, 2.8, 1H), 1.49 (dd, $J = 7.0$, 2.5, 3H). ¹³C NMR (125 MHz, CDCl₃): δ 172.6, 147.7, 136.4, 135.4, 128.1, 125.3, 121.0, 120.5, 110.7, 106.4, 87.5, 52.1, 52.0, 51.6, 51.3, 46.5, 40.7, 31.2, 26.2, 12.9.

3.10 References

- (1) For an example of an oxidative cleavage cascade, see: Wagnières, O.; Xu, Z.; Wang, Q.; Zhu, J. *J. Am. Chem. Soc.* **2014**, *136*, 15102–15108.
- (2) Nagata, H.; Kawamura, M.; Ogasawara, K. *Synthesis* **2000**, *13*, 1825–1834.
- (3) Sulfonamide **3.9** is commercially available from Aurora Fine Chemicals LLC (CAS No. 115462-23-0) or can be readily prepared in two steps from trans-4-aminocyclohexanol•HCl (See Section 3.9.2).
- (4) Rawal, V. H.; Michoud, C. *Tetrahedron Lett.* **1991**, *32*, 1695–1698.
- (5) For related Pd-catalyzed cyclizations, see: (a) Sole, D.; Piedro, E.; Bonjoch, J. *Org. Lett.* **2000**, *2*, 2225–2228. (b) Liao, X.; Zhou, H.; Yu, J.; Cook, J. M. *J. Org. Chem.* **2006**, *71*, 8884–8890. (c) Dounay, A. B.; Humphreys, P. G.; Overman, L. E.; Wroblewski, A. D. *J. Am. Chem. Soc.* **2008**, *130*, 5368–5377.
- (6) Nicolaou, K. C.; Montagnon, T.; Baran, P. S. *Angew. Chem., Int. Ed.* **2002**, *41*, 993–996.
- (7) For preparation of the stannane, see: (a) Danheiser, R. L.; Romines, K. R.; Koyama, H.; Gee, S. K.; Johnson, C. R.; Medlich, J. R. *Org. Syn.* **1993**, *71*, 133–139. For use of the reagent, see: (b) Buchanan, G. S.; Cole, K. P.; Tang, Y.; Hsung, R. P. *J. Org. Chem.* **2011**, *76*, 7027–7039.
- (8) For the original Dauben oxidation, see: Dauben, W. G.; Michno, D. M. *J. Org. Chem.* **1977**, *42*, 682–685.
- (9) Shibuya, M.; Ito, S.; Takahashi, M.; Iwabuchi, Y. *Org. Lett.* **2004**, *6*, 4303–4306.

- (10) Shibuya, M.; Tomizawa, M.; Iwabuchi, Y. *J. Org. Chem.* **2008**, *73*, 4750–4752.
- (11) Nagaoka, H.; Kobayashi, K.; Matsui, T.; Yamada, Y. *Tetrahedron Lett.* **1987**, *28*, 2021–2023.
- (12) Zhang, P.; Morken, J. P. *J. Am. Chem. Soc.* **2009**, *131*, 12550–12551.
- (13) Campagnole, M.; Delmond, B. *Synth. Commun.* **2007**, *37*, 1077–1090.
- (14) Reed, K. L.; Gupton, J. T.; Solarz, T. L. *Synth. Commun.* **1989**, *19*, 3579–3587.
- (15) Newton, R. F.; Wadsworth, A. H. *J. Chem. Soc., Perkin Trans. 1* **1982**, 823–830.
- (16) For a review, see: (a) Deutsch, C.; Krause, N.; Lipshutz, B. *Chem. Rev.* **2008**, *108*, 2916–2927. For examples, see: (b) Mahoney, W. S.; Brestensky, D. M.; Stryker, J. M. *J. Am. Chem. Soc.* **1988**, *110*, 291–293. (c) Baker, B. A.; Bošković, Ž. V.; Lipshutz, B. H. *Org. Lett.* **2008**, *10*, 289–292.
- (17) Ojima, I.; Kogure, T. *Organometallics* **1982**, *1*, 1390–1399.
- (18) Keinan, E.; Gleize, P. A. *Tetrahedron Lett.* **1982**, *23*, 477–480.
- (19) For the effect of silyl groups on controlling diastereoselective protonation, see: (a) Bouzide, A. *Org. Lett.* **2002**, *4*, 1347–1350. (b) Rodrigues Jr., M. T.; Gomes, J. C.; Smith, J.; Coelho, F. *Tetrahedron Lett.* **2010**, *51*, 4988–4990.
- (20) Hénon, H.; Mauduit, M.; Alexakis, A. *Angew. Chem., Int. Ed.* **2008**, *47*, 9122–9124.
- (21) Sabahi, A.; Novikov, A.; Rainier, J. D. *Angew. Chem., Int. Ed.* **2006**, *45*, 4317–4320.

- (22) (a) Jabri, S. Y.; Overman, L. E. *J. Org. Chem.* **2013**, *78*, 8766–8788. (b) He, F.; Bo, Y.; Altom, J. D.; Corey, E. J. *J. Am. Chem. Soc.* **1999**, *121*, 6771–6772.
- (23) Yang, D.; Zhang, C. *J. Org. Chem.* **2001**, *66*, 4814–4818.
- (24) Akbutina, F. A.; Torosyan, S. A.; Vyrypaev, E. M.; Furlei, I. I.; Miftakhov, M. S. *Russ. J. Org. Chem.* **1999**, *35*, 1386–1387.
- (25) VanRheenen, V.; Kelly, R. C.; Cha, D. Y. *Tetrahedron Lett.* **1976**, *17*, 1973–1976.
- (26) Burk, R. M.; Roof, M. B. *Tetrahedron Lett.* **1993**, *34*, 395–398.
- (27) Indolenine **3.29** and hydrate **3.30** readily interconverted in CDCl₃ or upon prolonged exposure to silica gel.
- (28) For examples of the Fischer indolization being employed in late-stage total synthesis of complex alkaloids, see: (a) Zu, L.; Boal, B. W.; Garg, N. K. *J. Am. Chem. Soc.* **2011**, *133*, 8877–8879. (b) Adams, G. L.; Carroll, P. J.; Smith, A. B., III. *J. Am. Chem. Soc.* **2012**, *134*, 4037–4040. (c) Adams, G. L.; Carroll, P. J.; Smith, A. B., III. *J. Am. Chem. Soc.* **2013**, *135*, 519–528. (d) Ban, Y.; Sato, Y.; Inoue, I.; Nagai, M.; Oishi, T.; Terashima, M.; Yonemitsu, O.; Kanaoka, Y. *Tetrahedron Lett.* **1965**, *6*, 2261–2268. (e) Ueda, H.; Satoh, H.; Matsumoto, K.; Sugimoto, K.; Fukuyama, T.; Tokuyama, H. *Angew. Chem., Int. Ed.* **2009**, *48*, 7600–7603. (f) Satoh, H.; Ueda, H.; Tokuyama, H. *Tetrahedron* **2013**, *69*, 89–95.
- (29) Yamashita, M.; Ohta, N.; Shimizu, T.; Matsumoto, K.; Matsuura, Y.; Kawasaki, I.; Tanaka, T.; Maezaki, N.; Ohta, S. *J. Org. Chem.* **2003**, *68*, 1216–1224.

- (30) Foos, J.; Steel, F.; Rizvi, S. Q. A.; Fraenkel, G. *J. Org. Chem.* **1979**, *44*, 2522–2529.
- (31) For a review on the nosyl protecting group, see: Kan, T.; Fukuyama, T. *Chem. Commun.* **2004**, 353–359.
- (32) (a) For the removal of nosyl groups using a solid-supported thiol reagent, see: Cardullo, F.; Donati, D.; Merlo, G.; Paio, A.; Salaris, M.; Taddei, M. *Synlett* **2005**, 2996–2998. (b) The thiol resin was obtained from SiliCycle Inc. (Product No. R51030B).
- (33) Mass spectral analysis of the crude reaction mixture suggests that nosyl cleavage occurred. However, efforts to purify products formed in the reaction were unsuccessful.
- (34) Kraus, G. A.; Roth, B. *J. Org. Chem.* **1980**, *45*, 4825–4830.
- (35) Although the MetSThiol reagent is typically used as a metal scavenger, this is the first example of this resin being used for the cleavage of a nosyl group.
- (36) Ferreira Batista, C. V.; Schripsema, J.; Verpoorte, R.; Rech, S. B.; Henriques, A. T. *Phytochemistry* **1996**, *41*, 969–973.
- (37) Frigerio, M.; Santagostino, M.; Sputore, S. *J. Org. Chem.* **1999**, *64*, 4537–4538.
- (38) Niu, C.; Pettersson, T.; Miller, M. J. *J. Org. Chem.* **1996**, *61*, 1014–1022.
- (39) Rawal, V. H.; Michoud, C. *Tetrahedron Lett.* **1991**, *32*, 1695–1698.
- (40) Danheiser, R. L.; Gee, S. K.; Perez, J. J. *J. Am. Chem. Soc.* **1986**, *108*, 806–810.

APPENDIX TWO

Spectra Relevant to Chapter Three:

Second-Generation Approach and Total Synthesis of Picrinine

Current Data Parameters
 NAME JM-1-Nosylketone
 EXPNO 2
 PROCNO 1

F2 - Acquisition Parameters
 Date_ 20140217
 Time 16:37
 INSTRUM av500
 PROBHD 5 mm DCH 13C-1
 PULPROG zg30
 TD 65536
 SOLVENT CDCl3
 NS 8
 DS 0
 SWH 10000.000 Hz
 FIDRES 0.152588 Hz
 AQ 3.2767999 sec
 RG 12.14
 DW 50.000 usec
 DE 10.00 usec
 TE 298.0 K
 D1 2.00000000 sec
 TD0 1

==== CHANNEL f1 =====
 SFO1 500.1330008 MHz
 NUC1 1H
 P1 10.00 usec
 PLW1 13.50000000 W

F2 - Processing parameters
 SI 65536
 SF 500.1300121 MHz
 WDW EM
 SSB 0
 LB 0.30 Hz
 GB 0
 PC 1.00

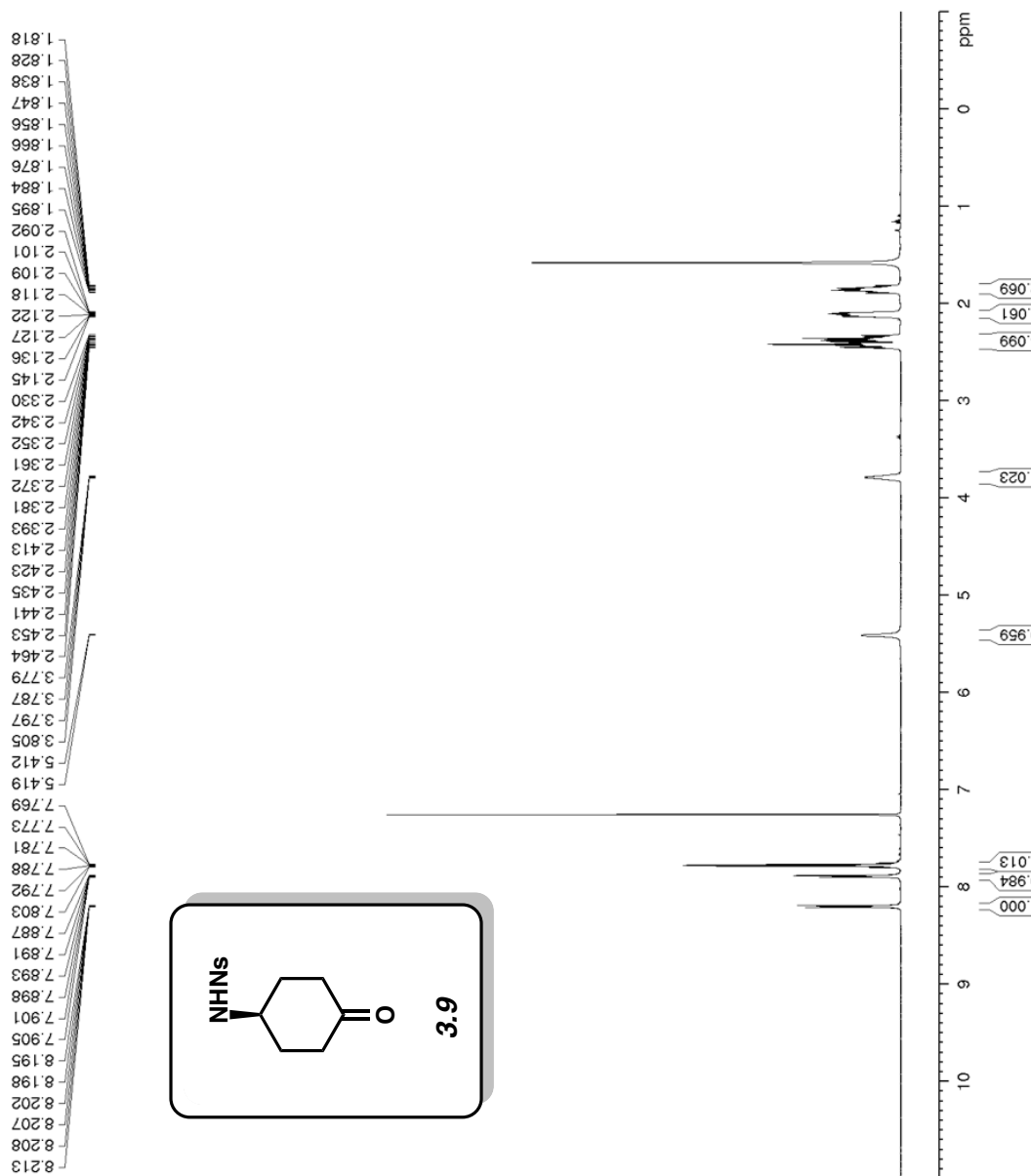


Figure A2.1 ¹H NMR (500 MHz, CDCl₃) of compound 3.9.

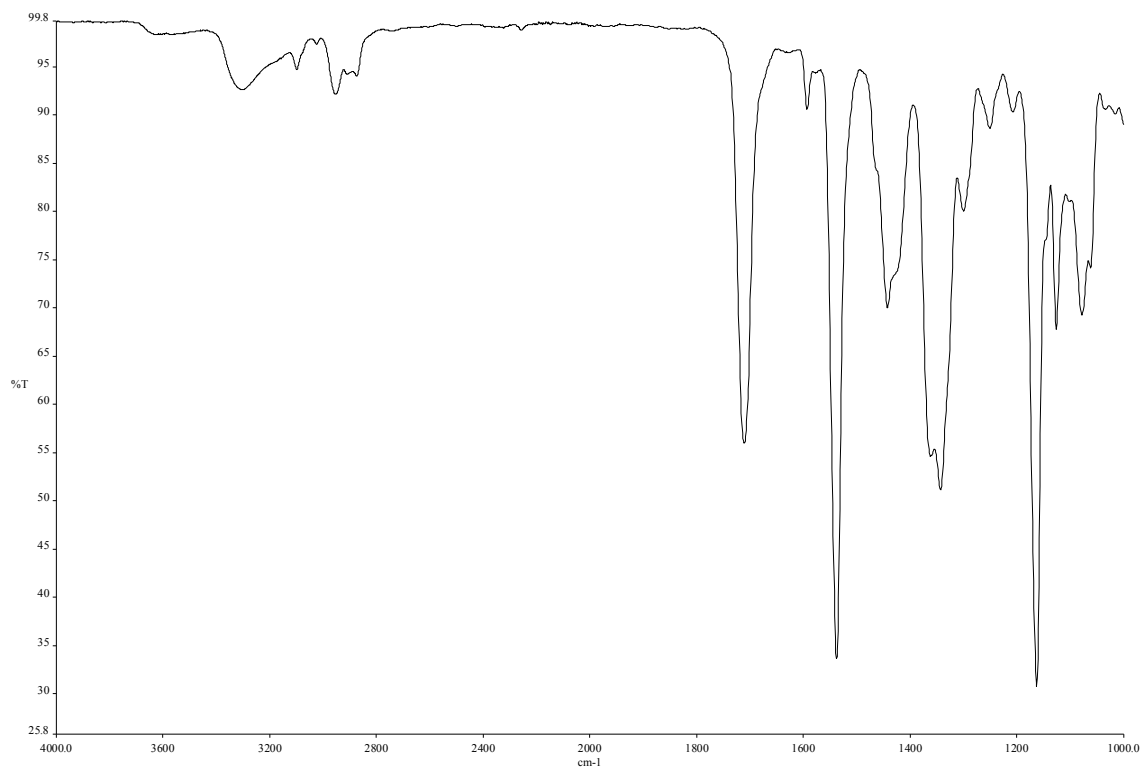


Figure A2.2 Infrared spectrum of compound **3.9**.

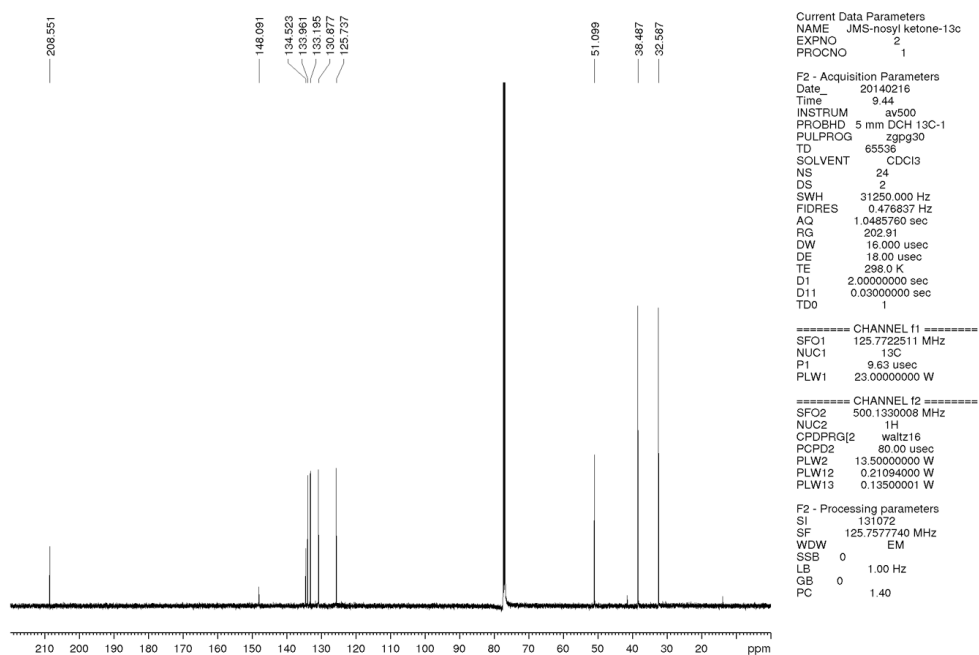


Figure A2.3 ¹³C NMR (125 MHz, CDCl₃) of compound **3.9**.

```

Current Data Parameters
NAME      JM-1-iodide
EXPNO    1
PROCNO   1

F2 - Acquisition Parameters
Date_    20140217
Time     16.42
INSTRUM  av500
PROBHD   5 mm DCH 13C-1
PULPROG  zg30
TD        65536
SOLVENT  CDCl3
NS        8
DS        0
SWH       10000.000 Hz
FIDRES    0.152588 Hz
AQ        3.2767999 sec
RG         12.14
DW         50.000 usec
DE         10.00 usec
TE         298.0 K
D1         2.00000000 sec
TD0        1

===== CHANNEL f1 =====
SFO1     500.1300008 MHz
NUC1      1H
P1        10.00 usec
PLW1     13.50000000 W

F2 - Processing parameters
SI        65536
SF        500.1300122 MHz
WDW       EM
SSB       0
LB        0.30 Hz
GB        0
PC        1.00

```

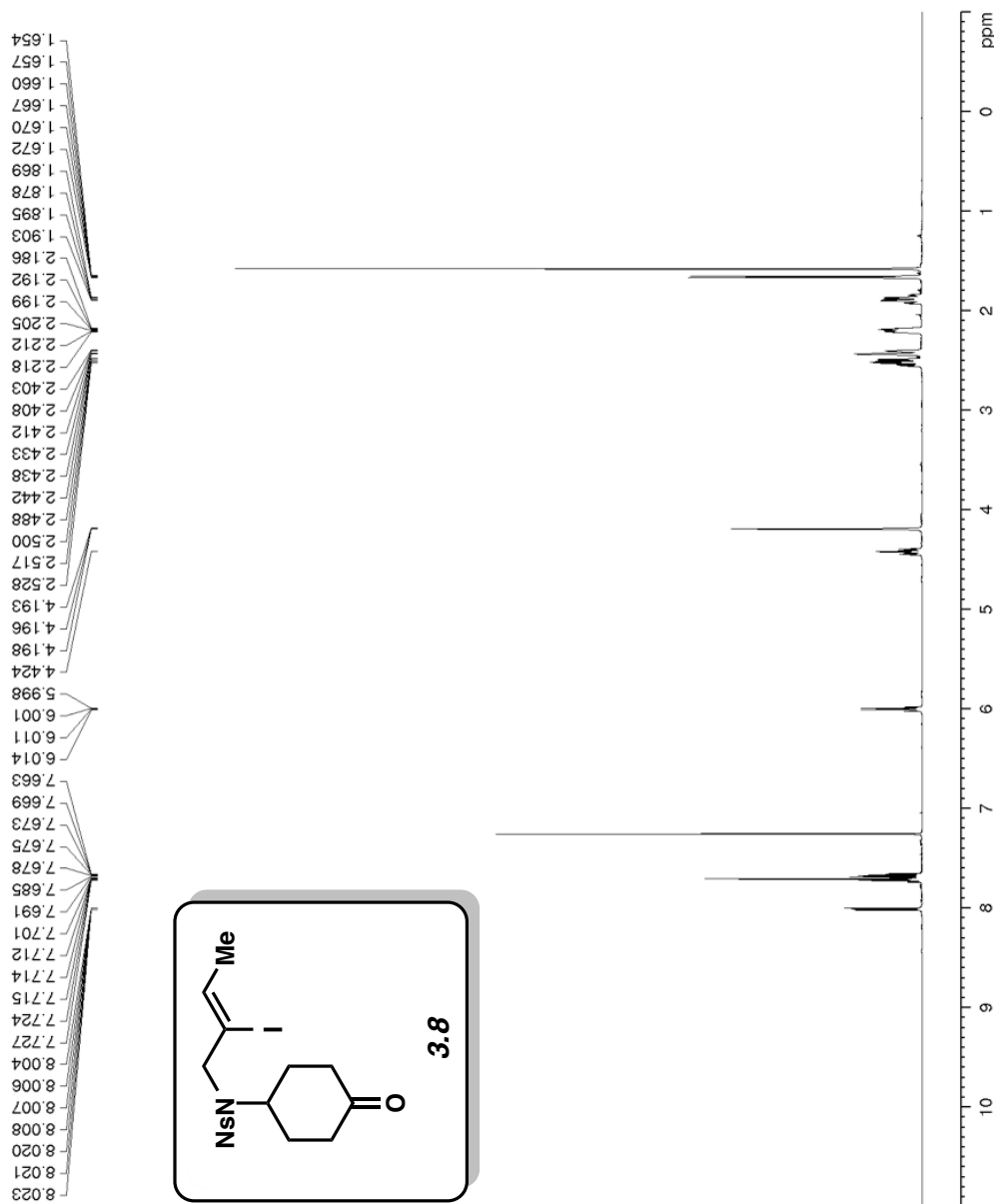


Figure A2.4 ¹H NMR (500 MHz, CDCl₃) of compound **3.8**.

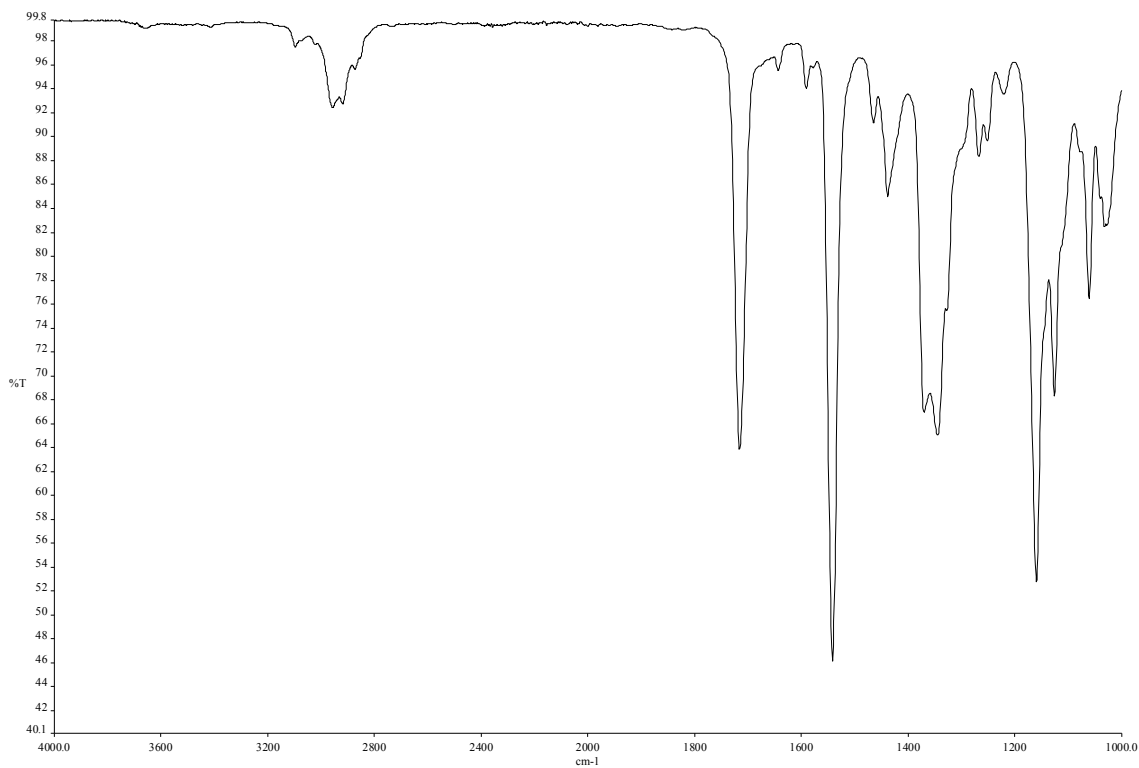


Figure A2.5 Infrared spectrum of compound **3.8**.

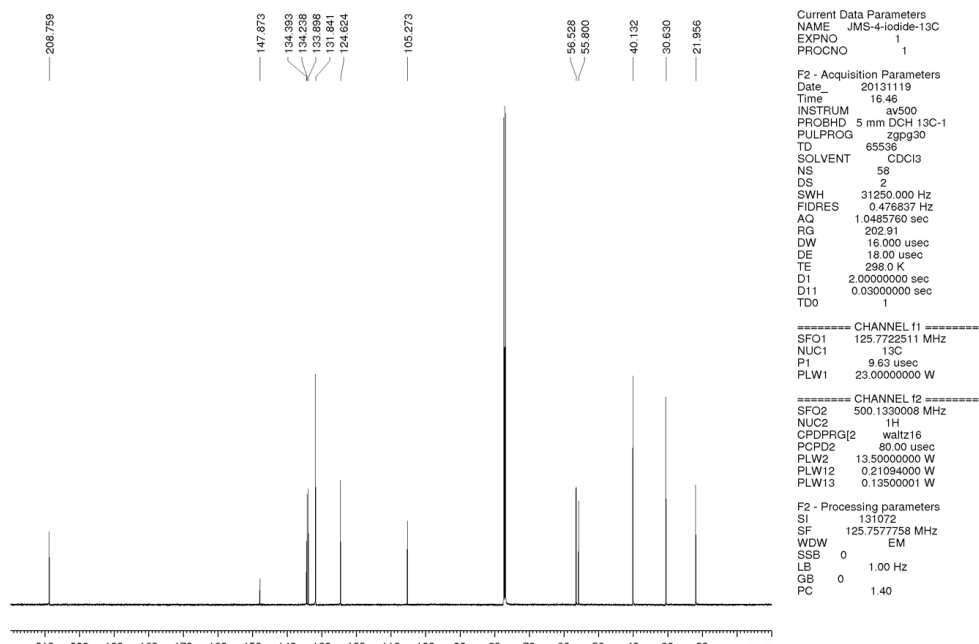


Figure A2.6 ^{13}C NMR (125 MHz, CDCl_3) of compound **3.8**.

```

Current Data Parameters
NAME      JM-1-45
EXPNO    2
PROCNO   1

F2 - Acquisition Parameters
Date_    20130204
Time_    19:47
INSTRUM  av300
PROBHD   5 mm PABBO BB-
PULPROG  zg30
TD        65536
SOLVENT  CDCl3
NS        8
DS        0
SWH       5995.204 Hz
FIDRES    0.091480 Hz
AQ         5.4657025 sec
RG         812.7
DW         83.400 usec
DE         6.00 usec
TE         297.6 K
D1         2.0000000 sec
TD0        1

===== CHANNEL f1 =====
NUC1      1H
P1        12.00 usec
PL1       -2.00 dB
PL1W      14.76977634 W
SFO1      300.1318008 MHz

F2 - Processing parameters
SI         65536
SF         300.1300124 MHz
WDW        EM
SSB        0
LB         0.30 Hz
GB         0
PC         1.40

```

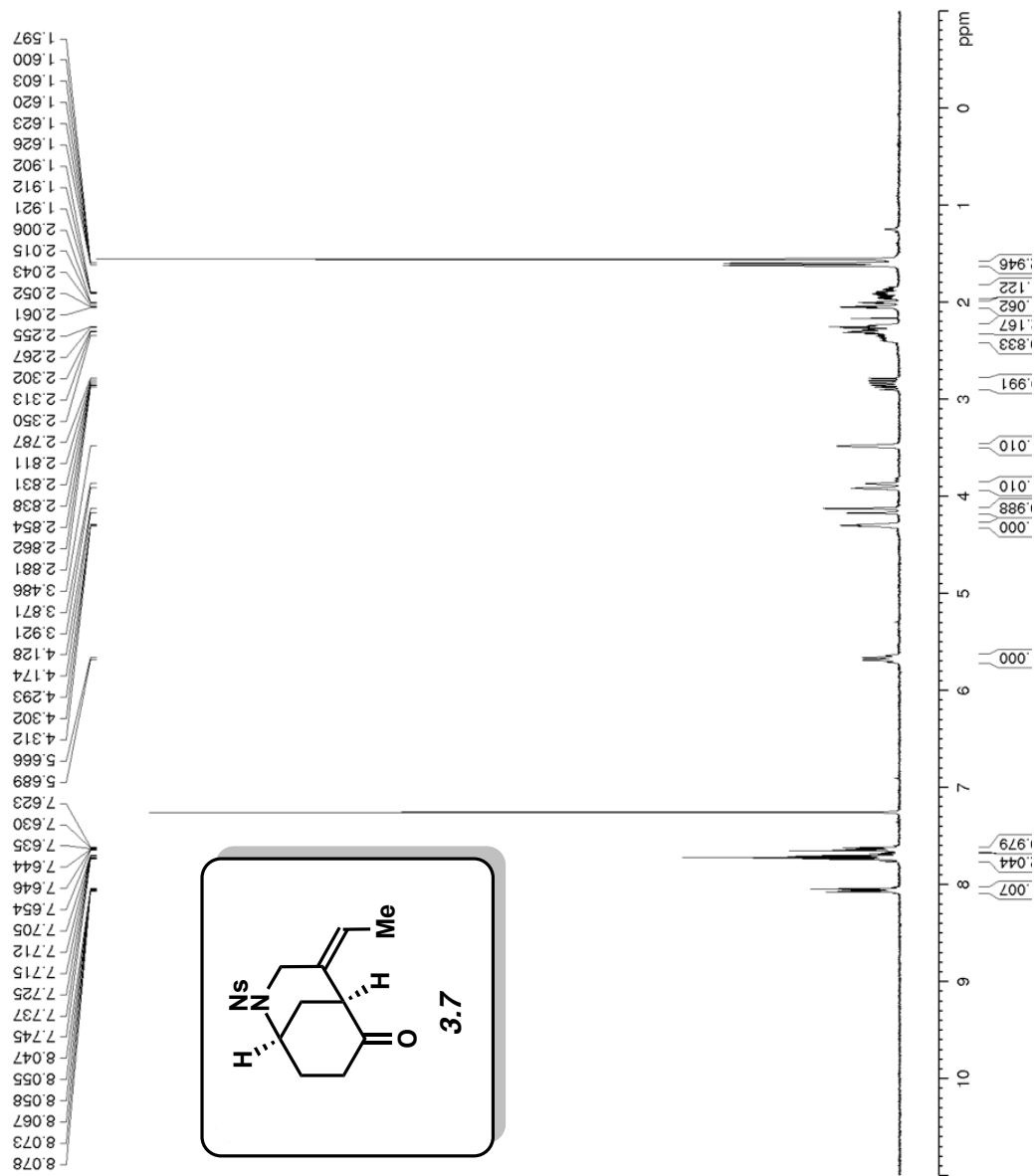


Figure A2.7 ¹H NMR (500 MHz, CDCl₃) of compound 3.7.

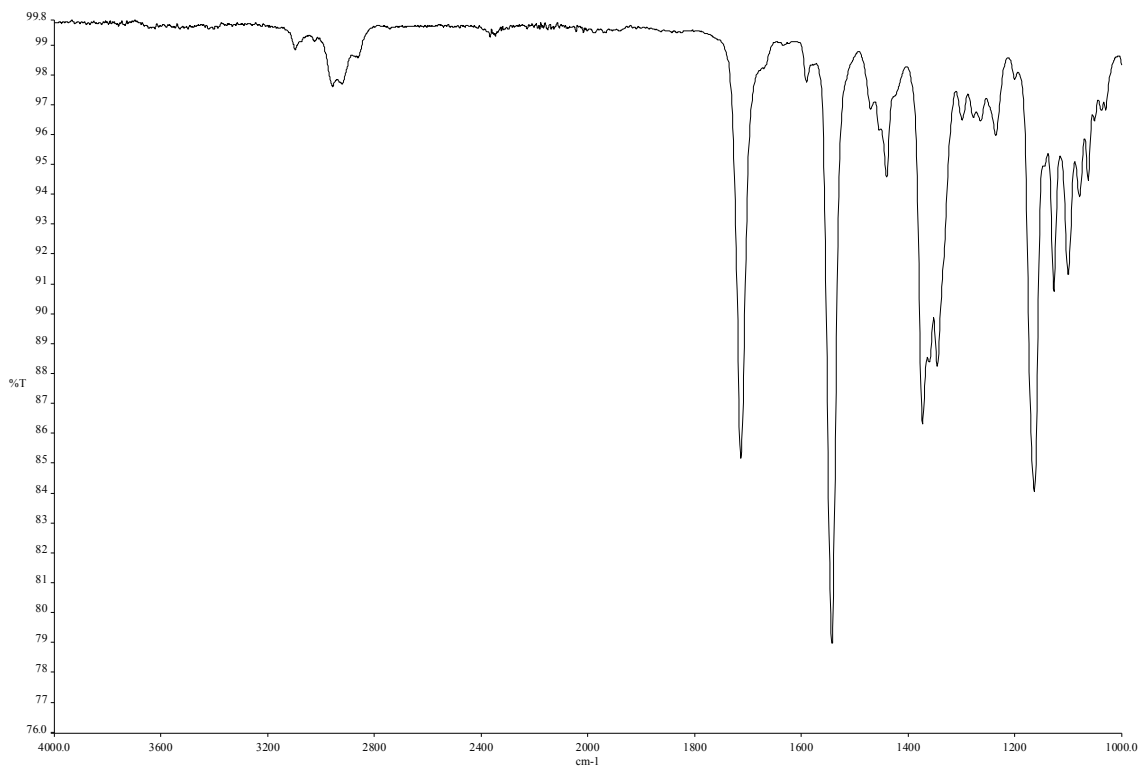


Figure A2.8 Infrared spectrum of compound **3.7**.

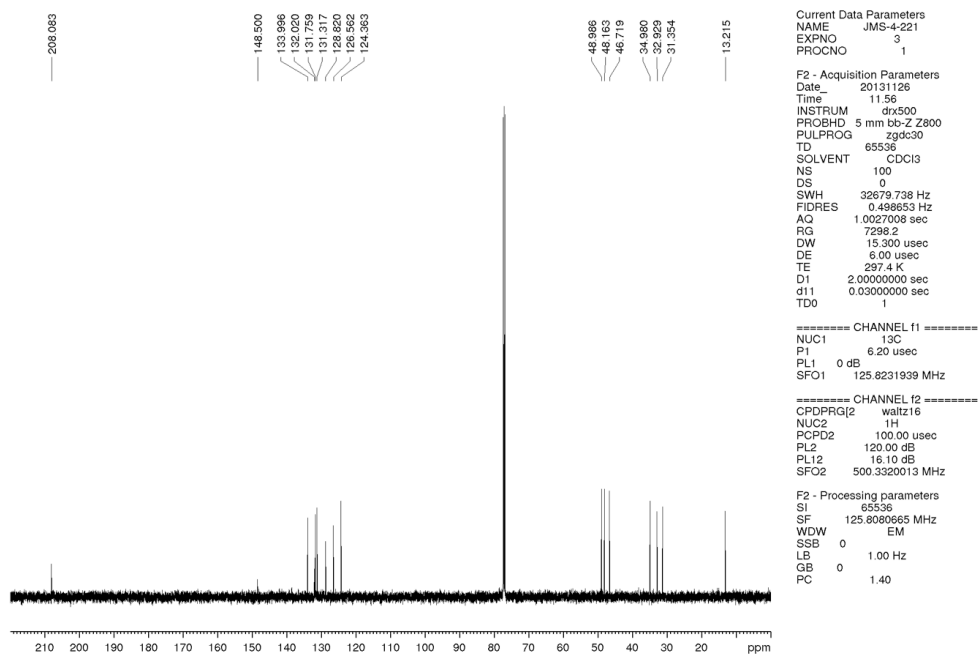


Figure A2.9 ¹³C NMR (125 MHz, CDCl₃) of compound **3.7**.

Current Data Parameters
 NAME JMS-4-219a
 EXPNO 1
 PROCNO 1

F2 - Acquisition Parameters
 Date_ 20131125
 Time 12.24
 INSTRUM av500
 PROBHD 5 mm DCH 13C-1
 PULPROG zg30
 TD 65536
 SOLVENT CDCl3
 NS 16
 DS 0
 SWH 10000.000 Hz
 FIDRES 0.152588 Hz
 AQ 3.2767989 sec
 RG 11
 DW 50.000 usec
 DE 10.00 usec
 TE 298.0 K
 D1 2.00000000 sec
 TD0 1

===== CHANNEL f1 =====
 SFO1 500.130008 MHz
 NUC1 1H
 P1 10.00 usec
 PLW1 13.50000000 W

F2 - Processing parameters
 SI 65536
 SF 500.1300121 MHz
 WDW EM
 SSB 0
 LB 0.30 Hz
 GB 0
 PC 1.00

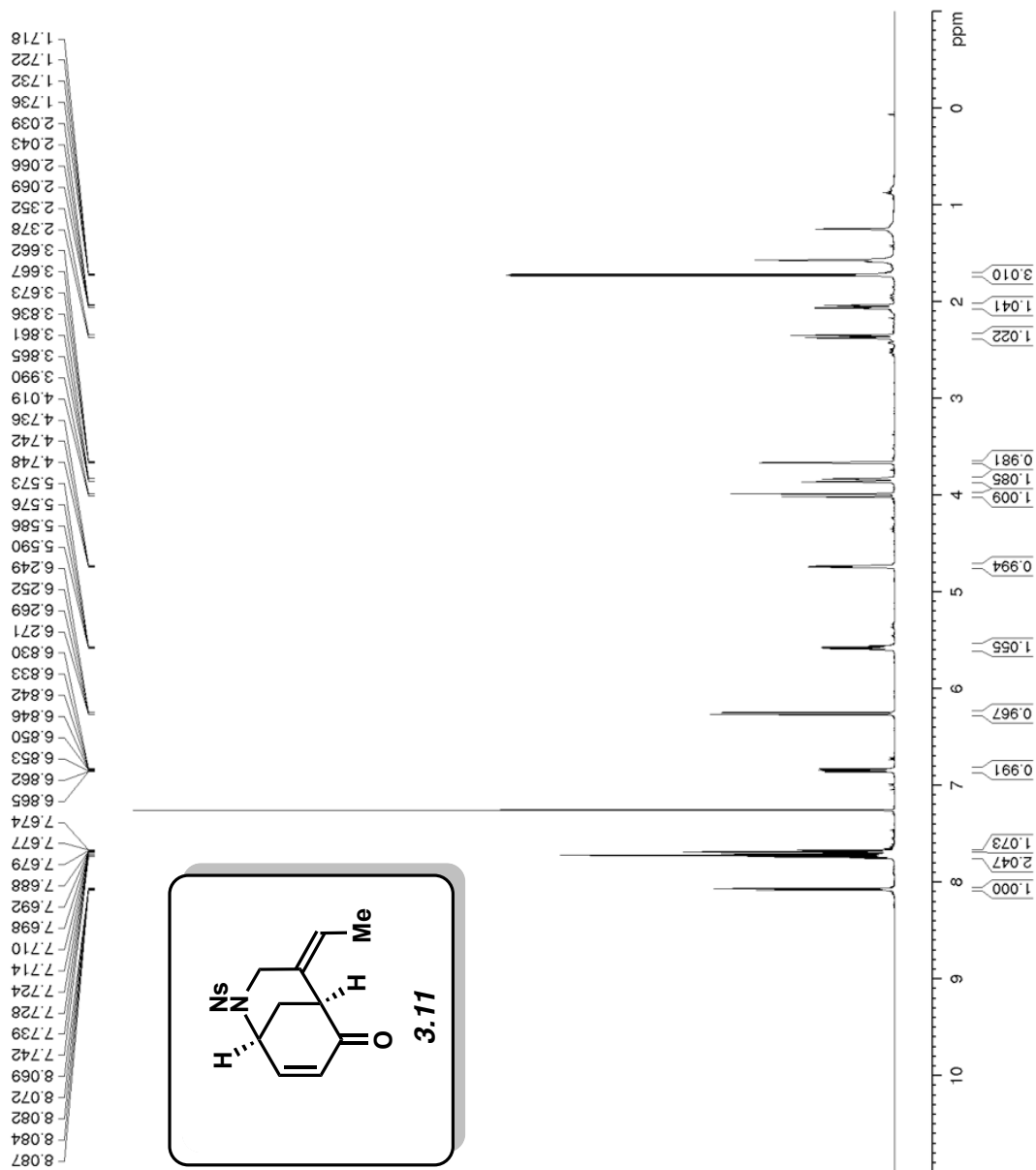


Figure A2.10 ¹H NMR (500 MHz, CDCl₃) of compound 3.11.

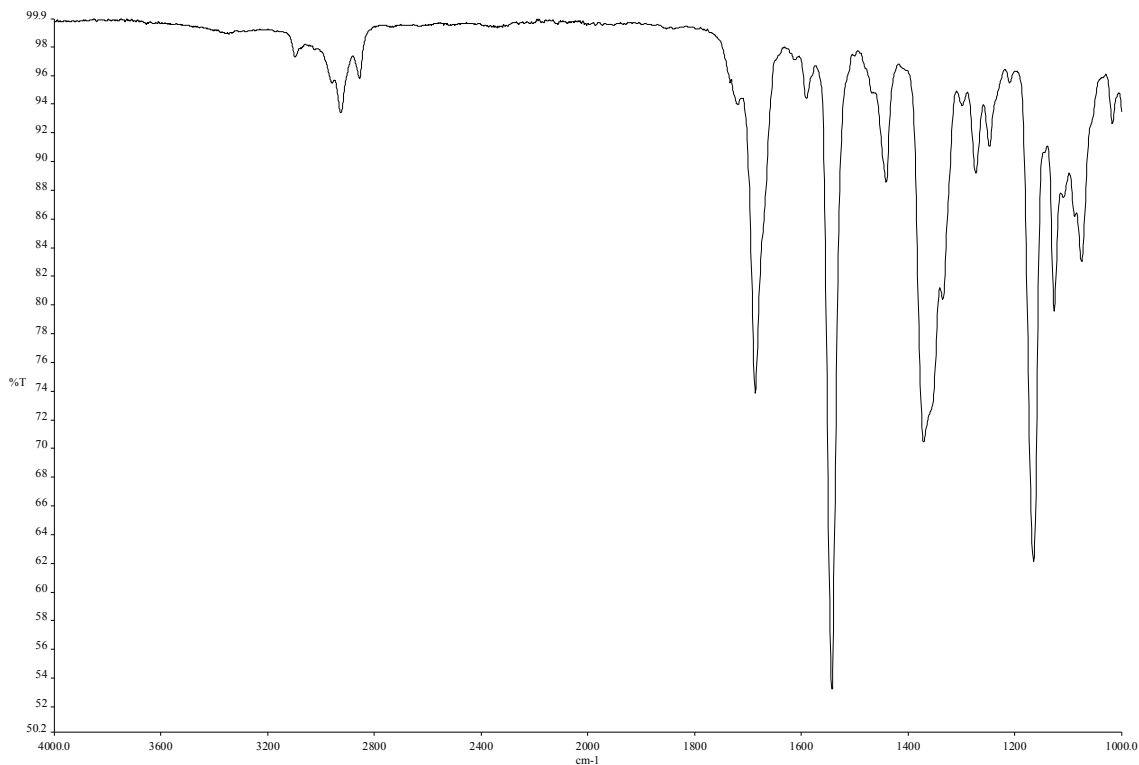


Figure A2.11 Infrared spectrum of compound **3.11**.

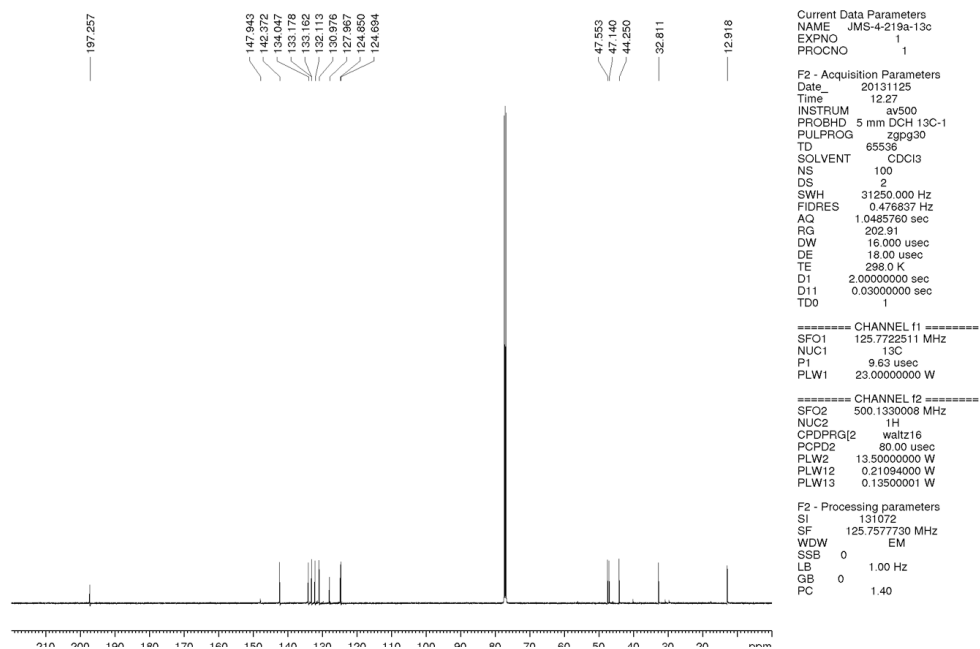


Figure A2.12 ^{13}C NMR (125 MHz, CDCl_3) of compound **3.11**.

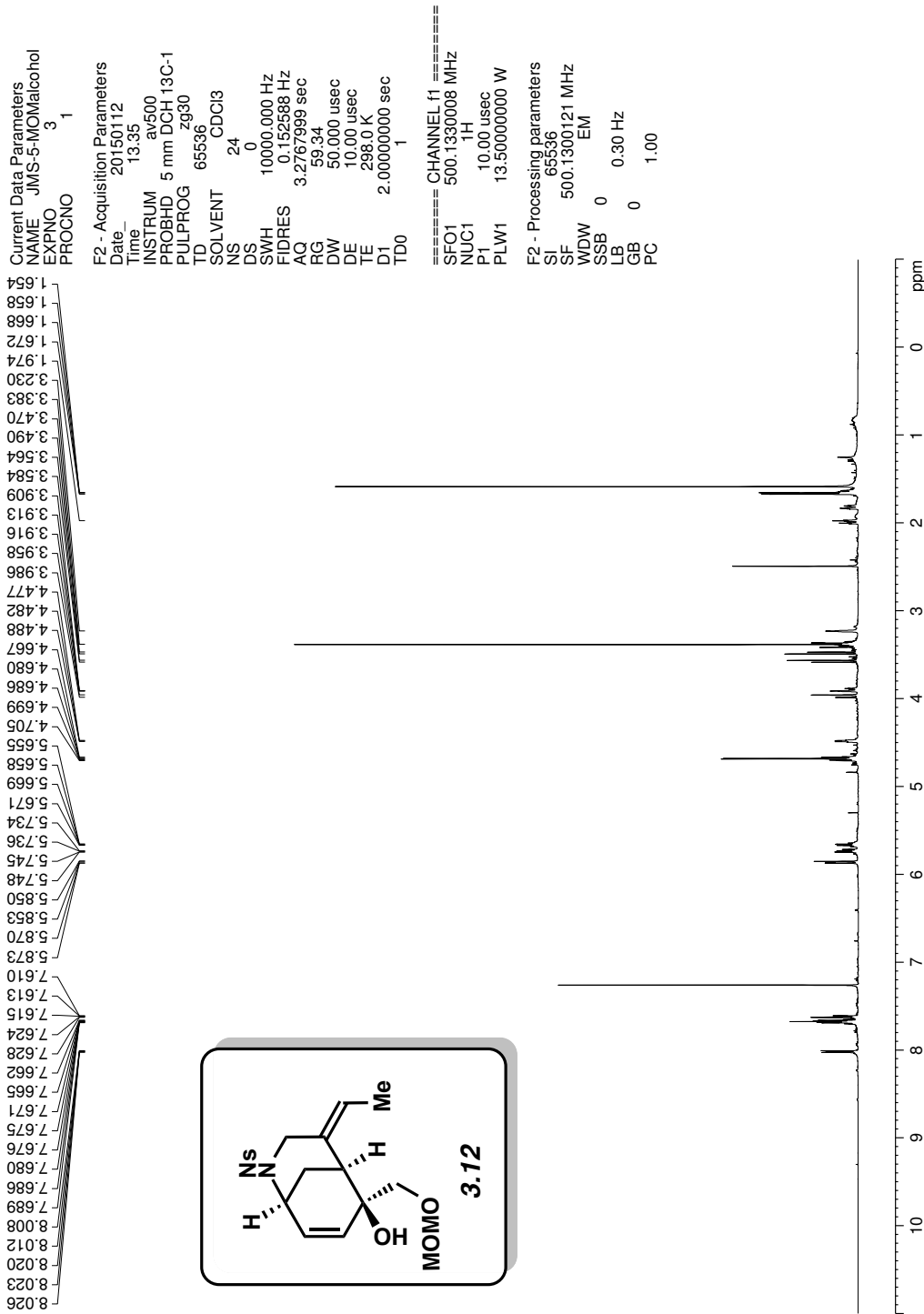


Figure A2.13 ¹H NMR (500 MHz, CDCl₃) of compound 3.12.

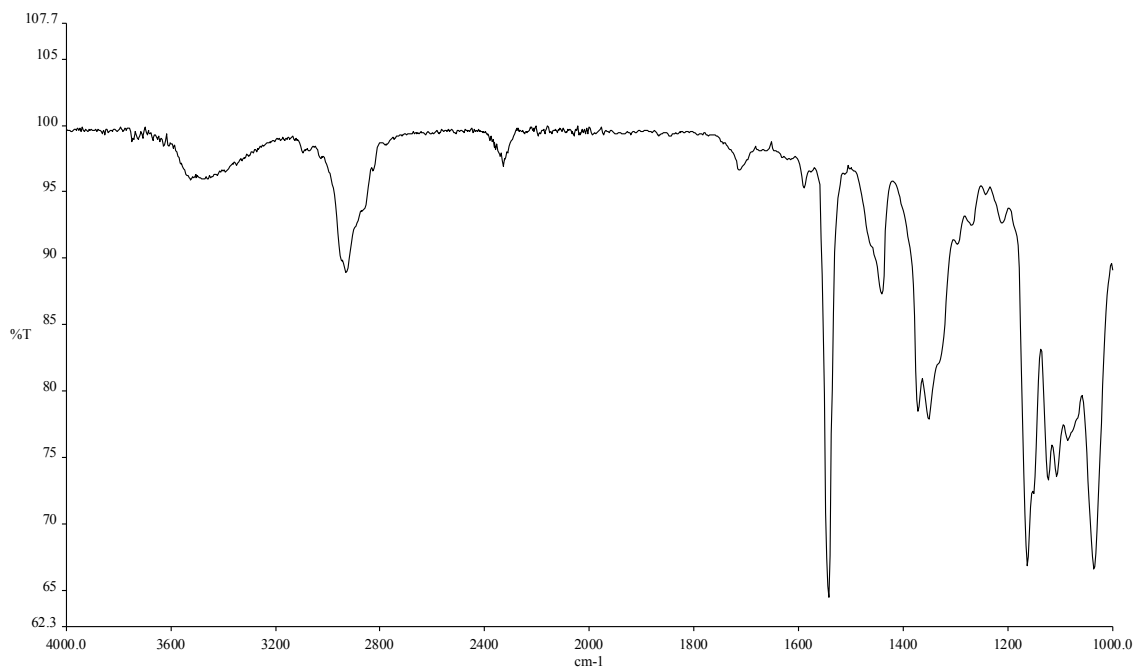


Figure A2.14 Infrared spectrum of compound **3.12**.

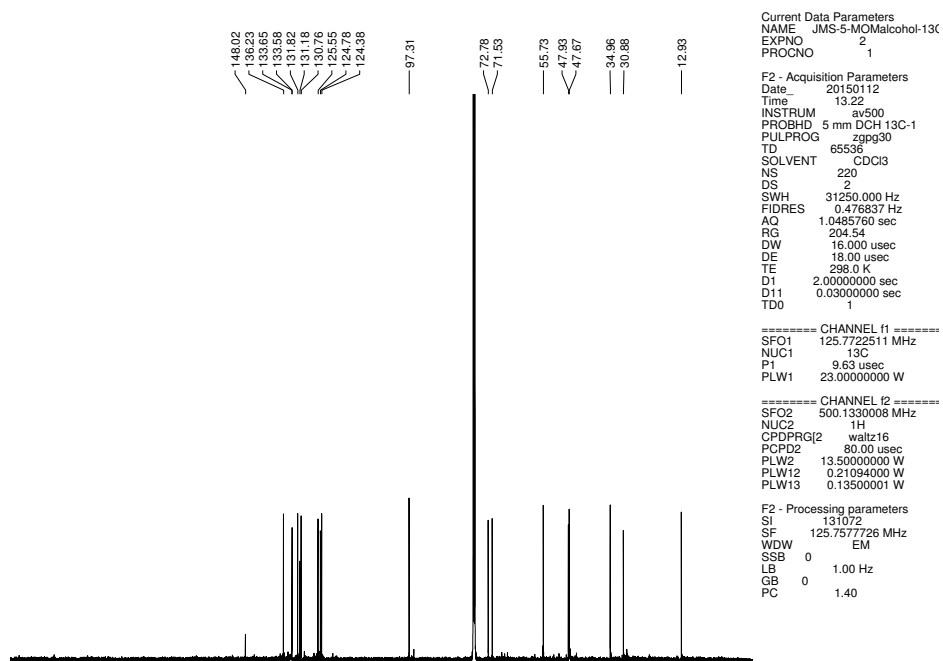


Figure A2.15 ^{13}C NMR (125 MHz, CDCl_3) of compound **3.12**.

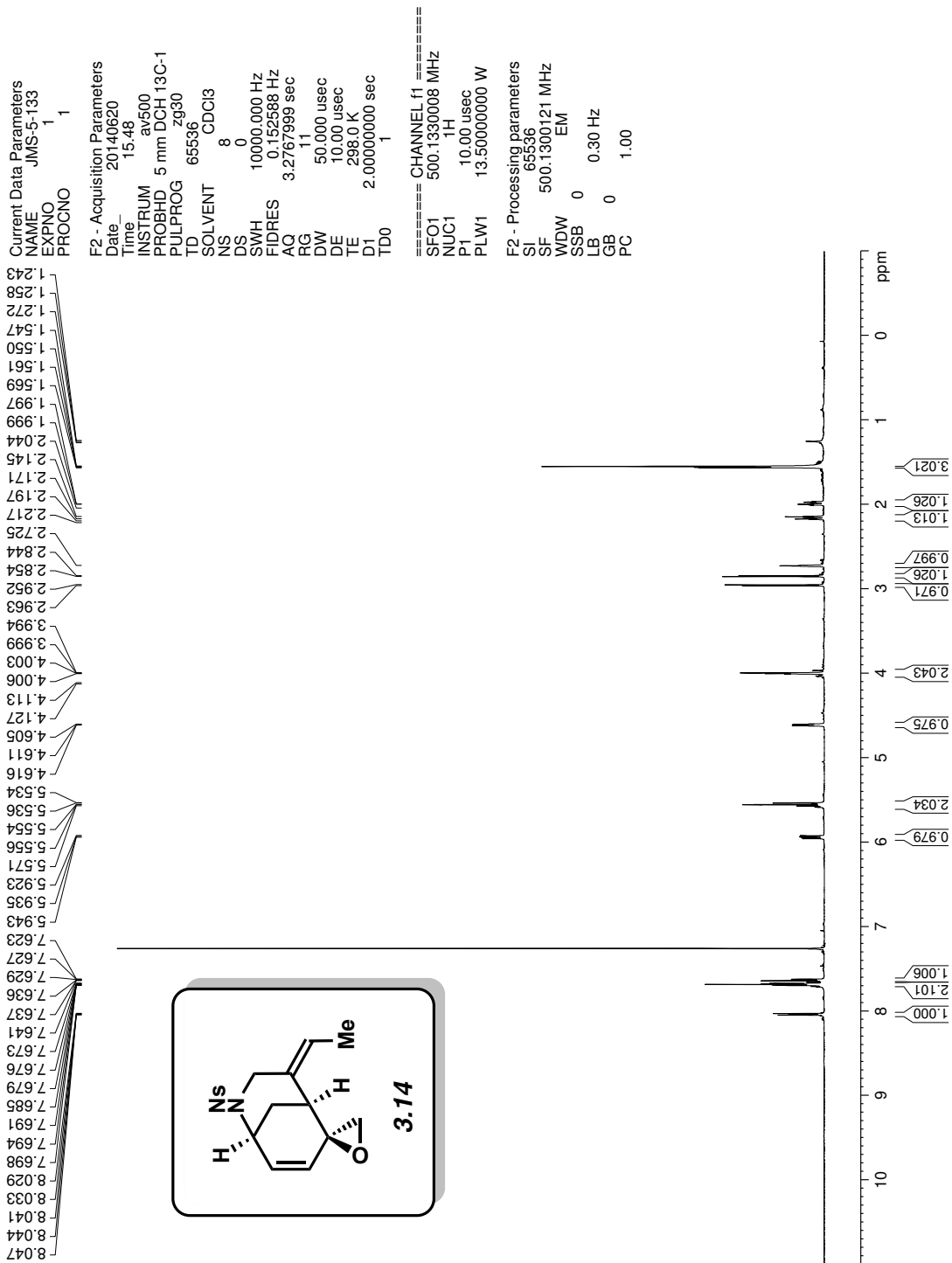


Figure A2.16 ^1H NMR (500 MHz, CDCl_3) of compound 3.14.

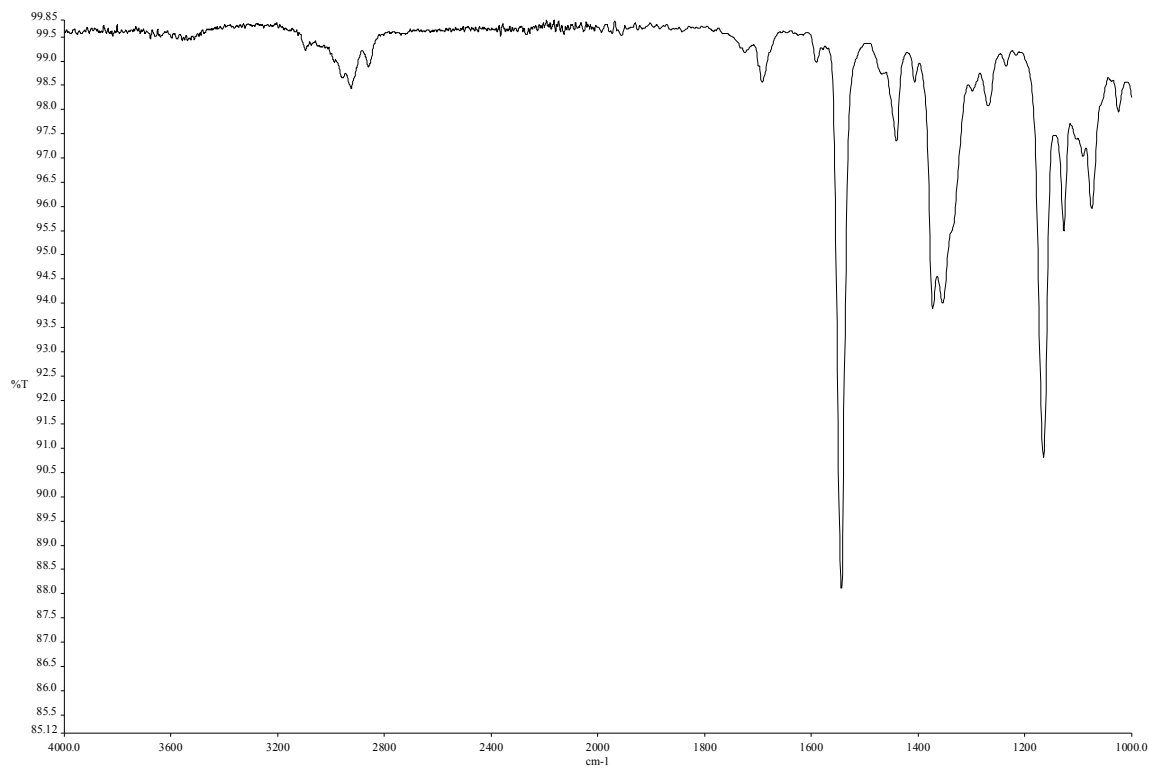


Figure A2.17 Infrared spectrum of compound **3.14**.

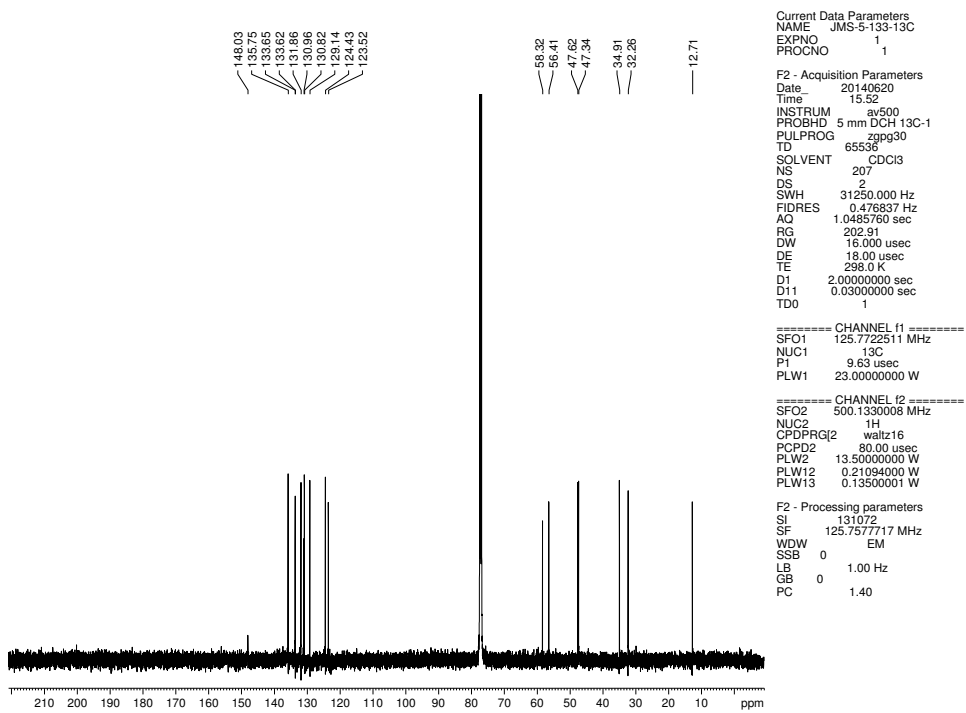


Figure A2.18 ^{13}C NMR (125 MHz, CDCl_3) of compound **3.14**.

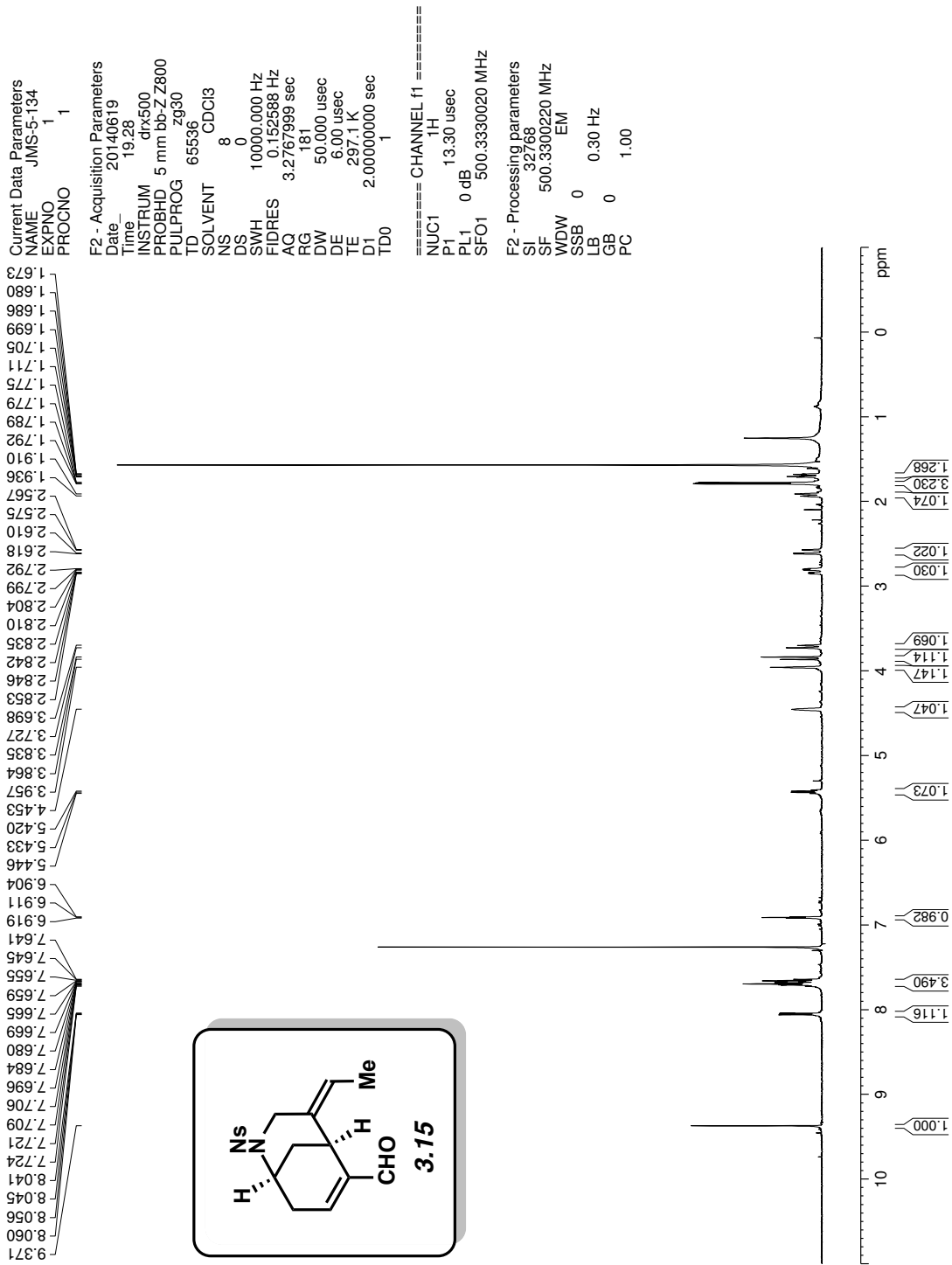


Figure A2.19 ¹H NMR (500 MHz, CDCl₃) of compound 3.15.

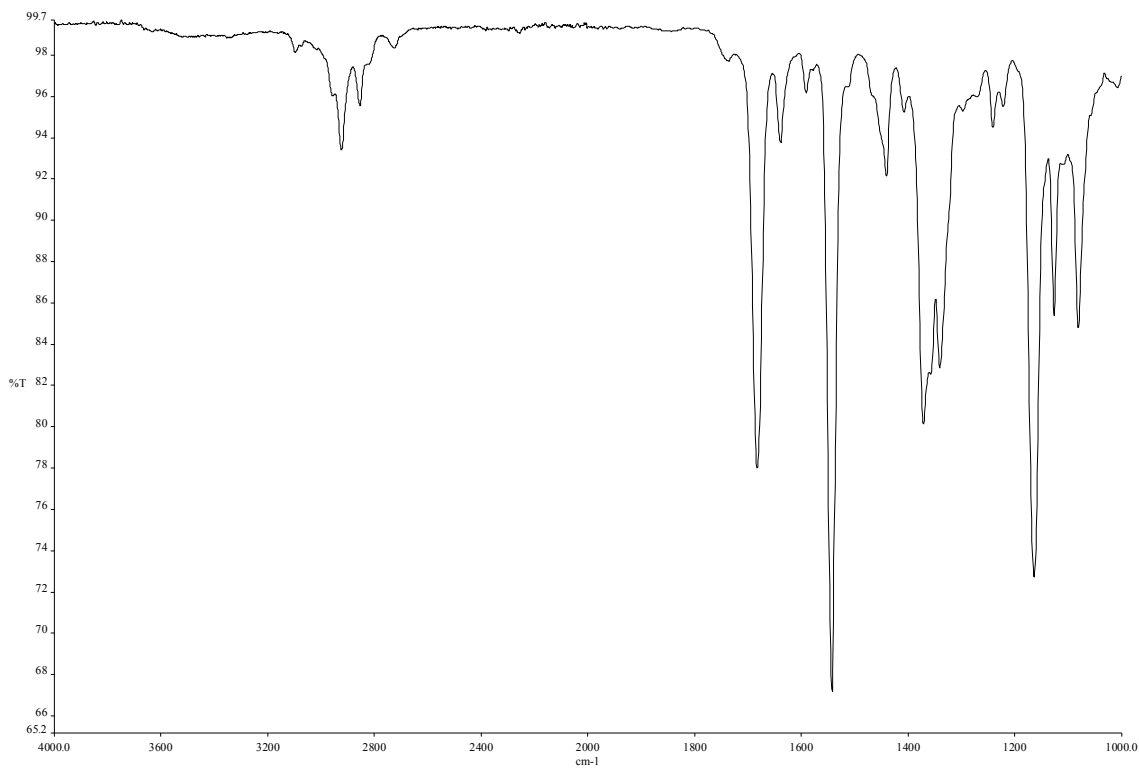


Figure A2.20 Infrared spectrum of compound **3.15**.

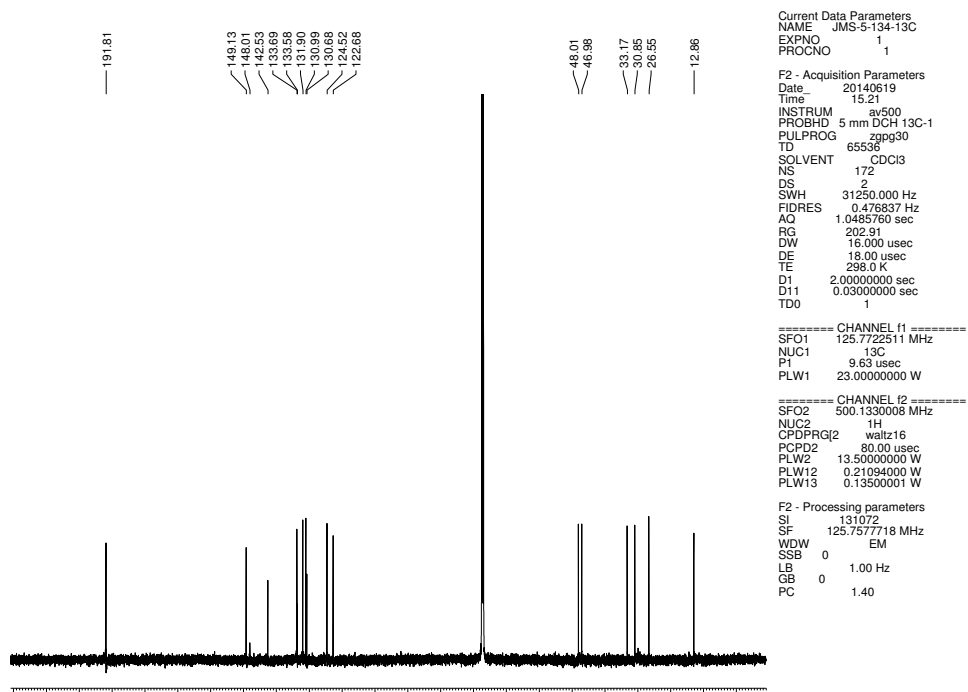


Figure A2.21 ^{13}C NMR (125 MHz, CDCl_3) of compound **3.15**.

```

Current Data Parameters
NAME   JMS-4-epoxide3
EXPNO  3
PROCNO 1

F2 - Acquisition Parameters
Date_  20131126
Time_  19.52
INSTRUM  dirx500
PROBHD  5 mm bb-Z Z800
PULPROG  zg30
TD      65536
SOLVENT  CDCl3
NS      16
DS      0
SWH     10000.000 Hz
FIDRES  0.152568 Hz
AQ      3.2767999 sec
RG      80.6
DW      50.000 usec
DE      6.00 usec
TE      297.1 K
D1      2.00000000 sec
TD0     1

===== CHANNEL f1 =====
NUC1    1H
P1      13.30 usec
PL1     0 dB
SFO1    500.3330020 MHz

F2 - Processing parameters
SI      32768
SF      500.3300220 MHz
WDW     EMI
SSB     0
LB      0.30 Hz
GB      0
PC      1.00

```

8.124
8.110
8.106
7.763
7.751
7.749
7.737
7.726
7.723
7.711
7.704
7.700
7.689
7.686
5.613
5.600
5.587
5.574
4.714
4.708
4.072
4.042
3.983
3.953
3.620
3.614
3.609
3.511
3.376
3.369
2.340
2.335
2.330
2.313
2.308
2.302

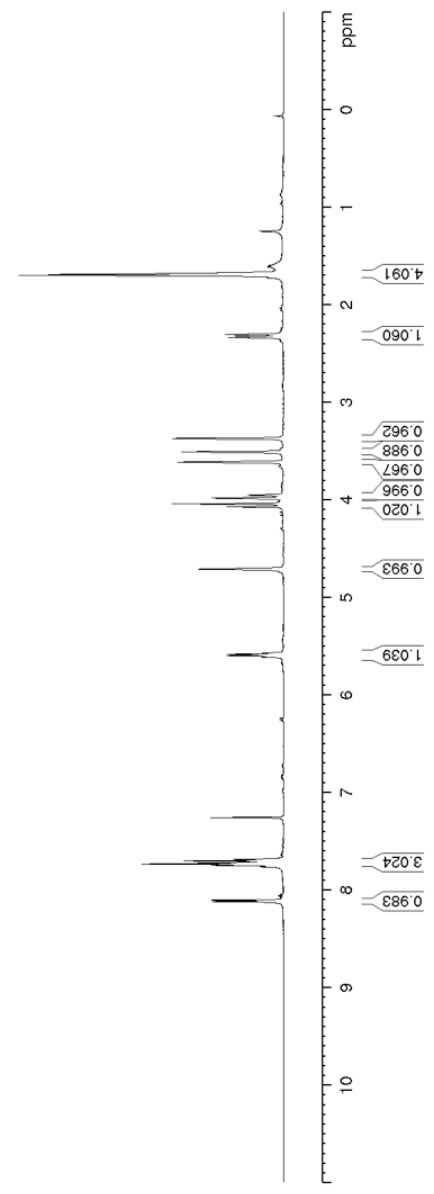
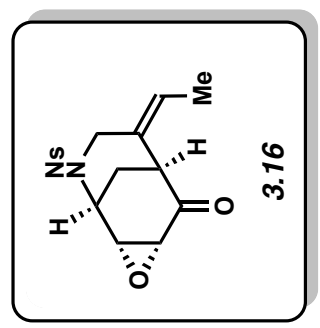


Figure A2.22 ¹H NMR (500 MHz, CDCl₃) of compound 3.16.

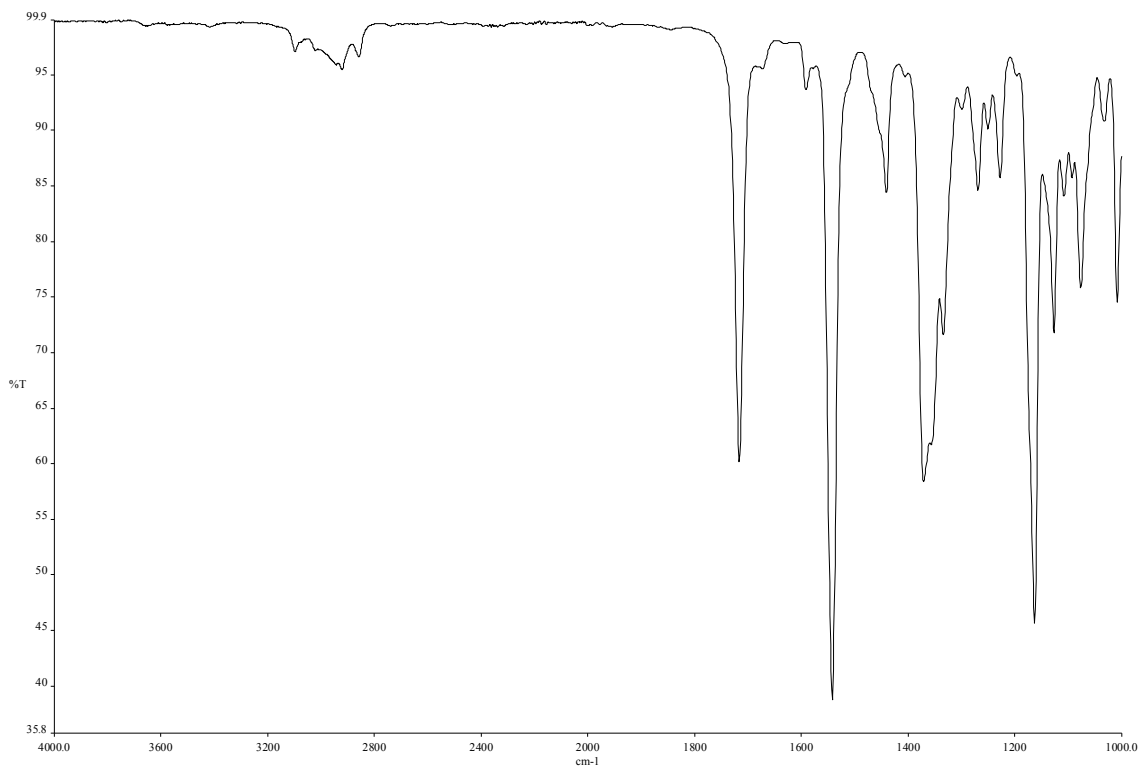


Figure A2.23 Infrared spectrum of compound **3.16**.

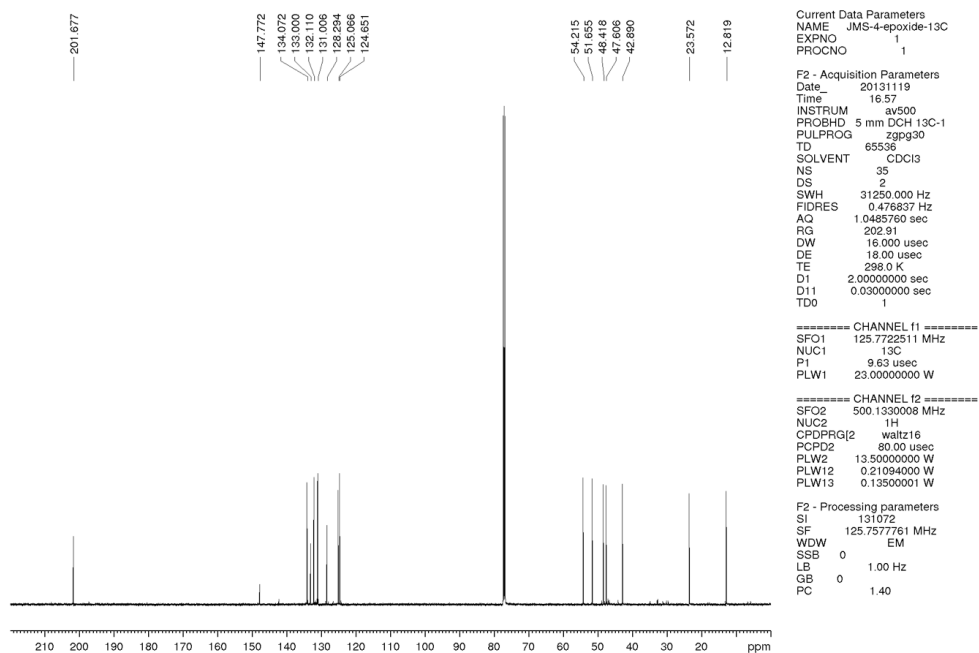


Figure A2.24 ^{13}C NMR (125 MHz, CDCl_3) of compound **3.16**.

Current Data Parameters
 NAME JMS-4-enal
 EXPNO 2
 PROCNO 1

F2 - Acquisition Parameters
 Date_ 20131119
 Time 13.30
 INSTRUM dx500
 PROBHD 5 mm bb-Z Z800
 PULPROG zg30
 TD 65536
 SOLVENT CDCIG
 NS 16
 DS 0
 SWH 10000.000 Hz
 FIDRES 0.152588 Hz
 AQ 3.2767999 sec
 RG 143.7
 DW 50.000 usec
 DE 6.00 usec
 TE 297.1 K
 D1 2.00000000 sec
 TD0 1

===== CHANNEL f1 =====
 NUC1 1H
 P1 12.25 usec
 PL1 0 dB
 SFO1 500.3330020 MHz

F2 - Processing parameters
 SI 32768
 SF 500.3300219 MHz
 WDW EM
 SSB 0
 LB 0
 GB 0
 PC 1.00

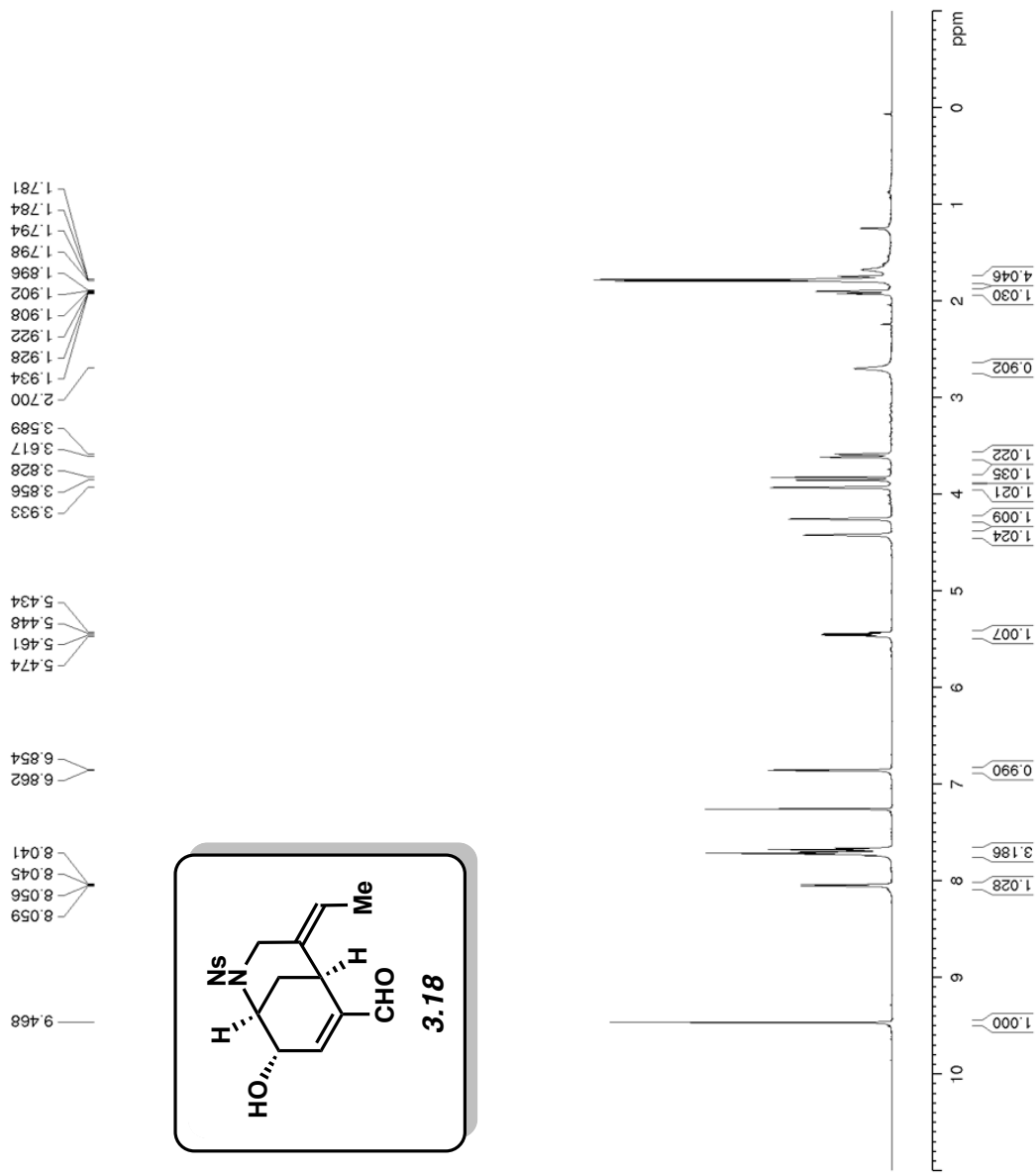


Figure A2.25 ¹H NMR (500 MHz, CDCl₃) of compound **3.18**.

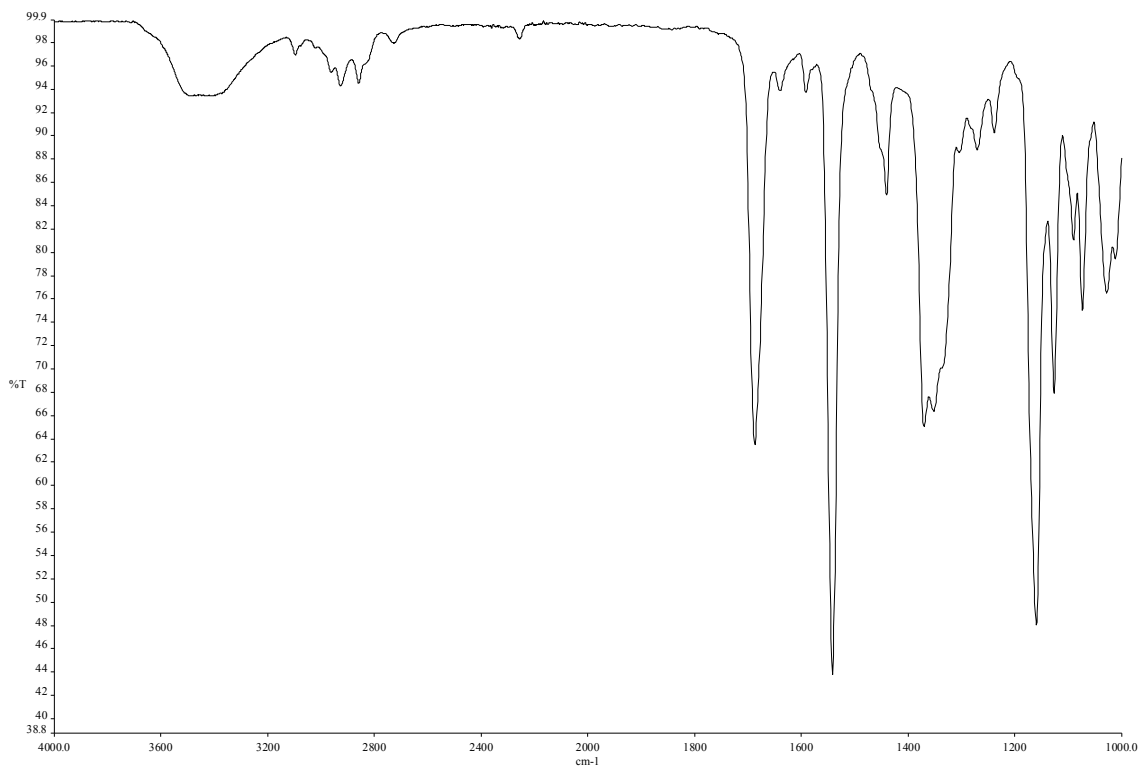


Figure A2.26 Infrared spectrum of compound **3.18**.

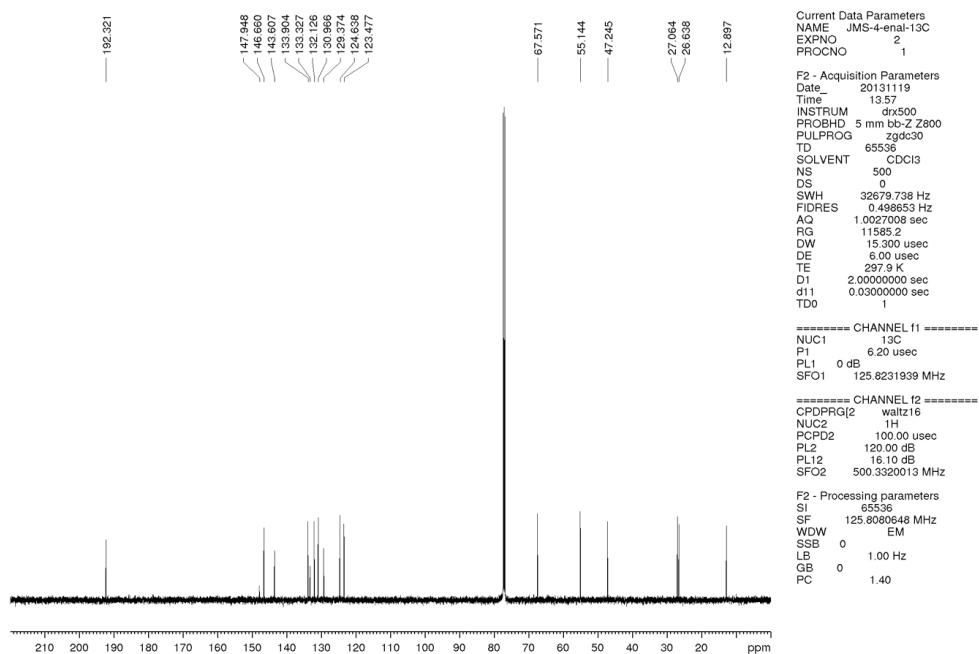


Figure A2.27 ¹³C NMR (125 MHz, CDCl₃) of compound **3.18**.

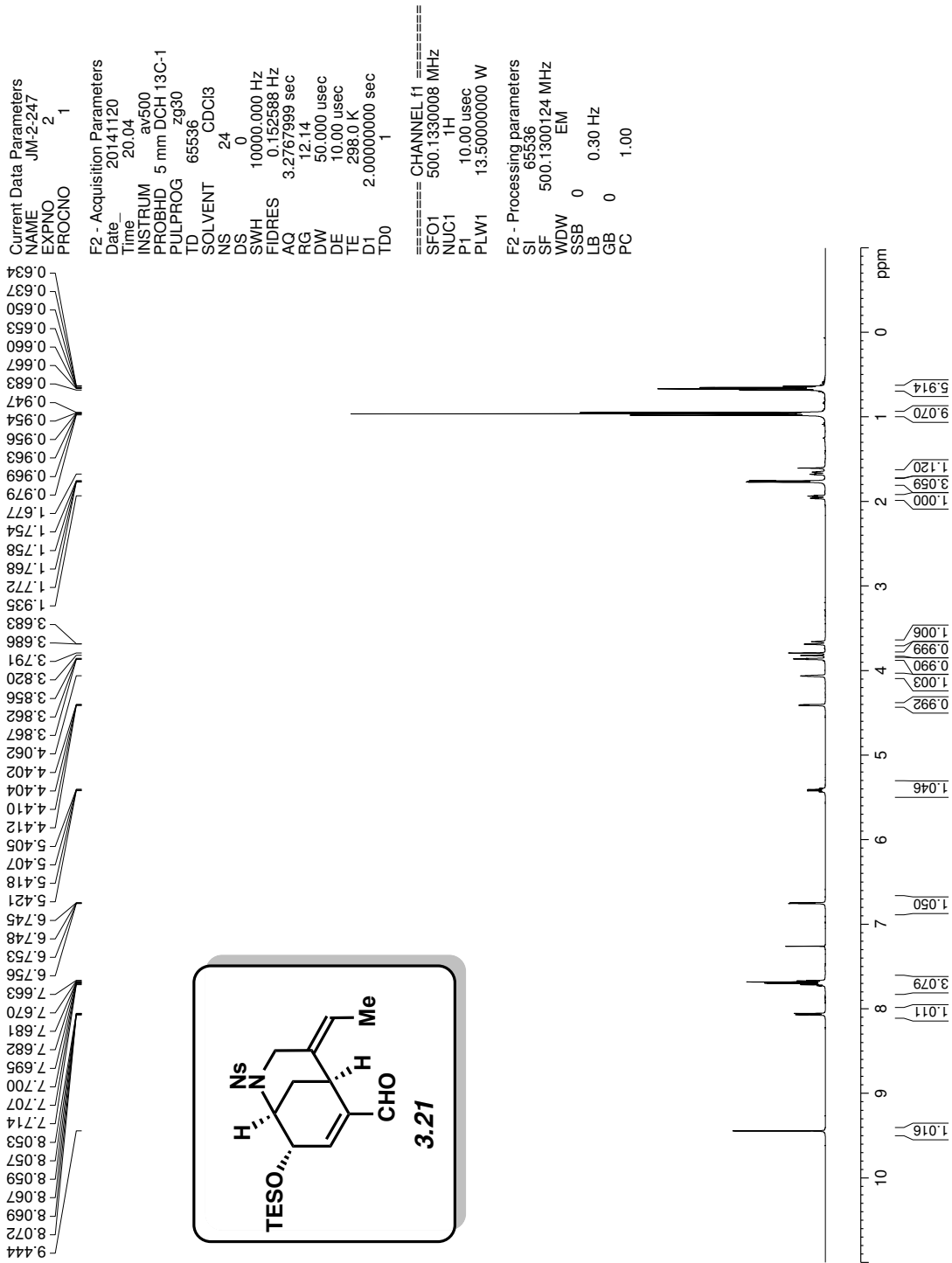


Figure A2.28 ¹H NMR (500 MHz, CDCl₃) of compound 3.21.

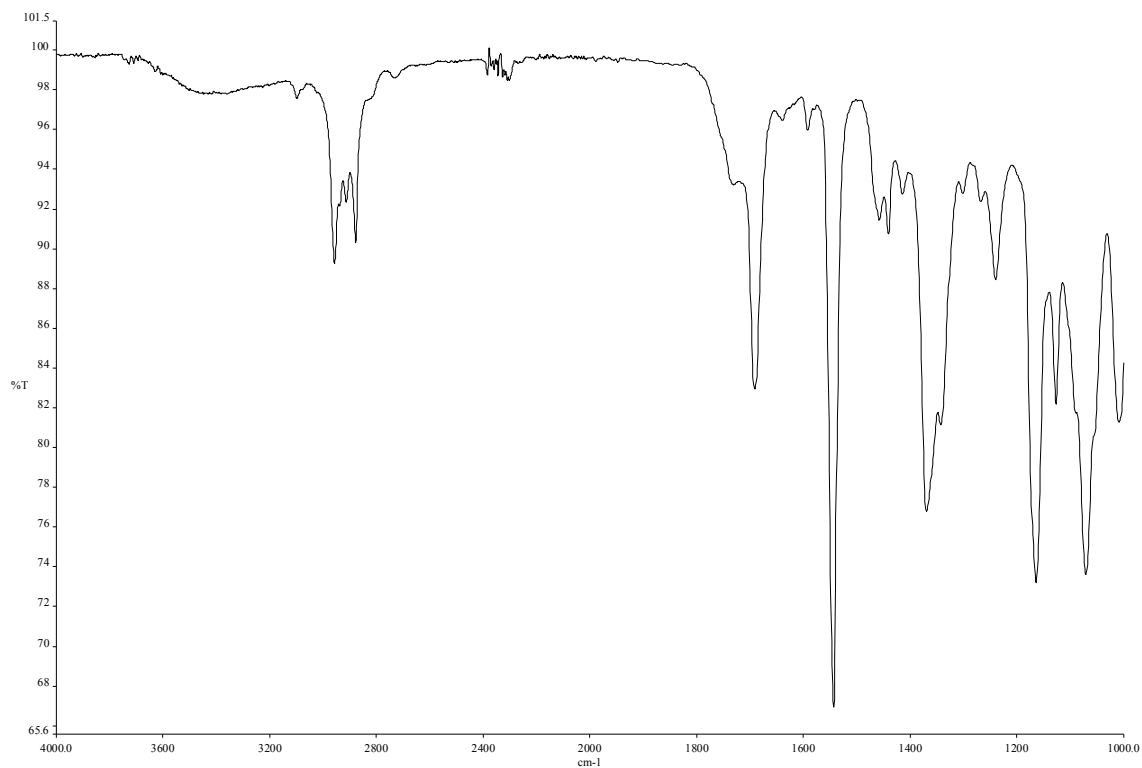


Figure A2.29 Infrared spectrum of compound **3.21**.

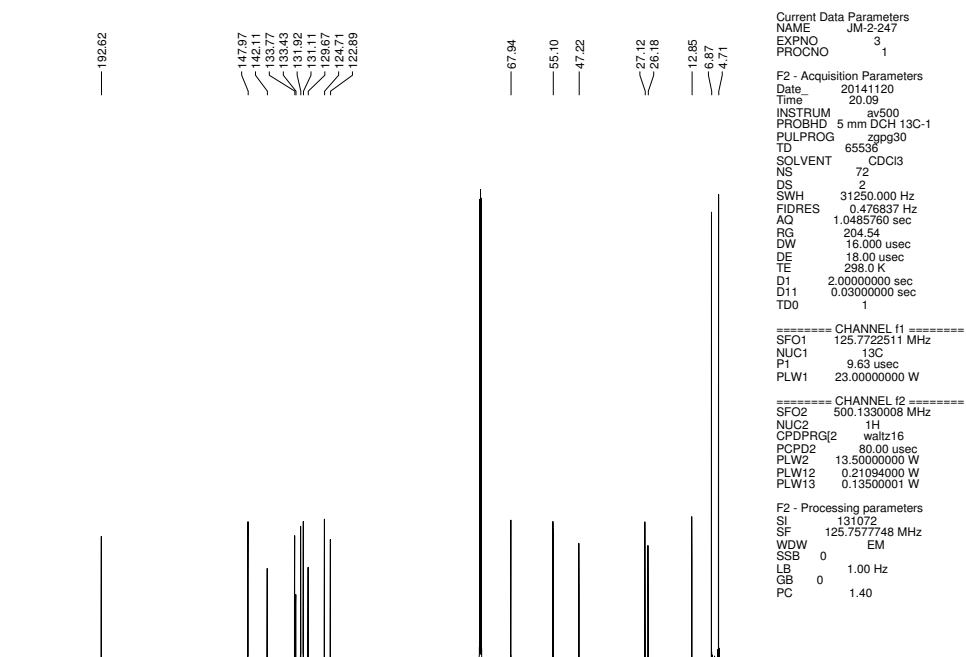


Figure A2.30 ^{13}C NMR (125 MHz, CDCl_3) of compound **3.21**.

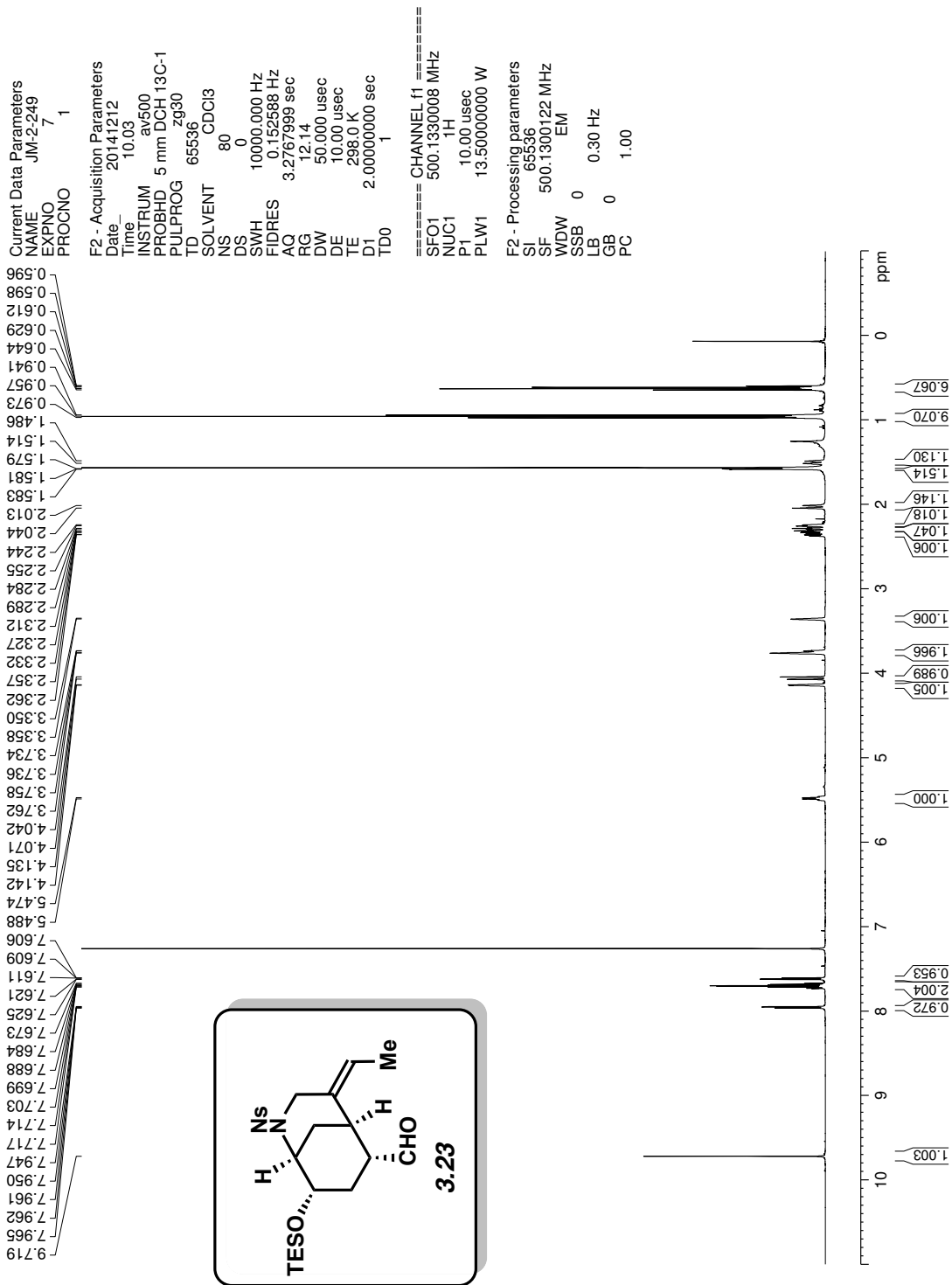


Figure A2.31 ¹H NMR (500 MHz, CDCl₃) of compound 3.23.

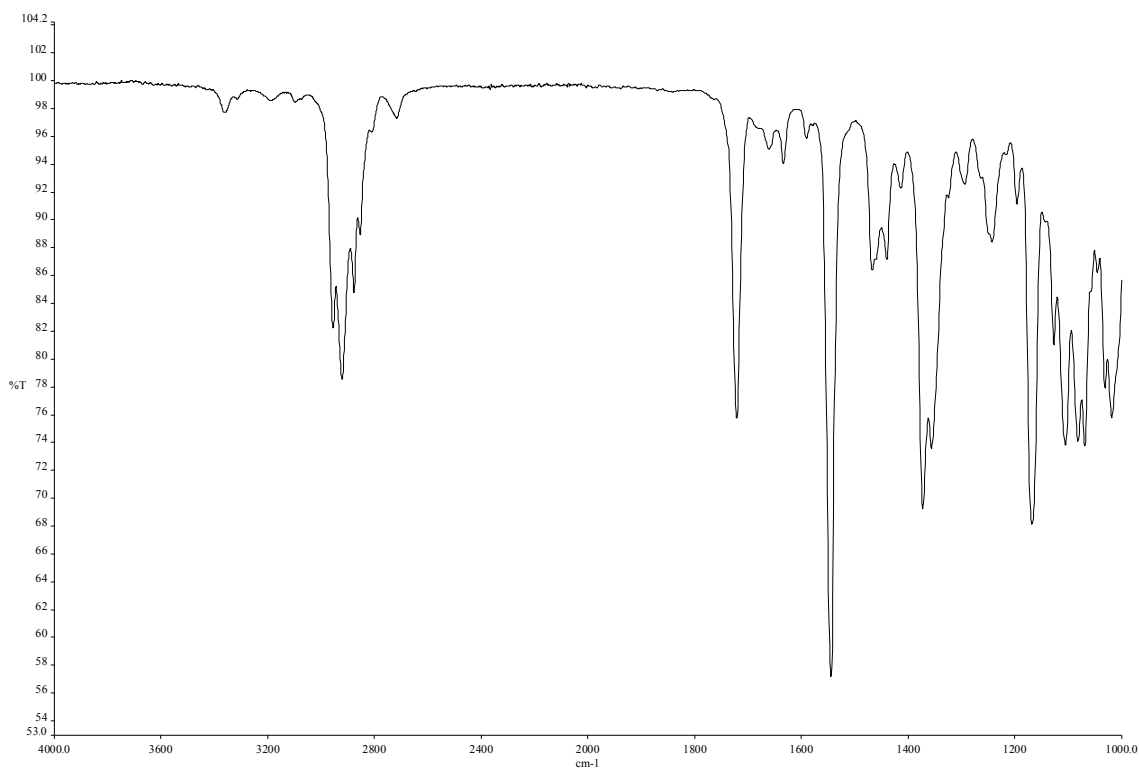


Figure A2.32 Infrared spectrum of compound **3.23**.

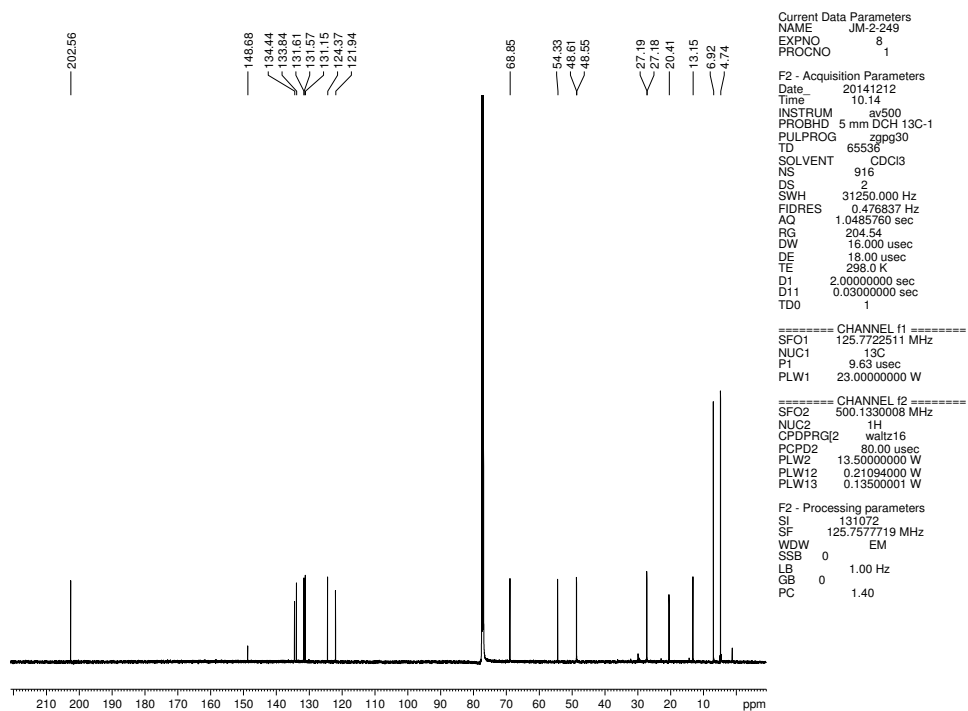


Figure A2.33 ^{13}C NMR (125 MHz, CDCl_3) of compound **3.23**.

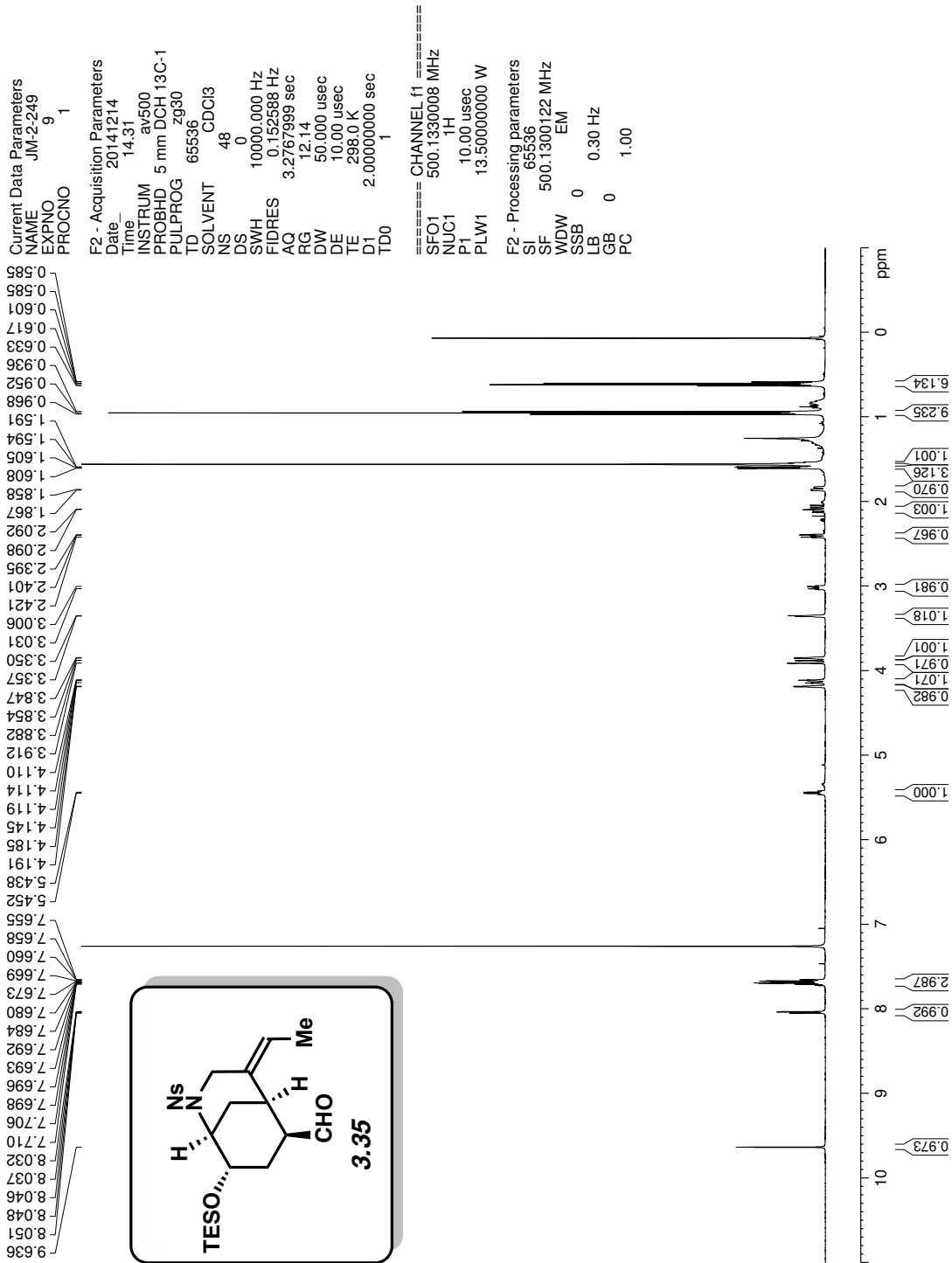


Figure A2.34 ¹H NMR (500 MHz, CDCl₃) of compound 3.35.

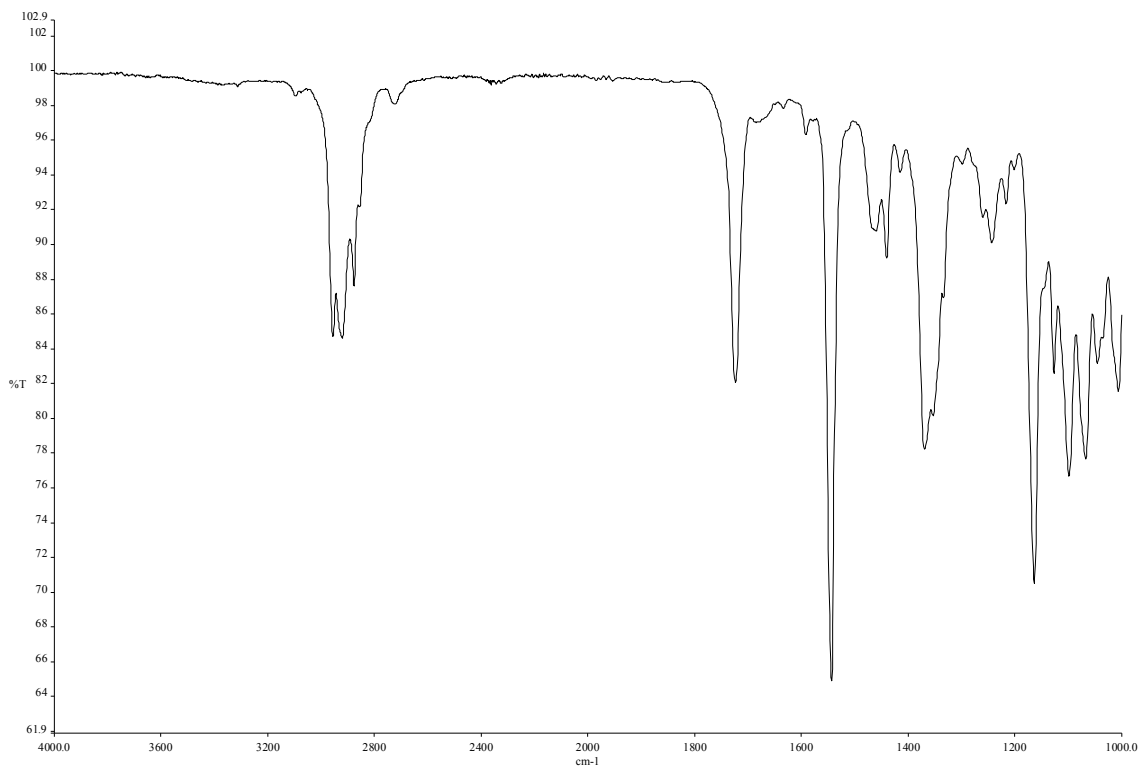


Figure A2.35 Infrared spectrum of compound **3.35**.

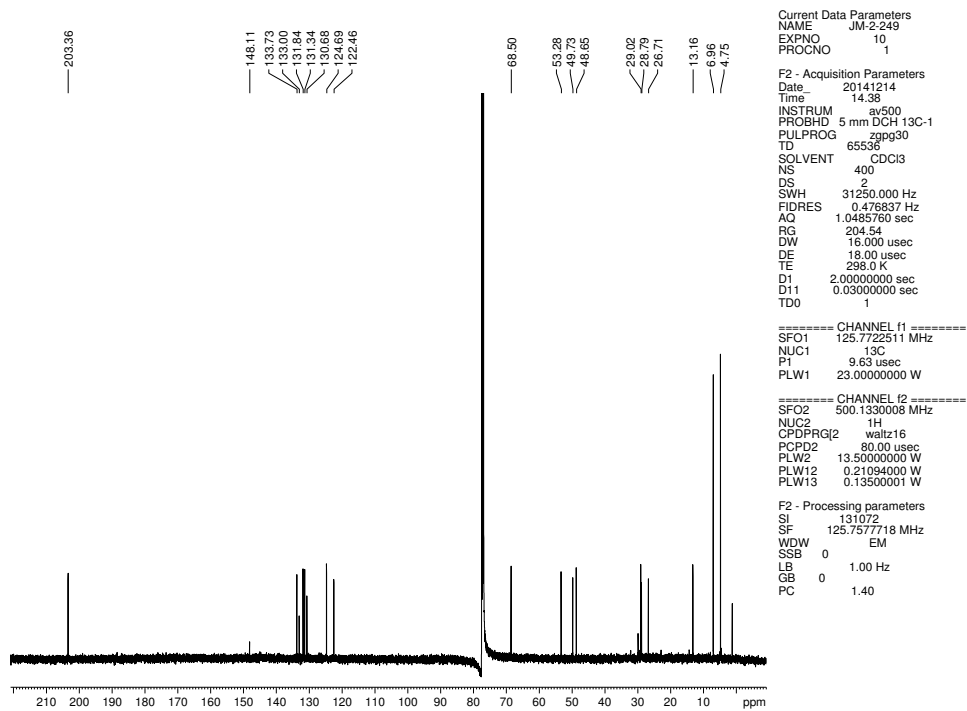


Figure A2.36 ^{13}C NMR (125 MHz, CDCl_3) of compound **3.35**.

```

Current Data Parameters
NAME      JMS-4-216c
EXPNO    1
PROCNO   1

F2 - Acquisition Parameters
Date_    20131120
Time     19:51
INSTRUM  av500
PROBHD   5 mm DCH 13C-1
PULPROG  zg30
TD        65536
SOLVENT  CDCl3
NS        16
DS         0
SWH       10000.000 Hz
FIDRES    0.152588 Hz
AQ         3.2767999 sec
RG         11
DW         50.000 usec
DE         10.00 usec
TE         298.0 K
D1         2.0000000 sec
TD0        1

===== CHANNEL f1 =====
SFO1     500.1330008 MHz
NUC1      1H
P1        10.00 usec
PLW1     13.50000000 W

F2 - Processing parameters
SI        65536
SF        500.1300120 MHz
WDW       EM
SSB       0
LB        0.30 Hz
GB         0
PC        1.00

```

9.641
8.055
8.052
8.049
8.041
8.036
7.722
7.718
7.712
7.708
7.707
7.703
7.697
7.693
7.682
7.683
7.659
7.650
7.648
7.645
5.454
4.244
4.131
4.105
4.100
4.096
4.020
4.014
3.938
3.908
3.404
3.397
3.050
3.024
2.421
2.415
2.400
2.394
2.388
2.172
2.148
2.141
2.123
2.115
1.970
1.960
1.655
1.635
1.629
1.617
1.614
1.604
1.600

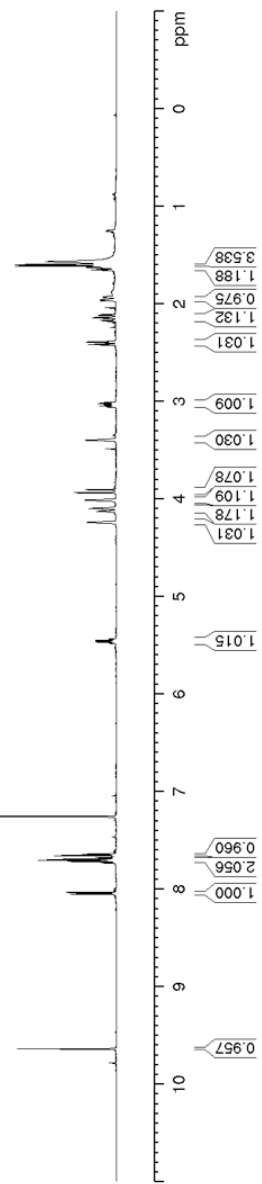
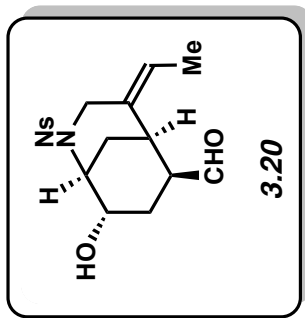


Figure A2.37 ¹H NMR (500 MHz, CDCl₃) of compound 3.20.

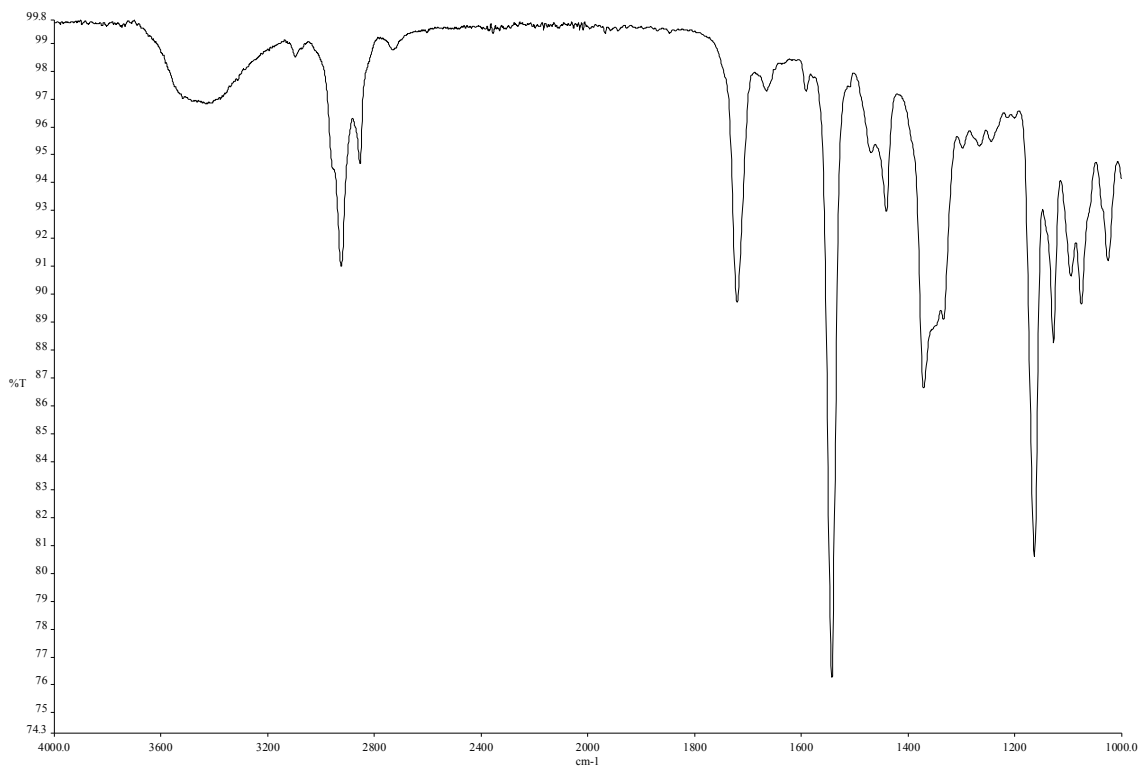


Figure A2.38 Infrared spectrum of compound **3.20**.

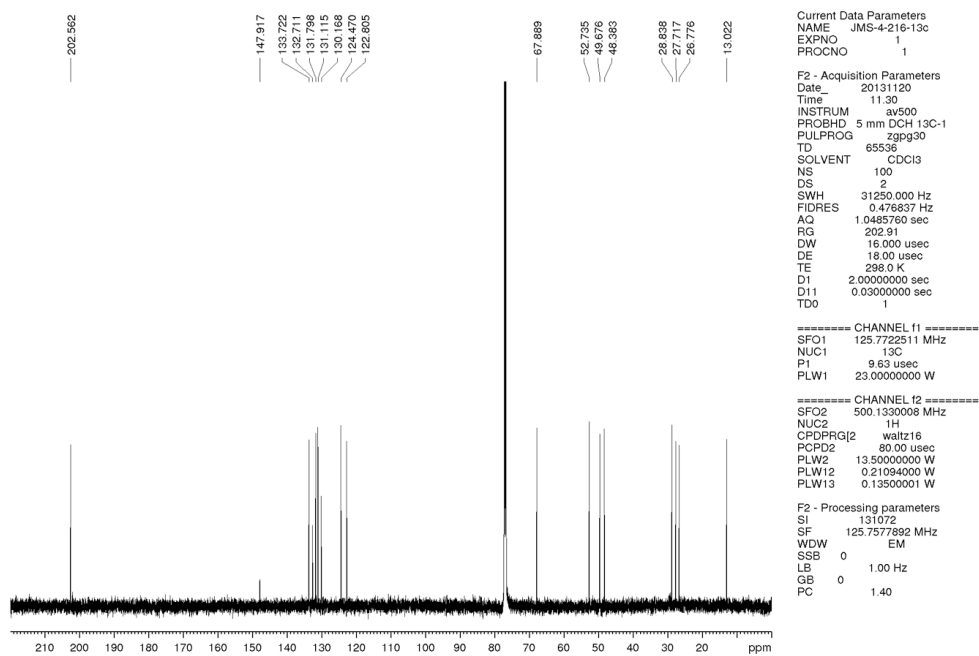


Figure A2.39 ^{13}C NMR (125 MHz, CDCl_3) of compound **3.20**.

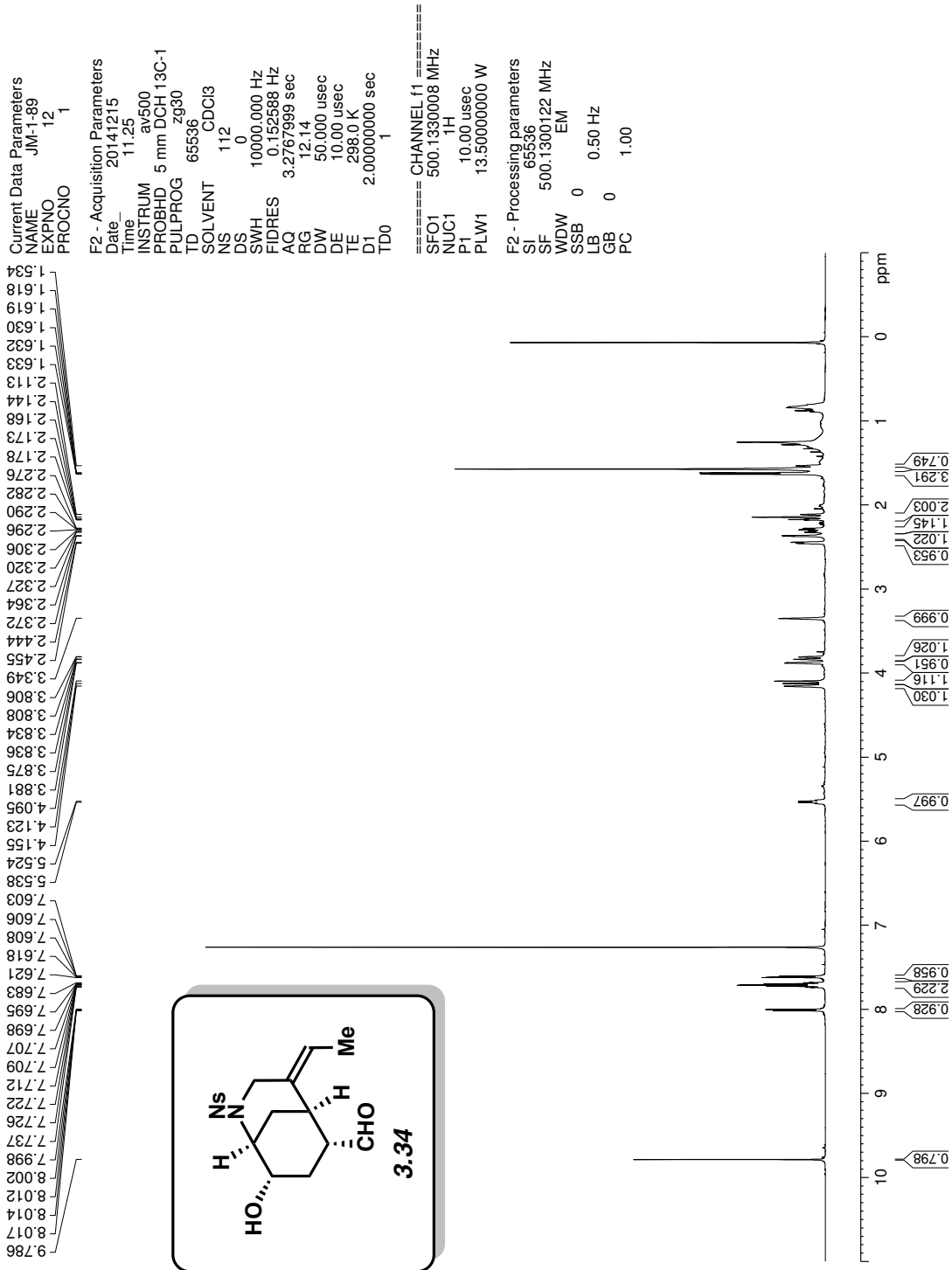


Figure A2.40 ¹H NMR (500 MHz, CDCl₃) of compound 3.34.

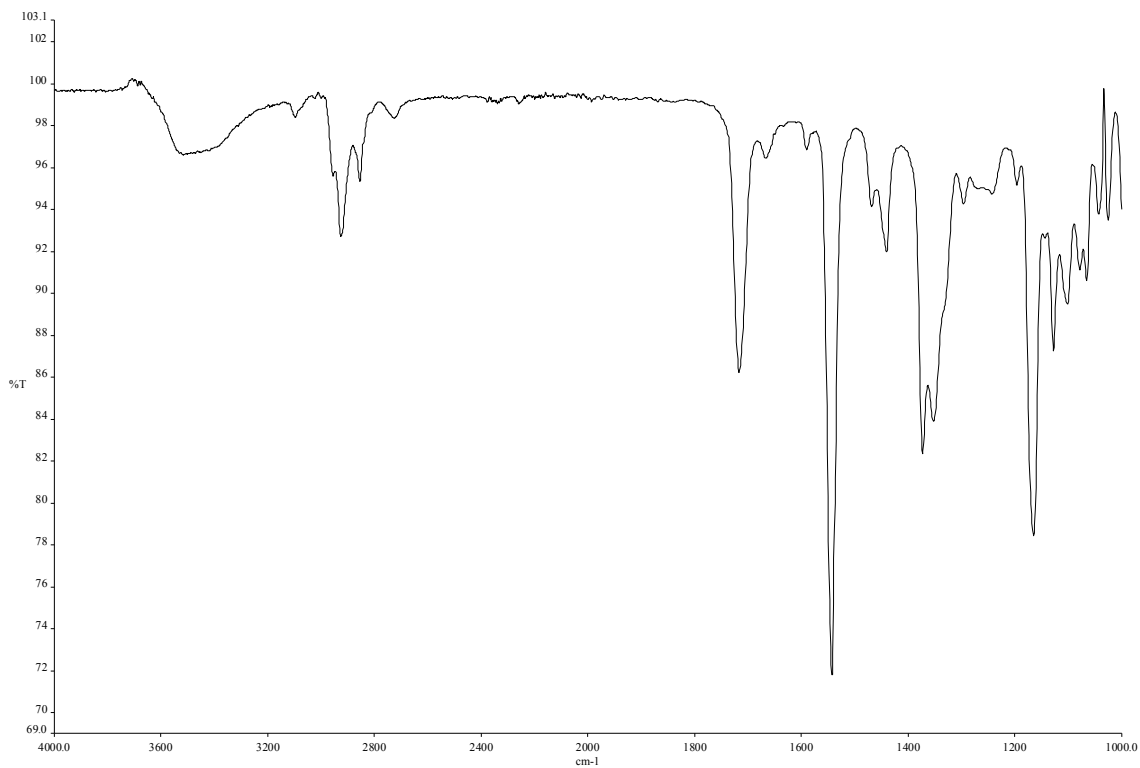


Figure A2.41 Infrared spectrum of compound **3.34**.

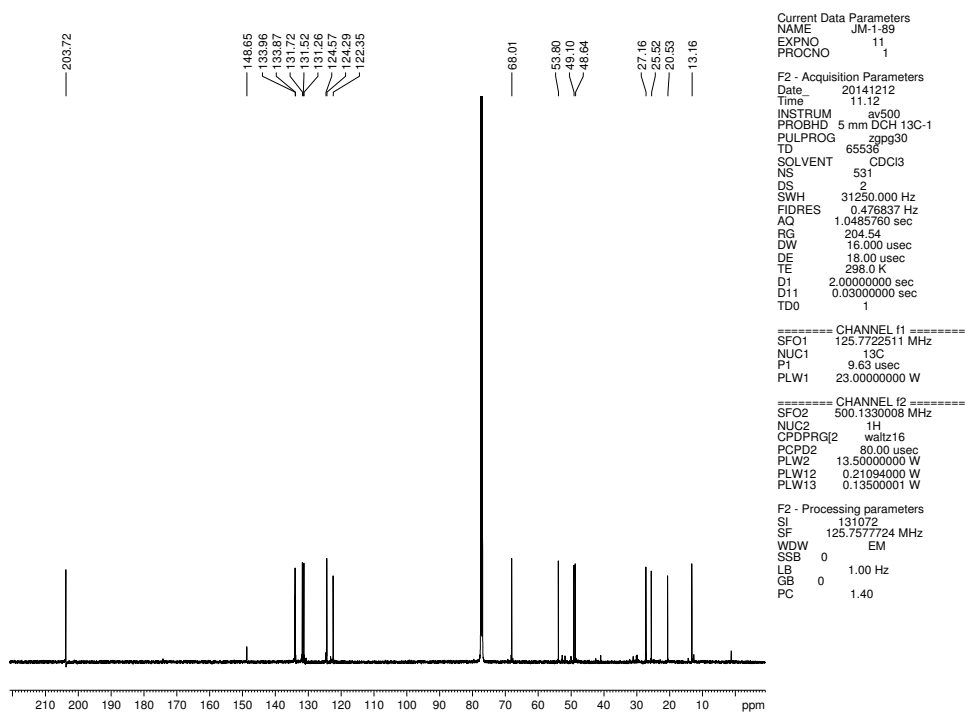


Figure A2.42 ^{13}C NMR (125 MHz, CDCl_3) of compound **3.34**.

```

Current Data Parameters
NAME      JMS-4-229
EXPNO    1
PROCNO   1

F2 - Acquisition Parameters
Date_    20131204
Time     15:07
INSTRUM  av500
PROBHD   5 mm DCH 13C-1
PULPROG  zg30
TD        65536
SOLVENT  CDCl3
NS        16
DS         0
SWH       10000.000 Hz
FIDRES    0.152568 Hz
AQ         3.2767999 sec
RG         11
DW         50.000 usec
DE         10.00 usec
TE         296.0 K
D1         2.00000000 sec
TD0        1

===== CHANNEL f1 =====
SFO1      500.1330008 MHz
NUC1       1H
P1         10.00 usec
PLW1      13.50000000 W

F2 - Processing parameters
SI         65536
SF         500.1300121 MHz
WDW        EMI
SSB         0
LB         0.30 Hz
GB         0
PC         1.00

```

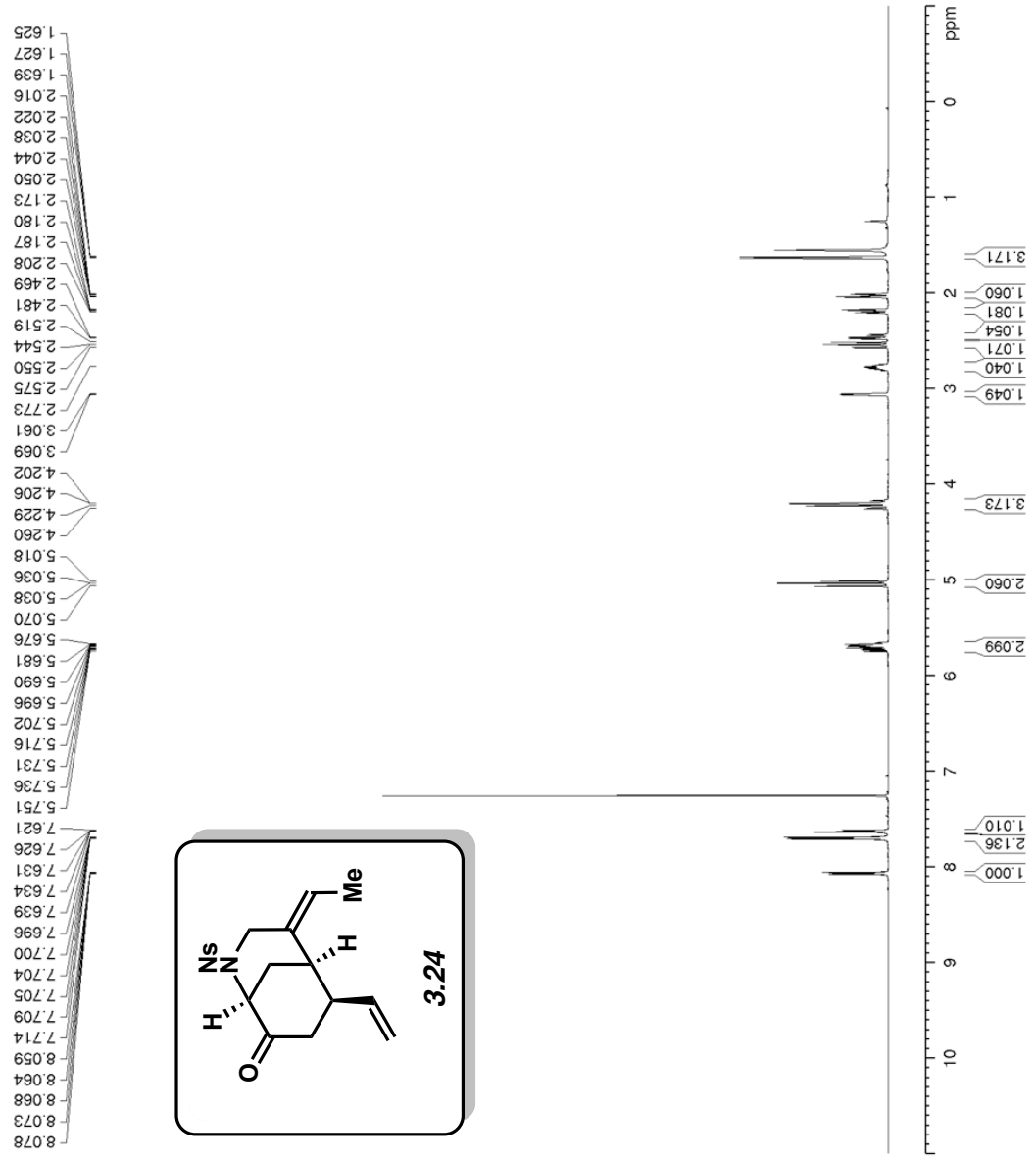


Figure A2.43 ¹H NMR (500 MHz, CDCl₃) of compound 3.24.

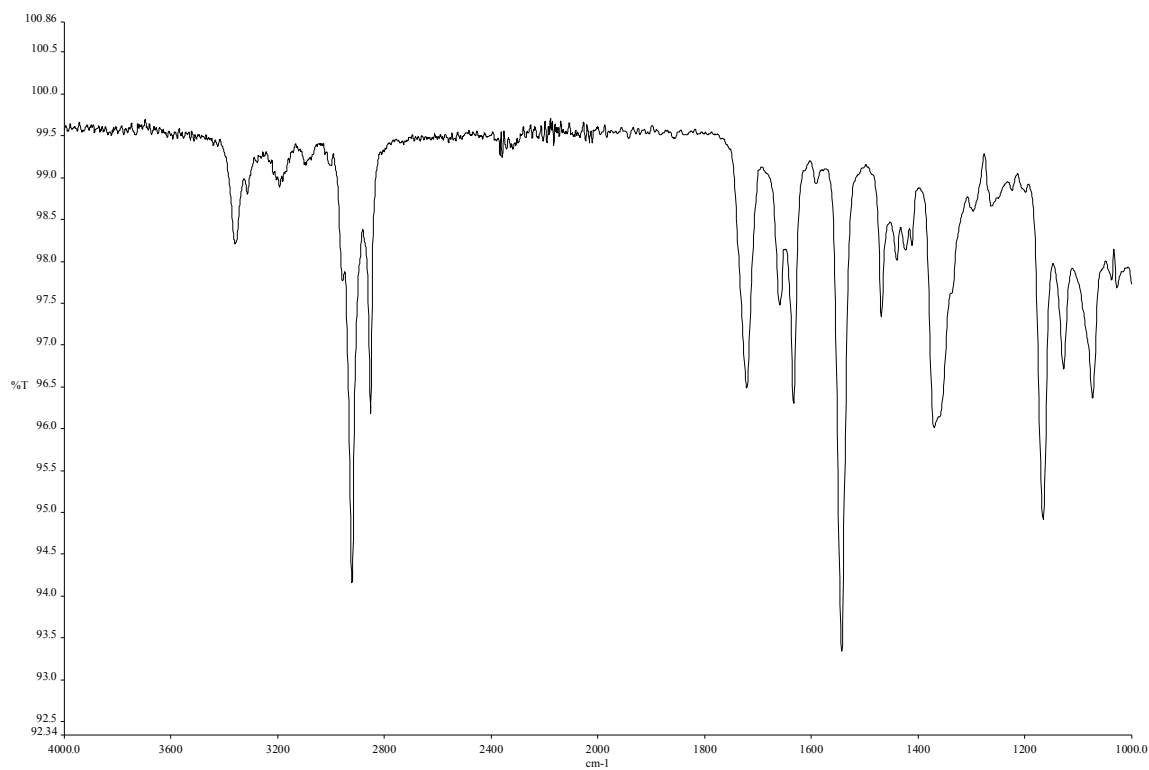


Figure A2.44 Infrared spectrum of compound 3.24.

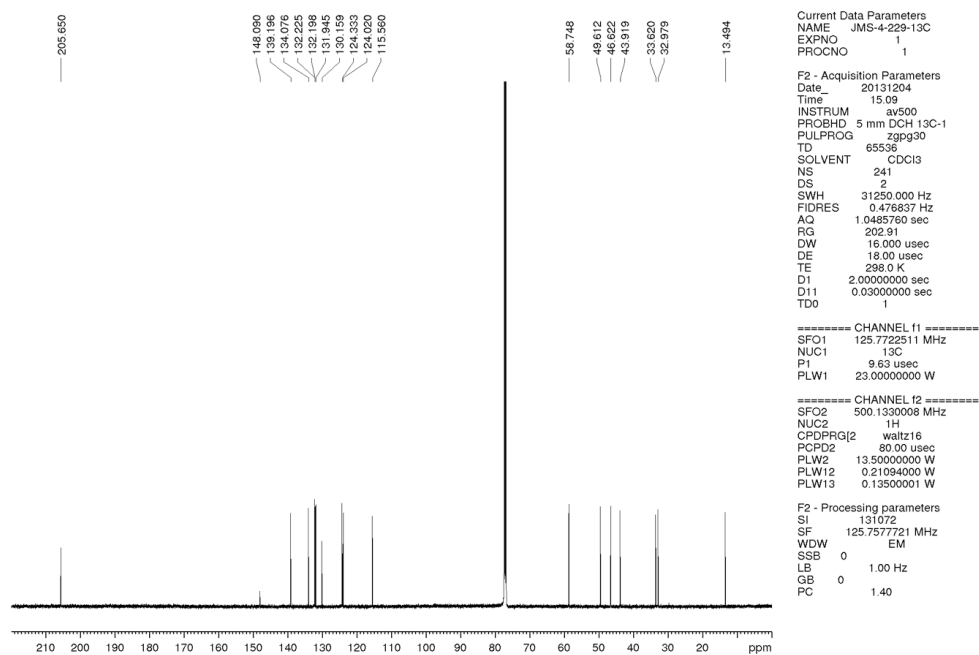


Figure A2.45 ¹³C NMR (125 MHz, CDCl₃) of compound 3.24.

```

Current Data Parameters
NAME      _JMS-4-232
EXPNO    1
PROCNO   1

F2 - Acquisition Parameters
Date_    20131206
Time     12.33
INSTRUM  av500
PROBHD   5 mm DCH 13C-1
PULPROG  zg30
TD        65536
SOLVENT  CDCl3
NS        32
DS        0
SWH       10000.000 Hz
FIDRES    0.152588 Hz
AQ        3.2767999 sec
RG        11
DW        50.000 usec
DE        10.00 usec
TE        298.0 K
D1        2.00000000 sec
TD0       1

===== CHANNEL f1 =====
SFO1     500.1330008 MHz
NUC1     1H
P1       10.00 usec
PLW1     13.50000000 W

F2 - Processing parameters
SI        65536
SF        500.1300122 MHz
WDW       EM
SSB       0
LB        0.30 Hz
GB        0
PC        1.00

```

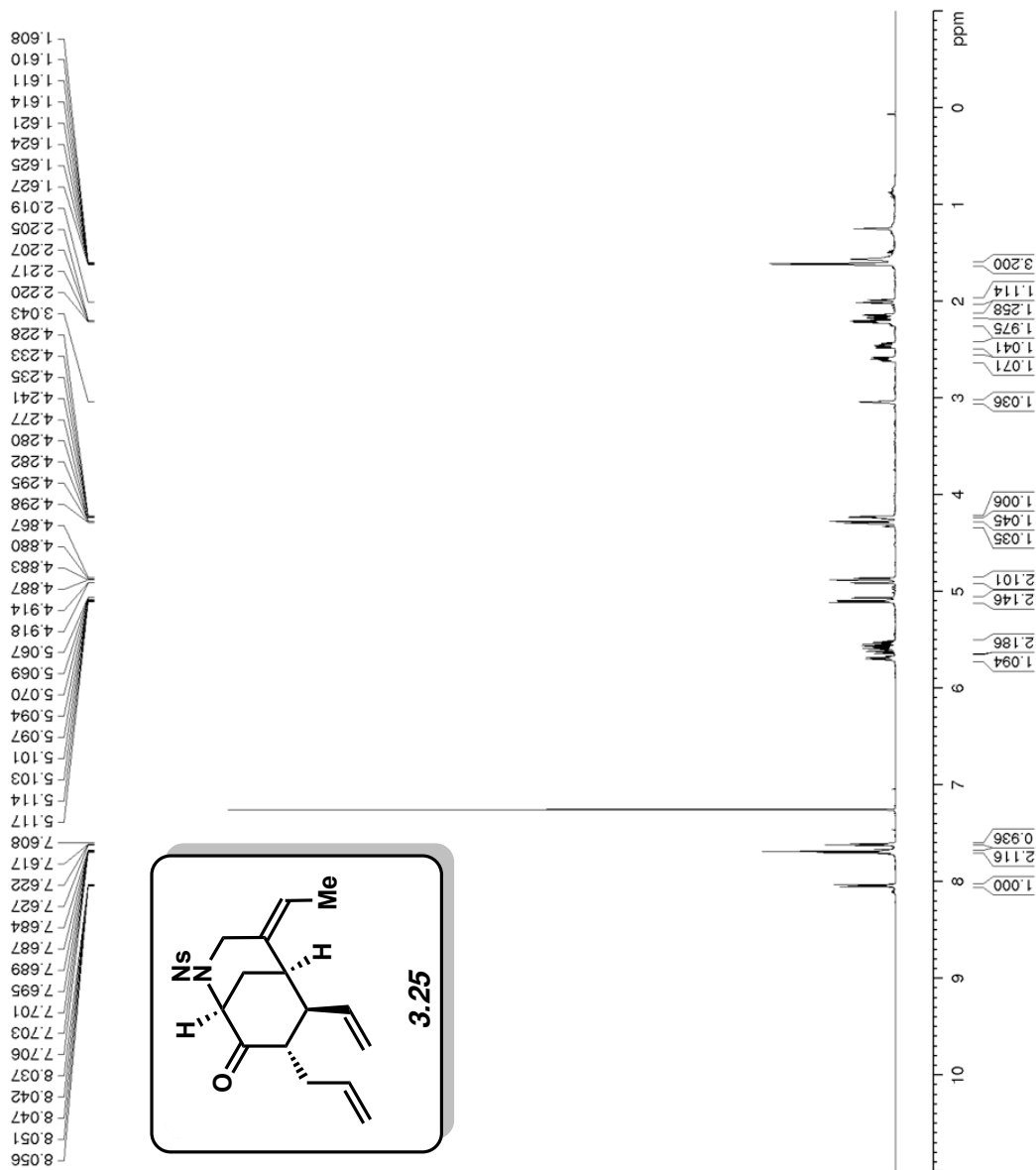


Figure A2.46 ¹H NMR (500 MHz, CDCl₃) of compound 3.25.

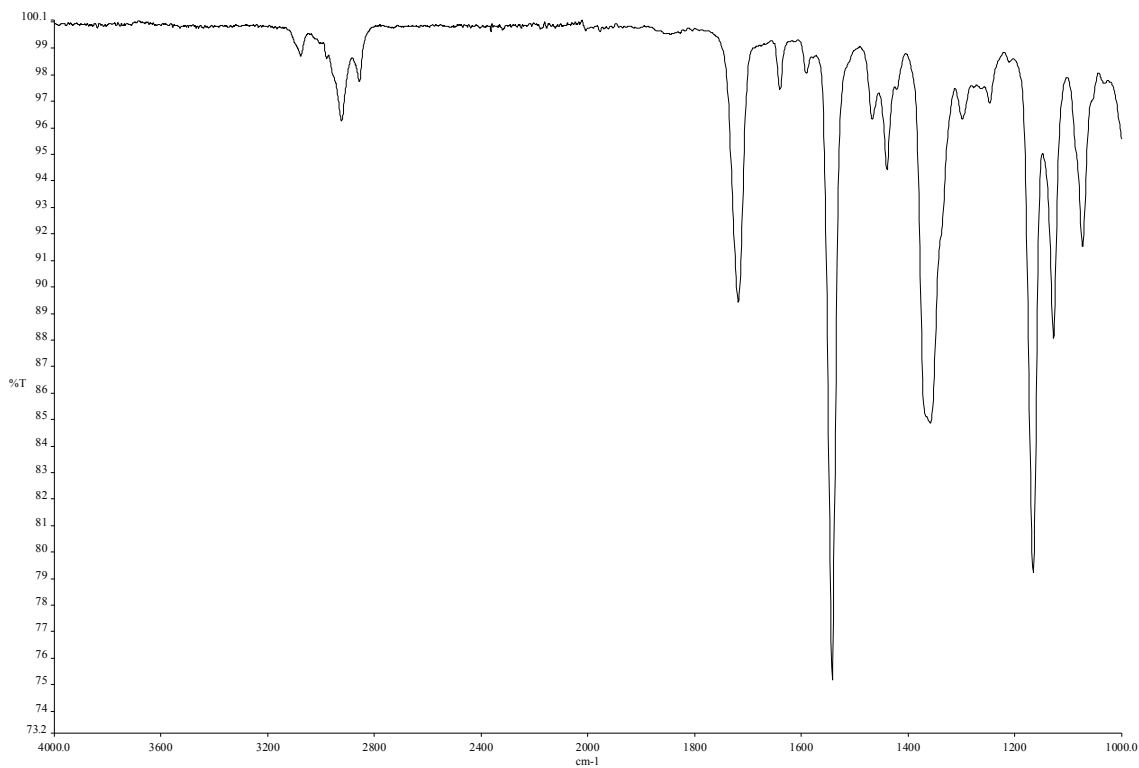


Figure A2.47 Infrared spectrum of compound 3.25.

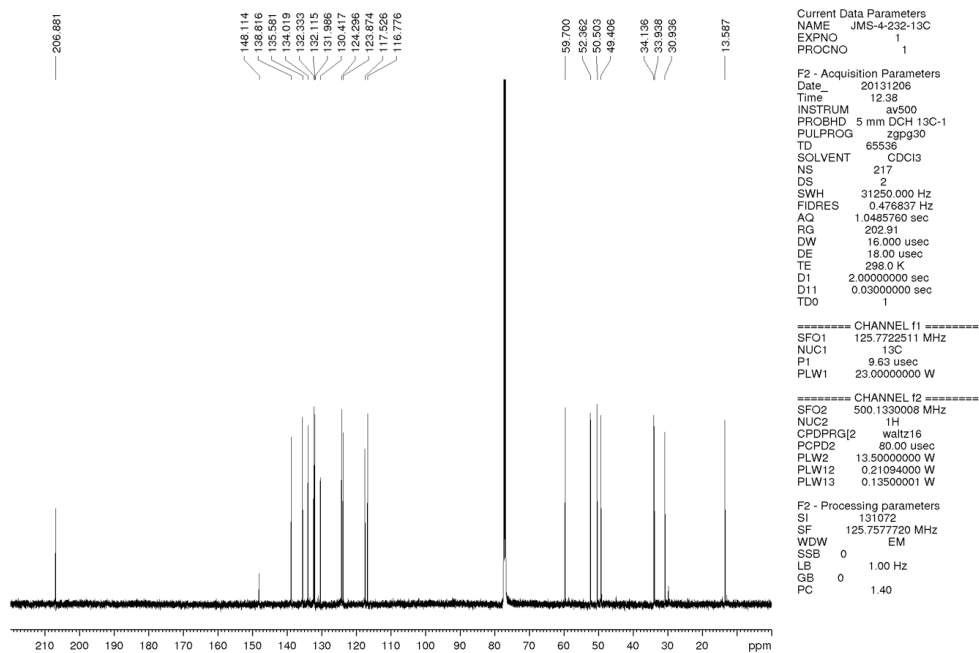


Figure A2.48 ^{13}C NMR (125 MHz, CDCl_3) of compound 3.25.

```

Current Data Parameters
NAME      JMS-4-211
EXPNO    1
PROCNO   1

F2 - Acquisition Parameters
Date_    20131113
Time     16.38
INSTRUM  av500
PROBHD   5 mm DCH 13C-1
PULPROG  zg30
TD       65536
SOLVENT  CDCI3
NS       8
DS       0
SWH      10000.000 Hz
FIDRES   0.152588 Hz
AQ       3.2767999 sec
RG       11
DW       50.000 usec
DE       10.00 usec
TE       298.0 K
D1       2.0000000 sec
TD0      1

===== CHANNEL f1 =====
SFO1    500.1330008 MHz
NUC1    1H
P1      10.00 usec
PLW1    13.5000000 W

F2 - Processing parameters
SI      65536
SF      500.1300120 MHz
WDW     EM
SSB     0
LB      0.30 Hz
GB      0
PC      1.00

```

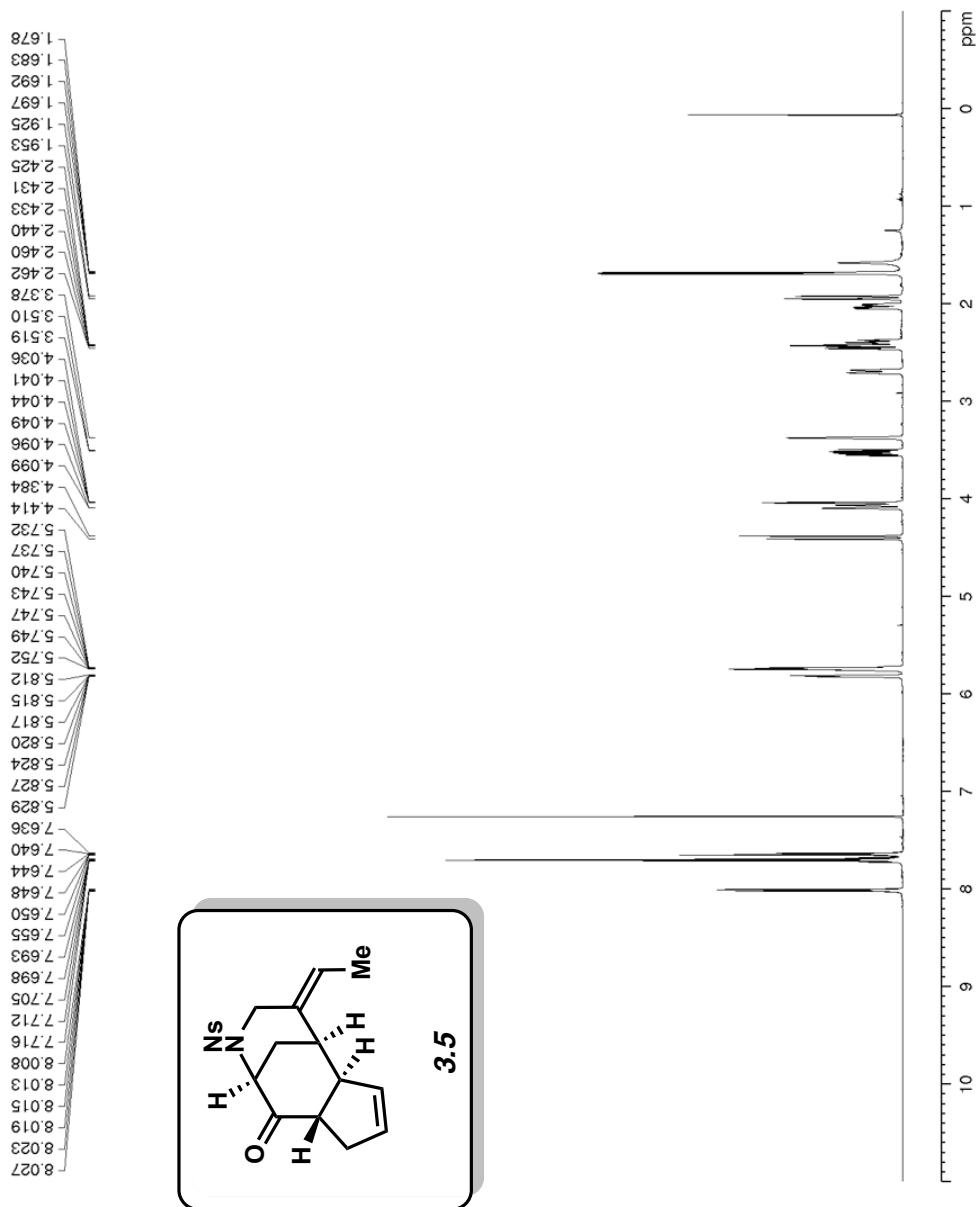


Figure A2.49 ¹H NMR (500 MHz, CDCl₃) of compound 3.5.

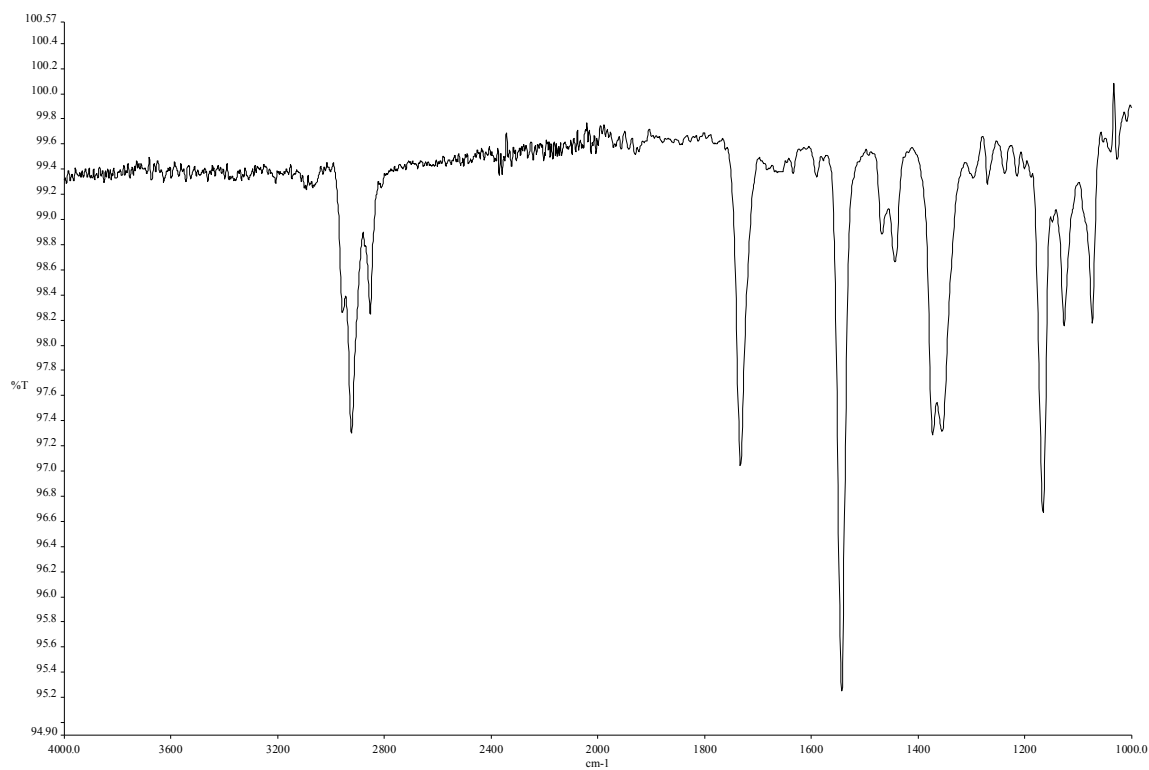


Figure A2.50 Infrared spectrum of compound **3.5**.

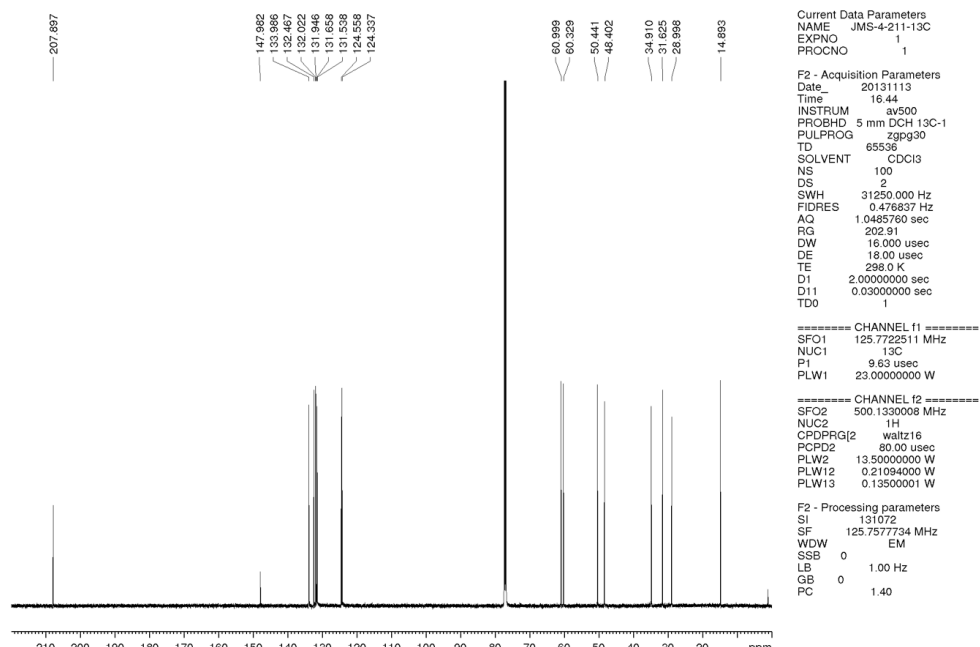


Figure A2.51 ^{13}C NMR (125 MHz, CDCl_3) of compound **3.5**.

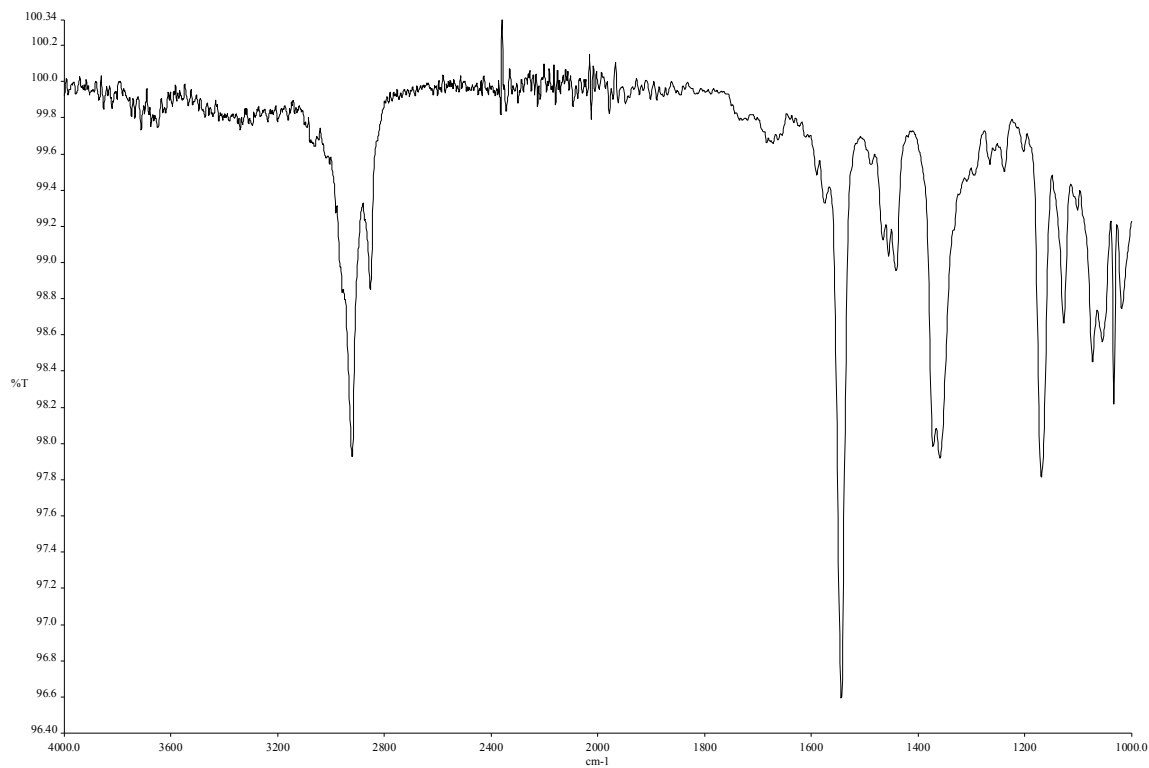


Figure A2.53 Infrared spectrum of compound **3.3**.

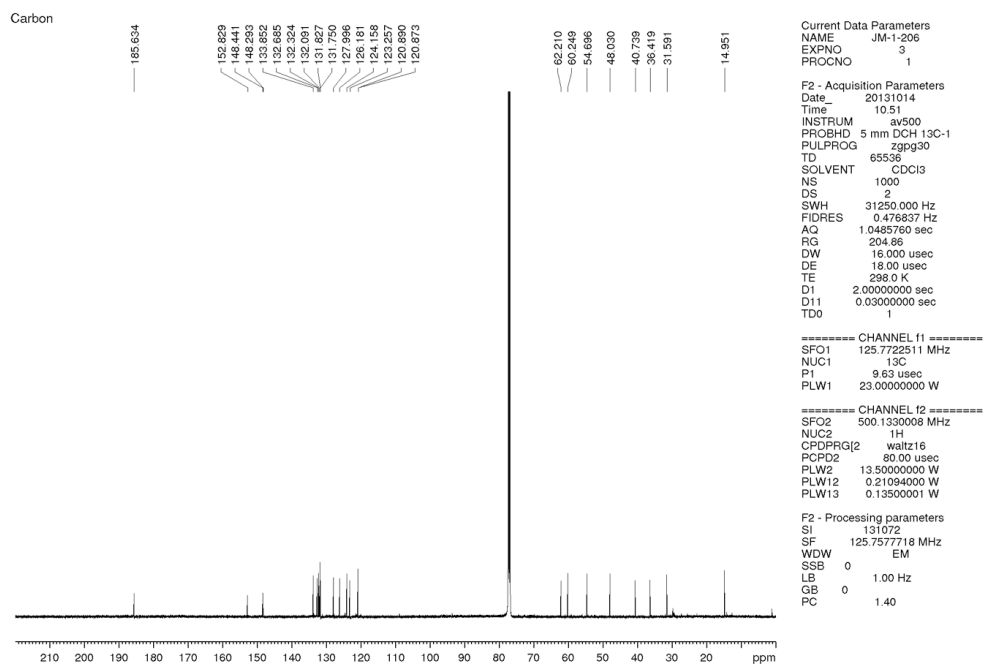


Figure A2.54 ^{13}C NMR (125 MHz, CDCl_3) of compound **3.3**.

```

Current Data Parameters
NAME      JM-1-208
EXPNO     2
PROCNO    1

F2 - Acquisition Parameters
Date_     20131119
Time      19:48
INSTRUM   av500
PROBHD    5 mm DCH 13C-1
PULPROG   zg30
TD         65536
SOLVENT   CDCl3
NS         33
DS         0
SWH        10000.000 Hz
FIDRES     0.152588 Hz
AQ         3.2767999 sec
RG         12.14
DW         50.000 usec
DE         10.00 usec
TE         298.0 K
D1         2.0000000 sec
TD0        1

===== CHANNEL f1 =====
SFO1      500.130008 MHz
NUC1       1H
P1         10.00 usec
PLW1      13.50000000 W

F2 - Processing parameters
SI         65536
SF         500.1300120 MHz
WDW        EM
SSB        0
LB         0.30 Hz
GB         0
PC         1.00

```

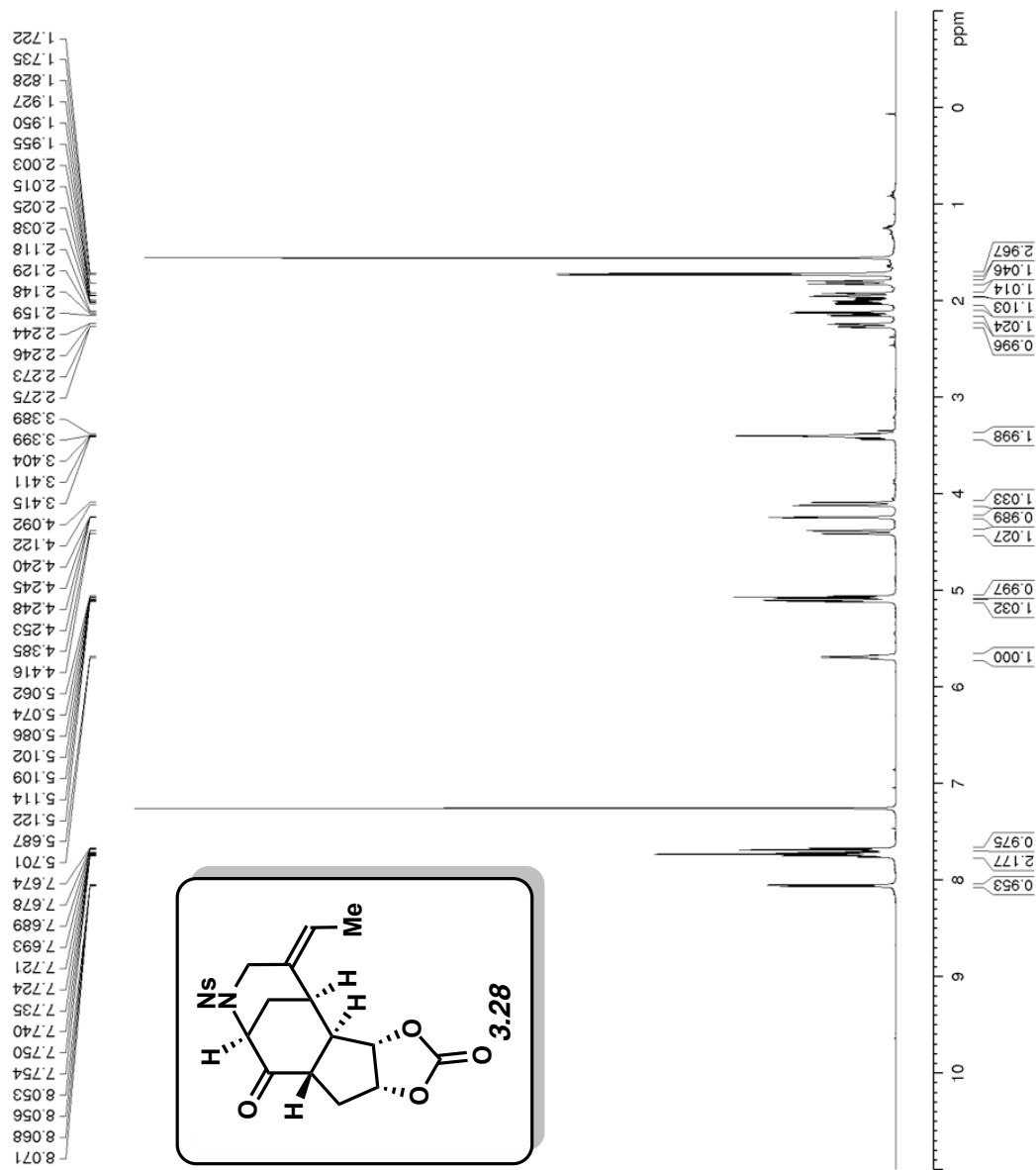


Figure A2.55 ¹H NMR (500 MHz, CDCl₃) of compound 3.28.

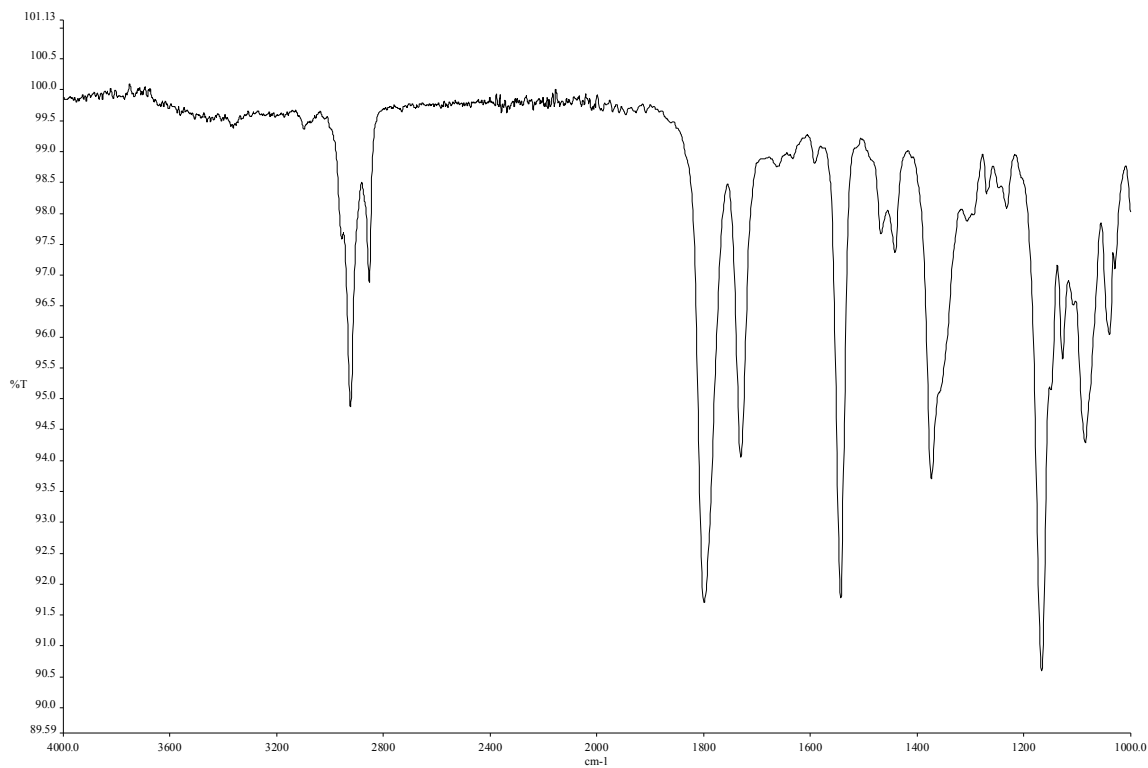


Figure A2.56 Infrared spectrum of compound **3.28**.

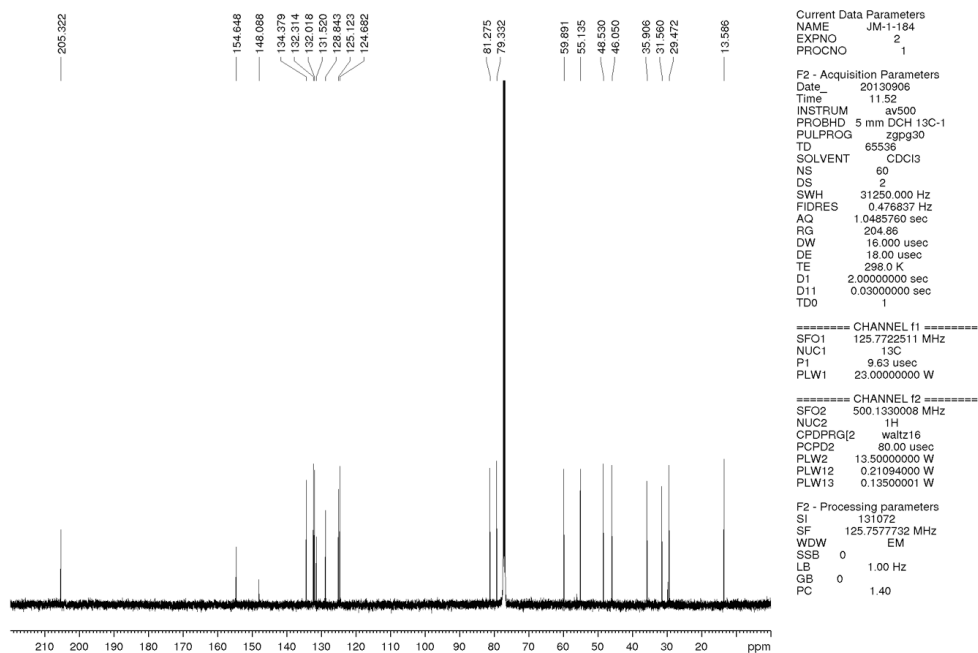


Figure A2.57 ¹³C NMR (125 MHz, CDCl₃) of compound **3.28**.

```

Current Data Parameters
NAME      JM-1-214
EXPNO     4
PROCNO    1

F2 - Acquisition Parameters
Date_     20131122
Time      9.33
INSTRUM   av500
PROBHD    5 mm DCH 13C-1
PULPROG   zg30
TD         65536
SOLVENT   C6D6
NS         24
DS         0
SWH        10000.000 Hz
FIDRES     0.152568 Hz
AQ         3.2767999 sec
RG         12.14
DW         50.000 usec
DE         10.00 usec
TE         296.0 K
D1         2.00000000 sec
TD0        1

===== CHANNEL f1 =====
SFO1      500.1330008 MHz
NUC1       1H
P1         10.00 usec
PLW1      13.50000000 W

F2 - Processing parameters
SI         65536
SF         500.1299960 MHz
WDW        EMI
SSB        0
LB         0.30 Hz
GB         0
PC         1.00

```

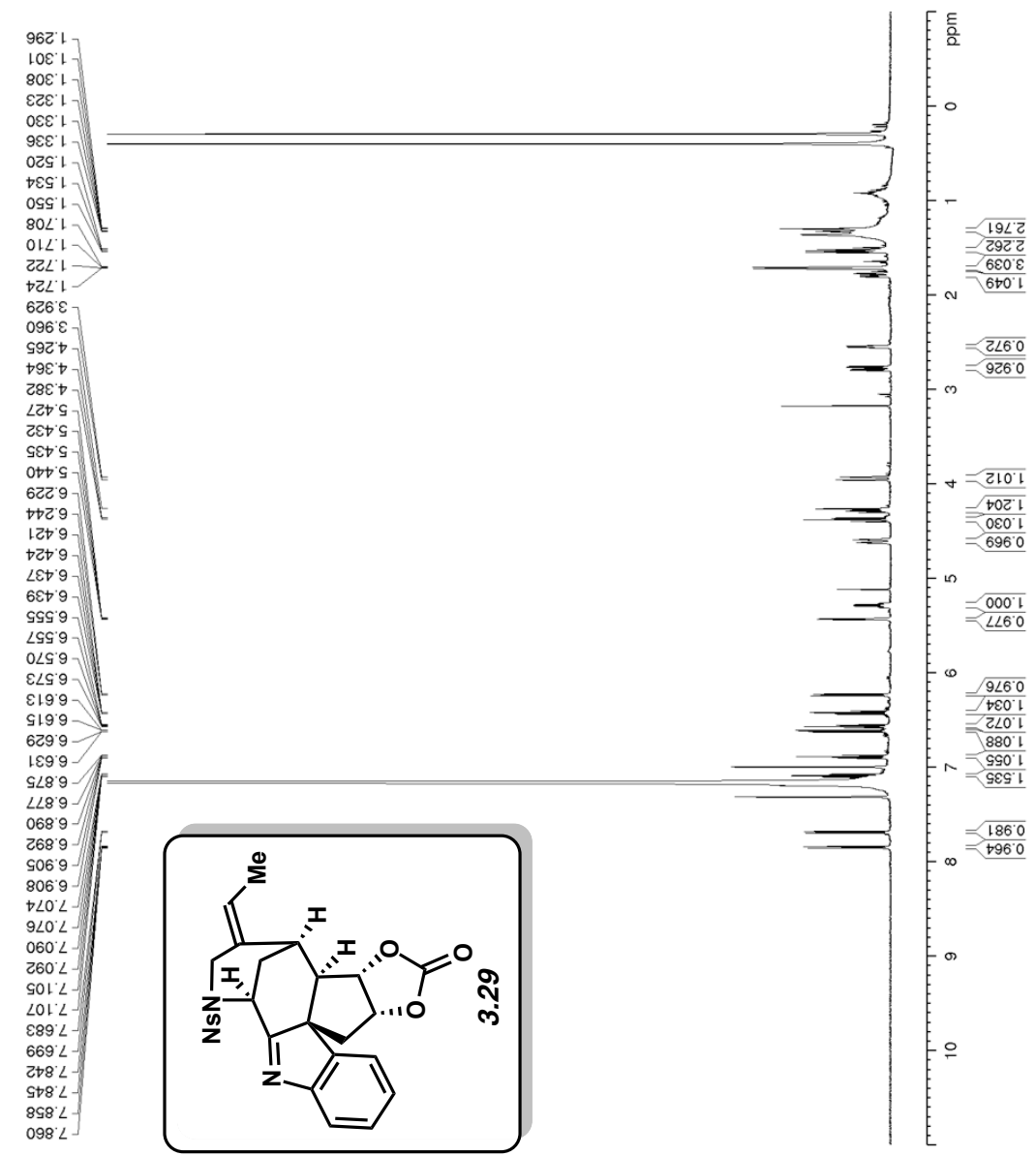


Figure A2.58 ¹H NMR (500 MHz, CDCl₃) of compound 3.29.

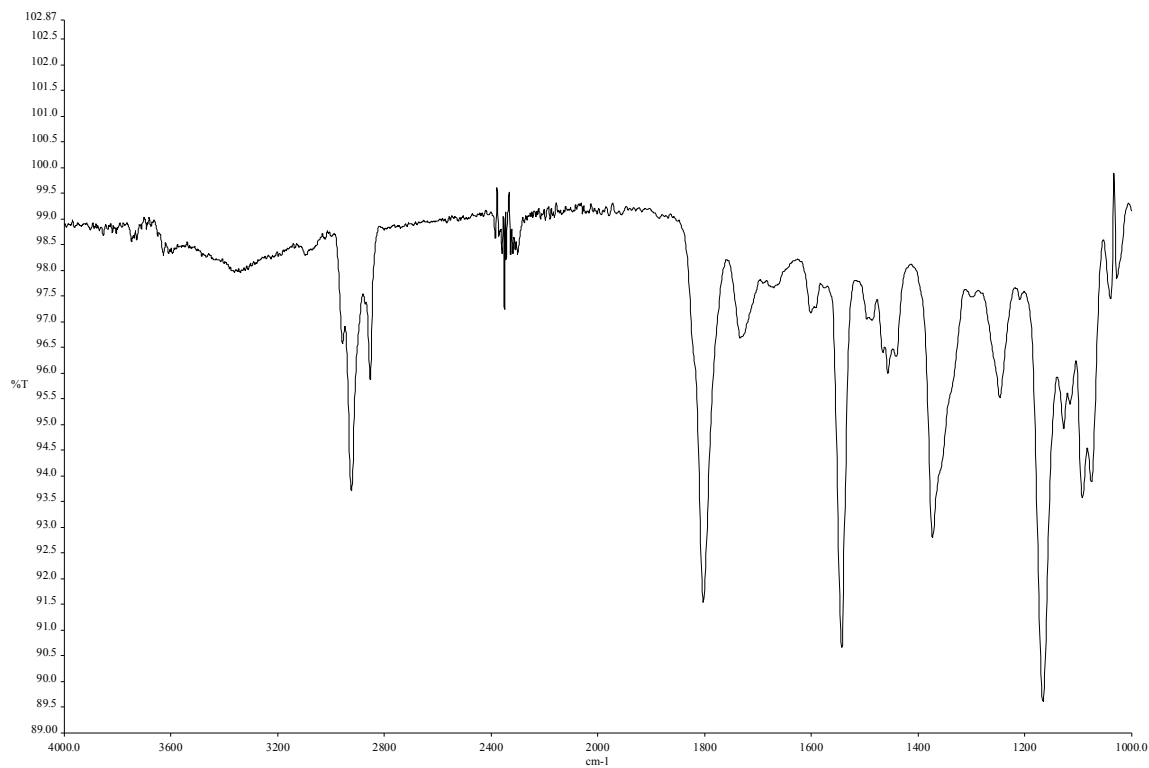


Figure A2.59 Infrared spectrum of compound **3.29**.

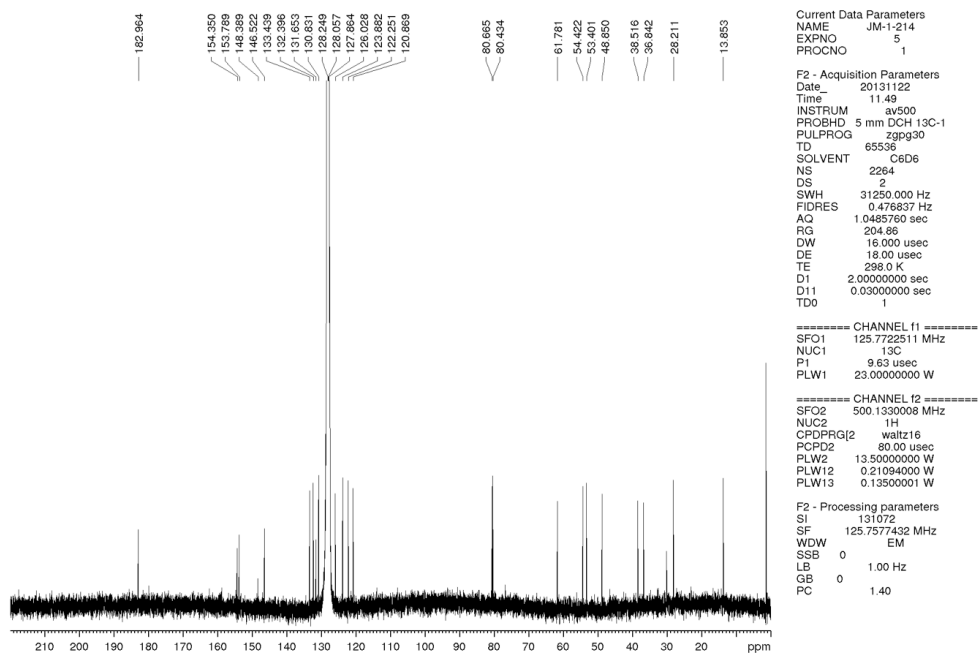


Figure A2.60 ^{13}C NMR (125 MHz, CDCl_3) of compound **3.29**.

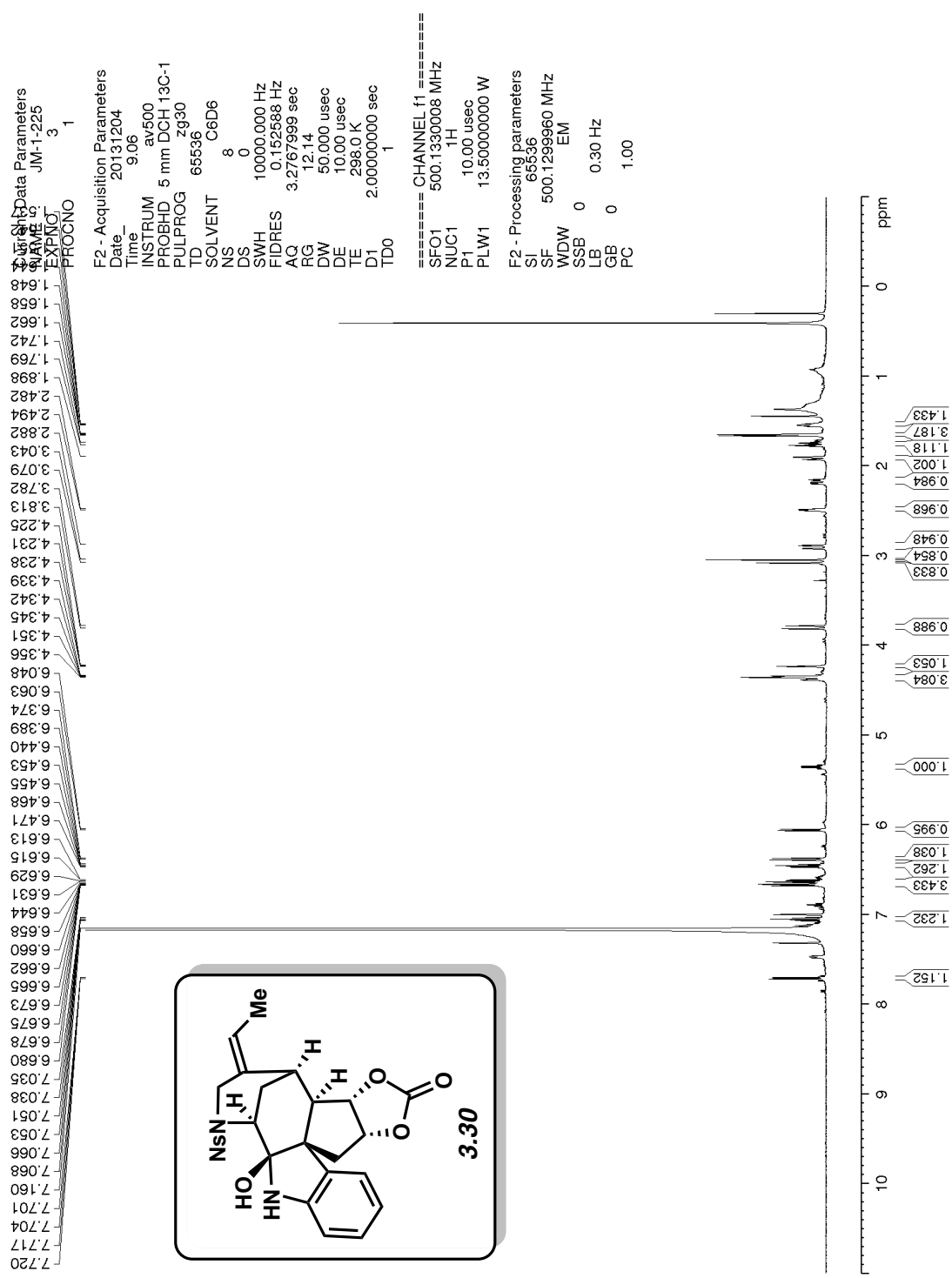


Figure A2.61 ¹H NMR (500 MHz, CDCl₃) of compound **3.30**.

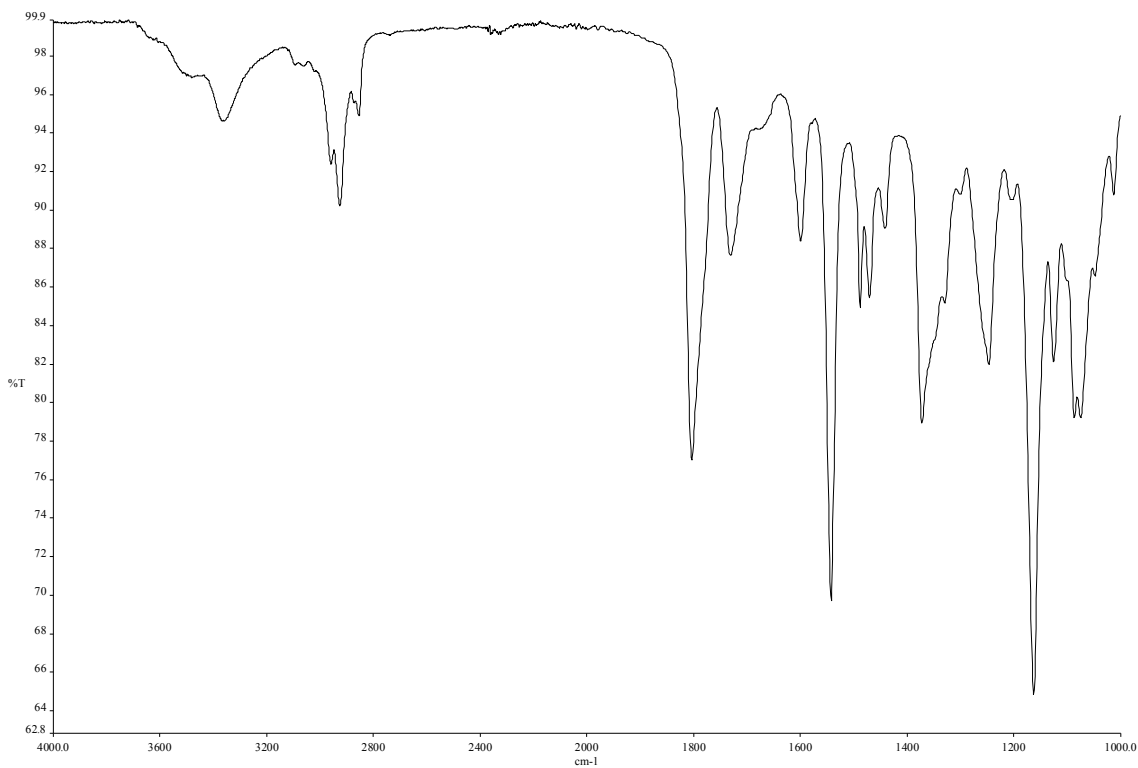


Figure A2.62 Infrared spectrum of compound **3.30**.

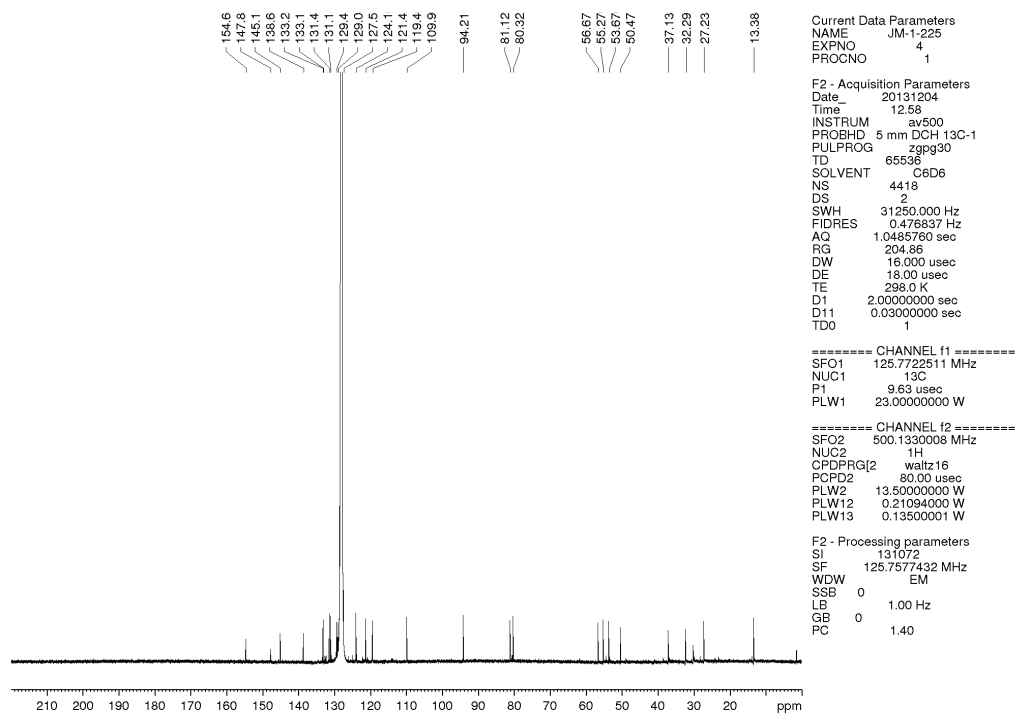


Figure A2.63 ^{13}C NMR (125 MHz, CDCl_3) of compound **3.30**.

```

Current Data Parameters
NAME      JM-1-218
EXPNO     2
PROCNO    1

F2 - Acquisition Parameters
Date_     20131126
Time      9.31
INSTRUM   av500
PROBHD    5 mm DCH 13C-1
PULPROG   zg30
TD         65536
SOLVENT   C6D6
NS         48
DS         0
SWH        10000.000 Hz
FIDRES     0.152568 Hz
AQ         3.2767999 sec
RG         21.36
DW         50.000 usec
DE         10.00 usec
TE         296.0 K
D1         2.00000000 sec
TD0        1

===== CHANNEL f1 =====
SFO1      500.1330008 MHz
NUC1       1H
P1         10.00 usec
PLW1      13.50000000 W

F2 - Processing parameters
SI         65536
SF         500.1299956 MHz
WDW        EMI
SSB        0
LB         0.30 Hz
GB         0
PC         1.00

```

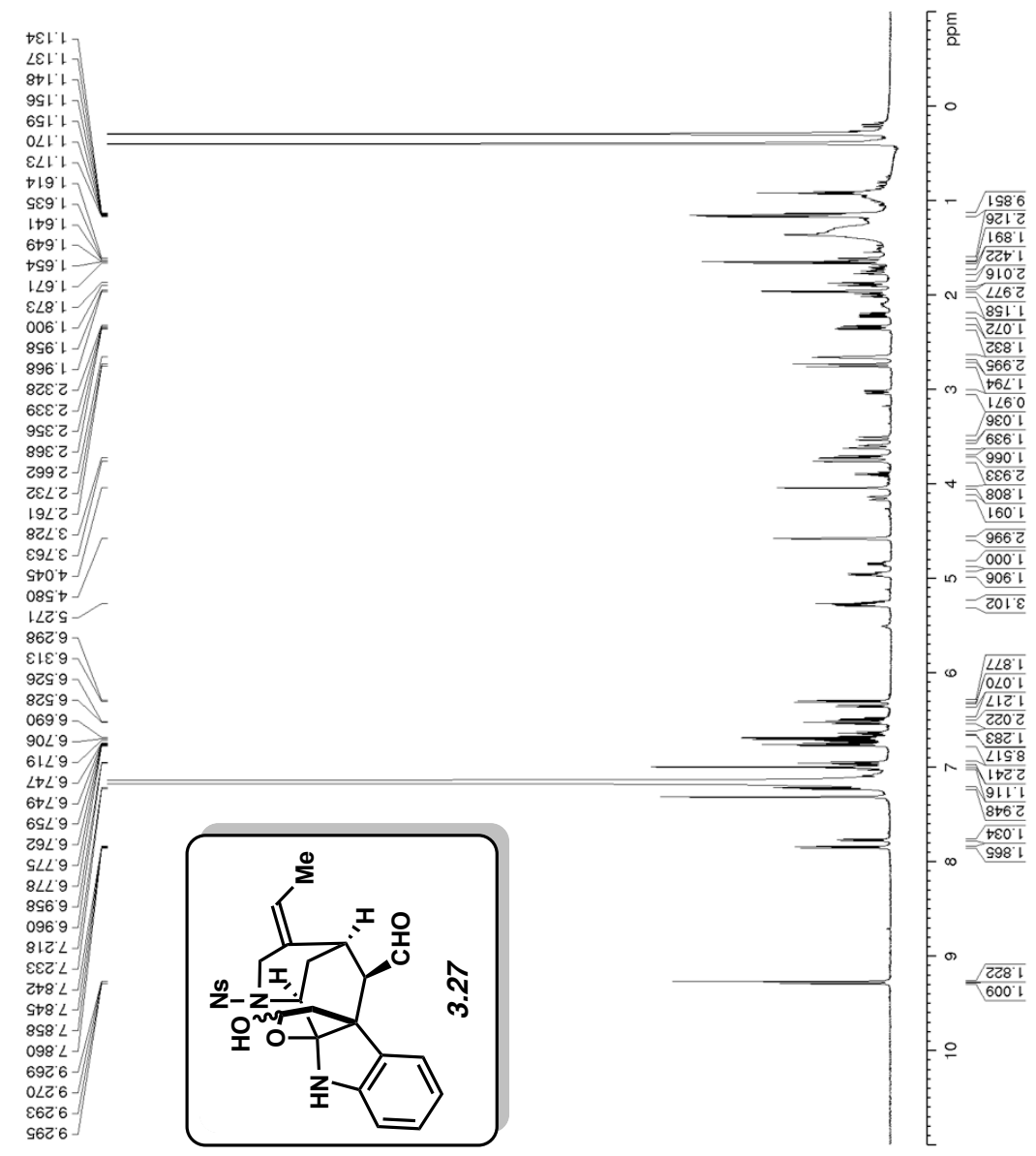


Figure A2.64 ¹H NMR (500 MHz, CDCl₃) of compound 3.27.

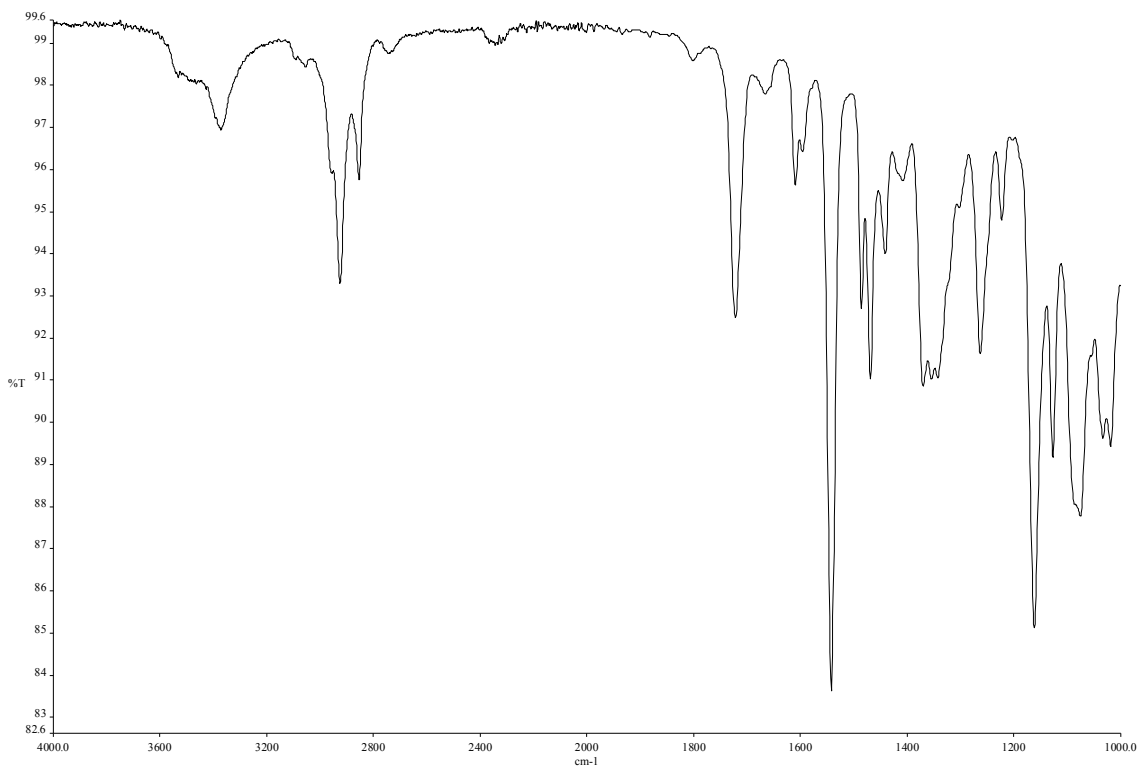


Figure A2.65 Infrared spectrum of compound **3.27**.

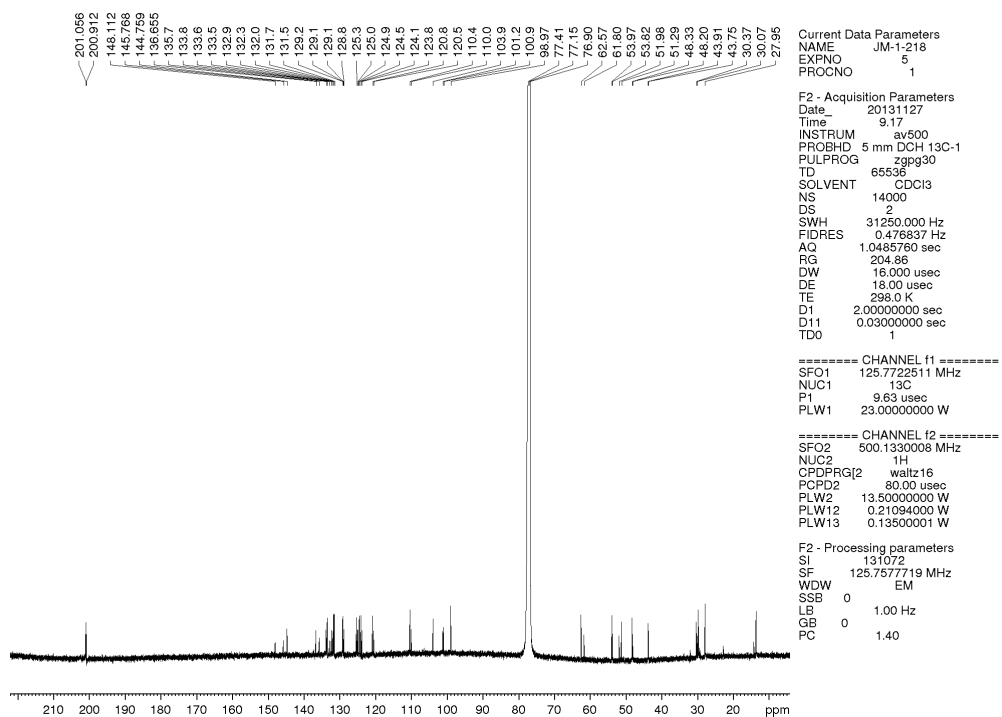


Figure A2.66 ¹³C NMR (125 MHz, CDCl₃) of compound **3.27**.

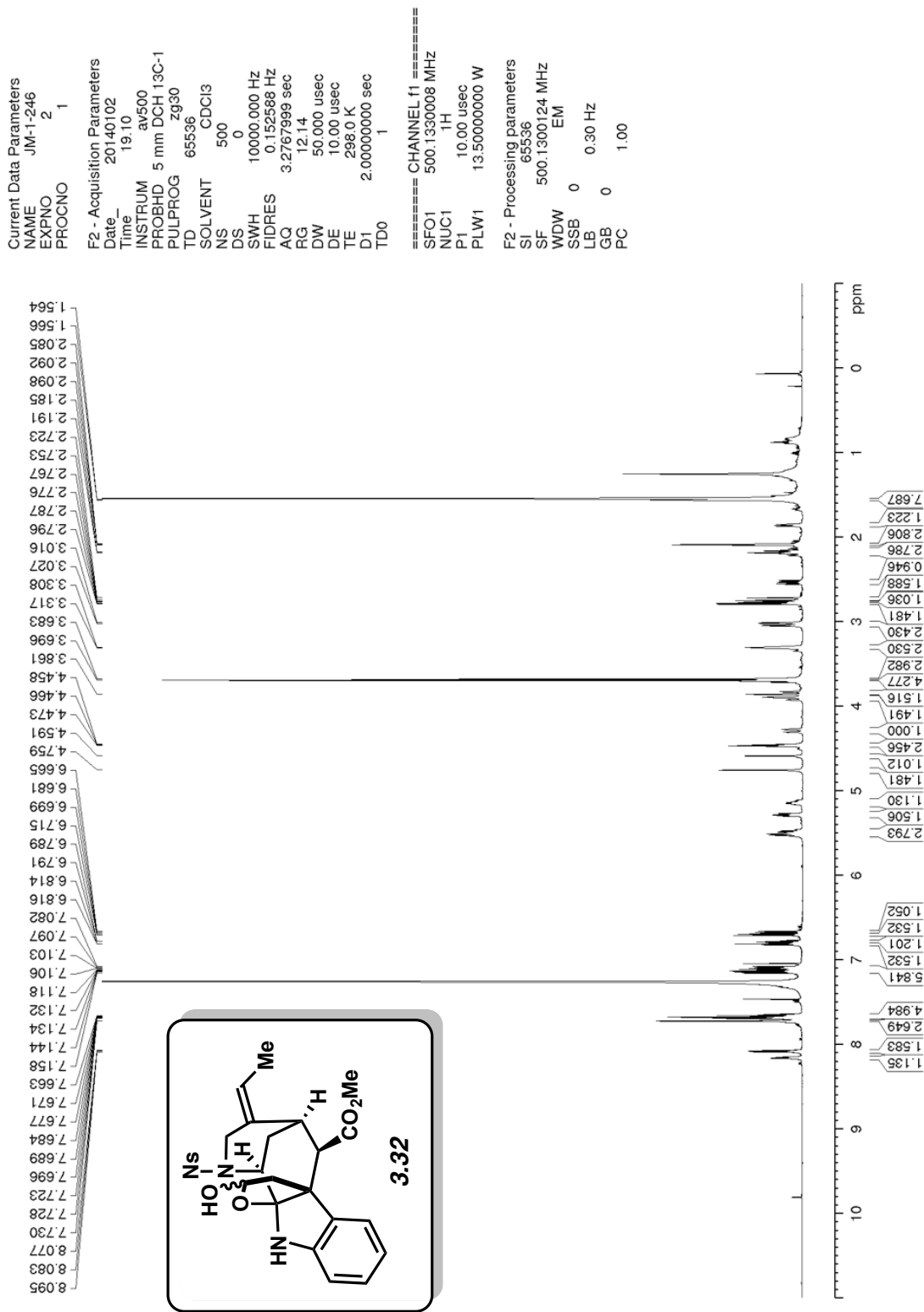


Figure A2.67 ¹H NMR (500 MHz, CDCl₃) of compound 3.32.

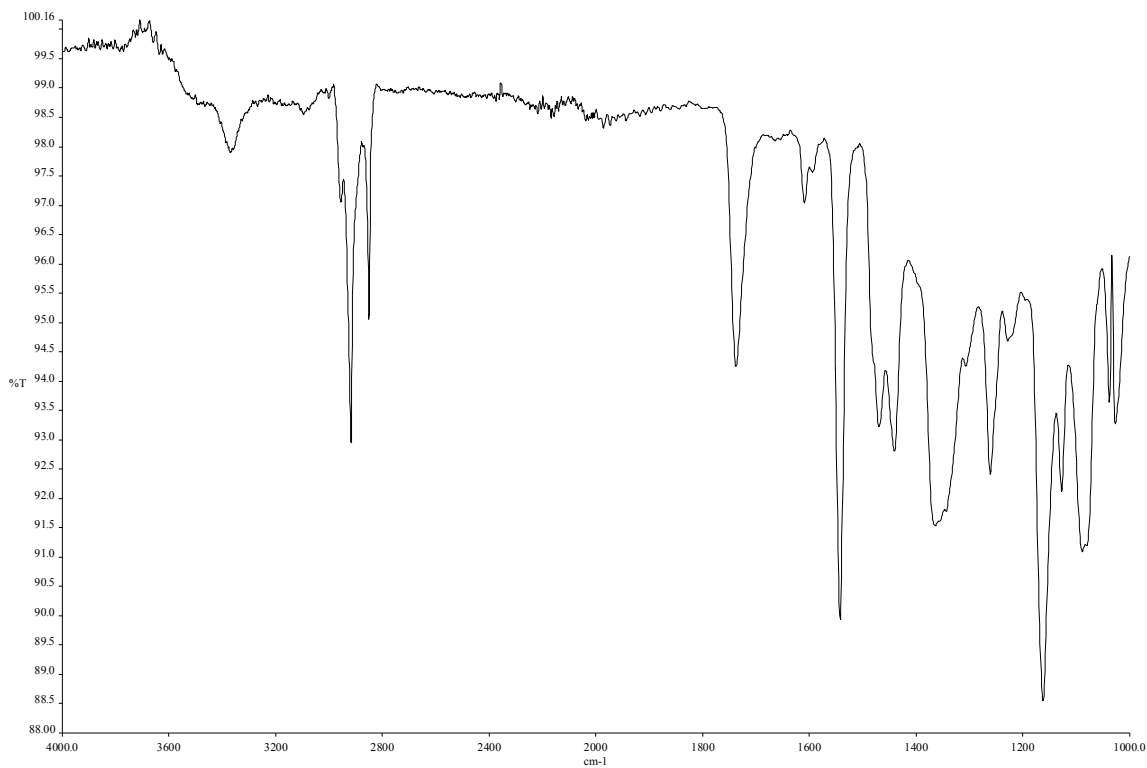


Figure A2.68 Infrared spectrum of compound 3.32.

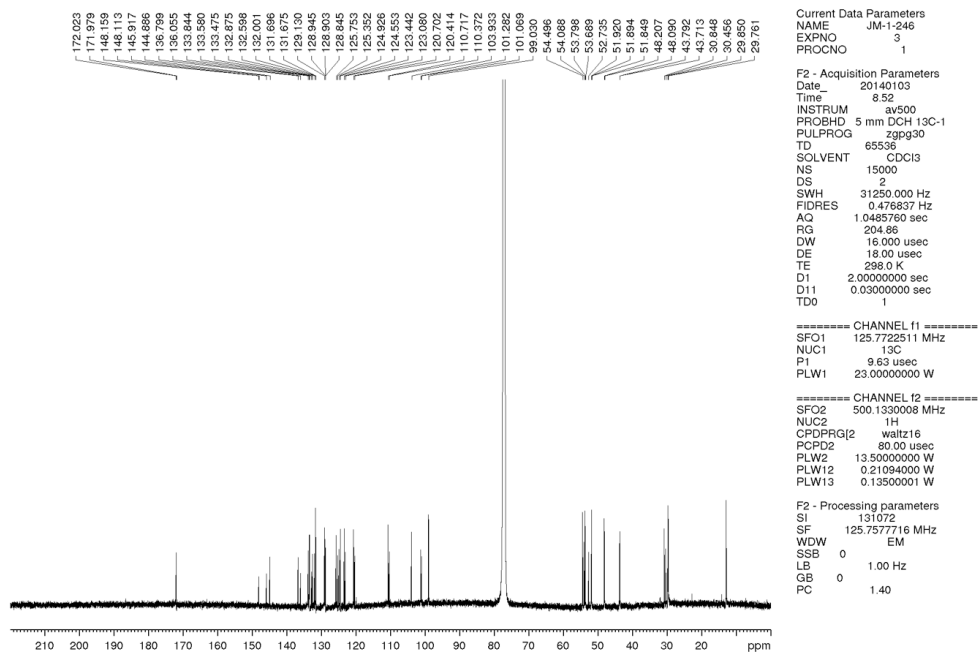


Figure A2.69 ^{13}C NMR (125 MHz, CDCl_3) of compound 3.32.

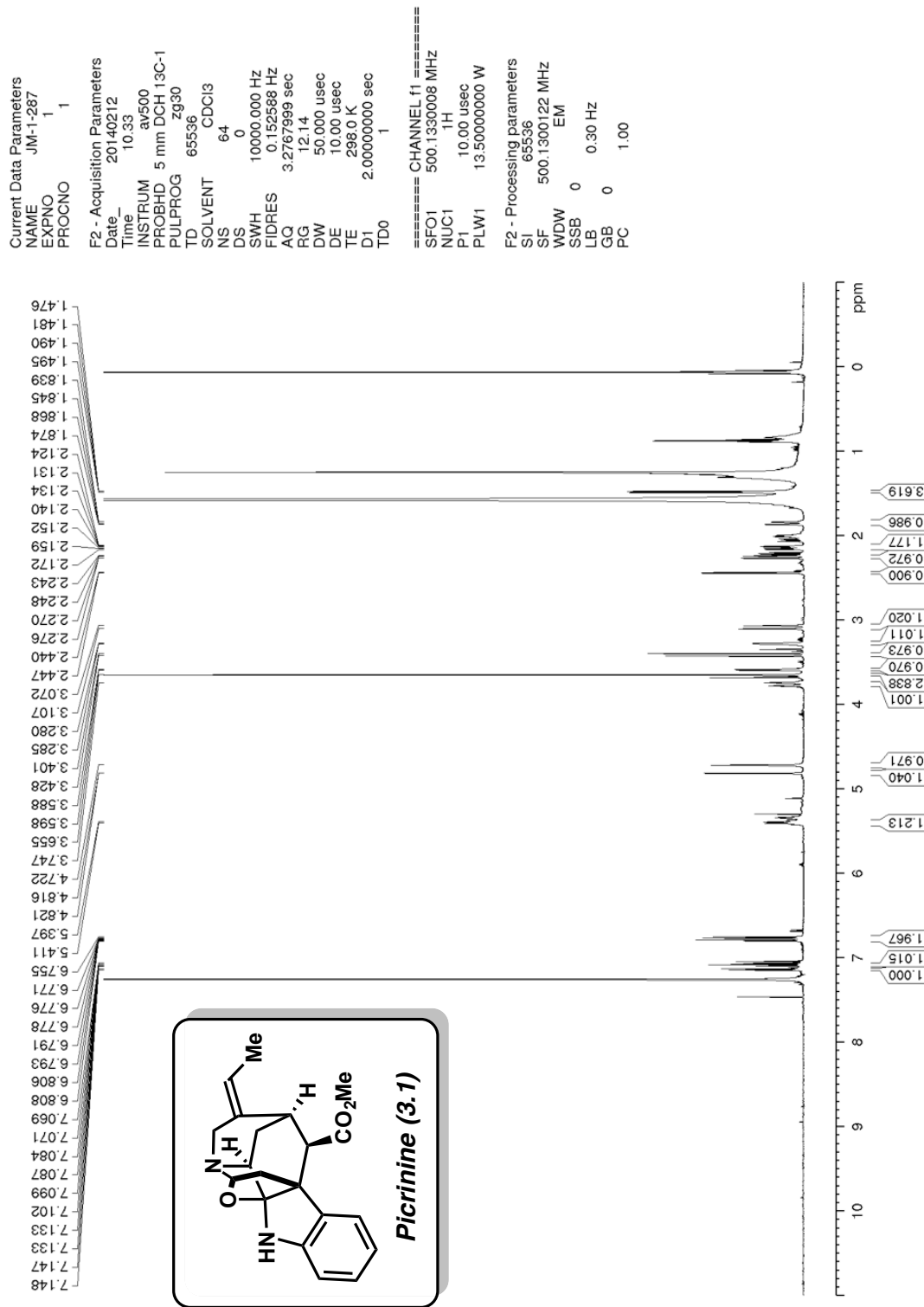


Figure A2.70 ¹H NMR (500 MHz, CDCl₃) of compound 3.1.

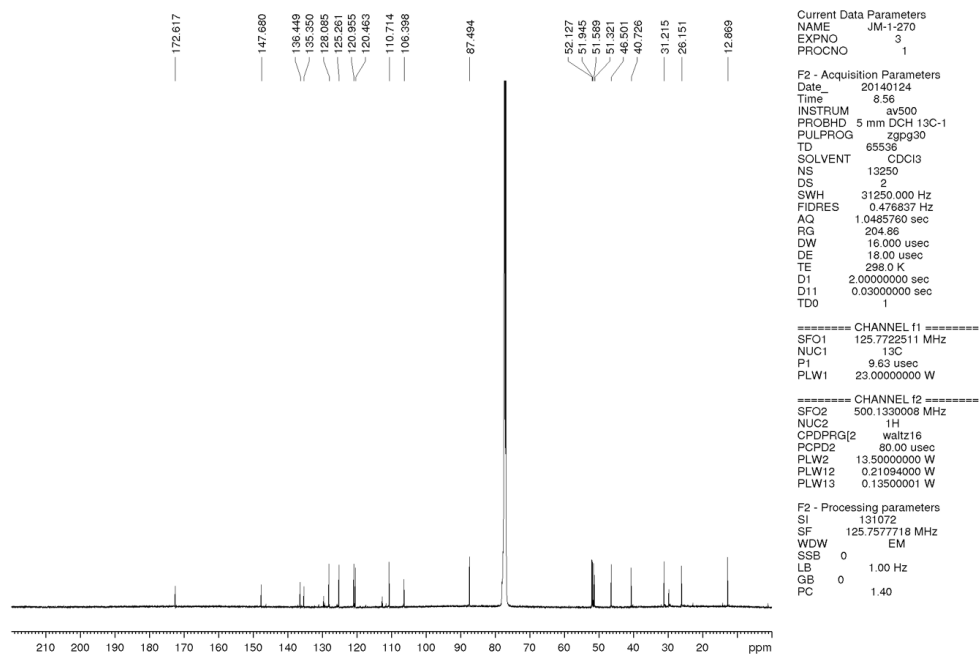


Figure A2.71 ¹³C NMR (125 MHz, CDCl₃) of compound **3.1**.

CHAPTER FOUR

Unified and Enantioselective Approach to the Akuammiline Alkaloids

4.1 Abstract

The akuammiline alkaloids are a family of natural products with a rich diversity of structural features. Although there have been many synthetic efforts toward the akuammilines, a central approach to their construction that hinges on synthetic divergence has not been disclosed. This chapter describes initial studies towards the development of a unified route to access the various akuammiline scaffolds. A key component of the approach is the use of the interrupted Fischer indolization as a fulcrum for overall synthetic unity. Additionally, an asymmetric route to the key [3.3.1]-azabicyclic akuammiline alkaloid core is demonstrated, which constitutes a formal enantioselective synthesis of several alkaloids.

4.2 Introduction

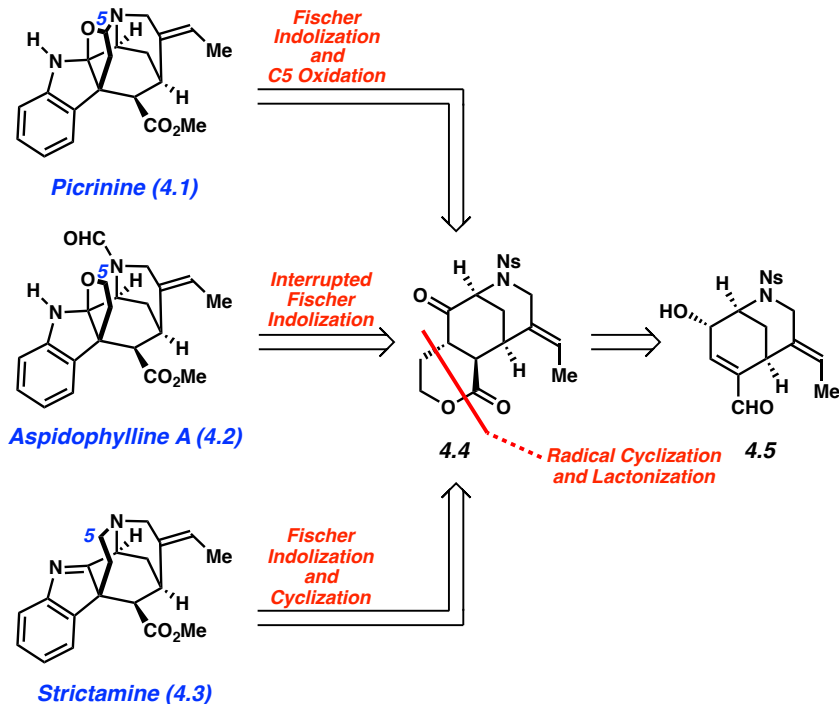
Akuammiline alkaloids, although intricate in their diverse structures, share a unifying biosynthetic origin (see Chapter 1).¹ Most members vary in their functionality or oxidation state at C5 (Figure 1), which is hypothesized to emerge late in their divergent biosynthetic pathway(s). Largely inspired by this phenomenon, we undertook the challenge of creating a parallel synthetic strategy that would serve as a platform to access several akuammiline scaffolds from a common intermediate.² Additionally, we were interested in rendering our synthetic approach asymmetric

in order to access these alkaloids in enantioenriched form. In this Chapter, an initial synthetic foray into a divergent strategy to the akuammiline alkaloids is described, along with a successful asymmetric route to the [3.3.1]-azabicyclic akuammiline framework.

4.3 Unified Route to the Akuammiline Alkaloids

The retrosynthetic analysis for our unified and divergent approach is depicted in Figure 1. It was envisioned that picrinine (**4.1**), aspidophylline A (**4.2**), and strictamine (**4.3**) could all be accessed from tricyclic lactone **4.4** through slightly differing pathways. First, picrinine (**4.1**) would arise from a Fischer indolization of lactone **4.4** and subsequent late-stage C5 oxidation. An interrupted Fischer indolization utilizing lactone **4.4** would allow access to the framework of aspidophylline A (**4.2**), and strictamine (**4.3**) would result from a strategic late-stage alkylation event at C5 to forge its methanoquinolizidine scaffold.³ Lactone **4.4**, the lynchpin intermediate for the divergent synthetic pathways, would be derived from enal **4.5** through a radical cyclization and lactonization strategy. Enal **4.5** would serve as a starting point for this endeavor, as it had been accessed in multigram scale in our successful synthesis of picrinine (**4.1**) (*vide supra*).⁴

Figure 4.1 Unified retrosynthetic strategy of akuammilines **4.1–4.3**.

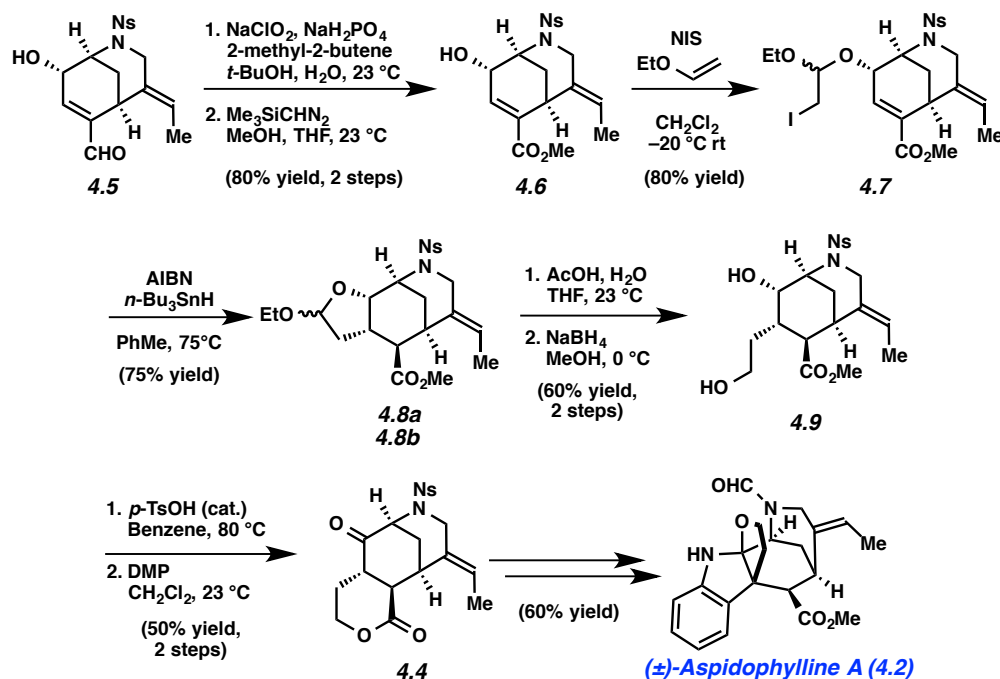


As a first goal, we aimed to access lactone **4.4** from enal **4.5**, and subsequently achieve a second-generation total synthesis of aspidophylline A (Scheme 1). Initial transformation of **4.5** to enoate **4.6** was achieved by Pinnick oxidation and subsequent methylation.⁴ Treatment of this enoate (**4.6**) with ethyl vinyl ether in the presence of *N*-iodosuccinimide (NIS) oxidatively forged iodide **4.7** in 80% yield as an equal mixture of diastereomers. Subjecting of this iodide (**4.7**) to Bu_3SnH and azobis(isobutyronitrile) (AIBN) promoted Ueno-Stork radical cyclization to afford mixed acetals **4.8a** and **4.8b** in 75% yield.⁵ Notably, this reaction proceeded with complete diastereoselectivity with regard to the two newly formed stereogenic centers. Mixed acetals **4.8a** and **4.8b** were then converted to diol **4.9** by acid-promoted hydrolysis and reduction with sodium

borohydride. Heating diol **4.9** in the presence of *p*-toluenesulfonic acid catalyzed lactone formation, and subsequent oxidation of the secondary alcohol gave the desired lactone **4.4**, the desired Fischer indolization substrate, in modest yield over 2 steps. Lactone **4.4** was then elaborated by my coworker Jesus Moreno to aspidophylline A (**4.2**), in a similar fashion to our laboratory's previously reported route.^{3,6}

This synthetic route to lactone **4.4** provides a scalable entryway to the akuammiline alkaloids through the divergent synthetic approach described above. Moreover, this effort marked a second-generation synthetic route to aspidophylline A (**4.2**), which proceeds in 16 steps from readily available starting materials.

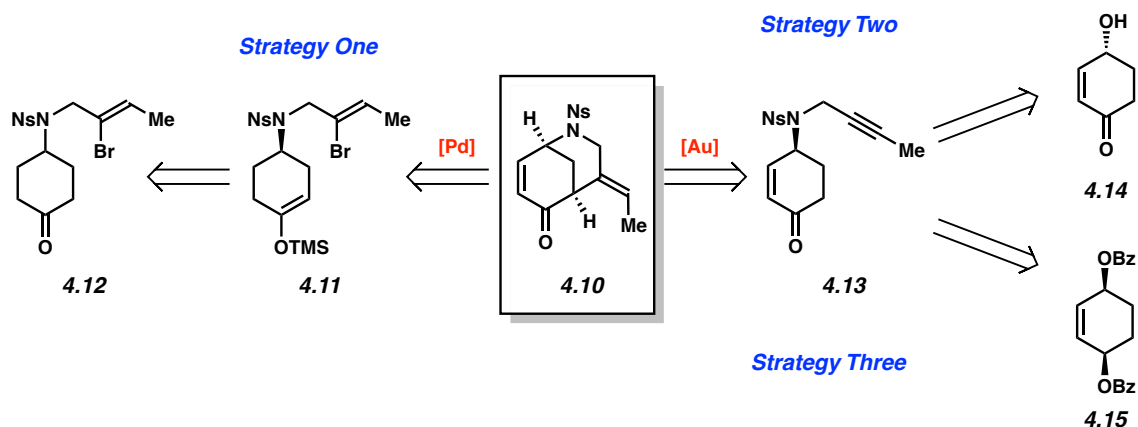
Scheme 4.1 Synthesis of lactone **4.4** from enal **4.5** and elaboration to aspidophylline A (**4.2**).



4.4 Enantioselective Approach to the Akuammiline Alkaloids

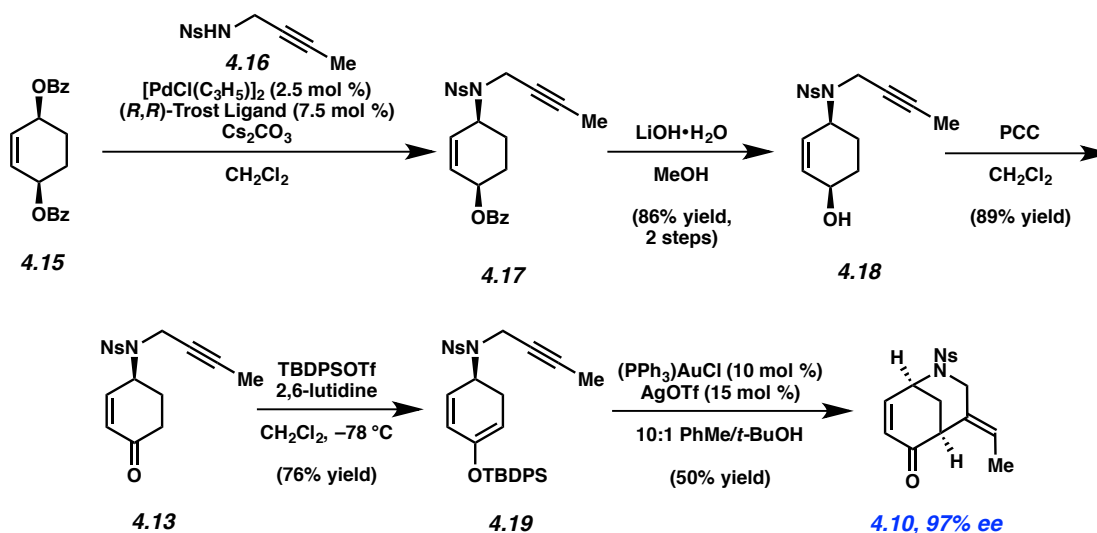
As outlined above, in addition to developing a divergent approach to the akuammiline alkaloids, we were interested in rendering our strategy asymmetric. This goal would entail modification of the synthetic strategy at the beginning of the synthesis. To this end, we targeted bicyclic enone **4.10**, an important intermediate from our racemic synthesis of picrinine (**4.1**), as our target for enantioselective synthesis (Scheme 4.2).⁴ Retrosynthetically, we envisioned a few strategic avenues by which to efficiently construct **4.10** in enantioenriched form. First, we envisioned the possibility of accessing the desired [3.3.1]-azabicyclic enone through a Pd-enolate cyclization of enol ether **4.11**.⁷ Enol ether **4.11** could theoretically be accessed through a desymmetrization of ketone **4.12** with a chiral lithium amide base (Strategy One, Scheme 4.2).⁸ Two other strategies both hinged on a successful gold (I)-catalyzed cyclization of alkyne **4.13** to access enone **4.10**.^{9,10} Strategy Two (see Scheme 4.2) would employ functionalization of cyclohexenone **4.14**, which can be accessed by a number of established synthetic strategies.¹¹ Finally, strategy three would utilize a modification of an established Pd-catalyzed desymmetrization of dibenzoate **4.15**.^{11a,12} Scouting experiments for each route led us to focus on Strategy Three, which held the most promise for providing **4.10** directly and in enantioselective form.

Scheme 4.2 Three approaches to the enantioselective synthesis of enone **4.10**.



The asymmetric synthesis of enone **4.10** is shown in Scheme 4.3. Dibenzoate **4.15**, which is readily available following a procedure by Trost, was treated with sulfonamide **4.16**¹³ in the presence of a catalytic amount of allylpalladium(II) chloride dimer, (*R,R*)-DACH-phenyl Trost ligand, and cesium carbonate in CH₂Cl₂ to afford allylic benzoate **4.17**.^{11a} The crude product was subjected to benzoate cleavage, resulting in the formation of allylic alcohol **4.18** in 86% yield over the two operations. Alcohol **4.18** was oxidized with PCC in excellent yield to deliver ketone **4.13**. Exposure of ketone **4.13** to TBDPSOTf and 2,6-lutidine at low temperature afforded the cross-conjugated silyl enol ether **4.19** in 76% yield. With **4.19** in hand, we were poised to attempt the key gold (I)-catalyzed cyclization. Upon treatment of **4.19** with 10 mol % (PPh₃)AuCl and 15 mol % AgOTf in a 10:1 mixture of toluene and *t*-BuOH, cyclization occurred to deliver enone **4.10** in 50% yield.¹⁰ Analysis of the product by chiral supercritical fluid chromatography showed that enone **4.10** had been synthesized in 97% ee. Accordingly, this effort constitutes formal enantioselective total synthesis of aspidophylline A (**4.2**) and picrinine (**4.1**).

Scheme 4.3 Asymmetric synthesis of enone **4.10**.



4.5 Conclusion

We have developed a unified, divergent approach to the akuammilines, which rests on the ability to efficiently access lactone **4.4**. The route to **4.4**, which begins from enal **4.5**, is eight steps, scalable, and relies on a Ueno–Stork radical cyclization. The synthesis of **4.4** also permitted a second generation synthesis of aspidophylline A (**4.2**). In addition, we have developed an asymmetric route to azabicyclic core of the akuammilines. Our strategy relies on a Trost-type desymmetrization reaction, followed by a gold-mediated cyclization, to construct the enone **4.10**. The successful enantioselective synthesis of enone **4.10** comprises a formal enantioselective synthesis of picrinine (**4.1**) and aspidophylline A (**4.2**). Both of these natural products have not been accessed enantioselectively previously, and this strategy provides a framework for the successful elaboration of the enantioenriched enone **4.10** to either natural product. The asymmetric synthesis of **4.10**, coupled with the divergent synthetic strategy outline

above, is expected to provide a unified and asymmetric entryway to the akuammiline family of monoterpene indole alkaloids.

4.6 Experimental Section

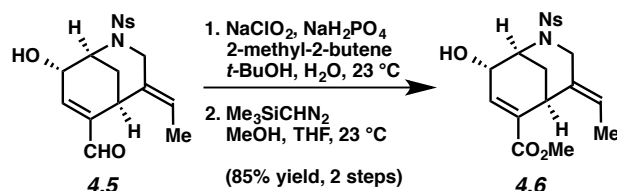
4.6.1 Materials and Methods

Unless stated otherwise, the reactions reported were carried out in flame-dried glassware under an atmosphere of nitrogen. The solvents were either freshly distilled or passed through activated alumina columns. Commercially available reagents were used as received unless otherwise specified. Sodium chlorite, 2-methyl-2-butene, 2,6-lutidine, (*R,R*)-DACH-phenyl Trost Ligand, pyridinium chlorochromate, and tributyltin hydride were obtained from Sigma-Aldrich. Cesium carbonate and lithium hydroxide monohydrate were obtained from Alfa-Aesar. Trimethylsilyldiazomethane and *tert*-butyldiphenylsilyl triflate were obtained from TCI. Chlorotriphenylphosphinegold (I), silver (I) triflate, and palladium allyl chloride dimer were purchased from Strem. *N*-Iodosuccinimide was purchased from Sigma-Aldrich and recrystallized from 1,4-dioxane. Unless stated otherwise, reactions were performed at room temperature (approximately 23 °C). Thin-layer chromatography (TLC) was conducted with EMD gel 60 F254 pre-coated plates (0.25 mm) and visualized using a combination of UV, anisaldehyde, and iodine staining. SiliCycle silica gel 60 (particle size 0.040–0.063 mm) was used for flash column chromatography. ¹H NMR spectra were recorded on Bruker spectrometers (300 and 500 MHz). Data for ¹H spectra are reported as follows: chemical shift (δ ppm), multiplicity, coupling constant (Hz), integration and are reference to the residual solvent peak 7.26 ppm for CDCl₃ and 7.16 ppm for C₆D₆. ¹³C NMR spectra are reported in terms of chemical shift (at 125 MHz) and

are reference to the residual solvent peak 77.16 for CDCl₃ and 128.06 for C₆D₆. IR spectra were recorded on a Perkin Elmer 100 spectrometer and are reported in terms of frequency absorption (cm⁻¹). Uncorrected melting points were measured using a Mel-Temp II melting point apparatus with a Fluke 50S thermocouple and a Digimelt MPA 160 melting point apparatus. High-resolution mass spectra were obtained on Thermo Scientific™ Exactive Mass Spectrometer with DART ID-CUBE. Determination of enantiopurity was carried out on a Mettler Toledo SFC (supercritical fluid chromatography) using a Daicel ChiralPak OD-H column.

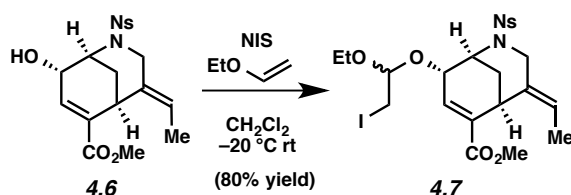
4.6.2. Experimental Procedures

4.6.2.1 Synthesis of Lactone 4.4



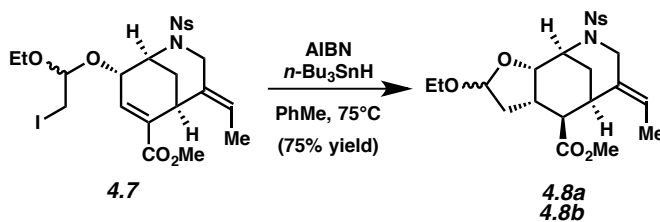
Enoate 4.6. To a solution of known enal **4.5** (0.400 g, 1.06 mmol) in *t*-BuOH (40.6 mL) and 2-methyl-2-butene (24.36 mL) at 0 °C was added a solution of sodium chlorite (524 mg, 5.81 mmol) and monobasic sodium phosphate (0.820 g, 6.86 mmol) in H₂O (40.6 mL). The reaction was allowed to warm to room temperature while stirring. After 12 h, the reaction mixture was poured into water (150 mL) and the resulting mixture was diluted with EtOAc (150 mL). The layers were separated and the aqueous layer was extracted with EtOAc (2 x 100 mL). The organic layers were combined and dried over MgSO₄. Evaporation of the solvent under reduced pressure afforded the corresponding acid, which was used in the subsequent step without further purification.

To a solution of crude acid in 5:3 THF:MeOH (106 mL) was added trimethylsilyldiazomethane (0.64 mL, 2.0 M solution in hexanes). After stirring for 1 h, the reaction mixture was poured into water (150 mL) and the resulting mixture was diluted with CH₂Cl₂ (150 mL). The layers were separated and the aqueous layer was extracted with CH₂Cl₂ (2 x 100 mL). The organic layers were combined and dried over MgSO₄ then concentrated under reduced pressure. The resulting residue was purified *via* flash chromatography (2:1 hexanes:EtOAc) to afford enoate **4.6** (0.388 g, 85% yield) as a yellow oil. Enoate **4.6**: R_f 0.56 (3:7 hexanes:EtOAc); ¹H NMR (500 MHz, CDCl₃): δ 8.04 (m, 1H), 7.74–7.63 (m, 3H), 7.05 (dd, *J* = 4.1, 1.2, 1H), 5.48 (q, *J* = 6.9, 1H), 4.24 (d, *J* = 4.2, 1H), 4.17 (br s, 1H), 3.93 (t, *J* = 3.0, 1H), 3.85 (d, *J* = 14.1, 1H), 3.74 (s, 3H), 3.67 (dt, *J* = 14.1, 1.9, 1H), 1.96 (dt, *J* = 13.0, 3.1, 1H), 1.76 (dd, *J* = 6.9, 1.9, 1H), 1.74 (dt, *J* = 13.0, 3.0, 1H); ¹³C NMR (125 MHz, CDCl₃): δ 166.0, 147.8, 137.9, 134.2, 133.7, 133.3, 132.0, 130.9, 130.0, 124.4, 123.0, 67.1, 54.2, 52.0, 47.1, 29.5, 27.1, 12.7; IR (film): 3485, 1954, 1716, 1543, 1371, 1163 cm⁻¹; HRMS–ESI (*m/z*) [M + H]⁺ calc for C₁₈H₂₁N₂O₇S⁺, 409.10640, found 409.10491.



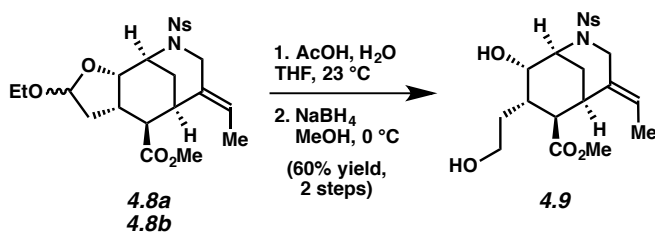
Acetal 4.7. To a solution of enoate **4.6** (0.503 g, 1.23 mmol) in CH₂Cl₂ (3.4 mL) at –20 °C was added NIS (1.66 g, 7.39 mmol). Ethyl vinyl ether (0.94 mL, 9.85 mmol) was then added dropwise over 2 min at –20 °C. The reaction was stirred at –20 °C for 2.5 h and then was quenched with sat. aq. sodium thiosulfate (150 mL). The resulting mixture was diluted with

CH₂Cl₂ (150 mL) and the layers were separated. The aqueous layer was extracted with CH₂Cl₂ (2 x 100 mL) and the organic layers were combined and dried over MgSO₄. Evaporation of the solvent under reduced pressure afforded the corresponding acetal **4.7** (0.596 g, 80% yield) as an inseparable mixture of diastereomers. Acetal **4.7** (diastereomer 1): mp: 88–92 °C as a mixture; R_f 0.73 (1:1 hexanes:EtOAc); ¹H NMR (500 MHz, CDCl₃): δ 8.09 (m, 1H), 7.74–7.64 (m, 3H), 7.07 (dd, *J* = 4.3, 1.2 1H), 5.47 (m, 1H), 4.83 (dd, *J* = 6.6, 4.2, 1H), 4.27 (m, 2H), 3.92 (t, *J* = 3.0, 1H), 3.80 (d, *J* = 14.2, 1H), 3.75 (d, *J* = 14.2, 1H), 3.73 (s, 3H), 3.70 (m, 1H), 3.62 (m, 1H), 3.25–3.20 (m, 2H), 1.94 (dt, *J* = 13.0, 3.1, 1H), 1.75 (dd, *J* = 6.9, 1.6, 3H), 1.70 (m, 1H), 1.24 (t, *J* = 7.0, 3H); (diastereomer 2) ¹H NMR (500 MHz, CDCl₃): δ δ 8.07 (m, 1H), 7.74–7.64 (m, 3H), 7.05 (dd, *J* = 4.3, 1.2 1H), 5.45 (m, 1H), 4.80 (t, *J* = 6.8, 1H), 4.22 (m, 2H), 3.90 (t, *J* = 3.0, 1H), 3.80 (d, *J* = 14.2, 1H), 3.75 (d, *J* = 14.2, 1H), 3.72 (s, 3H), 3.68 (m, 1H), 3.56 (m, 1H), 3.24–3.16 (m, 2H), 1.94 (dt, *J* = 13.0, 3.1, 1H), 1.73 (dd, *J* = 6.9, 1.6, 3H), 1.67 (m, 1H), 1.23 (t, *J* = 7.0, 3H); ¹³C NMR (42 of 44 observed, 125 MHz, CDCl₃): δ 166.0, 165.9, 147.8, 136.9, 136.5, 134.5, 134.3, 133.9, 133.8, 133.3, 133.2, 132.1, 132.0, 131.1, 131.0, 130.1, 130.0, 124.7, 124.6, 123.0, 122.9, 102.1, 101.8, 71.7, 71.4, 62.8, 62.7, 52.2, 52.1, 51.3, 47.2, 47.1, 29.4, 29.3, 27.3, 27.2, 15.4, 15.0, 12.81, 12.80, 5.8, 5.7; IR (film) as a mixture: 2976, 1717, 1516, 1438, 1369, 1342, 1250, 1162, 1126, 1090, 1021; HRMS–ESI (*m/z*) [*M* + *H*]⁺ calcd for C₂₂H₂₅N₂O₈SI⁺, 607.06056, found, 607.05525.



Tricycles 4.8 and 4.8b. To a solution of acetal **4.7** (0.452 g, 0.74 mmol) in toluene (3.7 mL) was added a solution of AIBN (0.020 g, 0.12 mmol) and *n*-Bu₃SnH (0.13 mL, 0.50 mmol) in toluene (1.2 mL) at 0 °C. The mixture was heated to 75 °C. After 1 h, a second identical solution of AIBN and *n*-Bu₃SnH in toluene was added. After a 2 h, a third identical solution of AIBN and *n*-Bu₃SnH in toluene was added. After 3 h, the resulting yellow solution was cooled to rt, concentrated under reduced pressure, and purified via flash chromatography (3:20 benzene:EtOAc) to afford tricycle **4.8a** and **4.8b** as a mixture of diastereomers (266 mg, 75% yield, 1:1 dr) as a white solid. Tricycle **4.8a**: mp: 88–92 °C; R_f 0.38 (9:1 benzene:EtOAc); ¹H NMR (500 MHz, CDCl₃): δ 8.08 (m, 1H), 7.71–7.63 (m, 3H), 5.48 (q, *J* = 6.8, 1H), 5.05 (d, *J* = 5.8, 1H), 5.25 (app q, *J* = 3.1, 1H), 4.09 (ddd, *J* = 5.9, 2.4, 1.2, 1H), 4.05 (d, *J* = 15.1, 1H), 3.93 (dt, *J* = 15.1, 2.1, 1H), 3.73 (m, 1H), 3.64 (s, 3H), 3.41 (m, 1H), 3.32 (m, 2H), 2.89 (m, 1H), 2.22 (ddd, *J* = 13.4, 7.1, 6.0, 1H), 2.11 (dt, *J* = 13.2, 2.7, 1H), 1.77 (d, *J* = 13.7, 1H), 1.66 (ddt, *J* = 13.4, 3.4, 1.5, 1H), 1.55 (dd, *J* = 6.9, 2.1, 3H), 1.19 (t, *J* = 7.1, 3H); ¹³C NMR (125 MHz, CDCl₃): δ 173.9, 147.8, 133.6, 133.5, 131.8, 131.0, 130.7, 124.5, 123.3, 103.1, 79.9, 63.3, 51.6, 50.4, 49.9, 47.2, 40.4, 35.4, 31.1, 29.7, 27.3, 15.3, 12.3; IR (film): 2919, 1732, 1543, 1439, 1373, 1196 cm⁻¹; HRMS–ESI (*m/z*) [M + H]⁺ calcd for C₂₂H₂₉N₂O₈S⁺, 481.16391, found 481.16224. Tricycle **4.8b**: mp: 88–92 °C; R_f 0.28 (9:1 benzene:EtOAc); ¹H NMR (500 MHz, CDCl₃): δ 8.07 (m, 1H), 7.72–7.63 (m, 3H), 5.49 (q, *J* = 7.0, 1H), 5.13 (dd, *J* = 5.7, 4.0, 1H), 4.34 (app q, *J* = 3.0, 1H), 4.10 (m, 1H), 4.13–4.05 (m, 2H), 4.03 (dt, *J* = 15.2, 2.1, 1H), 3.74 (ddd, *J* = 16.6, 9.5, 7.1, 1H), 3.65 (s, 3H), 3.43 (ddd, *J* = 16.6, 9.5, 7.1, 1H), 3.26 (app q, *J* = 3.4, 1H), 2.89 (ddd, *J* = 11.6, 7.6, 5.0, 1H), 2.48 (dd, *J* = 11.6, 4.3, 1H), 2.10 (ddd, *J* = 14.2, 7.5, 4.0, 1H), 2.06 (dt, *J* = 13.3, 2.9, 1H), 1.86 (dd, *J* = 14.2, 5.9, 1H), 1.64 (dt, *J* = 13.3, 3.6, 1H), 1.52 (dd, *J* = 6.9, 1.8, 3H), 1.17 (t, *J* = 7.1, 3H); ¹³C NMR (125 MHz, CDCl₃): δ 173.3, 147.8, 133.5, 133.4, 131.7,

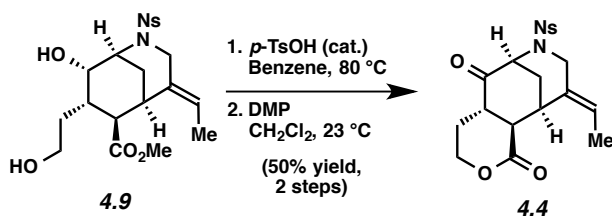
131.0, 130.1, 124.4, 123.5, 102.1, 75.9, 63.6, 51.8, 49.8, 49.5, 49.3, 41.3, 36.9, 31.5, 28.0, 15.2, 12.3; IR (film): 2922, 1733, 1544, 1439, 1373 cm^{-1} ; HRMS-ESI (m/z) [$M + H$] $^+$ calcd for $\text{C}_{22}\text{H}_{29}\text{N}_2\text{O}_8\text{S}^+$, 481.16, found 481.16224.



Diol 4.9. To a solution of tricycles **4.8a** and **4.8b** (0.331 g, 0.69 mmol) in THF (4.6 mL) and H₂O (4.6 mL) at 23 °C was added AcOH (13.7 mL, 240.8 mmol). The reaction vessel was heated to 75 °C for 12 h. After cooling to 23 °C the reaction was quenched with sat. aq. sodium bicarbonate (150 mL). The resulting mixture was diluted with EtOAc (150 mL) and the layers were separated. The aqueous layer was extracted with EtOAc (2 x 100 mL) and the organic layers were combined and dried over MgSO₄. Evaporation of the solvent under reduced pressure afforded the corresponding lactol, which was used in the subsequent step without further purification.

To a solution of the crude lactol (194 mg, 0.428 mmol) in MeOH (8.56 mL) at 0 °C was added NaBH₄ (32.4 mg, 0.86 mmol). The mixture was stirred at 0 °C for 1.5 h, diluted with EtOAc (100 mL) and then poured into H₂O (100 mL). The layers were separated and the aqueous layer was extracted with EtOAc (2 x 100 mL). The organic layers were combined, dried over MgSO₄, and concentrated under reduced pressure. The crude mixture was purified via flash chromatography (1:1 hexanes:EtOAc) to afford diol **4.9** (0.188 g, 60% yield over two steps) as a white solid. Diol **4.9**: mp: 151–154 °C; R_f 0.18 (1:1 benzene:EtOAc); ¹H NMR (500 MHz, CDCl₃): δ 8.05 (m, 1H), 7.72–7.63 (m, 3H), 5.44 (q, $J = 6.9$, 1H), 4.26 (dt, $J = 15.2, 2.4$, 1H),

4.19 (t, $J = 3.7$, 1H), 4.70 (app q, $J = 3.4$, 1H), 3.97 (d, $J = 15.2$, 1H), 3.76 (m, 2H), 3.62 (s, 3H), 3.40 (br s, 1H), 3.20 (app q, $J = 3.4$, 1H), 2.80 (dd, $J = 12.1, 4.5$, 1H), 2.38 (m, 1H), 2.31 (dt, $J = 13.4, 3.2$, 1H), 2.03 (br s, 1H), 1.67 (m, 2H), 1.55–1.48 (m, 3H); ^{13}C NMR (125 MHz, CDCl_3): δ 173.9, 148.0, 133.6, 132.9, 131.8, 131.1, 130.9, 124.4, 122.2, 69.0, 61.0, 52.9, 51.6, 49.8, 47.3, 36.7, 32.6, 31.8, 29.7, 26.4, 12.3; IR (film): 3397, 2951, 1728, 1542, 1162, 1128 cm^{-1} ; HRMS–ESI (m/z) $[\text{M} + \text{H}]^+$ calcd for $\text{C}_{20}\text{H}_{27}\text{N}_2\text{O}_8\text{S}^+$, 455.14826; found 455.14845.

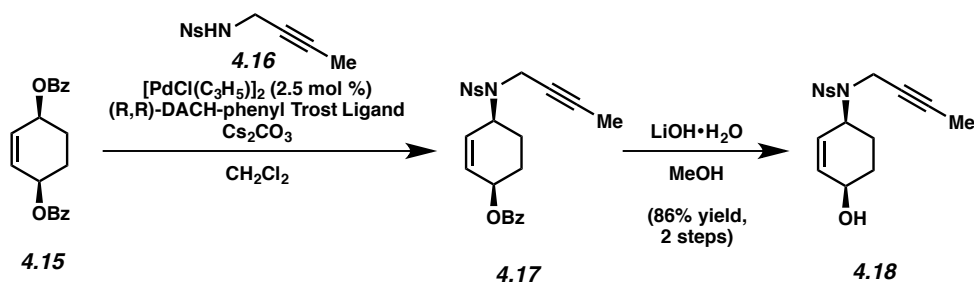


Lactone 4.4. To a solution of diol **4.9** (153 mg, 0.337 mmol) in benzene (17 mL) was added *p*-TsOH (16.0 mg, 0.084 mmol). The resulting mixture was placed into a preheated heating block at 80 °C for 1 h. After cooling to 23 °C, the reaction was diluted with EtOAc (100 mL) and then poured into H_2O (100 mL). The layers were separated and the aqueous layer was extracted with EtOAc (2 x 100 mL). The organic layers were combined and dried over MgSO_4 then concentrated under reduced pressure to afford the corresponding lactone, which was used subsequently without further purification.

To a solution of the crude lactone (0.337 mmol) in CH_2Cl_2 (3.5 mL) was added Dess–Martin periodinane (0.400 g, 0.944 mmol). The resulting mixture was heated to 40 °C. After 12 h, the reaction was cooled to room temperature and quenched with a 1:1 mixture of sat. aq. sodium thiosulfate (10 mL) and sat. aq. sodium bicarbonate (10 mL). The mixture was stirred for 5 min and then suspended in H_2O (50 mL). The resulting mixture was diluted with CH_2Cl_2 (50 mL) and the layers were separated. The aqueous layer was extracted with CH_2Cl_2 (2 x 50

mL) and the organic layers were combined, dried over MgSO_4 , and concentrated under reduced pressure. The crude mixture was purified via flash chromatography (3:2 benzene:EtOAc) to afford lactone **4.4** (0.071 g, 50% yield over two steps) as a yellow oil. Lactone **4.4**: R_f 0.49 (3:7 hexanes:EtOAc); ^1H NMR (500 MHz, CDCl_3): δ 8.09 (m, 1H), 7.77–7.66 (m, 3H), 5.72 (q, $J = 7.0$, 1H), 4.43 (ddd, $J = 11.6, 6.0, 3.8$, 1H), 4.39–4.27 (m, 3H), 4.19 (d, $J = 15.2$, 1H), 3.66 (q, $J = 3.2$, 1H), 3.14 (ddd, $J = 14.4, 10.4, 4.4$, 1H), 2.67 (dd, $J = 13.9, 3.5$, 1H), 2.19 (m, 2H), 2.07–1.98 (m, 2H), 1.83 (dd, $J = 7.0, 1.4$, 3H); ^{13}C NMR (125 MHz, CDCl_3): δ 203.2, 168.8, 147.9, 134.3, 132.1, 132.0, 131.7, 127.9, 127.0, 124.6, 68.0, 58.6, 50.6, 49.8, 45.2, 34.2, 28.7, 22.7, 13.5; IR (film): 2917, 1725, 1542, 1370, 1167, 1072; HRMS–ESI (m/z) $[\text{M} + \text{H}]^+$ calcd for $\text{C}_{19}\text{H}_{20}\text{N}_2\text{O}_7\text{S}^+$, 421.10640; found 421.10445.

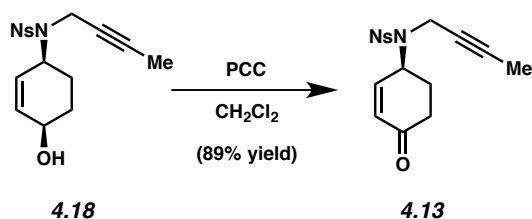
4.6.2.2 Enantioselective Synthesis of Azabicyclic 4.10



Alcohol 4.18. To a solution of $[\text{Pd}(\text{C}_3\text{H}_5)\text{Cl}]_2$ (0.028 g, .078 mmol), (R, R)-DACH-phenyl Trost ligand (0.161 g, 0.23 mmol), and Cs_2CO_3 (1.160 g, 3.57 mmol) in CH_2Cl_2 (5.5 mL) was added a solution of dibenzoate **4.15**^{11a} (1.00 g, 3.10 mmol) and sulfonamide **4.16**¹³ (0.910 g, 3.57 mmol) in CH_2Cl_2 (10 mL) at room temperature. After stirring for 30 min, the reaction was poured into a solution of sat. aq. NaHCO_3 (20 mL) and the layers were separated. The aqueous layer was extracted with EtOAc (3 x 50 mL) and the organic layers were combined, dried with MgSO_4 , and

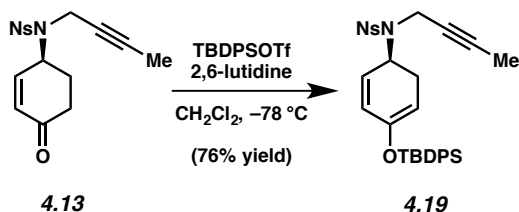
concentrated under reduced pressure. The crude benzoate **4.17** was used in the subsequent step without further purification.

To a solution of the crude benzoate **4.17** in methanol (14 mL) was added LiOH monohydrate (0.195 g, 4.66 mmol) at room temperature. After stirring for 2 h, the reaction was diluted with Et₂O (20 mL), poured into a pH 7-buffered solution (20 mL), and the layers were separated. The aqueous layer was extracted with Et₂O (3 x 50 mL) and the organic layers were combined, dried with MgSO₄, and concentrated under reduced pressure. The resulting residue was purified via flash chromatography (1:1 → 1:2 hexanes:EtOAc) to afford alcohol **4.18** (0.932 g, 86% yield over two steps) as a clear oil. Alcohol **4.18**: R_f 0.21 (3:7 hexanes:EtOAc); ¹H NMR (500 MHz, CDCl₃): δ 8.17 (m, 1H), 7.71–7.62 (m, 3H), 5.99 (m, 1H), 5.70 (d, *J* = 10.1, 1H), 4.49 (m, 1H), 4.13 (m, 1H), 4.09 (dq, *J* = 18.3, 2.3, 1H), 3.96 (dq, *J* = 18.3, 2.3, 1H), 2.05 (m, 1H), 1.90 (s, 1H), 1.88–1.75 (m, 3H), 1.60 (t, *J* = 2.3, 3H); ¹³C NMR (125 MHz, CDCl₃): δ 148.1, 134.2, 133.6, 133.4, 131.6, 131.5, 131.4, 124.2, 81.1, 74.7, 62.6, 55.8, 34.2, 29.9, 22.9, 3.5; IR (film): 3367, 2946, 1542, 1438, 1371, 1165, 1123, 1071, 1025; HRMS–ESI (*m/z*) [M + H]⁺ calcd for C₁₆H₁₉N₂O₅S⁺, 351.10092; found, 351.10003; [α]_D^{25.1} –4.0° (c = 1.0, CH₂Cl₂).



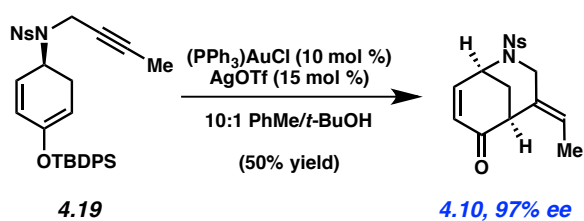
Enone 4.13. To a solution of pyridinium chlorochromate (0.860 g, 3.99 mmol) in CH₂Cl₂ (5 mL) was added a solution of alcohol **4.18** (0.932 g, 2.66 mmol) in CH₂Cl₂ (15 mL) at room temperature. After stirring for 2 h, celite (4 g) was added followed by Et₂O (20 mL). The mixture was filtered over a pad of celite (10 g) and basic alumina (5 g), and then washed with EtOAc

(500 mL). The filtrate was concentrated under reduced pressure and the resulting residue was purified via flash chromatography (1:1 hexanes:EtOAc) to afford enone **4.13** (0.821 g, 89% yield) as a clear oil. Enone **4.13**: R_f 0.68 (1:2 hexanes:EtOAc); ^1H NMR (500 MHz, CDCl_3): δ 8.22 (m, 1H), 7.77–7.68 (m, 3H), 6.92 (dt, $J = 10.3, 2.0$, 1H), 6.08 (ddd, $J = 10.3, 2.7, 1.0$, 1H), 5.00 (m, 1H), 4.08 (dq, $J = 18.4, 2.4$, 1H), 4.04 (dq, $J = 18.4, 2.4$, 1H), 2.64–2.48 (m, 2H), 2.40–2.23 (m, 2H), 1.61 (t, $J = 2.4$, 3H); ^{13}C NMR (125 MHz, CDCl_3): δ 197.4, 150.8, 148.1, 134.0, 133.9, 132.0, 131.9, 131.7, 124.5, 82.3, 73.9, 55.9, 37.1, 34.6, 29.0, 3.5; IR (film): 2922, 1685, 1541, 1439, 1356, 1296, 1251, 1209, 1164, 1125, 1082, 1016; HRMS–ESI (m/z) $[\text{M} + \text{H}]^+$ calcd for $\text{C}_{16}\text{H}_{17}\text{N}_2\text{O}_5\text{S}^+$, 349.08527; found, 349.08457; $[\alpha]_D^{25.1} -40.3^\circ$ ($c = 1.0$, CH_2Cl_2).



Enol Ether 4.19. To a solution of enone **4.13** (0.174 g, 0.50 mmol) and 2,6-lutidine (0.065 g, 0.60 mmol) in CH_2Cl_2 (3.3 mL) at -78°C was added TBDPSOTf (0.214 g, 0.55 mmol). After stirring for 1 h, the reaction was diluted with CH_2Cl_2 (5 mL) and poured into a solution of sat. aq. NaHCO_3 (4 mL). The layers were separated and the aqueous layer was extracted with CH_2Cl_2 (3 x 20 mL). The organic layers were combined, dried with MgSO_4 , and concentrated under reduced pressure. The resulting residue was purified via flash chromatography (10:1 \rightarrow 5:1 hexanes:EtOAc) to afford enol ether **4.19** (0.223 g, 76% yield) as a clear oil. Enol ether **4.19**: R_f 0.67 (3:7 hexanes:EtOAc); ^1H NMR (500 MHz, CDCl_3): δ 8.14 (m, 1H), 7.72–7.67 (m, 4H), 7.67–7.60 (m, 3H), 7.46–7.35 (m, 6H), 6.07 (dt, $J = 10.1, 2.1$, 1H), 5.64 (dd, $J = 10.1, 4.8$, 1H), 4.61 (m, 2H), 3.94 (dq, $J = 18.3, 2.3$, 1H), 3.73 (dq, $J = 18.3, 2.3$, 1H), 2.49 (ddd, $J = 18.6, 10.6$,

3.7, 1H), 2.39 (dt, $J = 18.6, 5.4$, 1H), 1.48 (t, $J = 2.3$, 3H), 1.03 (s, 9H); ^{13}C NMR (125 MHz, CDCl_3): δ (24 of 26 found) 148.1, 146.5, 135.64, 135.58, 134.6, 133.4, 132.93, 132.89, 131.8, 131.4, 130.4, 130.0, 127.88, 127.86, 125.5, 124.1, 102.0, 80.4, 74.9, 50.4, 34.4, 27.8, 26.6, 19.3, 3.5; IR (film): 2927, 2856, 1543, 1428, 1403, 1359, 1236, 1165, 1113, 1070; HRMS–ESI (m/z) $[\text{M} + \text{H}]^+$ calcd for $\text{C}_{26}\text{H}_{30}\text{N}_2\text{O}_5\text{SiS}^+$, 587.20305; found, 587.20078; $[\alpha]^{25.1}_{\text{D}} -72.0^\circ$ ($c = 0.10$, CH_2Cl_2).



Enone 4.10. To a solution of $(\text{PPh}_3)\text{AuCl}$ (0.017 g, 0.034 mmol) and enol ether **4.19** (0.200 g, 0.34 mmol) in toluene (8 mL) was added a solution of AgOTf (0.013 g, 0.051 mmol) in toluene (2 mL) and $t\text{-BuOH}$ (1 mL) at room temperature. After stirring for 3 h, the reaction was diluted with EtOAc (20 mL), poured into a solution of sat. aq. NaHCO_3 , and the layers were separated. The aqueous layer was extracted with EtOAc (3 x 20 mL) and the organic layers were combined, dried with MgSO_4 , and concentrated under reduced pressure. The resulting residue was purified via flash chromatography (3:2 hexanes: EtOAc) to afford enone **4.10** (0.059 g, 50% yield, 97% ee) as a clear oil. Enone **4.10**: For m. p., R_f , IR, HRMS–ESI, ^1H NMR, and ^{13}C NMR data, see Chapter 3 (Enone **3.11**). $[\alpha]^{25.1}_{\text{D}} -22.0^\circ$ ($c = 0.10$, CH_2Cl_2). Chiral SFC assay was run on a Daicel ChiralPak OD–H column at 35 °C with a 12% $i\text{-PrOH}$ isocratic solvent system and a flow rate of 2 mL/min. The retention times of the two enantiomers were 7.59 (minor) and 8.34 (major), respectively. The enantiomeric ratio (er) was 1.5:98.5, respectively.

4.7 References

- (1) For reviews on akuammiline alkaloids, see: (a) Ramírez, A.; García–Rubio, S. *Curr. Med. Chem.* **2003**, *10*, 1891–1915. (b) Eckermann, R.; Gaich, T. *Synthesis* **2013**, *45*, 2813–2823. (c) Smith, J. M.; Moreno, J.; Boal, B. W.; Garg, N. K. *Angew. Chem. Int. Ed.* **2015**, *54*, 400–412.
- (2) For a review on divergent synthesis, see: Serba, C.; Winssinger, N. *Eur. J. Org. Chem.* **2013**, 4195–4213.
- (3) Zu, L.; Boal, B. W.; Garg N. K. *J. Am. Chem. Soc.* **2011**, *133*, 8877–8879.
- (4) Smith, J. M.; Moreno, J.; Boal, B. W.; Garg, N. K. *J. Am. Chem. Soc.* **2014**, *136*, 4504–4507.
- (5) Bian, M.; Wang, Z.; Xiong, X.; Sun, Y.; Matera, C.; Nicolaou, K. C.; Li, A. *J. Am. Chem. Soc.* **2012**, *134*, 8078–8081.
- (6) Moreno, J.; Garg, N. K., unpublished results.
- (7) (a) For a review on the arylation of enolates and derivatives, see: Prim, D.; Marque, S.; Gaucher, A.; Campagne, J.-M. *Org. Reactions* **2012**, *76*, 49–279. For examples of arylation of silyl enol ethers using Pd, see: (b) Guo, Y.; Twamley, B.; Shreeve, J. M. *Org. Biomol. Chem.* **2009**, *8*, 1716–1722. (c) Kuwajima, I.; Urabe, H. *J. Am. Chem. Soc.* **1982**, *104*, 6831–6833. (d) Kosugi, M.; Hagiwara, I.; Sumiya, T.; Migita, T. *Bull. Chem. Soc. Jpn.* **1984**, *57*, 242–246. (e) Chae, J.; Yun, J.; Buchwald, S. L. *Org. Lett.* **2004**, *6*, 4809. (f) Su, W.; Raders, S.; Verkade, J. G.; Liao, X.; Hartwig, J. F. *Angew. Chem. Int. Ed.* **2006**, *45*, 5852–5855.
- (8) For a review on chiral amide bases, see: Harrison-Marchand, A.; Maddaluno, J. Advances in the Chemistry of Chiral Lithium Amides. In *Lithium Compounds in Organic Synthesis*; Luisi, R.; Capriati, V., Eds.; Wiley-VCH: Weinheim, 2014; 297–328.

- (9) For a recent review on gold-mediated cyclizations, see: Fensterbank, L.; Malacria, M. *Acc. Chem. Res.* **2014**, *47*, 953–965.
- (10) (a) Lu, Z.; Li, Y.; Deng, J.; Li, A. *Nat. Chem.* **2013**, *5*, 679–684. (b) Xiong, X.; Li, Y.; Lu, Z.; Wan, M.; Deng, J.; Wu, S.; Shao, H.; Li, A. *Chem. Comm.* **2014**, *50*, 5294–5297.
- (11) (a) Trost, B. M.; Masters, J. T.; Lumb, J.-P.; Fateen, D. *Chem. Sci.* **2014**, *5*, 1354–1360. (b) Dickmeiss, G.; De Sio, V.; Udmark, J.; Poulsen, T. B.; Marcos, V.; Joergensen, K. A. *Angew. Chem. Int. Ed.* **2009**, *48*, 6650–6653. (c) Bickley, J. F.; Evans, P.; Meek, A.; Morgan, B. S.; Roberts, S. M. *Tetrahedron: Asymmetry* **2006**, *17*, 355–362. (d) Suzuki, H.; Yamazaki, N.; Kibayashi, C. *J. Org. Chem.* **2001**, *66*, 1494–1496. (e) de March, P.; Escoda, M.; Figueredo, M.; Font, J.; Garcia-Garcia, E.; Rodriguez, S. *Tetrahedron: Asymmetry* **2000**, *11*, 4473–4483. (f) Marchand, A. P.; Xing, D.; Wang, Y.; Bott, S. G. *Tetrahedron: Asymmetry* **1999**, *6*, 2709–2714. (g) Carreno, M. C.; Garcia Ruano, J. L.; Garrido, M.; Ruiz, M. P.; Solladie, Guy *Tetrahedron Lett.* **1990**, *31*, 6653–6656.
- (12) For a review, see: Trost, B. M.; van Vranken, D. *Chem. Rev.* **1996**, *96*, 395–422.
- (13) Nishimura, T.; Maeda, Y.; Hayashi, T. *Org. Lett.* **2011**, *13*, 3674–3677.

APPENDIX THREE

Spectra Relevant to Chapter Four:

Unified and Enantioselective Approach to the Akuammiline Alkaloids

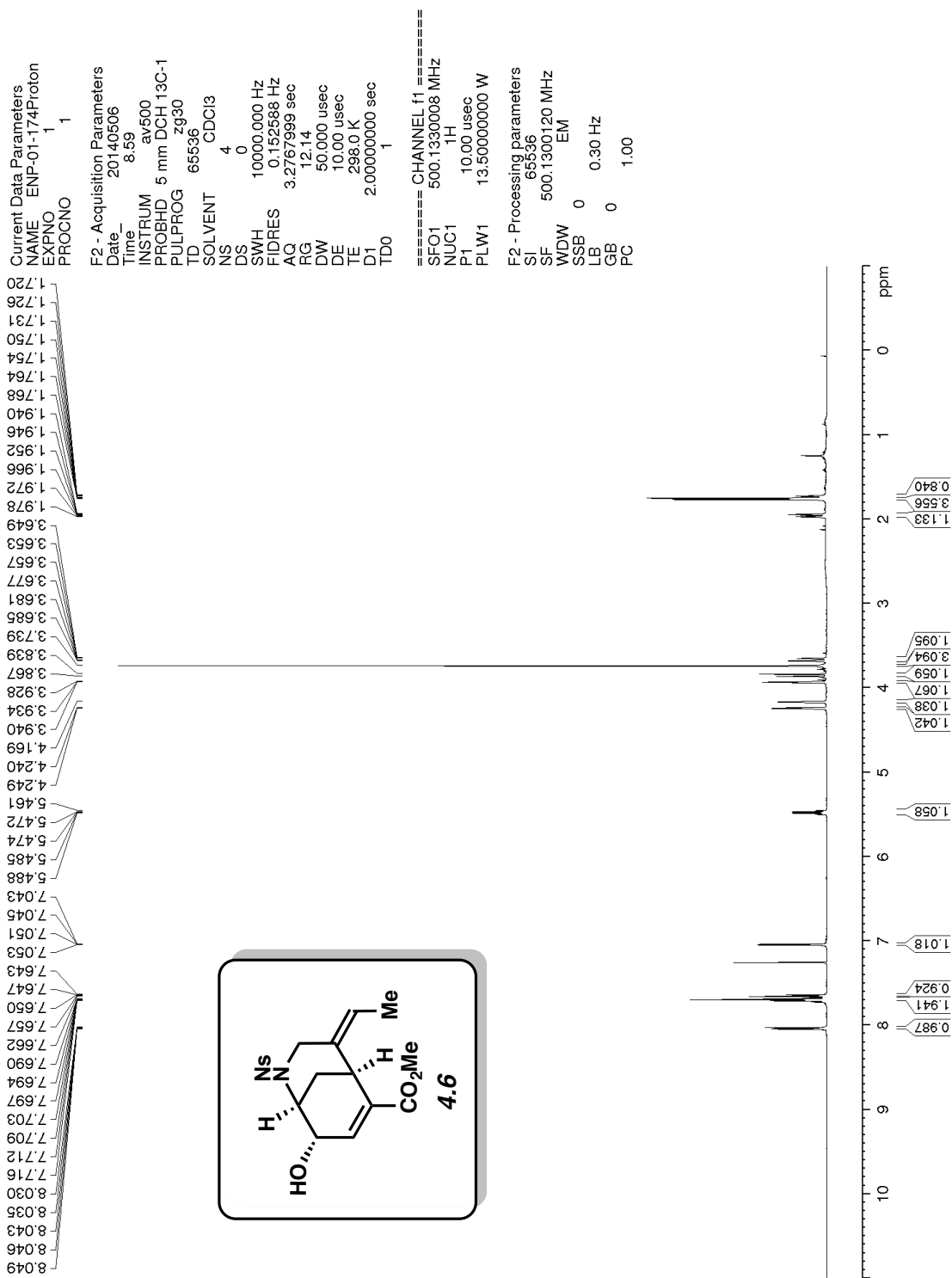


Figure A3.1 ¹H NMR (500 MHz, CDCl₃) of compound **4.6**.

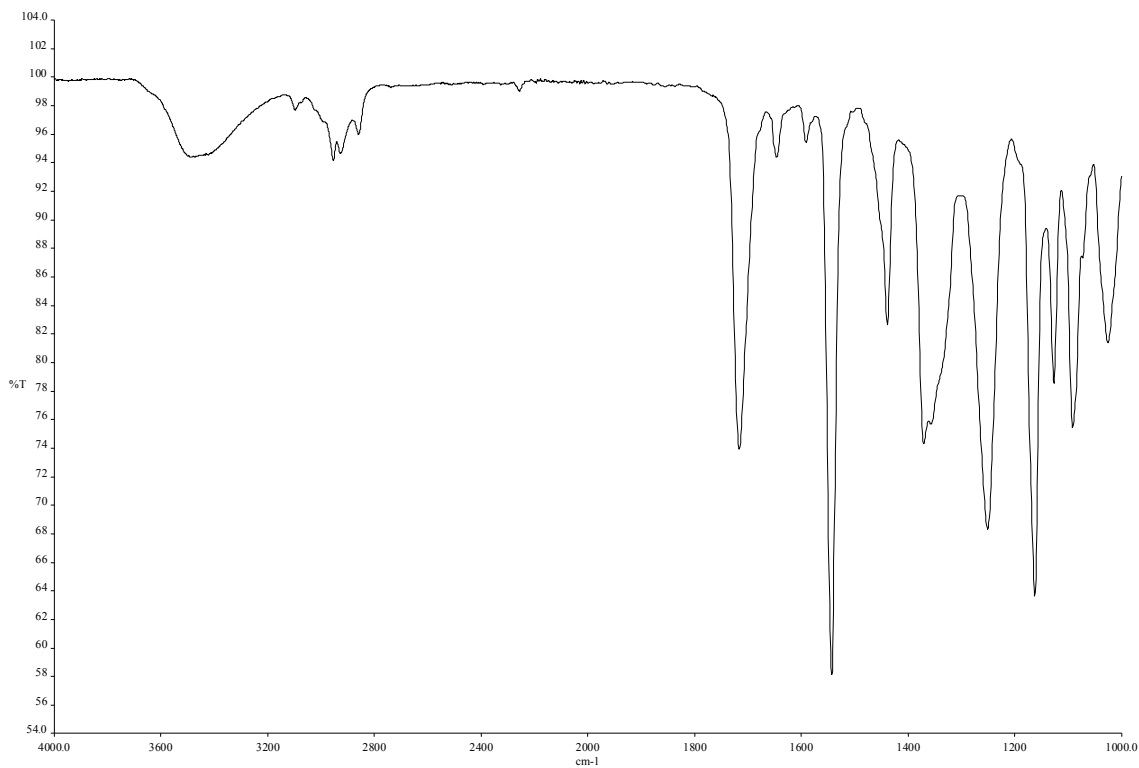


Figure A3.2 Infrared spectrum of compound 4.6.

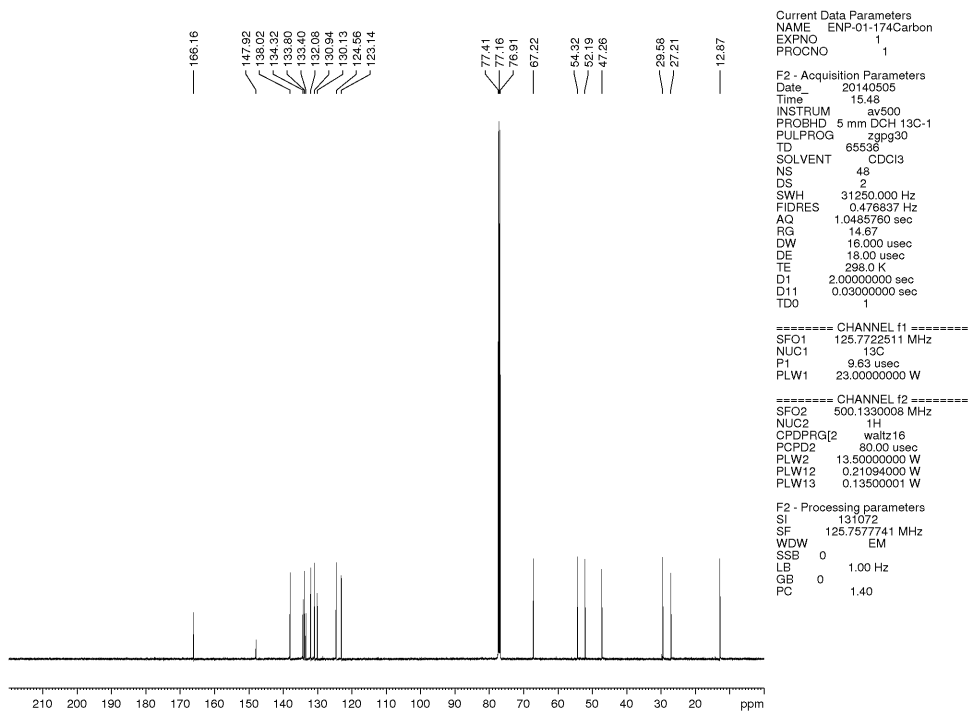


Figure A3.3 ^{13}C NMR (125 MHz, CDCl_3) of compound 4.6.

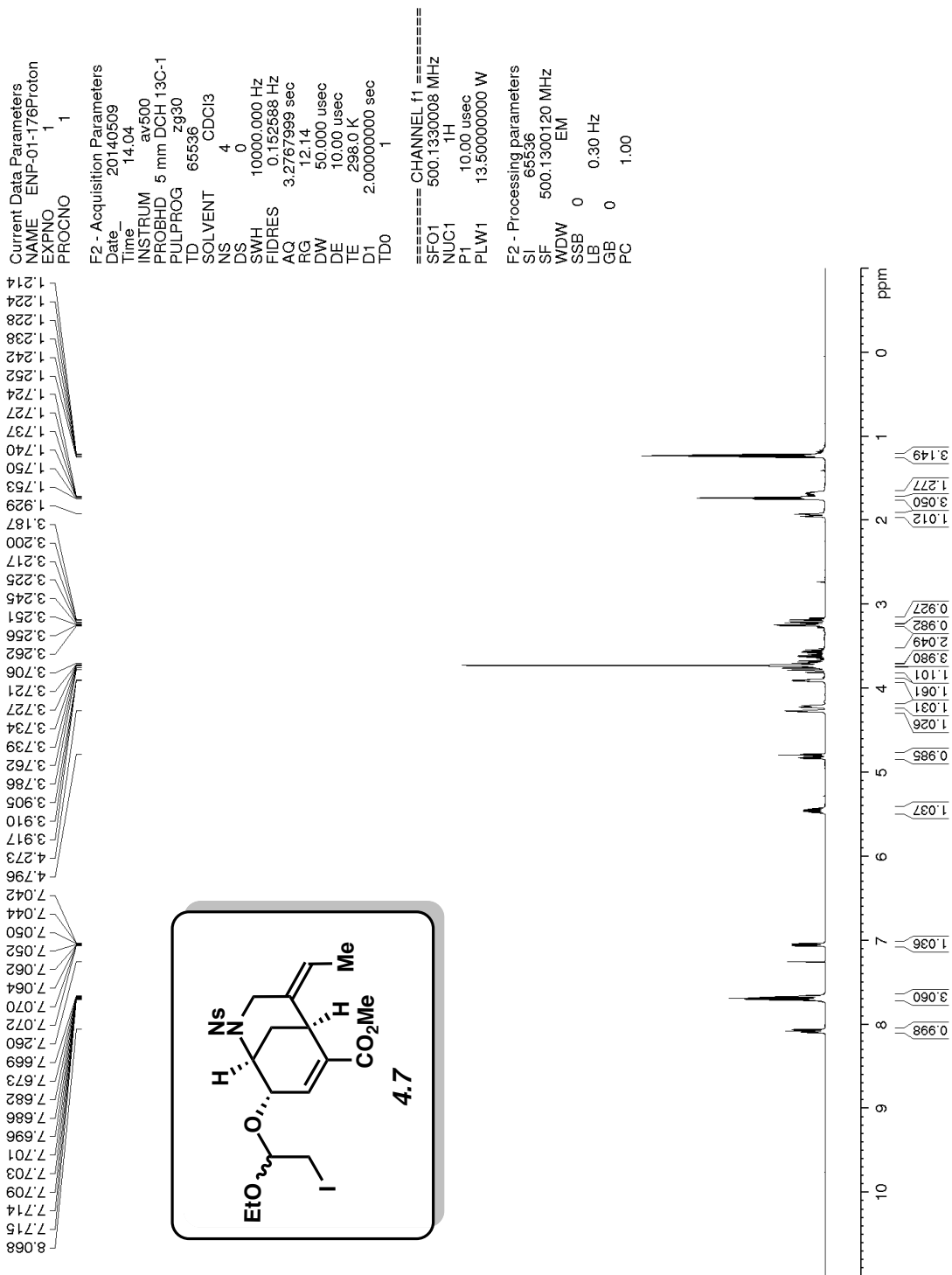


Figure A3.4 ¹H NMR (500 MHz, CDCl₃) of compound 4.7.

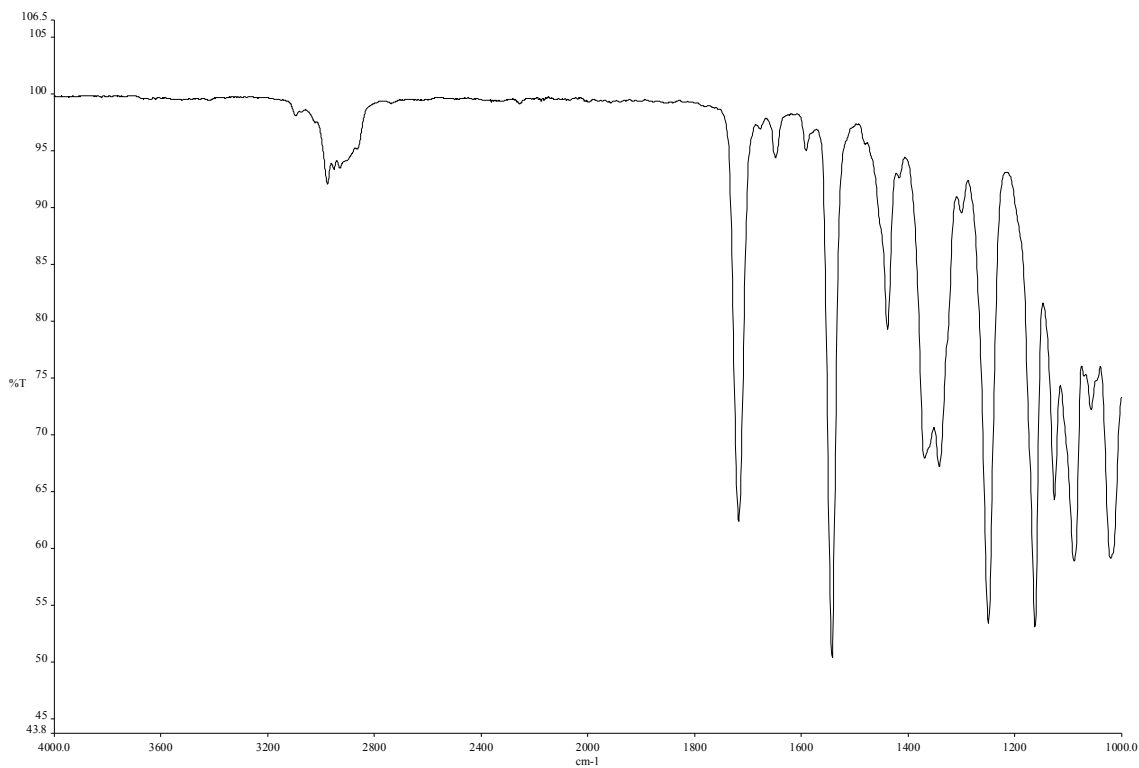


Figure A3.5 Infrared spectrum of compound 4.7.

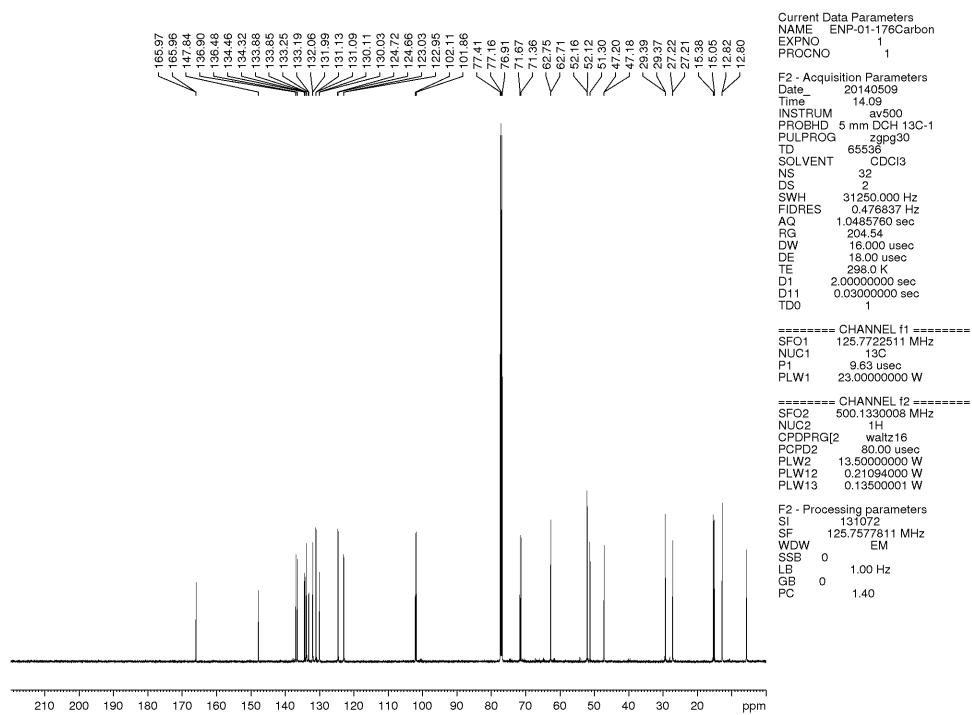


Figure A3.6 ^{13}C NMR (125 MHz, CDCl_3) of compound 4.7.

Current Data Parameters
 NAME ENP-01-186-2-D1Proton
 EXPNO 1
 PROCNO 1

F2 - Acquisition Parameters
 Date_ 20140527
 Time 21:20
 INSTRUM av500
 PROBHD 5 mm DCH 13C-1
 PULPROG zg30
 TD 65536
 SOLVENT CDCl3
 NS 14
 DS 0
 SWH 10000.000 Hz
 FIDRES 0.152588 Hz
 AC 3.2767999 sec
 RG 23.34
 DW 50.000 usec
 DE 10.00 usec
 TE 298.0 K
 D1 2.00000000 sec
 TD0 1

==== CHANNEL f1 =====
 SFO1 500.1330008 MHz
 NUC1 1H
 P1 10.00 usec
 PLW1 13.50000000 W

F2 - Processing parameters
 SI 65536
 SF 500.1300122 MHz
 WDW EM
 SSB 0
 LB 0 0.30 Hz
 GB 0
 PC 1.40

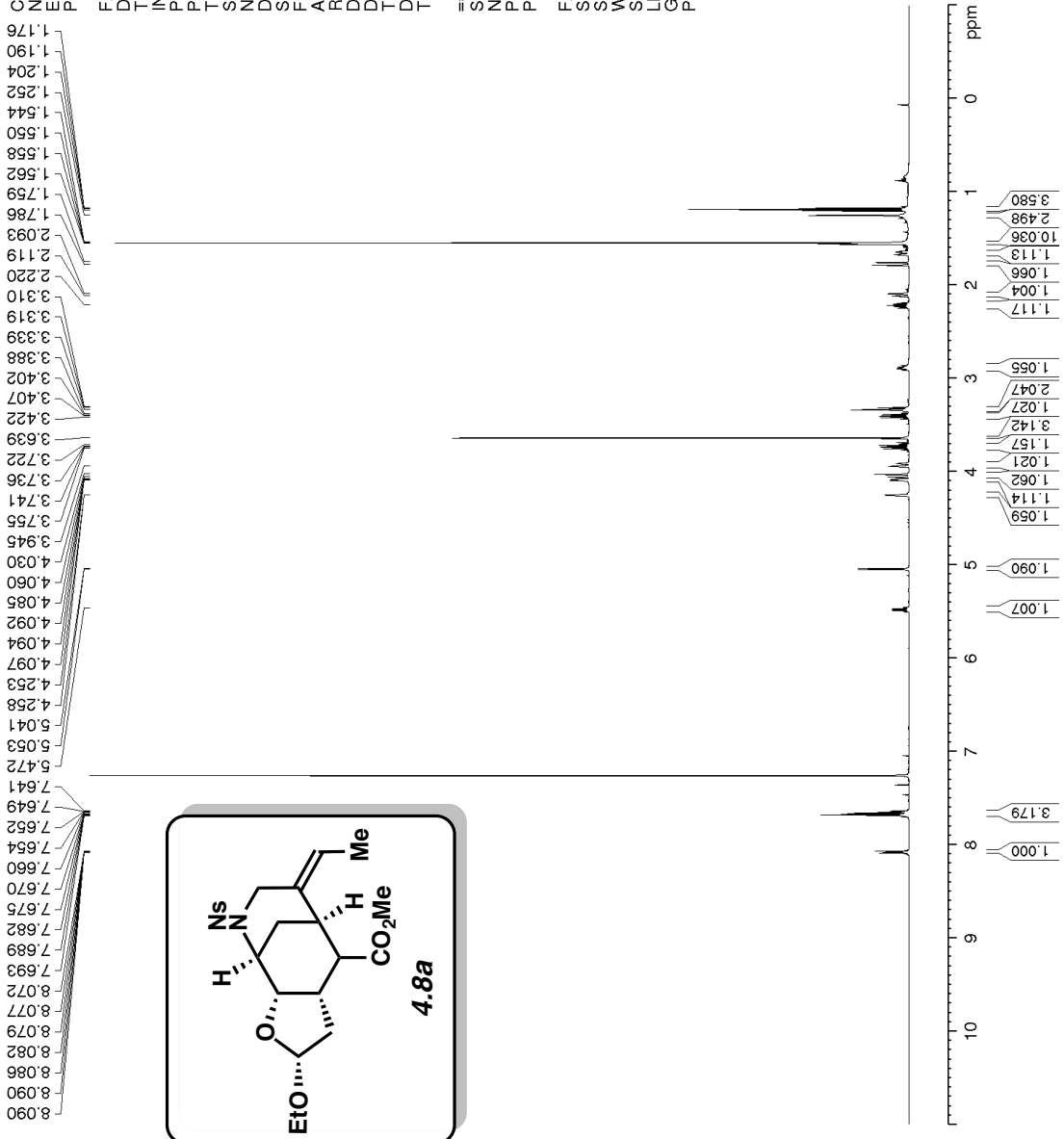


Figure A3.7 ¹H NMR (500 MHz, CDCl₃) of compound 4.8a.

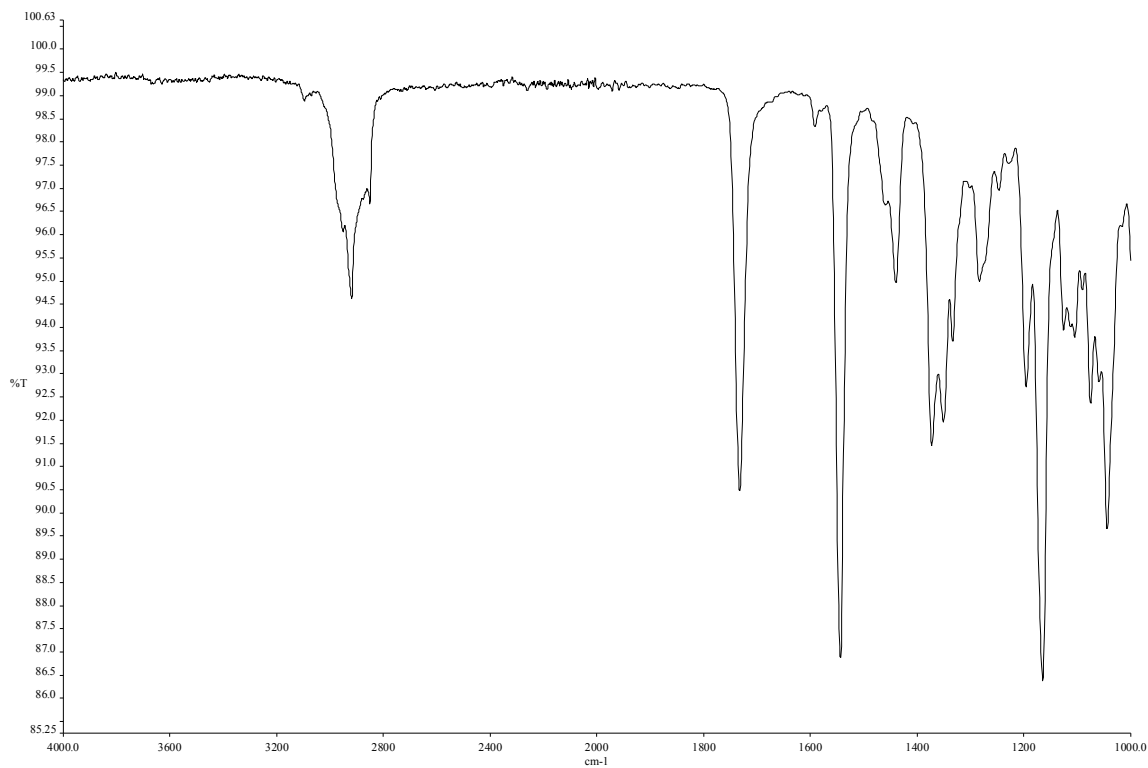


Figure A3.8 Infrared spectrum of compound **4.8a**.

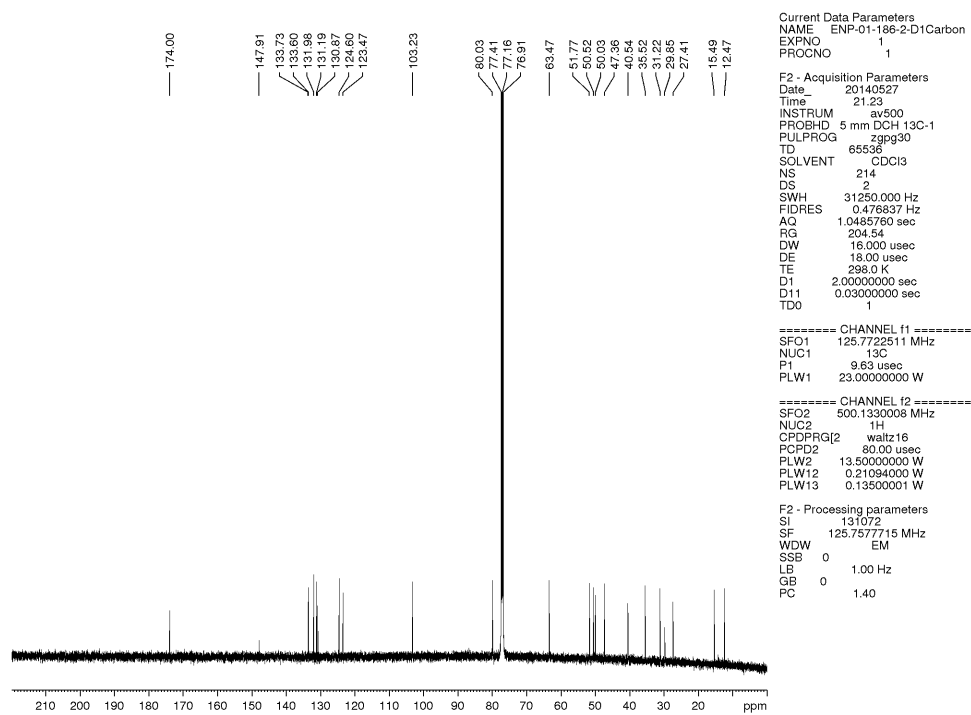


Figure A3.9 ^{13}C NMR (125 MHz, CDCl_3) of compound **4.8a**.

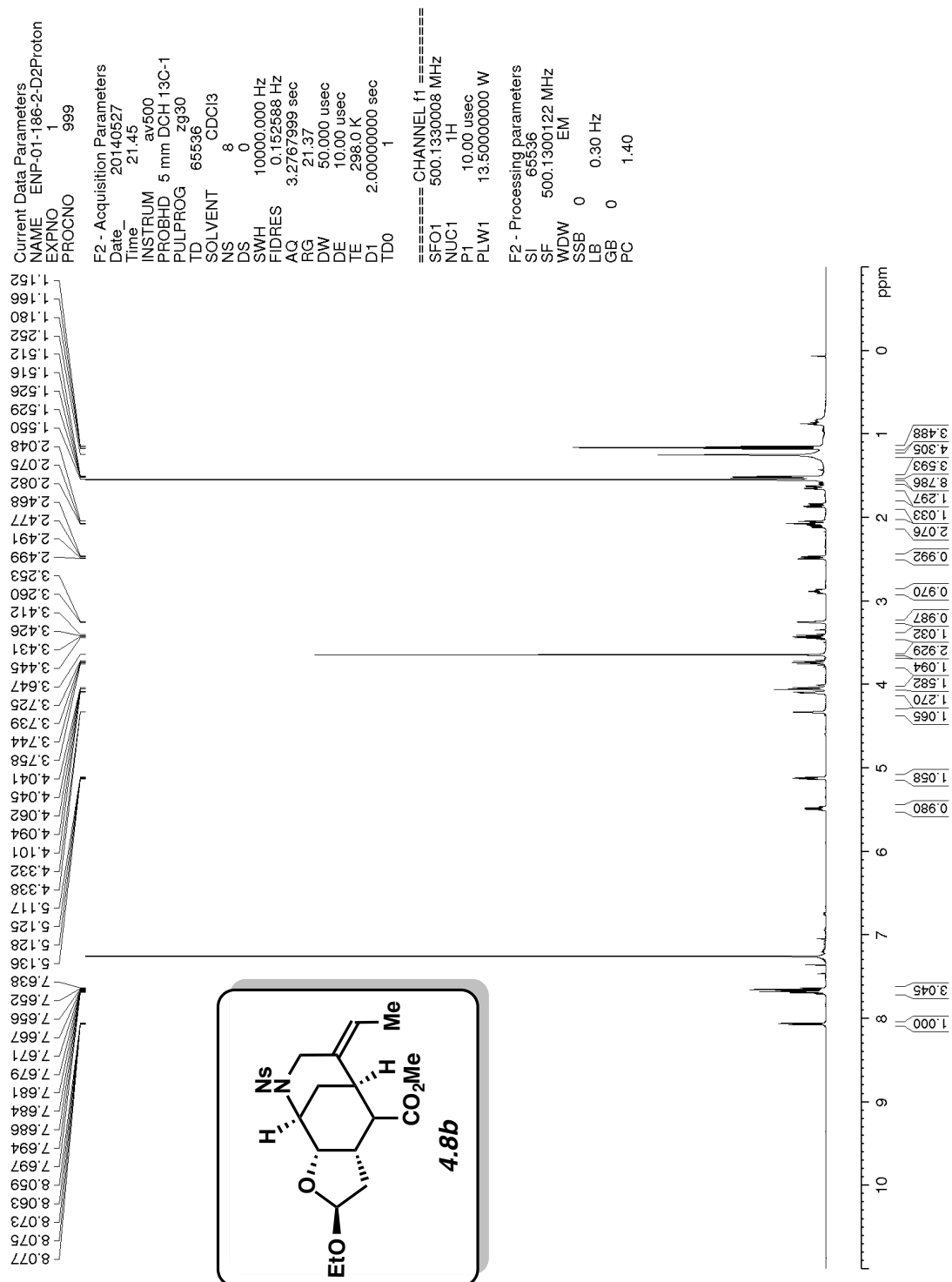


Figure A3.10 ¹H NMR (500 MHz, CDCl₃) of compound 4.8b.

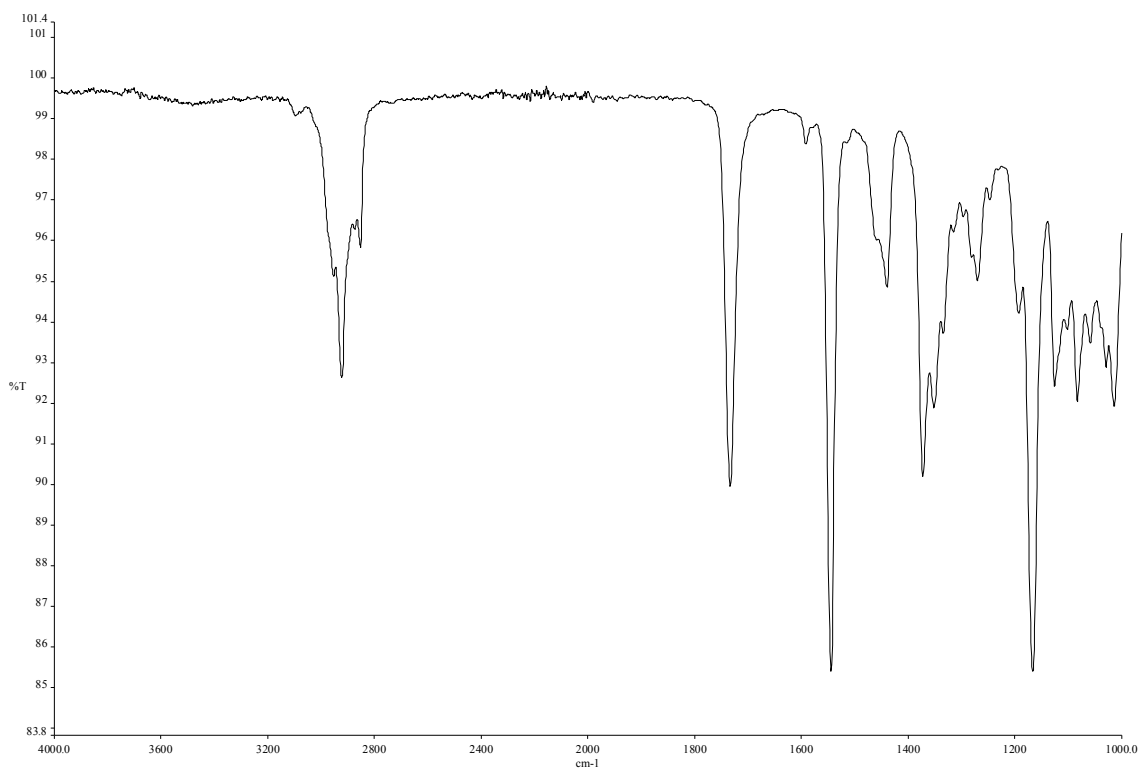


Figure A3.11 Infrared spectrum of compound **4.8b**.

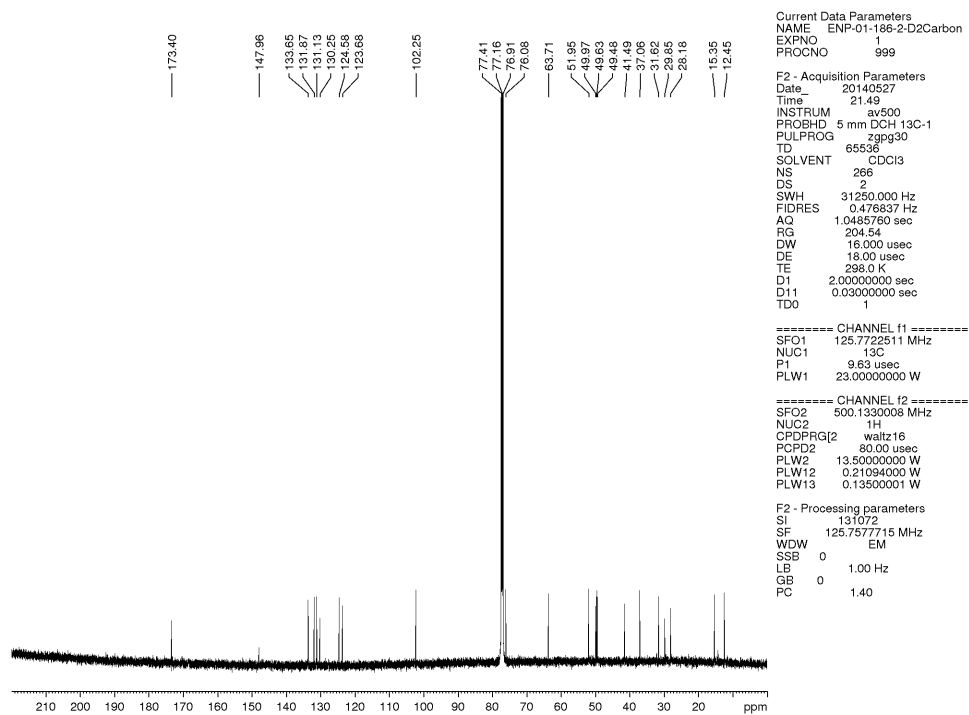


Figure A3.12 ^{13}C NMR (125 MHz, CDCl_3) of compound **4.8b**.

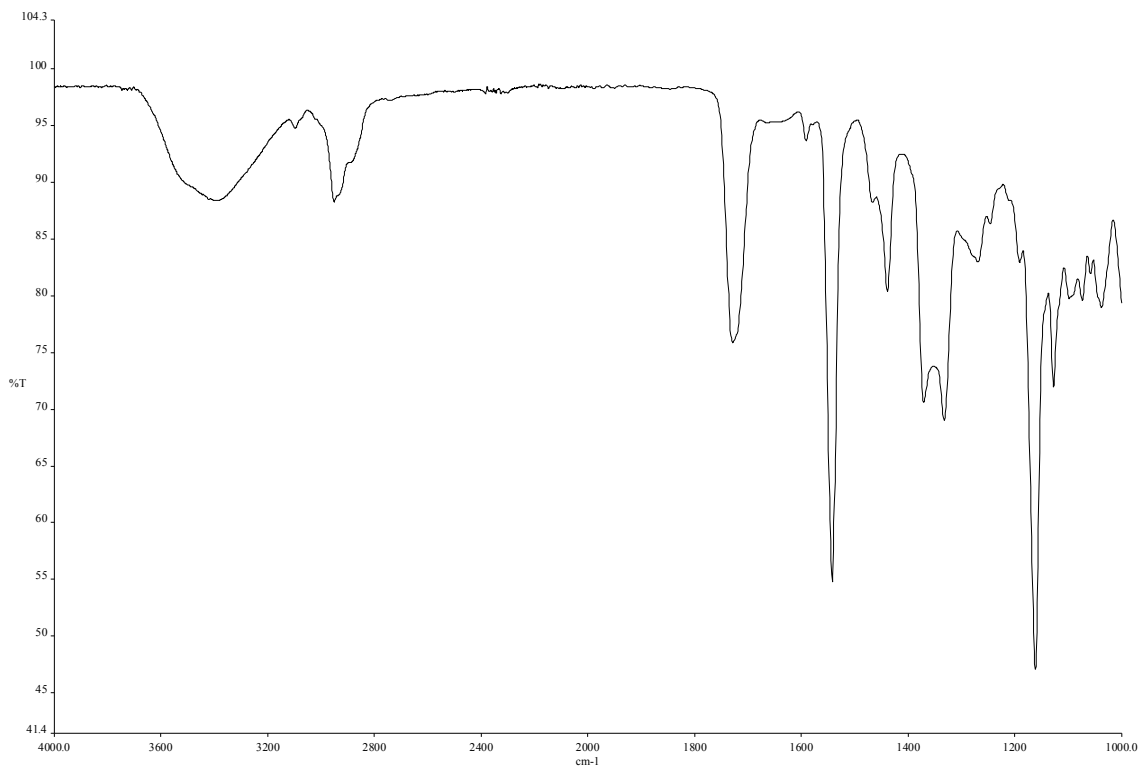


Figure A3.14 Infrared spectrum of compound **4.9**.

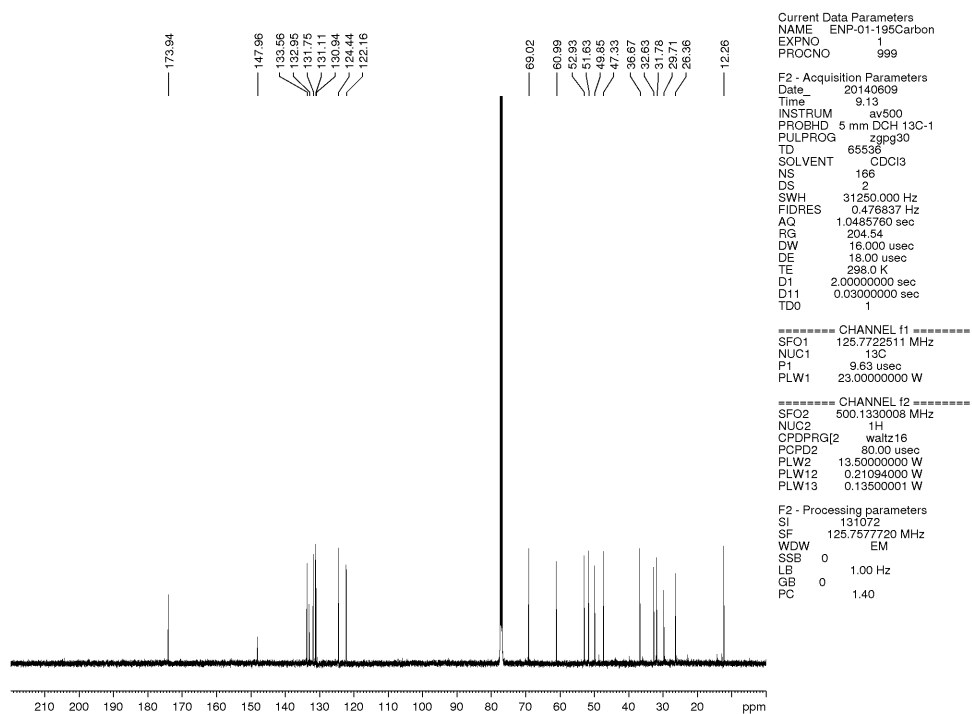


Figure A3.15 ¹³C NMR (125 MHz, CDCl₃) of compound **4.9**.

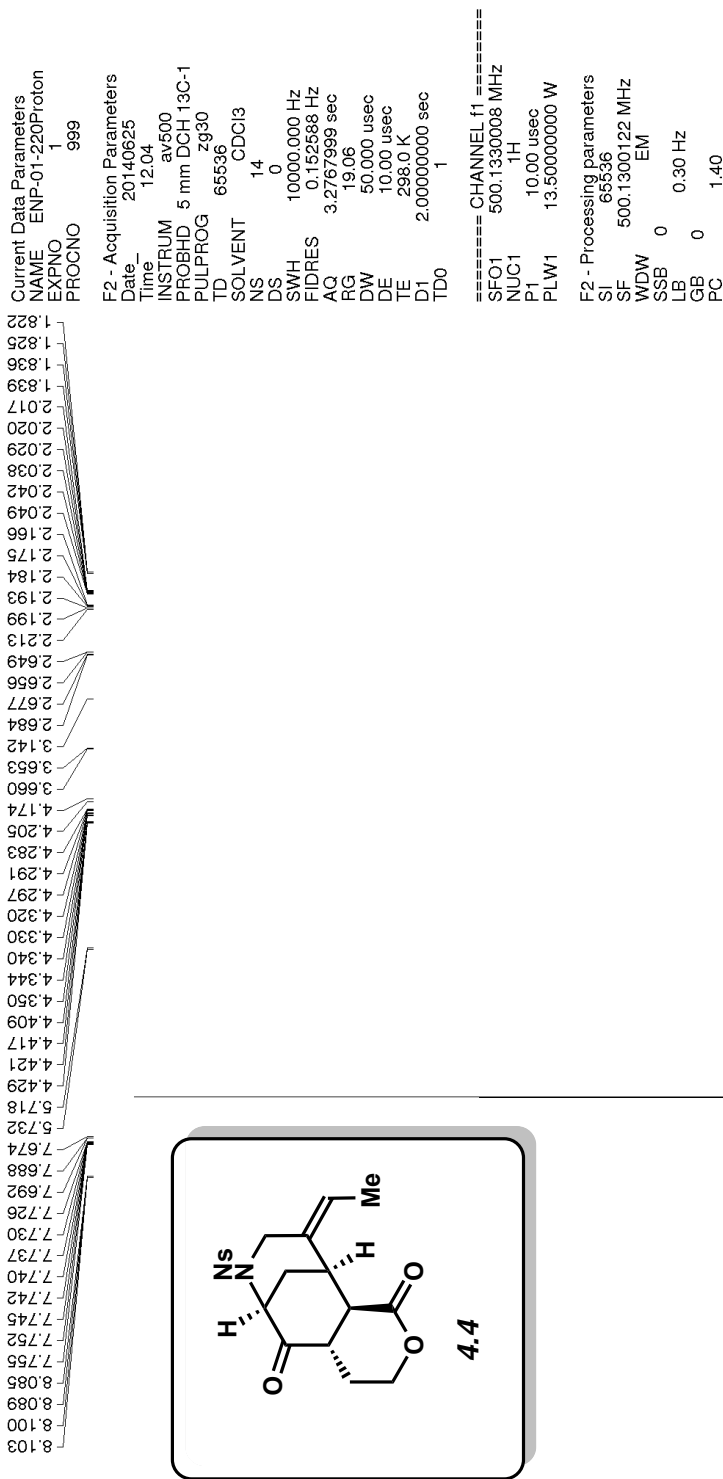


Figure A3.16 ¹H NMR (500 MHz, CDCl₃) of compound 4.4.

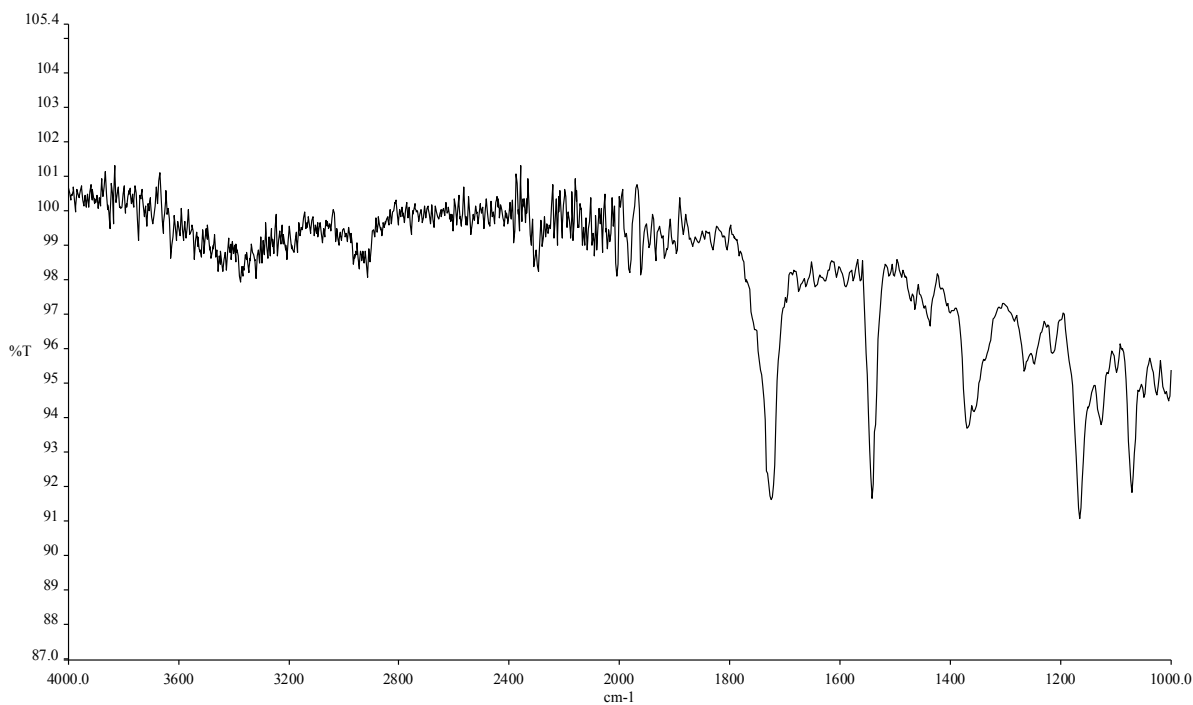


Figure A3.17 Infrared spectrum of compound **4.4**.

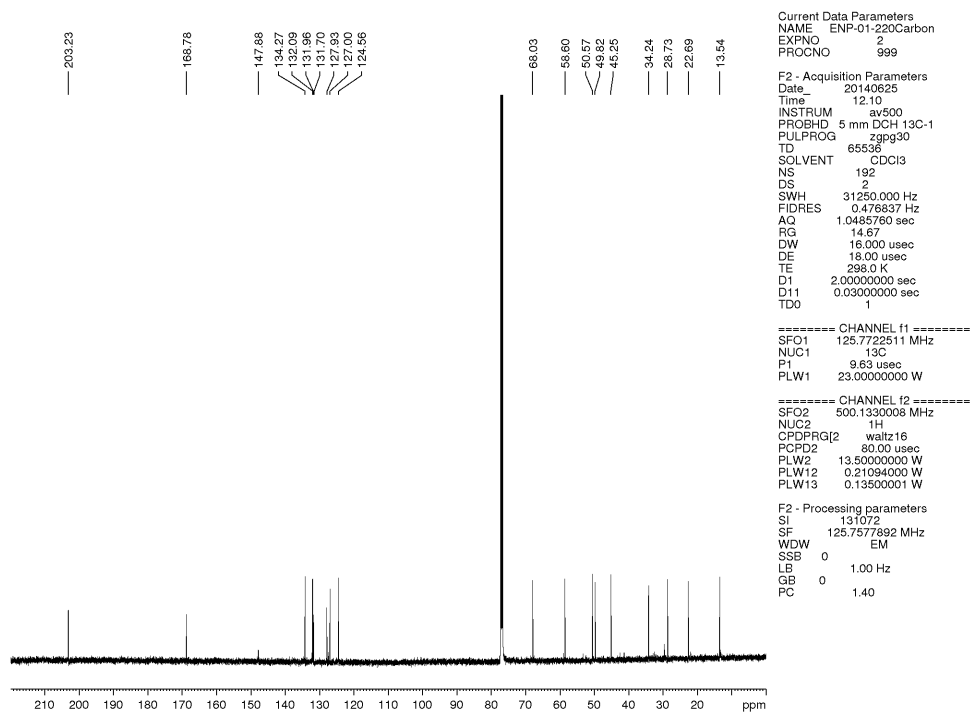


Figure A3.18 ^{13}C NMR (125 MHz, CDCl_3) of compound **4.4**.

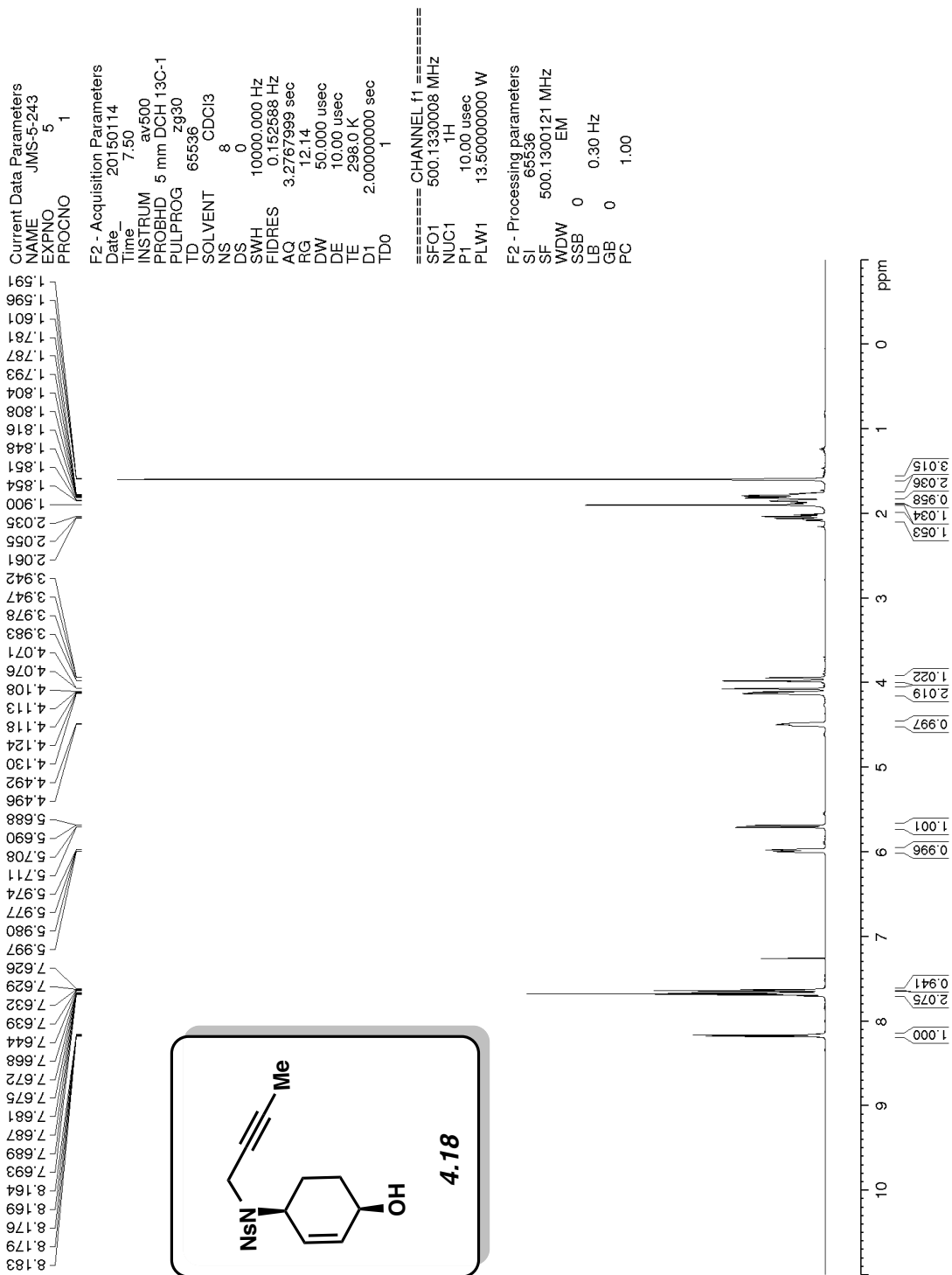


Figure A3.19 ¹H NMR (500 MHz, CDCl₃) of compound 4.18.

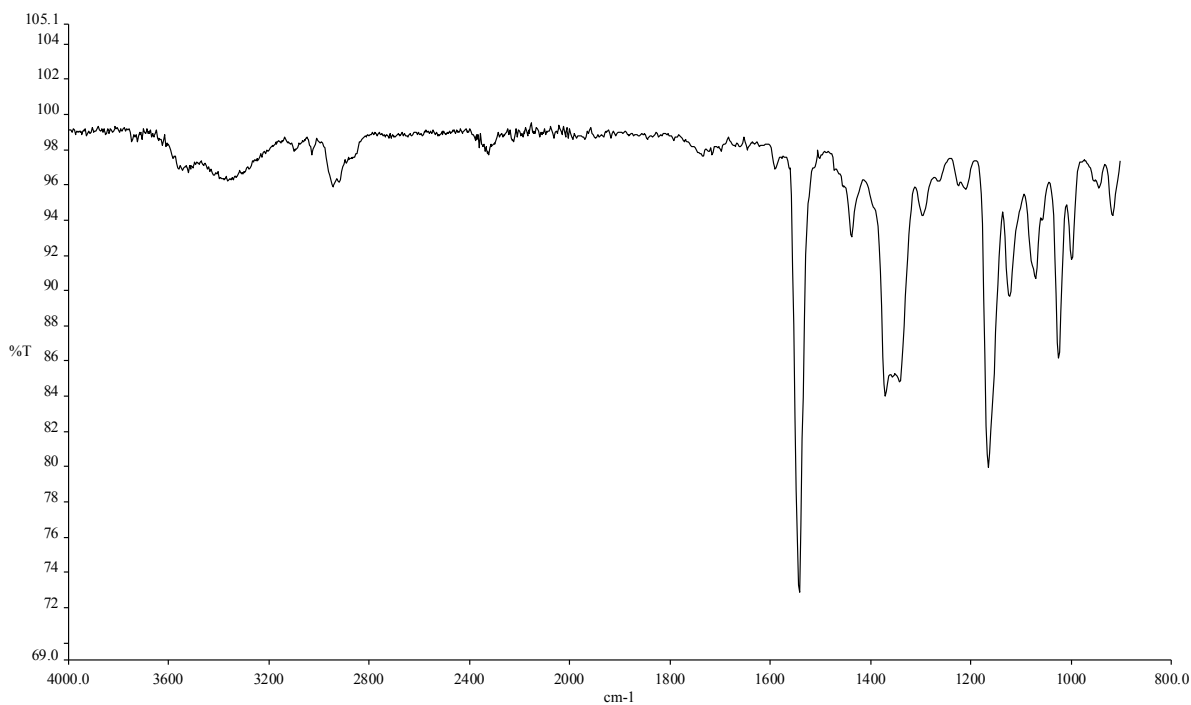


Figure A3.20 Infrared spectrum of compound **4.18**.

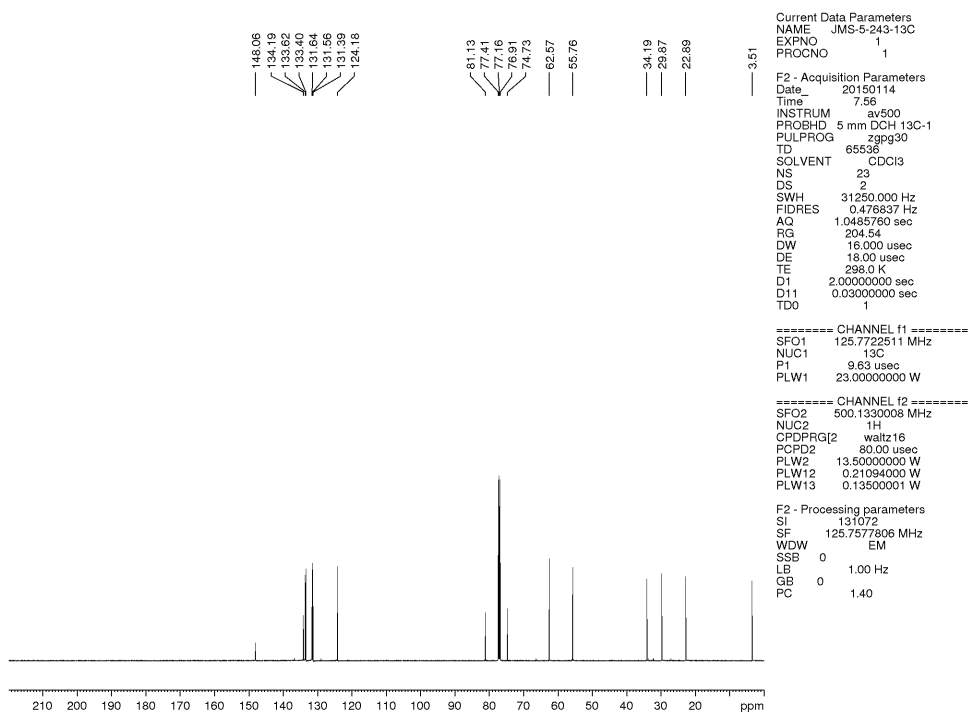


Figure A3.21 ^{13}C NMR (125 MHz, CDCl_3) of compound **4.18**.

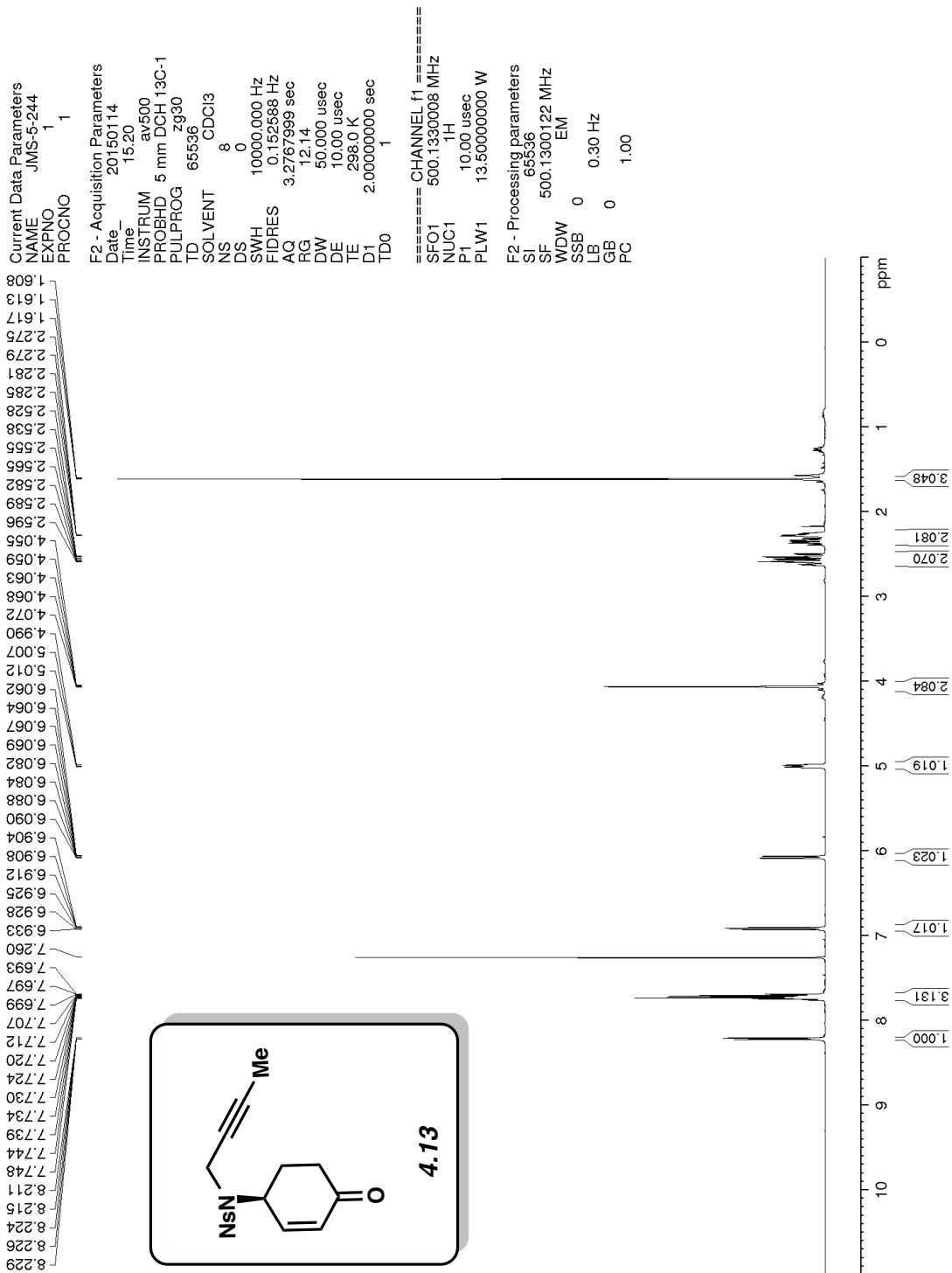


Figure A3.22 ¹H NMR (500 MHz, CDCl₃) of compound 4.13.

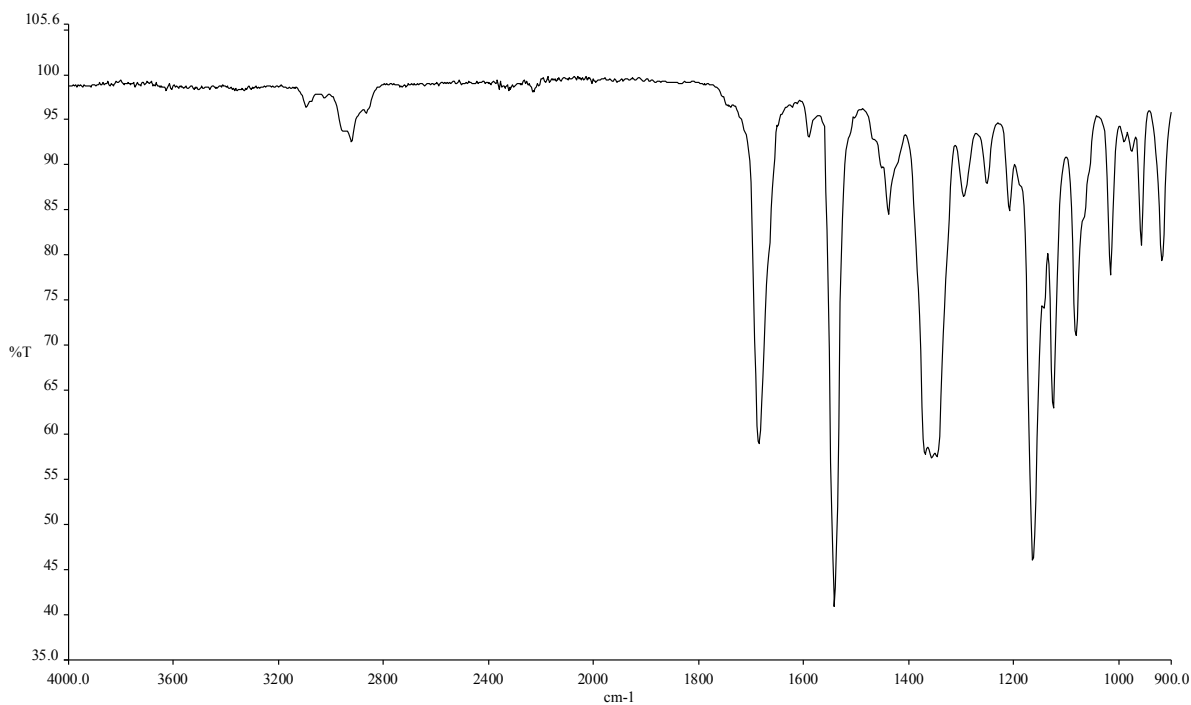


Figure A3.23 Infrared spectrum of compound **4.13**.

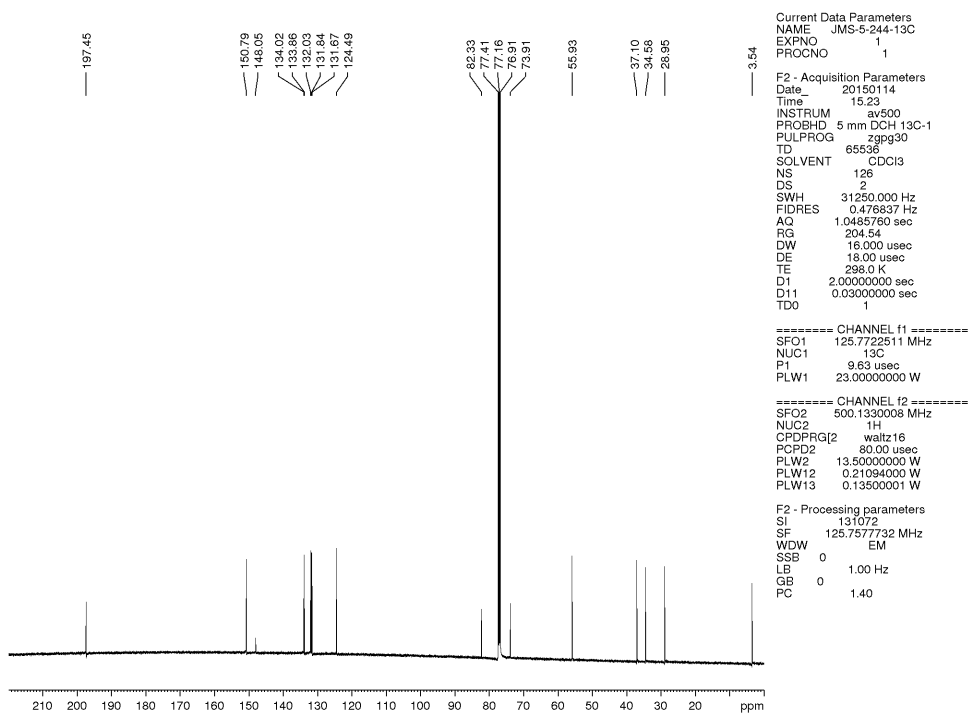


Figure A3.24 ^{13}C NMR (125 MHz, CDCl_3) of compound **4.13**.

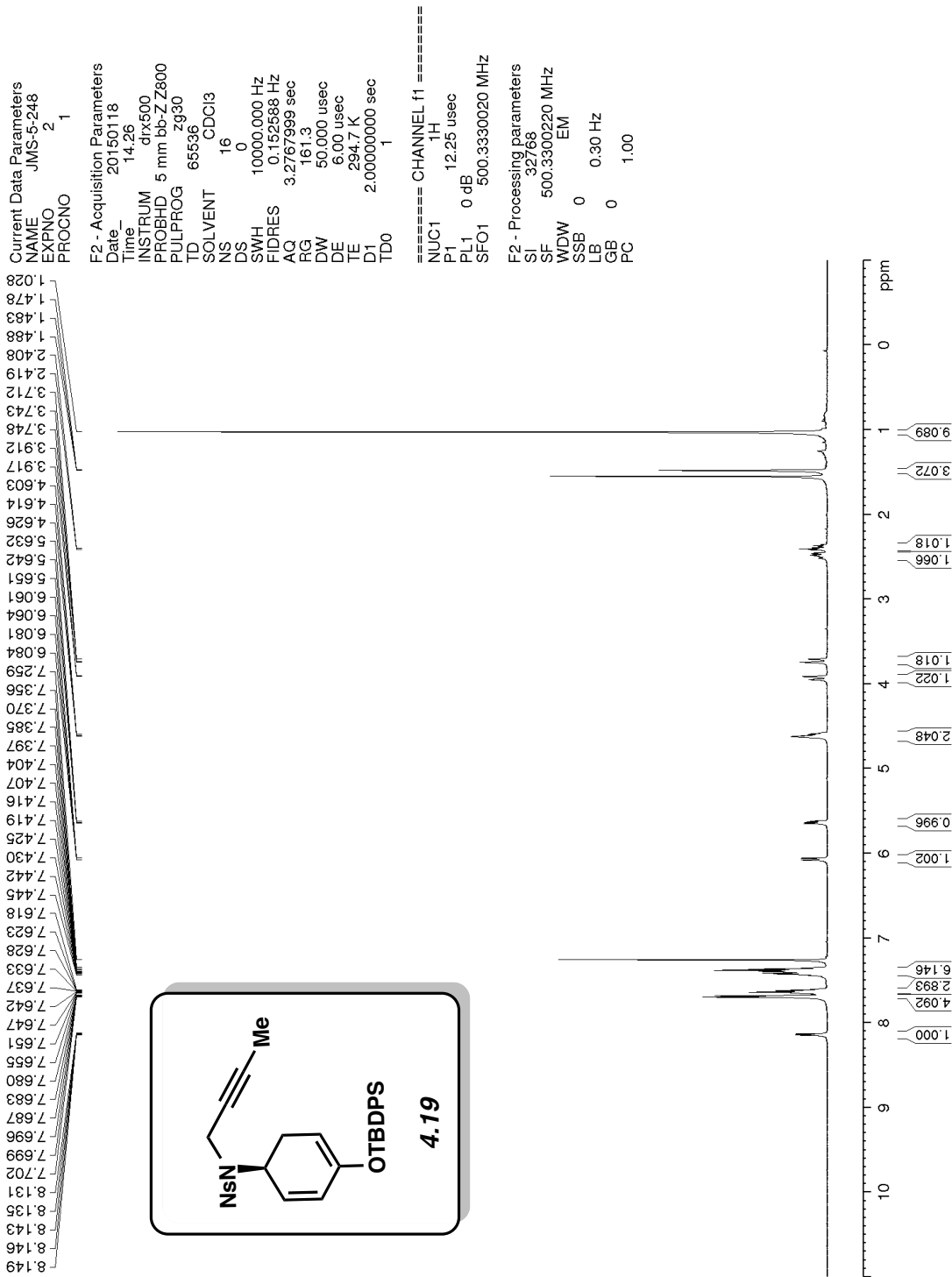


Figure A3.25 ¹H NMR (500 MHz, CDCl₃) of compound 4.19.

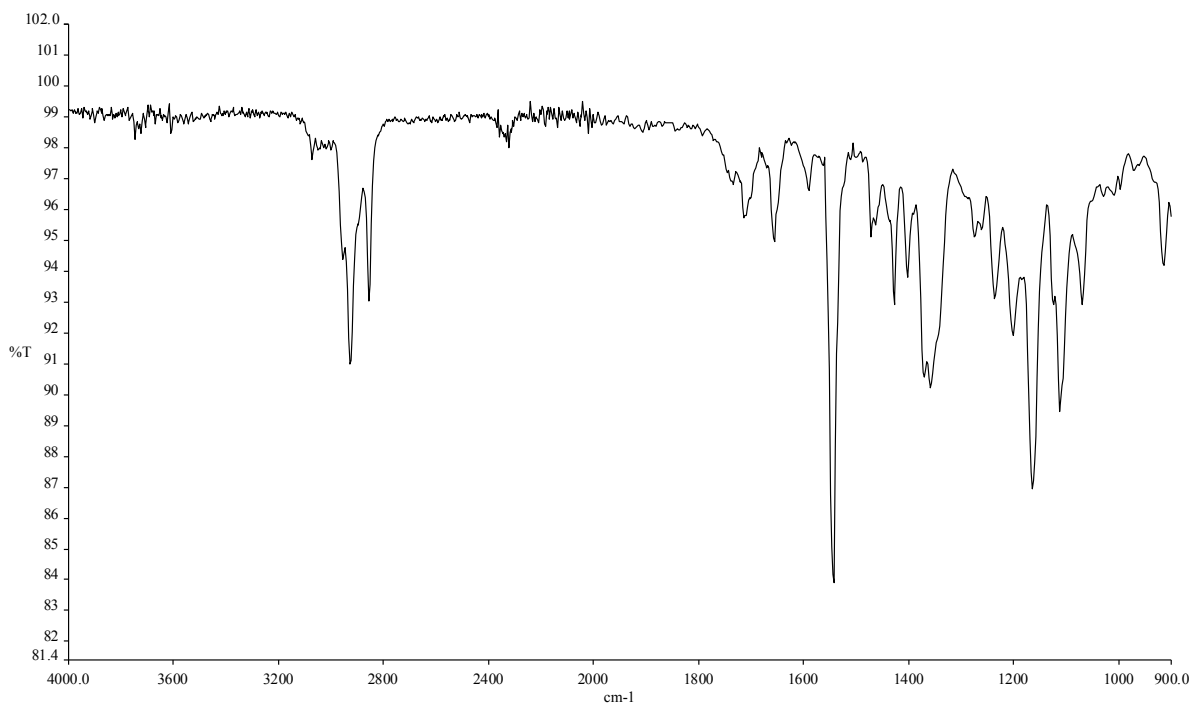


Figure A3.26 Infrared spectrum of compound 4.19.

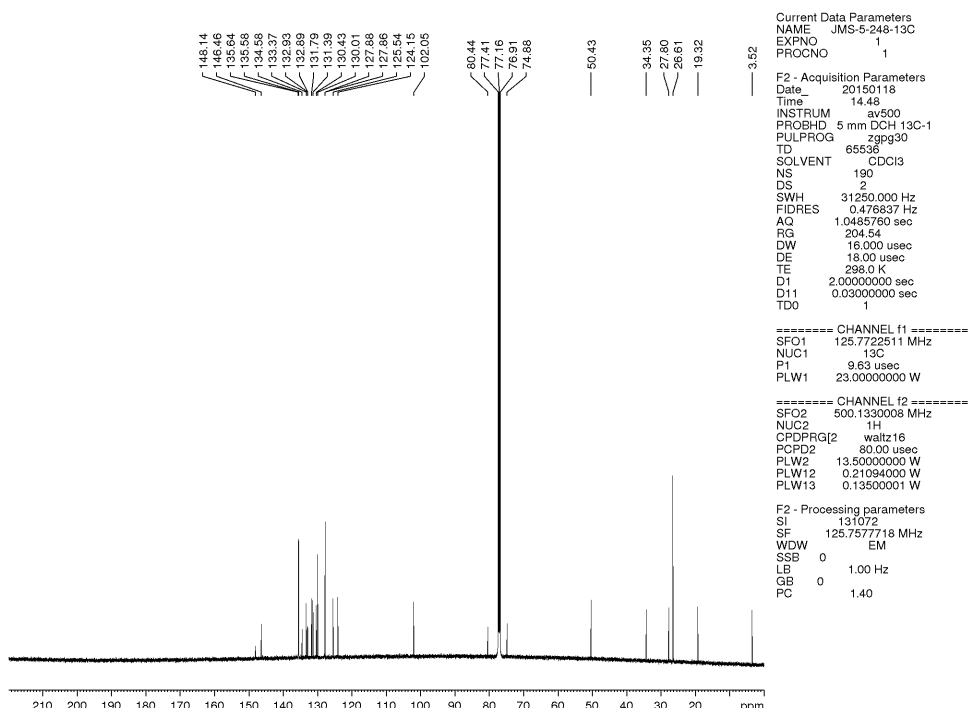
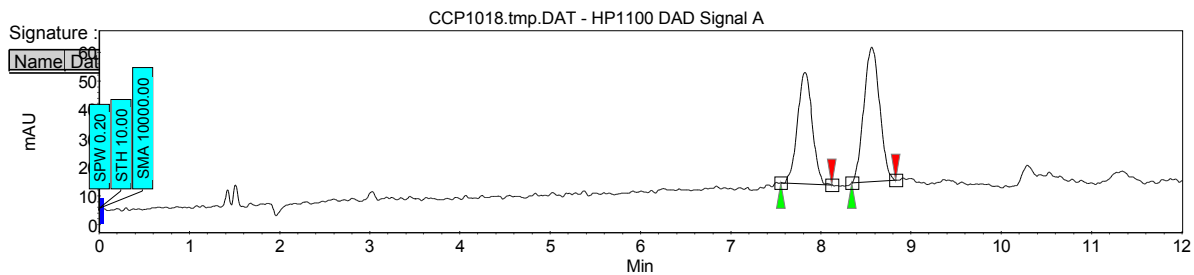
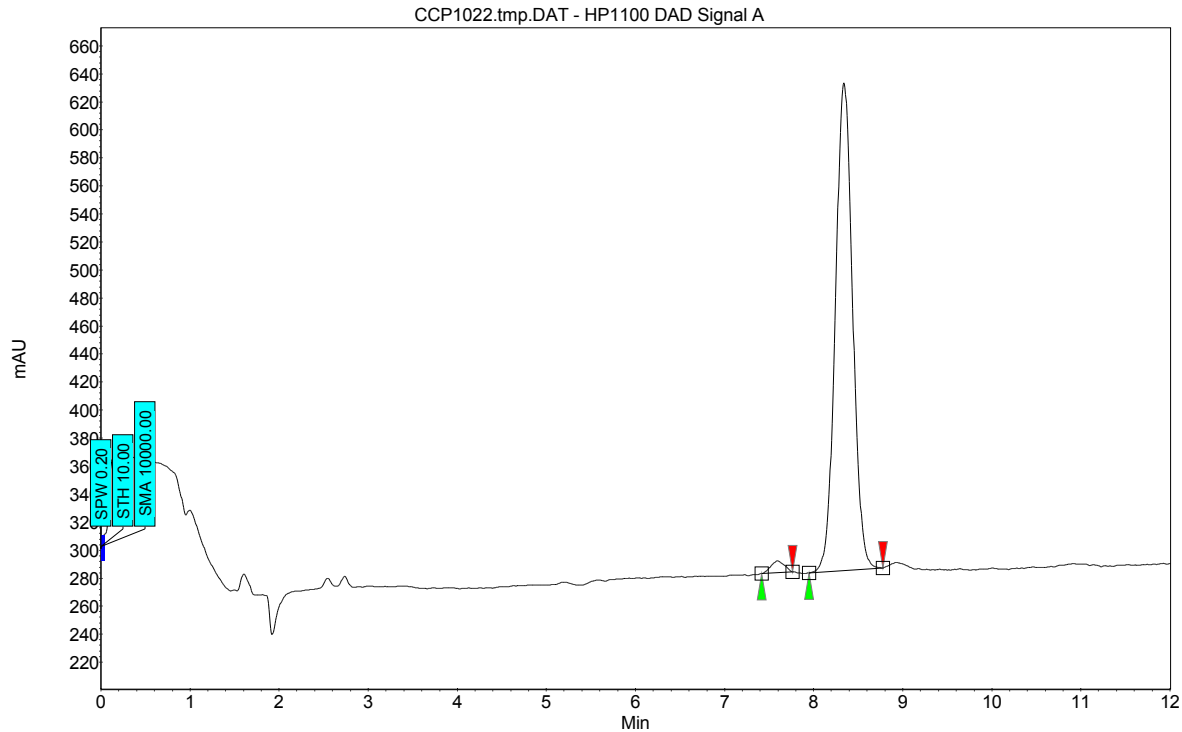


Figure A3.27 ^{13}C NMR (125 MHz, CDCl_3) of compound 4.19.



Index	Name	Start	Time	End	RT Offset	Quantity	Height	Area	Area
		[Min]	[Min]	[Min]	[Min]	[% Area]	[μ V]	[μ V.Min]	[%]
1	UNKNOWN	7.56	7.82	8.12	0.00	44.06	38.7	7.5	44.055
2	UNKNOWN	8.35	8.57	8.83	0.00	55.94	46.6	9.5	55.945
Total						100.00	85.3	16.9	100.000

Figure A3.28 Chiral SFC Trace of racemic compound **3.11** (see chapter 3).



Index	Name	Start	Time	End	RT Offset	Quantity	Height	Area	Area
		[Min]	[Min]	[Min]	[Min]	[% Area]	[μ V]	[μ V.Min]	[%]
1	UNKNOWN	7.42	7.59	7.77	0.00	1.83	8.4	1.5	1.830
2	UNKNOWN	7.95	8.34	8.78	0.00	98.17	348.0	78.0	98.170
Total						100.00	356.4	79.4	100.000

Figure A3.29 Chiral SFC trace of enantioenriched compound **4.10**.